Factors determining competence for *in vivo* glia-to-neuron conversion

Dissertation

Zur Erlangung des Grades

Doktor der Naturwissenschaften

Am Fachbereich Biologie

Der Johannes Gutenberg-Universität Mainz

Chiara Galante

Geboren am 23.03.1986 in Vicenza (Italien)

Mainz, 2019

1. Berictherstatter:
2. Berichterstatter:

Tag der mündlichen Prüfung: 09.10.2019

Foreward

The work presented in this thesis has been performed at *the Institut für Physiologische Chemie, Universitätsmedizin Mainz*, during my time as a PhD candidate of the Faculty of Biology at the Johannes Gutenberg-Universität Mainz. The projects here presented were initiated on basics of ideas of my supervisor, and conducted under the technical supervision of the postdoc overseeing my project.

The cloning of retroviral expression vectors has been designed and performed by myself; retroviral vectors used for the expression of *pAscl1* were produced in house, as a result of the shared efforts of all members of AG Berninger. All *in vitro* experiments were designed, performed and analysed by myself. Experimental design for the retroviral injections was done by myself and the postdoc overseeing my project, who also performed retroviral injections in the cortices of P5 pups. The subsequent processing of brains, immunohistochemistry, data analysis and interpretation were performed by me.

The strategy to adapt the StarTrack clonal labelling system to perform clonal analysis of induced neurons was devised by my supervisor, the postdoc supervising my projects and myself in collaboration with the Department of Molecular, Cellular and Developmental Neurobiology at the Instituto Cajal (Madrid, Spain). The cloning of constructs to express tamoxifen-inducible proneural factors was designed and performed by myself. The design of the all-in-one constructs for experiments in transgenic mouse lines has also been performed by me and the cloning is being carried on by Quimigen S.L. (Madrid, Spain). Preliminary *in utero* electroporation experiments shown in section 2.2 have been performed by me and the postdoc supervising my project. Animal care, tamoxifen injections, processing of the tissues and subsequent immunohistochemical and confocal analysis have been made by myself. Postnatal electroporations, consequent tissue preparation and confocal analysis have been performed by our collaborator at the Instituto Cajal (Madrid, Spain).

Electrophysiology recordings were performed and analysed by my colleague.

Finally, statistical analysis of all other data and their interpretation, graphs, and figures were all prepared by myself.

Declaration

I hereby declare that this thesis is my original work and that it has not been previously submitted to any other German or foreign university or comparable institution for the conferral of an academic degree.

I hereby declare that I have not unsuccessfully ended another doctoral or equivalent program in the subject area of the current doctoral program.

I hereby declare that I wrote the dissertation submitted without any unauthorised external assistance and used only sources acknowledged in the work. All the textual passages, which are appropriated verbatim or paraphrased from published and unpublished texts, as well as all information obtained from oral resources are duly indicated and listed in accordance with bibliographical rules. In carrying out research, I complied with the rules of standard scientific practice as formulated in the statues of Johannes Gutenberg University Mainz to ensure standard scientific practice.

I am aware that an untruthful declaration will have legal consequences.

_____

Place, Date, Name Signature

Table of contents

“With knowledge comes thought, and with thought comes power.”

Alexander von Humboldt

To my parents.

Abstract

In vivo glia-to-neuron conversion mediated by transcription factors is emerging as a possible cell replacement strategy to respecify brain resident cells into lost neuronal cell types and to reinstate the function of disrupted circuitries in the presence of injury, neuropsychiatric disorders or other insults. Different factors, such as the absence or presence of injury, the cell type of origin and the choice of transcription factors influence the ability to convert cortical glia into neurons *in vivo*. However, the role that post-translational modification of transcription factors or the intrinsic heterogeneity of the starting cell population have in this process is largely unknown.

In this thesis, I show that the ability of the proneural transcription factor ASCL1 to direct cell fate-switch in proliferative postnatal cortical glia is increased by the lack of protein phosphorylation. I found that, in postnatal cortical astrocytes cultures transduced with retroviruses encoding for three forms of ASCL1 differing in their phosphorylation states, the induction of a phospho-deficient mutant leads to increased reprogramming efficiency compared to the wild type protein or a phospho-mimetic mutant. However, independently on its phosphorylation state, ASCL1 is not able to efficiently convert postnatal cortical glia into neurons *in vivo* but rather decreases the proportion of astroglia favouring generation of oligodendroglia. The exogenous expression of both phospho-mutants leads to an increase in mature oligodendrocytes, consistent with a role of *Ascl1* in the differentiation of oligodendrocyte progenitors. Moreover, I demonstrated that co-transduction of *Bcl2* with *Ascl1* successfully induces glia-to-neuron conversion. Remarkably, when associated with *Bcl2*, both phospho-mutants showed a greater neurogenic ability compared to the wild type protein and the phospho-deficient mutant drove the formation of a higher proportion of NeuN-expressing neurons. In summary, while the phosphorylation state of ASCL1 does not seem to promote cell fate-switch per se, it influences the maturation level of reprogrammed postnatal cortical glia and the conversion efficiency in association with BCL2.

Furthermore, I describe an adaptation of a clonal labelling system, called StarTrack, for *in vivo* cortical astrocyte-to-neuron conversion and, eventually, clonal analysis of induced neurons. Here, I illustrate the results obtained from preliminary experiments in which the tamoxifen-activated proneural factors ASCL1ERT2 and NEUROG2ERT2 are induced in GFAP-expressing postnatal cortical astrocytes. These experiments revealed the limitations of the system, such as insufficient expression levels of the plasmids expressing *Ascl1ERT2* and *Neurog2ERT2* and the failure to induce formation of DCX-positive neurons to date. After identification of the pitfalls of the system, I describe a possible strategy to circumvent them. In the future, coupling tamoxifen-inducible activation of forced neurogenesis in astrocytes with clonal labelling of converted cells will permit the identification of the glial clones from which induced neurons are generated and, conversely, identification of the astrocytic populations that expressed the proneural factors but failed to reprogram.

Together, understanding the mechanisms favouring the execution of neurogenic programs instructed by transcription factors and the reasons, why some glial subpopulations fail to erase their original fate and switch lineage, will help developing strategies to improve cell fate conversion for regenerative medicine.

Zusammenfassung

Die Transkriptionsfaktor-vermittelte *in vivo* Glia-zu-Neuron Umwandlung, ist eine neu aufkommende, mögliche Zellersatz-Strategie um residente Zellen im Gehirn Zellen in verloren gegangene neuronale Zelltypen umzuwandeln und die Funktion angesichts von Verletzungen, neuropsychatrischer Krankheiten und weiterer Insulte unterbrochener Verschaltungen wiederherzustellen. Verschiedene Faktoren, wie z.B. das Vorhandensein oder Fehlen von Verletzungen, der Ursprungszelltyp und die Wahl der Transkriptionsfaktoren beeinflussen die Fähigkeit, kortikale Glia *in vivo* in Neuronen umzuwandeln. Die Rolle, die die post-translationale Modifikation von Transkriptionsfaktoren oder die intrinsische Heterogenität der Ausgangszellpopulation bei diesem Prozess spielen, ist allerdings weitestgehend unbekannt. In dieser Arbeit zeige ich, dass die Fähigkeit des proneuralen transkriptionsfaktors ASCL1 den Wechsel des Zellschicksals proliferativer postnataler kortikaler Glia zu dirigieren, durch das Fehlen der Proteinphosphorylierung erhöht wird. In postnatalen kortikalen Astrozytenkulturen, die durch Retrovieren mit verschiedenen Formen von ASCL transduziert werden, welche sich in ihrem Phosphorylierungsstatus unterscheiden, konnte ich feststellen, dass die Induktion einer phospho-defizienten Mutante, im Vergleich zum Wilttyp Protein oder einer phospho-mimetischen Mutante, zu einer erhöhten Reprogrammierungseffizienz führt. Unabhängig von seinem Phosphorylierungsstatus, ist ASCL1 jedoch nicht in der Lage, postnatale kortikale Glia in vivo effizient in Neuronen zu konvertieren. Vielmehr verringert es den Anteil an Astroglia, die die Bildung von Oligodendroglia begünstigen. Im Einklang mit der Rolle von *Ascl1* bei der Differnzierung von Oligodendrozyten-Vorläufern, führt die exogene Expression beider Phosphomutanten zu einem Anstieg reifer Oligodendrozyten. Darüberhinaus konnte ich zeigen, dass die Co-Transduktion von *Bcl2* mit *Ascl1* erfolgreich eine Glia-zu-Neuron Umwandlung induziert. Bemerkenswerterweise zeigten beide Phosphomutanten in Verbindung mit *Bcl2* eine erhöhte Neurogenität im Vergleich zum Wildtypprotein, die phosphodefiziente Mutante führte zu einer anteilig vermehrten Bildung NeuN-exprimieremder Neuronen. Zusammenfassend kann man sagen, dass, obwohl der Phosphorylierungsstatus von ASL1 per se keinen Zellschicksal-Wechsel zu fördern scheint, es in Verbindung mit BCL2 dennoch den Reifegrad reprogrammierter postnataler kortikaler Glia und die Umwandlungseffizienz beinflusst.

Des weiteren beschreibe ich die Anpassung eines klonalen Kennzeichnungssystems namens *StarTrack* zur in vivo Astrozyt-zu-Neuron Umwandlung und letzendlich klonalen Analyse induzierter Neuronen.

Hier verdeutliche ich Ergebnisse aus Vorversuchen, in welchen die Tamoxifen-aktivierten proneuralen Faktoren ASCL1ERT2 und NEUROG2ERT2 in GFAP-exprimierenden postnatalen kortikalen Astrozyten induziert werden. Diese Experimente zeigten die sogenannten „Stolperfallen“ des Systems auf, wie z.B. unzureichende Expressionslevel der *Ascl1ERT2* und *Neurog2ERT2* exprimierenden Plasmide und die bis

heute erfolglosen Versuche die Formation DCX-positiver Neuronen zu Induzieren. Nach Identifikation dieser Hindernisse im System, gehe ich weiterhin auf mögliche Strategien ein um diese zu verhindern. Die Kopplung von Tamoxifen-induzierbarer Aktivierung forcierter Neurogenese von Astozyten mit der klonalen Markierung umgewandelter Zellen wird es erlauben, gliale Klone zu identifizieren, aus denen Neuronen gebildet werden können. Umgekehrt wird auch die Identifikation astrozytischer Population welche zwar proneurale Faktoren exprimieren jedoch nicht umprogrammiert wurden möglich.
Das Verständnis der Mechanismen, die die Ausführung Transkriptionsfaktor-angewiesener neurogener Programme begünstigen, wie auch der Gründe, warum manche gliale Subpopulationen nicht in der Lage sind ihr Ursprungsschicksal zu überschreiben und ihre Abstammungs-/Entwicklungslinie zu wechseln, wird in Zukunft dabei helfen, neue Strategien zu entwickeln um die Umwandlung des Zellschicksals für die regenerative Medizin zu verbessern.

1 Introduction

1.1 Proneural transcription factors

During brain development, neurons forming the neocortex are derived from the division and differentiation of neural stem cells and neural progenitors residing in the germinal zones lining the ventricles, namely ventricular and subventricular zone (VZ/SVZ) (reviewed in Kriegstein and Alvarez-Buylla 2009). Specific genetic programs instructing the differentiation of neural progenitors into different subtype of neurons are activated by proneural factors, transcription factors that are necessary and sufficient to initiate differentiation of progenitor cells into neurons (reviewed in Bertrand et al. 2002). Knowing the mechanisms that instruct differentiation of diverse neuronal types has been of help to develop strategies to convert non-neuronal cell types into neurons, thus posing the basis for transcription factor-based reprogramming (reviewed in Masserdotti et al. 2016), which has the potential to become a cell-based therapy for brain repair (reviewed in Heinrich et al. 2015).

The work presented in this thesis explores the potential of two proneural factors to convert glial cells into neurons in the postnatal murine cortex, namely ASCL1 and NEUROG2. Throughout the manuscript, consistent with the Guidelines for Nomenclature of Genes, Genetic Markers, Alleles, and Mutations in Mouse and Rat (http://www.informatics.jax.org/mgihome/nomen/gene.shtml), genes' and proteins' symbols are going to be indicated as follows: italicised letters for genes (e.g. *Neurog2*, *Ascl1SA6*); regular, uppercase letters for proteins (e.g. NEUROG2, ASCL1SA6). The paradigm of forced conversion of one cell type into another will be named as: reprogramming; conversion; cell fate-switch; lineage conversion; lineage reprogramming. Those instances in which a specific concept or finding is summarised by the collection of numerous multiple works in a review are going to be indicated as "reviewed in".

1.1.1 Proneural transcription factors: origin, structure and function

Proneural transcription factors are a subset of basic Helix-Loop-Helix (bHLH) transcription factors. They were first identified in *Drosophila* as a group of genes necessary and sufficient to initiate development of nervous tissue and to promote specification and differentiation of neuronal cells (reviewed in Bertrand et al. 2002). They contain a basic Helix-Loop-Helix (bHLH) motif (Fig.1.1), first described by Villares & Cabrera in 1987 (Villares and Cabrera 1987). This motif comprises the basic domain and the HLH domain: the basic domain is involved in direct binding to the main groove of the DNA, while the HLH domain, composed by two *alpha*-helices connected by a loop, is involved in dimerization with the HLH domain of another proneural factor or of an E protein to form a four-helix bundle (reviewed in Bertrand et al. 2002; Villares and Cabrera 1987). The necessity of bHLH factors to dimerise was first

observed by Chien and colleagues in 1996. They demonstrated that while the bHLH motif of ATONAL was necessary to induce neurogenesis and specify the sensory organ of *Drosophila*, the aminoacidic residues required for this specification were actually not involved in DNA-binding, suggesting the requirement for dimerization with a co-factor (Chien et al. 1996).

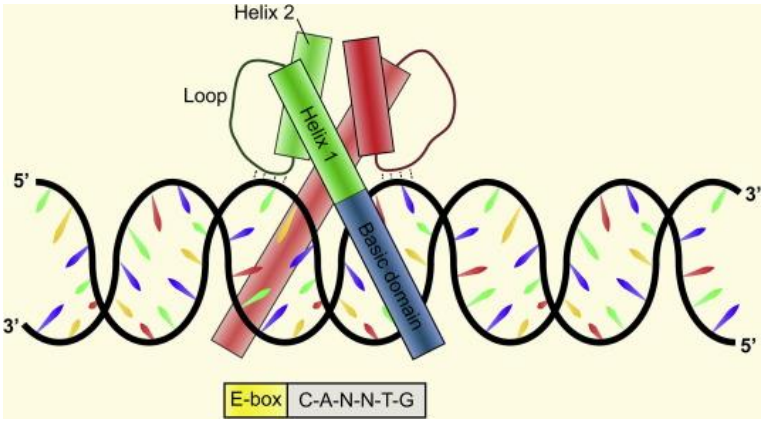

Fig.1.1 Structure of a basic Helix-Loop-Helix transcription factor. The basic Helix-Loop-Helix (bHLH) motif is constituted by a basic domain (blue) with affinity for the main groove of DNA and two alpha-helices joined by a loop (green). The consensus sequence for binding of bHLH transcription factors is CANNTG (E-box). Picture from Dennis et al. 2018.

The bHLH motif binds to a DNA sequence called E-box, a consensus sequence of six nucleotides (CANNTG) (Fig.1.1), and its presence is sufficient to have proneural function (reviewed in Bertrand et al. 2002; Hinz et al. 1994). After the discovery of bHLH transcription factors in *Drosophila*, several related genes have been discovered in vertebrates, including humans (reviewed in Dennis et al. 2018; Ho et al. 2008; Huang et al. 2014). The bHLH motif of vertebrate proteins is highly conserved among all neural bHLH factors, even though some portions are specific to each family of bHLH genes (reviewed in Bertrand et al. 2002; Ferré-D'Amaré et al. 1993). In vertebrates there are in total eight families of bHLH genes, but only a sub-set is actually classified as proneural: *Neurogenin1* (*Neurog1*) (Ma et al. 1996), *Neurogenin2* (*Neurog2*) (Fode et al. 1998; Ma et al. 1996), *Achaete Scute-Like1* (*Ascl1*) (Guillemot et al. 1993), *NeuroD4* (Tomita et al. 2000), *Atonal bHLH Transcription Factor1* (*Atoh1*) (Ben-Arie et al. 1997) and *Atonal bHLH Transcription Factor7* (*Atoh7*) (Brown et al. 2002) (reviewed in Bertrand et al. 2002, Dennis et al. 2018). The classification as proneural genes depends on whether they can promote neuronal differentiation and specification and whether they can activate NOTCH/DELTA-mediated lateral inhibition (as defined in Dennis et al. 2018). Proneural genes are regulating neurogenesis and the determination of neuronal identity in different areas of the brain, including dorsal telencephalon (Fode et al. 2000), ventral telencephalon (Casarosa et al. 1999; Fode et al. 2000), tectum (Tomita et al. 2000), cerebellum (Ben-Arie et al. 1997) and retina (Brown et al. 2002).

Their proneural activity is exerted through different mechanisms: activation of lateral inhibition via transactivation of *Delta* ligands (Castro et al. 2006; Hinz et al. 1994); activation of cascades of genes implementing a neuronal differentiation program (Hinz et al. 1994; Ma et al. 1996); positive-feedback loops in which proneural bHLH proteins promote the expression of other bHLH proteins which, in turn,

induce neuronal differentiation (Koyano-Nakagawa et al. 2000); repression of alternative glial fates (Cai et al. 2000; Inoue et al. 2002; Nieto et al. 2001; Tomita et al. 2000).

The proper orchestration of their activity is necessary for brain development and is mediated by several mechanisms. E proteins bind the HLH domain of proneural factors thus forming homodimers or heterodimers with other HLH proteins and acting as transcriptional cofactors (Le Dréau et al. 2018; Massari and Murre 2000). The presence of E proteins available for dimerization increases the half-life of proneural factors, as demonstrated by the double half-life of NEUROG2 upon co-expression of E12 as compared to NEUROG2 alone (Hindley et al. 2012). Another class of HLH proteins present in the cortex during development, namely ID proteins, act as transcriptional repressors by binding to E proteins and sequestering them (reviewed in Massari and Murre 2000; Wang and Baker 2015; reviewed in Yokota 2001). A further essential negative regulator of proneural factors is Notch signalling, acting via lateral inhibition; in fact, proneural genes themselves activate the expression of DELTA ligands (reviewed in Bertrand et al. 2002; Castro et al. 2006; Hinz et al. 1994). These ligands bind NOTCH receptors on neighbouring cells, which intracellularly release the NOTCH intracellular domain thus leading to the cell non-autonomous activation of their transcriptional targets, namely *Hes* genes. HES proteins are HLH transcription factors that repress transcription either via direct binding on enhancer sequences or via binding and sequestering of E proteins (reviewed in Bertrand e al. 2002; Chen et al. 1997; reviewed in Dennis etal. 2018). Another important developmental pathway, Wnt signalling, is involved in the timely regulation of proneural factors during early corticogenesis via induction of *Neurog1* and *Neurog2* expression by *beta*-catenin (Bluske et al. 2012). Wnt signalling is also involved in the induction of bHLH genes in the adult hippocampus, where *beta*-catenin directly binds the promoter region of *NeuroD1* to activate its transcription (Kuwabara et al. 2009). Similarly, Bone Morphogenetic Protein (BMP) signalling timely regulates the gene expression of *Neurog2* during development by activating its transcription (Segklia et al. 2012). BMP also induces increased expression of ID proteins, which can heterodimerise with E proteins, thus leading to increased instability of proneural factors and their subsequent degradation (Viñals et al. 2004), or with the bHLH factor OLIG2, thus inhibiting oligodendrogenesis (Samanta and Kessler 2004). Finally, Fibroblast Growth Factor (FGF) signalling is involved in the decision of neuronal cell fate by activating RAS/ERK signalling, which controls which proneural gene is to be expressed in the developing telencephalon via phosphorylation of ASCL1 (Li et al. 2014), as will be explained in more detail in section 1.2.2. FGF signalling also acts as downstream effector of Sonic Hedgehog (Shh) signalling to regulate expression and segregation of proneural factors in the diencephalon (Martinez-Ferre et al. 2016) .

In the following section, I will focus on the developmental role of the two proneural factors I used for my direct lineage-reprogramming studies, namely ASCL1 and NEUROG2.

1.1.2 *Achaete Scute-Like1* and *Neurogenin2*: role in development

The mouse proneural factors *Achaete Scute-like1* (*Ascl1*) and *Neurogenin2* (*Neurog2*) were first identified by Guillemot and Joyner in 1993 and by Fode and colleagues in 1998, respectively. These factors are expressed in a subset of neural progenitors constituting the ventricular zone during development (Fode et al. 2000). *Neurog2* is expressed in the dorsal telencephalon and thalamus (Fode et al. 2000), in the epibranchial placodes (Fode et al. 1998), in motor neuron precursor cells (Lee et al. 2005) and in the ventral midbrain (Kele et al. 2004). *Ascl1* is strongly expressed in the ventral telencephalon and thalamus and only at low level in the dorsal telencephalon (Fode et al. 2000), but is also found in the spinal cord and in the ventral midbrain (Borromeo et al. 2017; Guillemot and Joyner 1993; Kele et al. 2004). Both proneural factors are first detected in the telencephalon of the murine embryonic brain by embryonic day 10.5 (E10.5) and their expression is much more pronounced in ventricular progenitors by E12.5 (Guillemot and Joyner 1993; Lo et al. 1991; Sommer et al. 1996). The complete loss of *Ascl1* leads to perinatal death due to respiratory failure and feeding defects (Guillemot et al. 1993). Similarly, homozygous *Neurog2-/-* mutants mostly die within the first day of life, due to feeding defects; the few *Neurog2-/-* pups who can survive display severe growth retardation and die at postnatal stages (Fode et al. 1998). Heterozygotes for either *Ascl1-/+* or *Neurog2-/+* instead live and don't display obvious developmental defects (Fode et al. 1998; Guillemot et al. 1993).

The study of mutants for *Ascl1* and *Neurog2* revealed that they have a role in the specification of neurons along the dorsoventral axis of the telencephalon during cortical development (Fode et al. 2000). In fact, expression of *Neurog2* in neuronal progenitors is involved in cortical identity specification in the pallium, while expression of *Ascl1* in neuronal progenitors is involved in interneuronal specification in the subpallium (Casarosa et al. 1999; Fode et al. 2000) (Fig.1.2A). The maintenance of these two distinct domains is ensured by NEUROG2 expression, as demonstrated by the fact that *Neurog2* mutant embryos display ectopic expression of *Ascl1* in the dorsal telencephalon at E12.5-13.5 (Fode et al. 2000) and subsequent misexpression of a set of genes usually expressed in ASCL1-positive progenitors during the transition from proliferation to differentiation, namely *Dlx* genes (Fode et al. 2000; Porteus et al. 1994). Thus, NEUROG2 is restricting the expression of ASCL1 to the ventral telencephalon, but not vice versa, as highlighted by the fact that in *Ascl1* mutant embryos there is no ectopic expression of NEUROG2 (Fode et al. 2000). Similarly, *Neurog2* mutants show Wnt-mediated ectopic expression of ASCL1 in prethalamic progenitors at E12.5 but not at later stages (Bluske et al. 2012). Moreover, experiments in which the coding sequences of *Ascl1* and *Neurog2* were swapped in the mouse genome revealed that ASCL1 is an instructive developmental proneural factor (Parras et al. 2002). In fact, ectopic *Ascl1* expression in the ventral spinal cord is able to respecify the identity of a subset of spinal motor neurons, overriding the developmental instructive program (Parras et al. 2002). Conversely, misexpression of NEUROG2 during development does not change the fate of cells, but can

compensate for the loss of *Ascl1* in terms of neurogenesis (Parras et al. 2002). Interestingly, forced expression of *Neurog2* in the adult ventral subependymal zone (SEZ) re-specifies the identity of newborn neurons towards the glutamatergic lineage *in vivo* (Péron et al. 2017) but induces glutamatergic fate in neural stem cells of the adult ventral SEZ *in vitro* (Berninger et al. 2007).

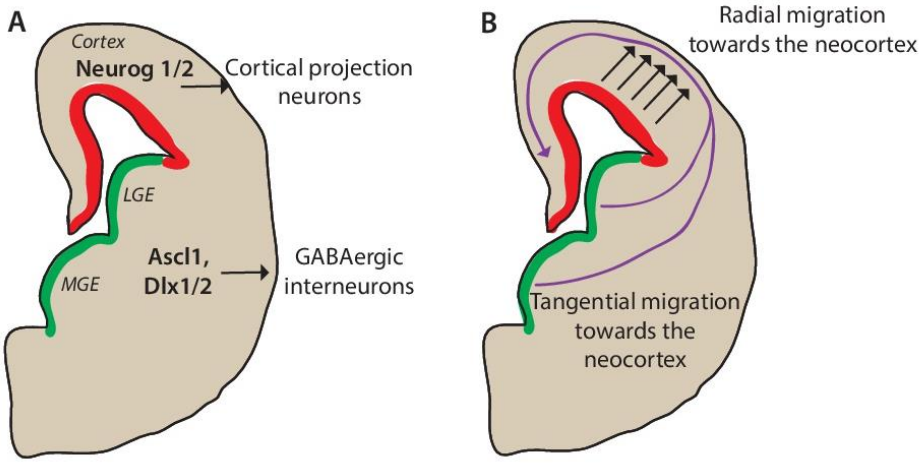

Fig.1.2 Developmental expression domain of NEUROG2 and ASCL1. A, During brain development, the proneural factors NEUROG1 and NEUROG2 are expressed in neural progenitors lining the ventricle (red), where they direct differentiation of cortical projection neurons. ASCL1 and its downstream targets DLX1/2 are expressed in progenitors lining the lateral ganglionic eminence (LGE) and medial ganglionic eminence (MGE) (green), directing differentiation of progenitors into GABAergic interneurons. B, Cortical neurons migrate from the VZ/SVZ to the cortex via radial migration, whereas interneurons generated in the ganglionic eminences reach the cortex via tangential migration.

Neurog2 is not the only Neurogenin expressed during cortical development and classified as proneural gene. *Neurog1* has in fact a similar pattern of expression and partial functional redundancy with *Neurog2* (Fode et al. 2000; Ma et al. 1999; Nieto et al. 2001). *Neurog1/2* contribute to the promotion of two different waves of neurogenesis during development (Dixit et al. 2014; Ma et al. 1999; Schuurmans et al. 2004). In the ventral pallium, until E12.5 *Neurog1/2* direct the formation of the early-born Cajal-Retzius neurons, which are generated before cortical glutamatergic neurons, and at later stages they both contribute to the specification of layer II/III neurons (Dixit et al. 2014). In the piriform cortex, Neurogenins exhibit different functions depending on the stage: *Neurog1* delays the genesis of deep-layer neurons at early stages (E12.5) while at later stages *Neurog2* specifies Cajal-Retius cells formation (Dixit et al. 2014), indicating that *Neurog1* can only induce cortical identity, while *Neurog2* can also specify Cajal-Retius neuronal fate (Dixit et al. 2014). In the neocortex instead, *Neurog1/2* are involved only in the first wave of neurogenesis, as until E14.5 they are both required to activate the specification of glutamatergic cortical early-born (deep-layer) neurons, while repressing the alternative GABAergic fate (Schuurmans et al. 2004). After this stage, in a second wave, upper-layer cortical neurons

are specified in a Neurogenin-independent manner, requiring instead *Pax6* and *Tlx* genes, also for the suppression of the GABAergic alternative fate (Schuurmans et al. 2004). The loss of *Neurog2* in mutant mice can be partially compensated by *Neurog1* (Fode et al. 2000; Ma et al. 1999). Neurogenins are also involved in the specification of neurons in the piriform cortex by inducing a dorsal phenotype; in fact, *Neurog1/Neurog2* double mutants show ventralisation of these cells and their subsequent death (Dixit et al. 2014). *Neurog2* also specifies the polarity of the leading process of pyramidal neurons at the initiation of radial migration (Fig.1.2B), as the mutation of a single amino acid on the protein leads to inhibition of radial migration and loss of unipolar morphology due to lack of phosphorylation and subsequent inability to bind NEUROG2's cofactors (Hand et al. 2005). This means that *Neurog2* is necessary for the specification of morphology of pyramidal neurons. NEUROG2 controls radial migration during corticogenesis through direct induction of the small GTP-binding protein RND2 (Heng et al. 2008). In the ventral midbrain, loss of *Neurog2* leads to a substantial loss of dopaminergic neurons which is due to the failure to differentiate into dopaminergic neurons of *Neurog2-/-* SOX2-expressing progenitors (Kele et al. 2004). Similarly, neural precursors of the epibranchial placodes in *Neurog2-/-* embryos fail to differentiate into cranial sensory neurons (Fode et al. 1998). *Neurog2* is also involved in specification of motor neurons (Lee et al. 2005; Ma et al. 2008). In fact, loss of phosphorylation of NEUROG2 leads to normal levels of neurogenesis but impaired motor neuron specification (Ma et al. 2008).

While Neurogenins are involved in the specification of glutamatergic neurons in the telencephalon, *Ascl1* is required for the specification and migration of GABAergic interneurons (Casarosa et al. 1999). ASCL1 directs in fact tangential migration of neuronal cells generated in the ventral telencephalon towards the neocortex (Fig.1.2B) through induction of *Ephb2* expression to define the migratory route (Liu et al. 2017). The guidance mechanism requires the presence of DLX2 for migration through the ventricular zone/subventricular zone, while ASCL1 is involved in the passage through the intermediate zone (Liu et al. 2017).

In addition to their role in neuronal specification, *Neurog2* and *Ascl1* play an important role in regulating neural progenitors' maintenance and differentiation. Interestingly, *Neurog2/Ascl1* double mutants show a disruption of the radial glial scaffold at the ventricle, accumulation of proliferating neural progenitors and a premature differentiation of progenitors into immature astrocytes during mid-to-late embryogenesis (Nieto et al. 2001). This indicates a role for both transcription factors in the lineage restriction of cortical progenitors, and their requirement to exit stemness and commit to a differentiated fate (Nieto et al. 2001). Moreover, it indicates that *Ascl1* and *Neurog2* are repressing the astroglial lineage (Nieto et al. 2001; Tomita et al. 2000). Double mutants also lose the expression of HES5, while single mutants don't, thus indicating a functional redundancy of ASCL1 and NEUROG2 in the activation of Notch signalling (Fode et al. 2000). The analysis of transcriptional targets of ASCL1 in

the developing ventral telencephalon shows that ASCL1 maintains the proliferative state of neural progenitors via activation of genes promoting cell cycle progression (Castro et al. 2011, 2006). ASCL1 binds both closed and open chromatin in proliferating neural progenitors. Binding to regions of closed chromatin is usually followed by increased chromatin accessibility, indicating that ASCL1 promotes the opening of genomic regions, and by transcriptional activation of ASCL1 target genes during cell differentiation (Raposo et al. 2015). One of *Ascl1* effectors, MYT1, promotes neuronal differentiation via direct binding on RBPJ-binding sites and repression of *Notch1* and several of its downstream targets (Vasconcelos et al. 2016). *Ascl1* has a role in regulating the proliferation and differentiation of neural progenitors also in the developing cortex (Garcez et al. 2015), where it is expressed at lower levels (Fode et al. 2000; Vasconcelos et al. 2016). In fact, in cortical progenitors of E14.5 embryos, ASCL1 activates its effector *CENPJ*, a centrosome associated protein regulating the plane of division of apical progenitors and the migration and morphology of neurons (Garcez et al. 2015). In the adult neurogenic niches, *Ascl1* is expressed in proliferating adult neural stem cells (aNSCs) and intermediate progenitors (Andersen et al. 2014; reviewed in Encinas and Fitzsimons 2017). The loss or reduction of *Ascl1* expression leads either to incapacity of adult neural stem cells to exit quiescence or to lower proliferation rates of active aNSCs, indicating a role of *Ascl1* in the promotion of the activation of aNSCs (Andersen et al. 2014). The exit from a quiescent state is mediated by ASCL1's transcriptional control of cell cycle-regulating genes (Andersen et al. 2014). Moreover, Ascl1 has a role in the specification of proliferating adult neural progenitors. In fact, overexpression of *Ascl1* respecifies subependymal zone-derived aNSCs expanded *in vitro* into GABAergic interneurons (Berninger et al. 2007).

Finally, *Ascl1* is also involved in the generation of oligodendrocyte progenitors (OPCs) in the murine ventricular zone (Nakatani et al. 2013; Parras et al. 2007; Parras et al. 2004). Here, a subset of PDGFRα-positive OPCs expresses ASCL1, which is necessary for the embryonic formation of an early population of OPCs between E11.5 and E13.5; the proneural factor cooperates with OLIG2 for the specification of oligodendrocytes at this stage (Parras et al. 2007). *Ascl1* has also an interesting role in postnatal stages, where it is expressed by progenitors of neuronal and oligodendroglial lineages and is necessary for the postnatal formation of OPCs derived from the subventricular zone (Nakatani et al. 2013; Parras et al. 2007). *Ascl1* mutants exhibited loss of neuronal precursors and OPCs at the subventricular zone and in the olfactory bulb at birth (Parras et al. 2004). Similarly, the deletion of *Ascl1* in OPCs of the embryonic and adult spinal cord results in decreased proliferation of these progenitors, while their differentiation potential remained unaltered, thus illustrating a role of this proneural factor in the regulation of the proliferative state of OPCs (Castro et al. 2011, 2006; Kelenis et al. 2018).

As for proneural genes in general, the regulation of *Ascl1* and *Neurog2* is exerted through similar pathways (reviewed in Bertrand et al. 2002, Dennis et al. 2018). For instance, in neural progenitors the BMP pathway transiently activates *Neurog2* at E14-15, thus regulating its transcripts' levels (Segklia et

al. 2012). Conversely, BMP-mediated activation of *Id1* leads to sequestering of the E protein E47, thus hampering E47 dimerization with ASCL1 and subsequently leading to degradation of ASCL1 (Viñals et al. 2004). This indicates a role of the balance of E proteins and Id proteins in the determination of the function and stability of ASCL1. Moreover, at low level of BMP induction in neural tube-derived neural stem cell (NSC) colonies *in vitro*, *Neurog2* and *Ascl1* promote sensory and autonomic neuronal fate, respectively (Lo et al. 2002). Another important regulator of proneural function is Notch signalling, through NOTCH-mediated lateral inhibition (reviewed in Bertrand et al. 2002). *Ascl1* is more sensitive than *Neurog2* to lateral inhibition, as demonstrated by the fact that, after treatment of NSCs colonies *in vitro* with a DELTA ligand, ASCL1-mediated neurogenesis is reduced more strikingly than the NEUROG2-mediated one (Lo et al. 2002). Interestingly, both proneural factors' expression levels oscillate every 2-3 hours in neural progenitors as an effect of lateral inhibition (reviewed in Guillemot and Hassan 2017; Imayoshi et al. 2013). Notably, the NOTCH-dependent mechanism acts on *Ascl1* gene expression generating an oscillatory pattern in which to high levels of ASCL1 correspond low levels of HES1 and OLIG2, and vice versa (Imayoshi et al. 2013). However, differentiating neurons display sustained expression of ASCL1, while differentiating astrocytes and oligodendrocytes have high (but not sustained) levels of HES1 and OLIG2, respectively (Imayoshi et al. 2013). Protein degradation is also involved in the regulation of proneural factors' activity. In fact, BMP-mediated induction of Id proteins and subsequent sequestering of E proteins leaves ASCL1 without a dimerization partner, thus leading to its proteasomal degradation (Viñals et al. 2004). Moreover, ASCL1 is degraded through the action of E3 ubiquitin ligase HUWE1, which adds ubiquitin moieties to the protein for its destabilisation and further proteasomal degradation (Gillotin et al. 2018; reviewed in Guillemot and Hassan 2017). Little is known about NEUROG2 destabilisation and degradation instead, besides that the presence of E proteins increases its stability (Hindley et al. 2012). Another mechanism of regulation of proneural factors is phosphorylation, as I will review in section 1.2.

1.2 Post-translational modifications of proneural transcription factors

1.2.1 Phosphorylation of proneural transcription factors

The importance of post-translational regulation of proneural transcription factors is gaining recognition, as several studies are demonstrating its role in modulating proneural activity and fate choice (reviewed in Dennis et al. 2018, Guillemot and Hassan 2017). Single-site or multi-site phosphorylation has in fact been shown to regulate and modulate a variety of aspects of the activity of bHLH factors (Hand et al. 2005; Hindley et al. 2012; Li et al. 2011; Li et al. 2012; Ma et al. 2008; Quan et al. 2016) (Fig.1.3).
The most prominently described proneural factor to be phosphorylated is NEUROG2. Hand and colleagues showed that Tyrosine 241 (Y241) is the acceptor site of a phosphoryl group. Phosphorylation

of this specific residue is necessary to induce radial migration of cortical neurons and to specify unipolar pyramidal morphology (Hand et al. 2005). Additional works on NEUROG2 demonstrated that it is target of phosphorylation by CDK2 and GSK3 (Ali et al. 2011; Hindley et al. 2012; Li et al. 2012). Two Serine residues, S231 and S234, located at the C-terminus of the protein, are phosphorylated by GSK3 to timely regulate NEUROG2 activity during cortical development and influence the choice of dimerization partner (Li et al. 2012; Ma et al. 2008). During early corticogenesis, *beta*-catenin negatively regulates *Gsk3*, thereby leading to homodimerization of NEUROG2 (Li et al. 2012). At later stages of corticogenesis, after E14.5, Wnt signalling is reduced thus no longer repressing *Gsk3* (Li et al. 2012). Subsequently, GSK3 directly phosphorylates NEUROG2, thus favouring heterodimerisation with E47 at the expense of more transcriptionally active interactions and consequently reducing its proneural activity (Li et al. 2012). The identification of nine Serine/Proline (SP) residues in *Xenopus* NEUROG2 (XNEUROG2) as targets of the cell cycle-dependent kinase CDK2, revealed that phosphorylation can also be involved in cell cycle coordination and cell differentiation (Ali et al. 2011). In fact, Ali and colleagues demonstrated that in presence of CyclinA/CDK2 XNEUROG2 is phosphorylated; this hampers its DNA binding activity thus maintaining the cells in a proliferative state. Conversely, a Serine/Alanine (SA) mutant which cannot be phosphorylated at CDK2-target sites (called phospho-deficient mutant) retains its neurogenic ability in a dosage-dependent manner (the higher the number of SP sites mutated, the higher the neurogenic potential) (Ali et al. 2011). Interestingly, not only this SA9 mutant (carrying mutation on all nine sites) is activating the downstream effector of *Neurog2, NeuroD1*, but it also seems to be less sensitive to lateral inhibition and to ubiquitination (Hindley et al. 2012), thus ensuring prolongation of the neurogenic effect. A similar mechanism has been described for another proneural factor of *Xenopus*, NeuroD4, which is phosphorylated at six SP and Threonine/Proline (TP) sites with a dosage-dependent effect (Hardwick and Philpott 2015). The phospho-deficient mutant showed increased neurogenic ability and control of lateral inhibition via upregulation of *Delta* ligand gene (Hardwick and Philpott 2015).

A more recent study, comprising *Drosophila* as well as mouse proneural factors, demonstrated the existence of one Serine or Threonine residue within the bHLH motif of different proneural proteins, the position of which is highly conserved, that is target of phosphorylation. Interestingly, the authors generated both phospho-deficient mutants (S>A or T>A) and phospho-mimetic mutants. In the latter, the substitution of the Serine or Threonine with an aspartic acid residue (D) mimics the constitutive presence of the large negatively charged phosphoryl group (Quan et al. 2016). This conserved residue acts as a binary switch for neurogenesis: phospho-deficient mutants have neurogenic capacity and bind the DNA; phospho-mimetic mutants behave as a strong loss of function allele for neurogenesis and cannot bind the DNA, probably due to the repulsion between the negative charges of DNA and aspartic acid (Quan et al. 2016).

Besides proneural factors, another bHLH factor has been described to be target of phosphorylation, namely OLIG2. When S147 is phosphorylated, OLIG2 forms homodimers and the fate of a group of neural stem cells in the spinal cord is directed toward motor neuron generation (Li et al. 2011). However, S>A mutation prevents motor neuron formation while promoting oligodendrocytes formation (Li et al. 2011). This switch between lineages is due to the choice of a different dimerization partner, as unphosphorylated OLIG2 prefers NEUROG2 or other bHLH proteins as cofactors (Li et al. 2011).

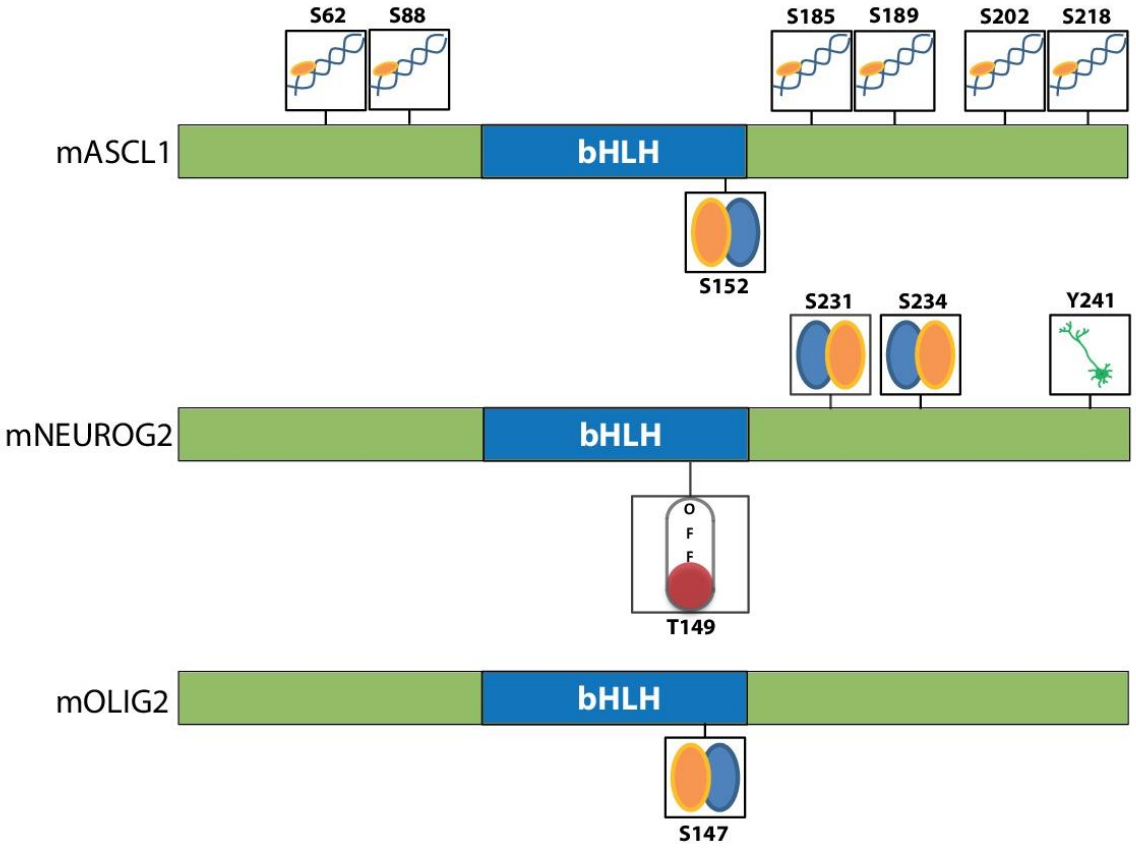

Fig.1.3 Phosphorylation of murine bHLH factors. Phosphorylation sites of murine bHLH transcription actors so far described lead to different consequences upon post-translational modification. Some change the DNA-binding affinity, like the six serine residues targeted on mouse ASCL1, while others change the choice of dimerization partner (e.g. S147 on mOLIG2). Phosphorylation of a tyrosine residue on mNEUROG2 is required for migration and maturation of cortical neurons, while T149, which is located within the bHLH of mNEUROG2, acts as an on-off switch of proneural activity by affecting the binding of the proneural factor to DNA. m=mouse.

1.2.2 Phosphorylation of ASCL1

Similarly to what described for NEUROG2 (Ali et al., 2011; Hand et al., 2005), ASCL1 contains six SP residues which are target of phosphorylation by CDK2 during *Xenopus* development (Ali et al. 2014; Wylie et al. 2015). The phosphorylation of these residues maintains progenitor cells in proliferative state and blocks neurogenesis (Ali et al., 2014; Wylie et al., 2015). Loss of phosphorylation via S>A mutation of these residues confers neurogenic activity both *in vivo* and *in vitro*, resistance to lateral inhibition and to CyclinA/CDK2-mediated cell cycle regulation; the effect seems to be dosage-dependent (Ali et al. 2014). Interestingly, in a neuroblastoma model in *Xenopus*, in which the wild type form of *Xenopus* ASCL1 is highly phosphorylated, cells fail differentiating into neurons but neurogenic differentiation is restored upon exogenous expression of the phospho-deficient mutant (Wylie et al. 2015).

Another important pathway regulating mouse ASCL1 proneural function is the RAS/ERK signalling pathway. The pathway is directly phosphorylating six SP residues in the mouse protein, thus activating the neurogenic and gliogenic differentiation programs while inhibiting cell proliferation (Li et al. 2014). The direct phosphorylation on the proneural factor has been demonstrated via serum starvation of cells *in vitro*, which by reducing RAS/ERK activity leads to reduced phosphorylation of ASCL1, and via exogenous expression of activated ERK *in vivo* during corticogenesis, which increased phosphorylation of ASCL1 (Li et al. 2014). A phospho-deficient mutant ASCL1 has increased neurogenic potential compared to the wild type protein (Li et al. 2014). Interestingly, the effect on ASCL1 is depending on the level of activity of RAS/ERK: when the pathway is activated, wild type ASCL1 activates the gliogenic differentiation pathway via transactivation of *Sox9* and the neurogenic pathway via transactivation of *Dlx1/2*, whereas in the presence of boosted activity of RAS GTPase the protein responds by increasing transactivation of *Sox9* (Li et al. 2014). The phospho-deficient is instead resistant to RAS/ERK activity, as its transactivation potential does not change when RAS is boosted (Li et al. 2014). Interestingly, the phospho-deficient mutant cannot transactivate *Dlx1/2* (Li et al. 2014), thus hinting at the necessity of intact SP sites to bind the promoter and at a different mechanism to promote its neurogenic potential. Thus, it seems that SA6 phosphorylation of ASCL1 *in vivo* is balancing the neurogenic and oligodendrogenic activity of ASCL1.

1.3 Direct reprogramming

1.3.1 Direct cell fate-conversion: an historical perspective

Differentiation was thought to be an irreversible process from which the cell would assume its final, unchangeable identity. Notably, developmental biologist Waddington theorised that the epigenetic landscape of the cell is like a series of valleys and hills, where the differentiated state corresponds to one of the valleys (reviewed in Ladewig et al. 2013; Waddington 1957). In order to go from one

differentiated state to the other, the cell would have to overcome various hurdles represented by the hills (reviewed in Amamoto and Arlotta 2014, Ladewig et al. 2013; Waddington 1957). In 1962 Gurdon demonstrated that nuclei from the blastula or from hatched tadpole gut cells of *Xenopus laevis* contained all the information necessary to generate one adult frog individual and the potential to do it (Gurdon 1962). This work on somatic cell nuclei transplantation was the first one to ever demonstrate that is was possible to revert the state of a differentiated cell, like that of tadpole gut cells, to a pluripotent state that can generate all tissues of the organism (reviewed in Amamoto and Arlotta 2014; Gurdon 1962). Another important milestone in the field of reprogramming was reached in 2006, when Takahashi and Yamanaka successfully identified four transcription factors, namely OCT4, SOX2, KLF4 and c-MYC, that were capable of reverting differentiated fibroblasts to a pluripotent state. This work, which led to the generation of human induced pluripotent stem cells (hiPSCs) (Takahashi and Yamanaka 2006), was the premise to many other studies on cell fate-switch.

Almost thirty years after Gurdon's reprogramming of tadpole gut cells into pluripotent stem cells, the first demonstration of direct conversion of one differentiated cell type into another has been published. MYOD was in fact identified as the first bHLH transcription factor able to induce direct lineage-reprogramming, converting cultured mouse embryonic fibroblasts into myocytes (Fig.1.4) (Tapscott et al. 1988). The first direct reprogramming of a non-neuronal cell type into neurons was achieved in 2002, when cortical postnatal astrocytes were converted into neurons via exogenous expression of *Pax6* (Heins et al. 2002) (Fig.1.4). The quest for understanding how to overcome the hurdles a cell faces to change its lineage (Waddington's hills), brought researchers to learn from developmental factors, as direct lineage-conversion partially recapitulates development (Camp et al. 2015; reviewed in Masserdotti et al. 2016). Thus, many transcription factors involved in the development of organs have to-date been used to force lineage-conversion of cells (reviewed in Amamoto and Arlotta 2014, Masserdotti et al. 2016). Besides heart and neuronal cells, researchers obtained also other cell types through direct cell fate-switch, such as astrocytes, OPCs, *beta*-cells in the pancreas (Caiazzo et al. 2015; reviewed in Heinrich et al. 2015; Yang et al. 2013; Yang et al. 2011).

The successful conversion of astrocytes into neurons (Heins et al. 2002) opened the lead to a vast area of research (reviewed in Amamoto and Arlotta 2014, Masserdotti et al. 2016). Soon, other murine or human cell types were converted in neuronal cells, like fibroblasts, hepatocytes and pericytes (reviewed in Amamoto and Arlotta 2014; Karow et al. 2012; Vierbuchen et al. 2010), and the first attempts to directly specify subtypes of induced neurons brought to the conversion of fibroblasts into dopaminergic neurons and motor neurons (Caiazzo et al. 2011; Son et al. 2011). Moreover, in 2015 for the first time some groups have identified cocktails of small molecules able to induce conversion of fibroblasts or astrocytes into neurons *in vitro* (Li et al. 2015; reviewed in Masserdotti et al. 2016; Zhang et al. 2015).

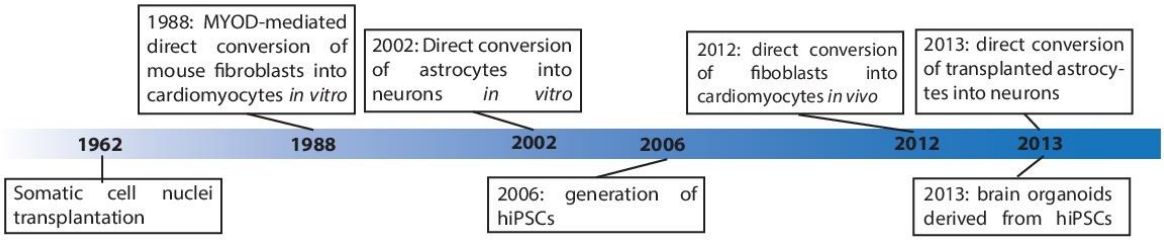

Fig.1.4 Timeline of major milestones in the field of cellular reprogramming.

Further advances came recently, with pioneering work on *in vivo* direct reprogramming (Heinrich et al. 2014; Niu et al. 2013; Qian et al. 2012; Torper et al. 2013). The first instance of such work was published in 2012, when murine cardiac fibroblasts were converted into cardiomyocytes via the exogenous expression of *Gata4*, *Tbx* and *Mef2c* (Qian et al. 2012). The *in vivo* conversion of non-neuronal cells into neurons was achieved for the first time one year later, when endogenous astrocytes or transplanted fibroblasts expressing exogenous transcription factors were converted into neurons in the mouse brain (Niu et al. 2013; Torper et al. 2013). Noteworthy, the availability of hiPSCs as a tool opened the way to conversion of hiPSCs into different cell types, including neurons, and to the generation of 3D-human brain organoids (reviewed in Amamoto and Arlotta 2014, Heinrich et al. 2015; Lancaster et al. 2013). The possibility to have a 3D structure recapitulating the developing human brain in a dish is giving access to a model that mimics a functional brain circuitry (Quadrato et al. 2017), thus allowing to screen for further factors instructing human brain development that could be employed for direct neuronal reprogramming (reviewed in Amamoto and Arlotta 2014, Heinrich et al. 2015).

1.3.2 Direct neuronal reprogramming: lessons from *in vitro* paradigms

The first instance of forced conversion of a cell type into neurons came in 2002, when Heins and colleagues directly reprogrammed cultured cortical astrocytes via exogenous expression of *Pax6*. Such neuronal induction seemed to be mediated by interactions with bHLH factors, as PAX6 reduced the expression of *Ascl1* and *Olig2* (Heins et al. 2002). More recently, it has been demonstrated that co-expression of *Ascl1* with *Dlx2* increases the reprogramming success from circa 30% to circa 90% of transduced cells converted into neurons (Heinrich et al. 2010). *Ascl1*- and *Neurog2*-induced neurons usually acquire identities matching to the specification role of these proneural factors during development (Heinrich et al. 2010; Karow et al. 2012, 2018). *Neurog2* induction yields in fact glutamatergic neurons (Heinrich et al. 2010), while *Ascl1* alone or in combination with *Dlx2* or *Sox2* induces formation of GABAergic interneurons from astroglia or pericytes (Heinrich et al. 2010; Karow et al. 2018, 2012), as indicated by marker expression and electrophysiological recordings. Nevertheless, recent work from Karow and colleagues showed with single cell RNA sequencing that in human

pericytes-to-neurons reprogramming cells can be converted into neurons of two different lineages (Karow et al. 2018), as I will discuss later.

Mouse embryonic fibroblasts induced by three factors together, namely *Ascl1*, *Brn2* and *Myt1l* (BAM), generate both glutamatergic and GABAergic neurons (Vierbuchen et al. 2010). The exogenous expression of *Ascl1* alone is sufficient to induce the cell fate-switch, but co-expression of *Ascl1* with *Brn2* and *Myt1l* greatly increases conversion efficiency (Vierbuchen et al. 2010). More recently, some of the mechanisms underpinning the BAM-mediated conversion were elucidated. In fibroblasts and neural progenitors, ASCL1 alone binds chromatin at genomic loci that are very similar to those it binds in the BAM combination (Wapinski et al. 2013). The direct binding of ASCL1 is possible thanks to a trivalent chromatin state present in fibroblasts; conversely, BRN2 is recruited by ASCL1 to bind ASCL1 target sites (Wapinski et al. 2013). Thus, ASCL1 has been described to be an "on-site pioneer" factor capable of binding chromatin immediately (Wapinski et al. 2013) and is able to initiate an early response through expression of neuronal genes (Treutlein et al. 2016). Within 12 hours from its binding to target sites, ASCL1 opens the chromatin, thus leading to the gain of accessibility of many neuronal-related genes (Wapinski et al. 2017). Eventually, also MYT1L has a role in the neuronal fate-switch. In fact, it represses fibroblast-identity programs and other somatic programs, such as a later-emerging competing myogenic program, in order to maintain neuronal identity of induced neurons (Mall et al. 2017; Treutlein et al. 2016). A similar repressive role has been described for the transcriptional repressor REST in the context of astrocyte-to-neuron conversion. The activation of the tamoxifen-dependent protein NEUROG2ERT2 after 6 days of culture fails to induce neuronal conversion, as compared to the activation of the protein after 2 days of culture (Masserdotti et al. 2015). This delayed activation results in lower binding of NEUROG2 to its target genomic loci, which is mediated by REST at early stages and by increased presence of the repressive marker H4K20me3 at later stages, thus hampering NEUROG2-mediated activation of transcription (Masserdotti et al. 2015).

These studies show that in fibroblasts and postnatal cortical astrocytes ASCL1 can activate the neuronal program to convert cells into neurons either alone or with other factors, in this case DLX2 or BRN2 and MYT1L (Heinrich et al. 2010; Vierbuchen et al. 2010). Nevertheless, the activity of ASCL1 appears to be context-dependent, as demonstrated also by the fact that alone it fails to convert human brain-derived pericytes into neurons (Karow et al. 2012). The fate-switch from the mesodermal cell type to neurons requires the co-expression of the transcription factor SOX2, which acts synergistically with ASCL1 to induce a neural stem cell-like gene expression program that eventually leads to conversion into neurons (Karow et al. 2018). This synergistic action allows the modulation of different signalling pathways that contribute to direct reprogramming and the maintenance of induced neurons. Interestingly, in this context the ASCL1/SOX2-mediated conversion leads to the formation of two distinct neuronal populations: the activation of a *Dlx*-driven program gives rise to GABAergic neurons, while the activation

of a *Neurog2*-driven program generates glutamatergic neurons (Karow et al. 2018), suggesting that the direct conversion happens through a bipotent-progenitor state. Such context-dependent behaviour might hold true also for other transcription factors involved in forced lineage-conversion.

Interestingly, also miRNAs have a role in direct cell fate-switch (Abernathy et al. 2017; Lee et al. 2018; Victor et al. 2014; Yoo et al. 2011). In fact, the expression of the neuronal-specific miR-9/9* and miR-124 in human fibroblasts leads to changes in DNA methylation, chromatin accessibility and transcriptome that eventually result in the opening of neuronal-subtype specific loci (Abernathy et al. 2017; Lee et al. 2018; Yoo et al. 2011). Interestingly, the two miRNAs don't need co-expression with neuronal-specification factors to induce the cell fate-switch, meaning that non-translated elements such as miRNAs or long non-coding RNAs might have a role in forced neuronal mediation and specification (Abernathy et al. 2017; Karow et al. 2018; reviewed in Masserdotti et al. 2016). Moreover, co-expression of miR-9/9* and miR-124 with lineage-specific transcription factors induces formation of striatal medium spiny neurons human fibroblasts *in vitro* (Victor et al. 2014), thus further hinting at a role for miRNAs in forced neurogenesis.

Another aspect of importance recently emerged for cell fate-switch is the metabolic state of cells. The forced conversion of fibroblasts or cortical astrocytes mediated by *Neurog2* or *Ascl1* seems in fact to activate a transcriptional program causing oxidative stress in the cells (Gascón et al. 2016). The action of reactive oxygen species thus generated leads to cell death and reduced reprogramming efficiency, which is consequent to the switch from a glycolytic metabolism to an oxidative phosphorylation-sustained metabolism (Gascón et al. 2016; Kim et al. 2018). However, the co-expression of the proneural factors with *Bcl2* or co-treatment with antioxidants helps the cells to overcome this metabolic hurdle by inhibiting a cell death program called ferroptosis, thus surviving and successfully converting into neurons (Gascón et al. 2016).

1.3.3 Direct neuronal reprogramming: lessons from *in vivo* paradigms

In vitro paradigms are useful to understand the mechanisms underpinning direct cell-lineage conversion, to screen for novel factors in the quest for the generation of specific neuronal subtypes and to investigate the functional properties and the integration of induced neurons after transplantation (reviewed in Heinrich et al. 2015; Torper et al. 2013; Yang et al. 2013). However, the necessity to find successful strategies to replace neuronal cells lost in the brain after traumatic or neurodegenerative stimuli, drove several groups to investigate the possibility of performing *in vivo* direct conversion of brain resident cells into neurons (reviewed in Amamoto and Arlotta 2014, Heinrich et al. 2015). One of the first studies to bridge *in vitro* direct reprogramming with *in vivo* paradigms, described transduction of fibroblasts or astrocytes with Cre-dependent lentiviral vectors expressing the BAM factors (*Brn2*, *Ascl1*, *Myt1l*). After injecting the viruses in the adult rodent striatum, they activated the transcription

factors and identified successful neuronal reprogramming of injected cells, specifically generating dopaminergic neurons (Torper et al. 2013). Following this report of the successful induction of direct neuronal cell-fate conversion of transplanted cells in the rodent brain, other studies described cell-fate conversion of non-neuronal brain resident cells into neurons (Heinrich et al. 2014; Liu et al. 2015; Niu et al. 2013, 2015; Su et al. 2014).

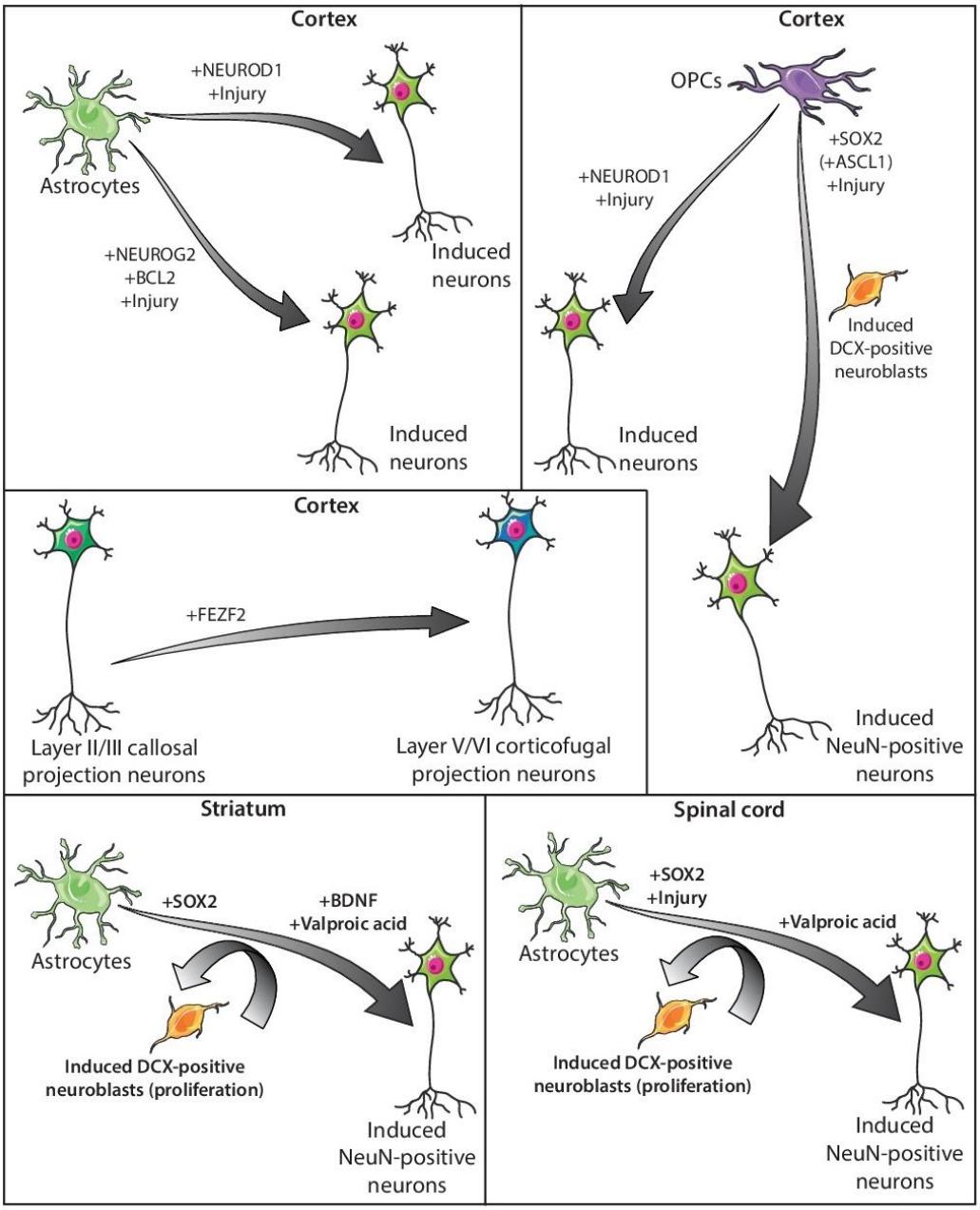

Fig.1.5 Main advances in the field of direct neuronal cell fate-switch mediated by transcription factors *in vivo*. Direct conversion of brain resident cells into neurons has been successfully achieved from different starting populations: astrocytes, OPCs and newly generated neurons in the cortex; astrocytes in striatum and spinal cord. In most cases it is required to induce a reactive state of glial cells, e.g. via stab wound injury. Direct conversion of astrocytes in striatum and spinal cord goes through the formation of neuroblasts, which proliferate in situ, and mature when induced with valproic acid or BDNF.

A proneural factor prominently used *in vitro* to convert postnatal cortical astrocytes into neurons, namely ASCL1, fails to reprogram endogenous adult reactive cortical glia *in vivo* (Heinrich et al. 2014). However, expression of *Ascl1* in reactive astrocytes of the dorsal midbrain induces neurons *in vitro* and *in vivo* (Liu et al. 2015). Moreover, by combining ASCL1 with the transcription factor SOX2 it is possible to convert transduced OPCs into doublecortin (DCX)-positive neuroblasts after stab wound injury (Fig.1.5) (Heinrich et al. 2014). Surprisingly, also *Sox2* alone induces the generation of DCX-positive neuroblasts; such induced cells progressively mature through time and by 21 days post injection some of them actually express the mature neuronal marker NeuN (Heinrich et al. 2014; reviewed in Heinrich et al. 2015). Moreover, *Sox2*-induced cells do not seem to be significantly different in terms of morphology and maturation than the *Ascl1/Sox2*-induced cells, thus indicating the forced neurogenic potential of this factor in the adult injured murine cortex (Heinrich et al. 2014; reviewed in Heinrich et al. 2015). Exogenous expression of *Sox2* can convert also adult striatal astrocytes into DCX-positive neuroblasts expressing ASCL1 protein (Niu et al. 2015, 2013). Noteworthy, conditional deletion of *Ascl1* hampers the formation of *Sox2*-induced neuroblasts, hinting at the requirement of the proneural factor for the switch to the neurogenic lineage (Niu et al. 2015). Such induced neuroblasts proliferate *in situ* and become postmitotic mature neurons, expressing NeuN, only after treatment with neurotrophic factors or valproic acid (Niu et al. 2015, 2013). The same group showed that SOX2 alone is able to force the fate-switch of astrocytes upon spinal cord injury both *in situ* and after transplantation (Su et al. 2014). Induced DCX-positive neuroblasts mature into GABAergic neurons only when treated with the deacetylase inhibitor valproic acid (Su et al. 2014), indicating that the epigenetic state of the cells is involved in the maturation of induced neurons (Niu et al. 2015; Su et al. 2014).

Some groups have successfully converted cortical glia into glutamatergic neurons *in vivo*, such as via the exogenous expression of *NeuroD1* in adult cortical astrocytes after stab wound injury or in a model of Alzheimer disease (Guo et al. 2014), and via the expression of the proneural factor *Neurog2* (Gascón et al. 2016) (Fig.1.5). Notably, *Neurog2* alone fails reprogramming reactive adult cortical glia (Gascón et al. 2016). However, when co-expressed with *Bcl2* or upon associated treatment with vitamin E to reduce oxidative stress in cells undergoing direct reprogramming, *Neurog2* successfully converts reactive adult cortical glia (Gascón et al. 2016).

Coming to the fine-tuning of cellular identity, the work of the group of Paola Arlotta identified FEZF2, a transcription factor that during development specifies subcortical projection neurons, as sufficient for the direct conversion of one neuronal cell type into another (Rouaux and Arlotta 2013, 2010). After *in utero* electroporation at E14.5, the exogenous expression of *Fezf2* converts progenitors fated to generate medium spiny neurons into corticofugal neurons (Rouaux and Arlotta 2010). Surprisingly, forced expression of *Fezf2* in callosal projection neurons from layers II/III during embryonic development or at early postnatal stages induces their conversion into corticofugal projection neurons

of layers V/VI (Rouaux and Arlotta 2013). Converted neurons changed their axonal projections, directing them to ipsilateral subcortical structures (Rouaux and Arlotta 2013). The fact that it is possible to convert one neuronal subtype into another one at early developmental stages, means that also postmitotic cells might have a plasticity-window for the specification of their neuronal subtype (Rouaux and Arlotta 2013).

The plasticity of the starting population is of great importance to achieve conversion into neurons. In fact, the vast majority of *in vivo* studies require a pre-existing injury to induce a reactive phenotype of glial cells present in the brain (reviewed in Heinrich et al. 2015) (Fig.1.5). Some paradigms activate glia through mechanical means, such as cortical stab wound injury or spinal cord hemisection (Gascón et al. 2016; Heinrich et al. 2014, 2015; Su et al. 2014), whereas others exploit pathological conditions that induce reactive astrogliosis, such as stroke models or neurodegeneration models (Guo et al. 2014; reviewed in Heinrich et al. 2015; Torper et al. 2013). The necessity of a reactive phenotype of cortical astrocytes in the brain is likely to depend on the fact that it coincides with the acquisition of neural stem cell-like properties (reviewed in Heinrich et al. 2015, Robel et al. 2011). Similarly, striatal astrocytes are able to spontaneously induce neurogenesis after stroke or in an Huntington's disease model through activation of a neurogenic program which induces proliferating DCX-positive neuroblasts (Magnusson et al. 2014; Nato et al. 2015). While most experimental paradigms require a pre-existing injury, some studies performed by expressing SOX2 in striatal glia did not require an injury to induce a reactive phenotype of the starting cell population (Niu et al. 2015, 2013).

1.4 Astrocytes

1.4.1 Origin and function of astrocytes

Astrocytes are glial cells that originate from the same developmental precursors of neurons, namely radial glia (RG). At perinatal stage, once radial glial cells (RGCs) have generated neurons and their role in the guidance of newly born neurons to their final position in the cortical plate is concluded, some RGCs undergo a series of transcriptional and morphological transformations to become astrocytes while others remain as neural stem cells in dedicated postnatal niches (Barry & McDermott 2005; Culican et al. 1990; Fuentealba et al. 2015; Furutachi et al. 2015; reviewed in Kriegstein & Alvarez-Buylla 2009). RGCs first lose the attachment to the ventricle, then migrate to the developing cortex via soma translocation (reviewed in Kriegstein and Alvarez-Buylla 2009). Here, newly generated astrocytes locally proliferate and divide symmetrically to generate more astrocytes until postnatal day 21 (P21) (Ge et al. 2013). Astroglial cells generated postnatally in the cortex will also mature and integrate into the network, coupling with neighbouring astrocytes and oligodendrocytes via formation of gap-junctions (Ge et al. 2013; reviewed in Nagy & Rash 2007). Interestingly, progenitors generate neurons and

astrocytes in a columnar way (Magavi et al. 2012). Each cortical column contains pyramidal neurons and protoplasmic astrocytes, the latter usually in clusters containing several astroglial cells (Magavi et al. 2012).

As mentioned in section 1.1.2, proneural factors regulate neurogenesis and inhibit gliogenesis during embryonic brain development (Nieto et al. 2001). Several mechanisms are involved in the inhibition of gliosis. The signalling pathway most prominently involved in promotion of astrogenesis is the JAK/STAT pathway; its inhibition by bHLH factors, especially NEUROG1, during neurogenesis leads to the repression of astrogenesis (He et al. 2005; reviewed in Kanski et al. 2014; Sun et al. 2001). The modulation of JAK/STAT pathway activity goes through the physical sequestering of the acetyl-transferase p300/CBP, which during neurogenesis binds NEUROG1, thus not being available for dimerization with STAT3 (reviewed in Kanski et al. 2014; Sun et al. 2001). However, given the presence of other proneural factors during development, such as NEUROG2 and ASCL1, known to inhibit astrogenesis (Nieto et al. 2001), it is possible that p300/CBP is sequestered by other bHLH proteins. Another pathway modulating proneural factors, namely RAS/ERK, has been described to regulate ASCL1 functions via direct phosphorylation. The RAS/ERK pathway becomes transiently upregulated during late neurogenesis, at E15.5; in conditions of high RAS/ERK activity, ASCL1 is phosphorylated and promotes activation of a gliogenic program, inducing *Sox9*-expressing glial precursors (Li et al. 2014).

One of the main changes permitting gliogenesis is the opening of chromatin at the promoter of the *Glial Fibrillary Acidic Protein* (*GFAP*) gene, expressing a protein involved in gliogenesis and widely used as an astroglial marker (Cheng et al. 2011; reviewed in Kanski et al. 2014, Sofroniew and Vinters 2010). Different factors contribute to a change in chromatin accessibility. To begin with, after the end of neurogenesis there is no more sequestering of p300/CBP from proneural factors, thus leading to dimerization of p300/CBP with STAT3 and to the activation of a gliogenic program (He et al. 2005; reviewed in Kanski et al. 2014). In addition to this, Notch signalling induces astrogenesis via its downstream target *NFIA* (reviewed in Kanski et al. 2014; Namihira et al. 2009), which contributes to demethylation of the *GFAP* promoter (Wilczynska et al. 2009). NFIA is also cooperating with SOX9 and ZBTB20 to regulate astrocytic specification via repression of the BRN2-mediated neurogenic program in neural progenitors (Nagao et al. 2016). It has recently been demonstrated that NFIA binds enhancer regions of their target genes that are primed, thereby switching them to an activated state (Tiwari et al. 2018). The increased accessibility of chromatin in these regions results in transcription of genes driving astrocyte differentiation (Tiwari et al. 2018).

After specification of progenitors into astrocytes, astrocytic fate-commitment is promoted by BMP signalling (Gross et al. 1996; reviewed in Kanski et al. 2014), which induces the transcriptional repressor REST (Gross et al. 1996; reviewed in Kanski et al. 2014; Kohyama et al. 2010). The repressor protein occupies the promoter of neuronal genes, thus suppressing neurogenesis (Kohyama et al. 2010;

reviewed in Kanski et al. 2014), similarly to what was found in late-stage cultures of postnatal cortical astrocytes (Masserdotti et al. 2015).

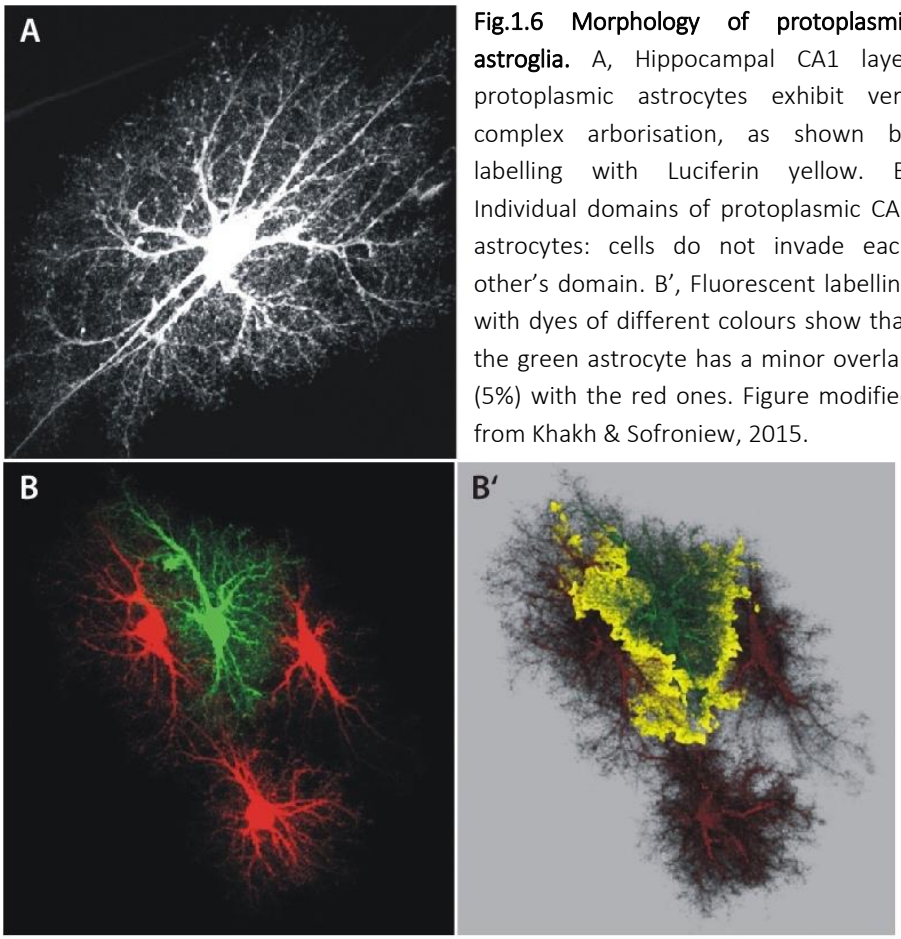

Fig.1.6 Morphology of protoplasmic astroglia. A, Hippocampal CA1 layer protoplasmic astrocytes exhibit very complex arborisation, as shown by labelling with Luciferin yellow. B, Individual domains of protoplasmic CA1 astrocytes: cells do not invade each other's domain. B', Fluorescent labelling with dyes of different colours show that the green astrocyte has a minor overlap (5%) with the red ones. Figure modified from Khakh & Sofroniew, 2015.

Astrocytes are organised in the cortex as individual domains in which one cell does not extensively overlap with the neighbouring astroglial cell but rather has only the most distal end-feet interdigitating with each other and forming gap junctions (Ge et al. 2013; reviewed in Sofroniew & Vinters 2010) (Fig.1.6B-B'). Cortical astrocytes contacts blood vessels and protoplasmic astrocytes envelope synapses, while fibrous astrocytes contact Ranvier nodes (Herrmann et al. 2008; reviewed in Sofroniew and Vinters 2010). Moreover, they exert many important functions, as reviewed by Sofroniew and colleagues (reviewed in Khakh and Sofroniew 2015, Sofroniew and Vinters 2010). Astrocytes express on their membrane sodium and potassium channels (Higashi et al. 2001; Pappalardo et al. 2015; Tong et al. 2014), have low membrane resistance and can have evoked inward currents, albeit not being able to propagate an action potential (Higashi et al. 2001; reviewed in Khakh and Sofroniew 2015, Sofroniew and Vinters 2010). They also show excitability due to increase of intracellular calcium concentration, either via release from internal storage or triggered by neurotransmitters (Cornell-Bell et al. 1989;

reviewed in Khakh and Sofroniew 2015, Sofroniew and Vinters 2010). This elevated calcium concentration in astrocytes can be propagated to neighbouring astroglial cells and elicit release of neurotransmitters, thus evoking receptor-mediated currents in neurons (Ma et al. 2016; Sofroniew & Vinters 2010). This last effect is linked to the role that astrocytes have in the maintenance of transmitter homeostasis: they indeed uptake neurotransmitters released by neurons, thus clearing the synaptic space, and convert them into neurotransmitter precursors which they will release back in the synaptic space, whereby neurotransmitter precursor molecules are recycled via conversion into active transmitters (Clements et al. 1992; Norenberg and Martinez-Hernandez 1979; Yu et al. 1983). Astroglia also contributes to the maintenance of homeostasis of ions, pH and fluids, to neurovascular coupling, to guidance of axonal migration and to the formation of functional synapses (Powell and Geller 1999; reviewed in Sofroniew and Vinters 2010). The homeostatic control of water can be exerted via Aquaporine 4 (AQP4), a water channel expressed on the astrocytic membrane and densely expressed at contact with blood vessels (Schummers et al. 2008; Sofroniew & Vinters 2010). Given the fact that cortical astrocytes make contacts with blood vessels and synapses, the homeostatic control of fluids contributes also to the regulation of blood flow depending on the synaptic activity, as demonstrated via two-photon calcium-imaging (Schummers et al. 2008; Sofroniew and Vinters 2010). The increase in astrocytic calcium concentration that follows neuronal activity induces vasodilation or vasoconstriction: to a modest increase corresponds dilation of arterioles, whereas to a larger increase corresponds vasoconstriction (Girouard et al. 2009; reviewed in Mishra 2017). In addition to these roles, the metabolic state of astrocytes is very important too (reviewed in Sofroniew and Vinters 2010). In fact, astroglial cells have a glycolytic metabolism (Zhang et al. 2014) and constitute the major storage of glycogen granules in the central nervous system, which they can use to support neuronal activity during high activity or hypoglycaemia (Cataldo and Broadwell 1986).

Astrocytes have also a role in pathological conditions, most notably through reactive astrogliosis and scar formation (reviewed in Dimou and Gotz 2014, Sofroniew and Vinters 2010, Sofroniew 2009). Upon invasive injury, such as a stab wound, ischemia, or inflammation, local astrocytes assume a “reactive” phenotype: they become hypertrophic and upregulate GFAP expression, proliferate and acquire neural stem cell-like properties (reviewed in Robel et al. 2011; Sirko et al. 2013; reviewed in Sofroniew and Vinters 2010, Sofroniew 2009). Moreover, they undergo a series of molecular changes mediated by different pathways, including JAK/STAT and Shh (Sirko et al. 2013; reviewed in Sofroniew 2009). In case of severe injury, reactive astrogliosis is accompanied by glial scar formation (Anderson et al. 2016; reviewed in Robel et al. 2011, Sofroniew 2009, Sofroniew and Vinters 2010). The scar is a dense and compact fibrotic tissue made of reactive scar-forming astrocytes derived from proliferation (Bardehle et al. 2013) (with overlapping domains and elongated morphology), fibrotic cells and inflammatory cells (reviewed in Sofroniew 2009; Wanner et al. 2013). The scar creates a barrier against inflammatory

agents and infectious agents, thereby protecting the healthy tissue. However, some consider the scar to have negative effects, via the formation of neurotoxic astrocytes induced by activated microglia, which inhibit axonal regeneration and induce death of neurons and oligodendrocytes (Liddelow et al. 2017; reviewed in Sofroniew 2009; Sofroniew and Vinters 2010). In opposition to these data, it has been recently demonstrated that ablation of scar-forming astrocytes from a spinal cord injury site hampers axonal regeneration, and that the cells present at the lesion site upregulate molecules supporting axonal growth (Anderson et al. 2016; reviewed in Sofroniew 2009, Sofroniew and Vinters 2010), thus pointing at the fact that the actual mechanisms triggered by cell types and molecules involved in a glial scar formation are not yet completely understood. Interestingly, in the spinal cord a sub-population of a non-glial cell type, namely pericytes, forms the core of the scar and gives rise to stromal cells (Goeritz et al. 2011). The progeny of stromal cells invades the damaged tissue and deposits extracellular matrix, thereby contributing to the formation of the scar (Goeritz et al. 2011).

1.4.2 Heterogeneity of astrocytes

Astrocytes are a very heterogeneous population in terms of morphology, functions and reaction to injury. Mouse astrocytes are morphologically characterized as protoplasmic (Fig.1.6) and fibrous, which are located in the grey matter or white matter, respectively (Hu et al. 2016; reviewed in Sofroniew & Vinters 2010). Some astrocytes, at the border of the scar-forming area during reactive astrogliosis, acquire an elongated morphology which differentiates them from the others (Wanner et al. 2013), while astroglial cells of the cerebellum and retina (Mueller glia, Bergmann glia, Velate astrocytes) have region-specific characteristics (Farmer et al. 2016; reviewed in Farmer & Murai 2017). Astrocytes make contacts with blood vessels; protoplasmic astrocytes make also contacts with synapses, while fibrous astrocytes contact Ranvier nodes, thus having different functions at the synapse and in myelination, respectively (Herrmann et al. 2008; reviewed in Sofroniew and Vinters 2010).

Protoplasmic astrocytes are known to have a big arborisation, with branches, branchlets and leaflets constituting 90-95% of their volume (Bushong et al. 2002; reviewed in Khakh and Sofroniew 2015) (Fig.1.6A). They are organised in individual non-overlapping domains, with only about 5% of their surface (the leaflets) overlapping with nearby astroglial cells (Bushong et al. 2002; reviewed in Khakh and Sofroniew 2015, Sofroniew and Vinters 2010) (Fig.1.6B-B'). Interestingly, cortical layering seems to be required for the emergence of heterogeneity among cortical astrocytes. Their morphological and molecular properties depend in fact on cortical layers, such that deep layer astrocytes expand tangentially (horizontal, in relation to the pial surface) whereas upper layer astrocytes expand radially (vertical, in relation to the pial surface) (Lanjakornsiripan et al. 2018). Moreover, layer II/III astrocytes occupy a bigger volume and cortical astroglia exhibits layer-specific morphology (Lanjakornsiripan et al.

2018). Cortical layering influences also the formation of the tripartite synapse, as layer II/III astrocytes appear to have a broader ensheathment of the synapse (Lanjakornsiripan et al. 2018).

In subcortical regions, astroglial cells behave differently depending on their location. Striatal astrocytes are in fact larger than hippocampal ones, and differ from the latter in terms of transcriptome, proteome, electrophysiological properties and proximity to the synapse (Chai et al. 2017). Moreover, Shh signalling displays differential effects on astrocytes of different brain areas (reviewed in Farmer & Murai 2017). For instance, neuronal induction of Shh signalling in hippocampal astrocytes translates into expression of the potassium channel Kir4.1 (Farmer et al. 2016), while in cerebellar Velate astrocytes (VA) it promotes a switch from expression of VA typical markers to markers of Bergmann glia (Farmer et al. 2016).

Astrocytes exhibit also diverse expression of markers used for their identification. GFAP is in fact expressed by some, but not all, astrocytes, by neural stem cells and by reactive astrocytes and is not detected in adult cortical astroglia (Levitt et al. 1981, 1983; reviewed in Kriegstein and Alvarez-Buylla 2009, Sofroniew and Vinters 2010). The channel Kir4.1 is highly expressed in astrocytes of hippocampus and cerebellum, but not in the rest of the brain (Poopalasundaram et al. 2000); the expression of the glutamate transporter GLAST is higher in the cerebellum than in the rest of the brain, whereas the expression of the glutamate transporter GLT-1 is higher in cortex, hippocampus and striatum (Lehre et al. 1995); connexins are heterogeneously expressed and *Connexin30* is expressed only in the grey matter, although with regional patterning (reviewed in Khakh & Sofroniew 2015; Nagy et al. 1999; reviewed in Nagy & Rash 2007).

There is also increasing evidence of the regionalisation of astrocytic function, as suggested by transcriptional and activity-dependent diversity. First of all, the heterogenous distribution of connexins' expression results in different density of gap junctions in different brain regions, which implies regional variations in the coupling of astrocytes (Houades et al. 2008). Astroglial cells can have also different responsiveness to Ca^{2+}-signalling, with different types of Ca^{2+}-signals observed (reviewed in Khakh and Sofroniew 2015). These signals can be spontaneous, mediated by neurons, arousal-evoked, specific to branches and branchlets or specific to the soma and large branches (Cornell-Bell et al. 1989; Ma et al. 2016; reviewed in Khakh and Sofroniew 2015; Sasaki et al. 2014). At a molecular level, it has been recently demonstrated that there is a gradient of transcribed proteins in astrocytes, from the cortex to the thalamus, indicating heterogenous molecular footprints (Morel et al. 2017). The different transcriptional profile seems to be linked to the different region-selective functions of cortical and subcortical areas (Morel et al. 2017).

Astrocytes are heterogeneous also in their response to injury. A fraction of the cells at the border with the injury site proliferates, possibly due to Shh-responsiveness, and generates the scar-forming astrocytes (Bardehle et al. 2013; Farmer et al. 2016; Sirko et al. 2013; Wanner et al. 2013). Two-photon

imaging experiments performed by Bardhele and colleagues in 2013 showed how astrocytes at the site of injury behave after traumatic brain injury. Surprisingly, cells involved in reactive astrogliosis at the site of injury do not migrate and only a small proportion of reactive astrocytes proliferates (14%), while the rest of the astroglial cells polarize or simply acquire a hypertrophic morphology (45% and 47%, respectively) (Bardehle et al. 2013). Cells that polarize and extend towards the injury site, polarize 3-5 days after injury and maintain the elongated processes for weeks. Interestingly, the majority of astrocytes that proliferate are juxtavascular, with their somata in contact with the glio-vascular basement membrane (Bardehle et al. 2013), which hints at the role of this sub-set of reactive astrocytes in limiting infiltration of other cells contributing to inflammation or fibrosis.

1.5 *PiggyBAC* transposons

1.5.1 *PiggyBAC* transposase: mechanism of action

Part of the work presented in this thesis is aimed at adapting a clonal labelling system based on *PiggyBAC*-mediated transposition of genetic elements to be used for direct conversion of astrocytes into neurons. The *piggyBAC* transposon is an autonomous DNA element capable of moving itself from one location of the genome to another thanks to the enzyme transposase. Originally isolated from the cabbage looper moth (*Trichoplusia ni*), we know today that it belongs to a superfamily of elements found in several non-insect species, including *Homo sapiens* (reviewed in Yusa 2014; Yusa et al. 2011). The *piggyBAC* transposon originally contains: the gene for the transposase, flanked by 5' and 3' terminal inverted repeats (TIR) to signal where the enzyme should bind; the tetranucleotide TTAA for specific insertion (Fraser et al. 1985; reviewed in Yusa 2014). The transposase contains a DDE/D domain, necessary to catalyse all steps of transposition: nicking, hairpin resolution and target joining (reviewed in Yusa 2014; Yuan and Wessler 2011). At first, the transposase nicks the 3' ends of the transposon at each strand, thus generating free 3'-OH ends. These free ends are then attached to the 5' end of the flanking TTAA tetranucleotide on the complementary strand, forming a hairpin. While the genome is being repaired at the nicked sites via joining of the TTAA free ends, the transposase resolves the hairpin by nicking it and leaving again free 3'OH ends. At the new target site, the TTAA sequences are nicked at their 5' end in each strand and the free 3'OH ends are joined via ligation of the 5' overhangs (Mitra et al. 2008; reviewed in Yusa 2014) (Fig.1.7). Given the formation of overhanging TTAA ends, the *piggyBAC* transposase does not require DNA replication and does not leave a footprint (reviewed in Yusa 2014; Yusa et al. 2011).

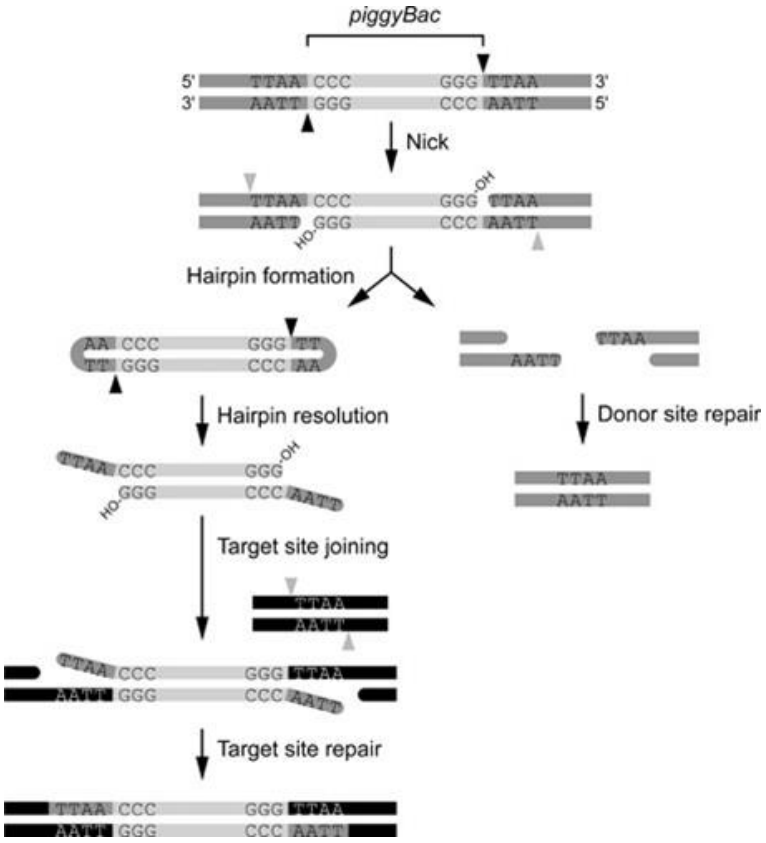

Fig.1.7 Transposition mechanism catalysed by the *PiggyBAC* transposase. The PiggyBAC transposase catalyses transposition via three different actions: nicking at the TTAA sites and formation of a hairpin containing the transposon, hairpin resolution, nicking of the target site for transposition and ends joining. Figure taken from Yusa, 2014.

1.5.2 *PiggyBAC* transposase: tool for mammalian expression systems

In order to use the *PiggyBAC* transposase as a genetic tool, different versions have been engineered. The most prominent changes to the system are the generation of a hyperactive *PiggyBAC* transposase containing seven aminoacidic mutations that highly increase its transposition efficiency, the separation of the system in two independent elements (the transposon and the transposase) and the generation of an inducible transposase (Cadiñanos and Bradley 2007; Yusa et al. 2011; reviewed in Yusa 2014). The separation of enzyme and mobile element allows the use of this tool for integration of genomic elements that are up to 10Kb long (Li et al. 2011). The hyperactive form of the transposase, called hyPBase, does not affect genomic integrity and introduces about 1% of point mutations due to integration in unspecific (non-TTAA) sites (Li et al. 2013; Yusa et al. 2011). Studies on mouse embryonic stem cells revealed that the hyPBase integrates the transposon preferentially at TA-rich and GC-rich regions, thus indicating a preference for coding regions. Moreover, integration happens predominantly in regions with open chromatin, with H3K4me3 enrichment, DNase I-hypersensitivity and Polymerase II

binding (Li et al. 2013). Interestingly, transposons prefer to be mobilised in chromosomal locations at less than 5Kb of distance, upstream or downstream, to coding genes and they favour loci with genes that are highly expressed (Li et al. 2013).

1.5.3 StarTrack clonal labelling system

In order to track cells *in vivo*, it is useful to have a combinatorial labelling system which tags cells with fluorescent proteins and allows to follow them and their progeny. Among the most famous tools used in the mouse central nervous system, is the Brainbow (Livet et al. 2007). This tool is multi fluorophore-based and it is possible to generate mouse lines stably expressing the Brainbow fluorophores under the control of cell type-specific promoters; moreover, the combinatorial expression of the fluorophores is Cre-dependent, thus allowing precise temporal induction of labelling (Livet et al. 2007). However, in order to achieve a resolution of combinatorial labelling that allows clonal analysis of treated cells, e.g. in gain/loss of function experiments, there would be no fluorescent channels left to identify them. In addition to this, the possible necessity to treat animals with tamoxifen for several days in order to activate a specific protein, would lead to Cre-dependent recombination of all Lox sites on the Brainbow constructs, thus reducing the possibilities of combinatorial labelling.

An *in vivo* clonal analysis system that circumvents these problems is the StarTrack clonal labelling system (García-Marqués and López-Mascaraque 2013). It was established for tracking of astroglia, thanks to the human GFAP promoter-driven expression of the fluorophores, and exploits *in utero* electroporation for the delivery of the plasmids. Thus, there are no transgenic mouse lines generated but rather a series of plasmids encoding for six fluorophores (Fig.1.8A) that can be injected in the lateral ventricle of embryos or pups as a mix (Figueres-Oñate et al. 2015; García-Marqués & López-Mascaraque 2013). The plasmids are randomly internalised by the progenitors lining the ventricle through electroporation (García-Marqués and López-Mascaraque 2013).

In order to stably integrate the genes to express in the genome of the host cell, the Startrack system exploits transposons. In fact, each gene is encoded by an operon containing also the promoter and a polyA sequence; such operon is part of the *PiggyBAC* transposon, as it is flanked by the 5' and 3' terminal repeats (TR) recognised by the *PiggyBAC* transposase (García-Marqués and López-Mascaraque 2013). Given the fact that transposition requires the catalytic activity of the enzyme, in the plasmid mixture there is also a plasmid encoding for the hyPBase (García-Marqués and López-Mascaraque 2013). Moreover, each fluorophore is present in two variants: one with cytoplasmic localisation and one with nuclear localisation, thanks to the fusion with the Histone 2B protein (García-Marqués and López-Mascaraque 2013). Thus, the resolution power of the combinatorial labelling is determined by the number of fluorophores (six), their subcellular localisation (cytoplasmic or nuclear) and the stochastic integration in the genome of ventricular progenitors of different copies of each transposon (Figueres-

Onãte et al. 2016). Due to genomic integration of the transposons, the progeny of targeted progenitors will express the same barcode, namely the same combination of fluorophores of the cell of origin. This allows lineage tracking and clonal analysis of electroporated cells by colour-barcoding and spatial location (García-Marqués & López-Mascaraque 2013; Garcia-Marques et al. 2014).

Analysis of adult brains electroporated at E14 with the StarTrack system revealed for instance that astroglial progenitors are specialised to generate a very heterogeneous population (García-Marqués and López-Mascaraque 2013). Protoplasmic (grey matter) and fibrous (white matter) astrocytes were never clonally related, while cortical astrocytes exhibited different morphological characteristics. Cortical clones contained up to 50 cells and were bigger than callosal clones. Moreover, they were usually organised in columnar domains that associated to a single blood vessel. Pial clones were instead either made of protoplasmic astrocytes or of fibroblast-like astrocytes and expressed GFAP protein (García-Marqués and López-Mascaraque 2013). Similarly, the StarTrack system allowed the clonal study of OPCs, to reveal that the size of clones increases with life and clones grow up to hundreds of cells originating from pallial progenitors (Garcia-Marques et al. 2014).

A more recent version of this tool, the ubiquitous StarTrack, allows tracking of cells from every lineage thanks to the human ubiquitin promoter (Figueres-Onãte et al. 2016) (Fig.1.8D). The generation of this method highlighted a caveat of the technique: since transposons are randomly transposed in the genome by the transposase, some of them are not integrated and remain as episoms in the cell (Figueres-Onãte et al. 2016; Figueres-Oñate et al. 2015). Episoms can be diluted or lost during cell proliferation, thus leading to a different amount of gene copies per each fluorophore in the cells of the same clone. This translates into an interference with clonal analysis of glial cells, which proliferate after electroporation, but not of neurons, which are postmitotic (Figueres-Oñate et al. 2015). In order to circumvent this, the ubiquitous StarTrack has been engineered in order to insert LoxP sites at strategic locations: one LoxP site is upstream of the gene (inside the transposon) and one LoxP site is downstream of the 3'TR (outside of the transposon) (Fig.1.8C). Cre-dependent recombination allows excision and loss of the genes that are present as episoms, but not of the genes stably integrated in the host genome (Figueres-Oñate et al. 2015). The ubiquitous StarTrack thus requires to include in the plasmid mixture also a plasmid encoding for a tamoxifen-dependent Cre recombinase (Figueres-Onãte et al. 2016).

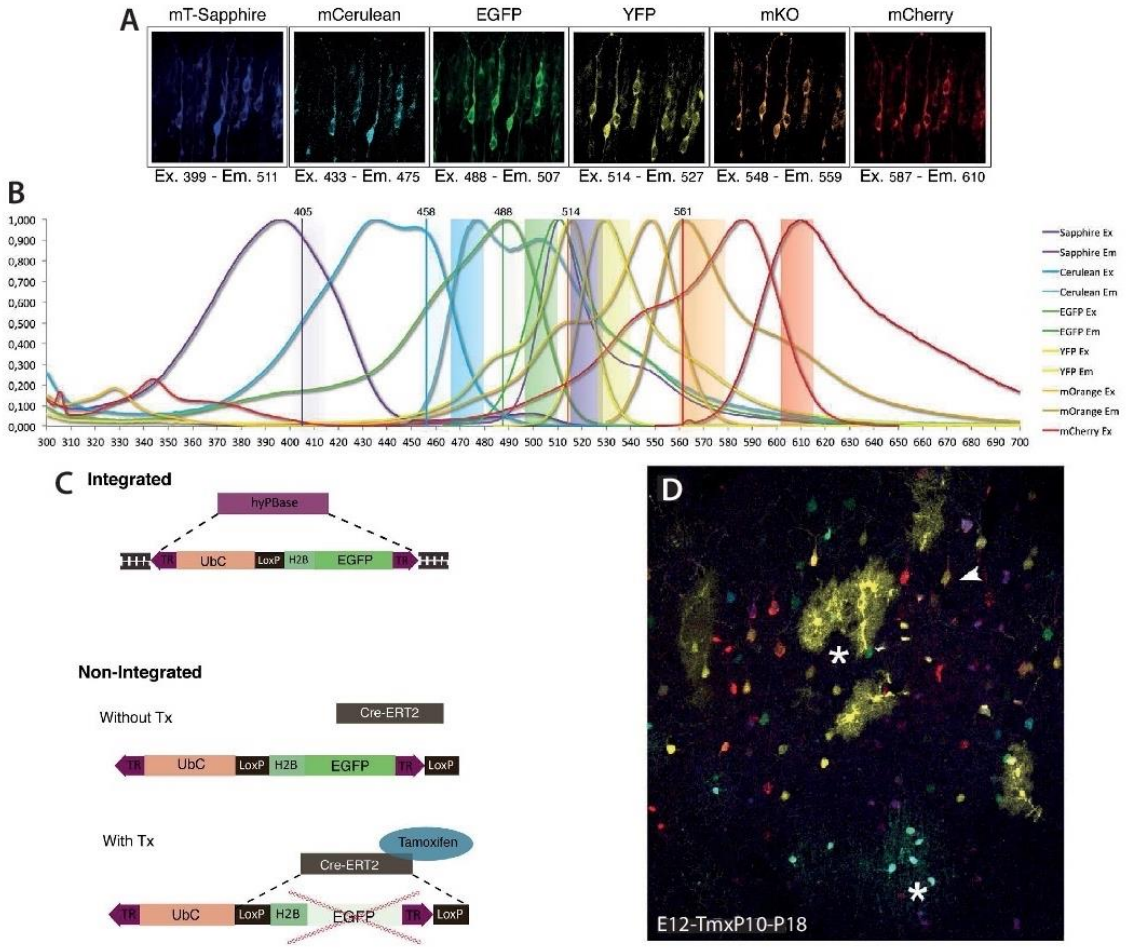

Fig.1.8 StarTrack clonal labelling system. A, The six fluorophores used by the StarTrack system, with their excitation and emission wavelengths. B, Spectral separation of the StarTrack fluorescent proteins. C, Overview of the location of the LoxP sites in plasmids of the ubiquitous StarTrack system that either integrated or not in the genome of the cell. Episomal copies that do not integrate are sensitive to Cre-dependent recombination, which excides the fluorophore. D, Illustration of the result of an electroporation performed at E12 with the ubiquitous StarTrack. Cre-mediated recombination was induced at P10 via one single intraperitoneal injection of tamoxifen and the clonal analysis was performed at P18. Astrocytes (asterisks) and neurons (arrowhead) can be distinguished by their characteristic morphology. Figure modified from Figueres-Onate et al., 2016.

As mentioned above, there are six fluorophores in the StarTrack clonal labelling system: mTSapphire, mCerulean, eGFP, eYFP, mKO, mCherry. The fluorescent proteins can be detected at a confocal microscope using acquisition settings that don't overlap between each other (Figueres-Oñãte et al. 2016) (Fig.1.8B). Even though the probability of integrating each transposon should be the same, the percentage of detection of the six fluorophores in labelled cells is different, with eGFP, mTSaphhire and mCherry being the most frequently expressed ones. Conversely, eYFP and mKO are not frequently expressed (Figueres-Oñãte et al. 2016). Thus, the StarTrack is a tool suitable for clonal analysis of cells in gain/loss of function experiments *in vivo*, or for other paradigms in which it is required to follow the progeny of specific cells.

1.6 Aim of the study

Proneural transcription factors-mediated direct conversion of cortical glia into neurons *in vivo* has so far been achieved via modulation of different aspects, such as the choice of transcription factors (Heinrich et al. 2015) or the induction a reactive glial phenotype, either through stab wound injury or disease models (reviewed in Heinrich et al. 2015, Robel et al. 2011). Taking advantage of a model in which glial cells proliferate in the absence of injury (Ge et al. 2013) and can be converted into neurons using retrovirus-mediated forced expression of neurogenic transcription factors (unpublished data), namely the early postnatal mouse brain, we aimed in this study at deciphering the influence of specific biological aspects on the reprogramming outcome. Understanding the mechanisms underpinning forced cell fate-switch will help improving the efficiency of this approach for generating new neurons for brain repair.

The first aspect investigated was phosphorylation of ASCL1, a proneural factor which successfully converts cortical astrocytes into GABAergic interneurons when exogenously expressed alone *in vitro* (Berninger et al. 2007; Heinrich et al. 2011). Phosphorylation of ASCL1 on six serine/proline (SP) residues modulates its neurogenic ability both during development *in vivo* and in the context of direct conversion of human fibroblasts into neurons *in vitro* (Ali et al. 2014; Li et al. 2014). Thus, I studied whether the phosphorylation state of ASCL1 influences its ability to induce cortical glia-to-neuron conversion in the uninjured brain of postnatal mice. In order to do this, I first subcloned the coding sequences of: the wild type *Ascl1* gene; a phospho-deficient *Ascl1* mutant carrying S>A mutations at the six SP residues above mentioned; a phospho-mimetic *Ascl1* mutant carrying S>D mutations at the six SP residues into a Moloney-Murine Leukaemia Virus (MoMLV) retroviral backbone. The three forms of ASCL1 with different phosphorylation states are collectively called pASCL1. The cell populations transduced by MoMLV retroviruses in the postnatal murine cortex correspond to astroglia and oligodendroglia (Fig.2.4), thus allowing the exogenous expression of transgenes in cortical glia. After injecting retroviruses encoding for *pAscl1* in the postnatal cortex, I performed immunohistochemistry at 12 days post injection to assess the fate of transduced cells and determine the impact of the three different phosphorylation states on the reprogramming outcome:

- Wild type ASCL1 alone has been shown to induce astrocyte-to-neuron conversion *in vitro* and to instruct developmental neurogenesis *in vivo* (Ali et al. 2014; Li et al. 2014). Thus, I expected to observe neuronal induction upon its exogenous expression (Fig.1.9, left).
- ASCL1SA6, the phospho-deficient mutant, increases the efficiency of forced neurogenesis *in vitro* and developmental neurogenesis *in vivo* (Ali et al. 2014; Li et al. 2014). Thus, I expected to observe increased neuronal induction upon its exogenous expression (Fig.1.9, middle).
- ASCL1SD6, the phospho-mimetic mutant, mimics constitutive phosphorylation of the protein. It has been shown that high levels of RAS/ERK signalling pathway activation, which directly

phosphorylates the six SP residues of ASCL1 during mouse cortical development, lead to increased transactivation of *Sox9*, expressed by glial progenitors (Li et al. 2014). Thus, I expected to observe increased gliogenesis upon its exogenous expression (Fig.1.9, right).

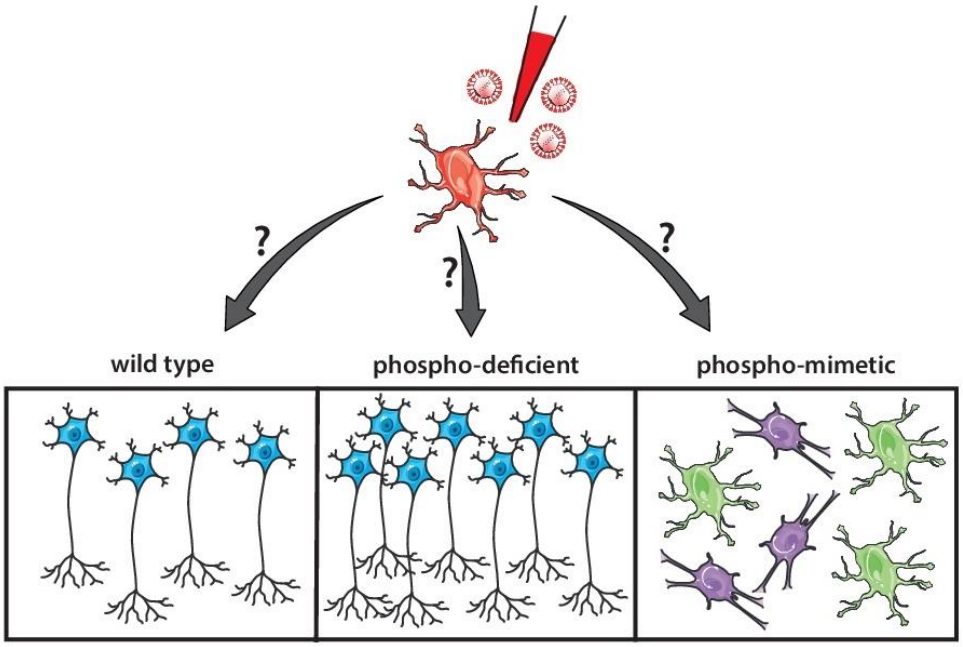

Fig.1.9 Graphical abstract of the experimental hypothesis for section 2.1 By means of retroviral transduction, the *pAscl1* genes have been exogenously expressed in cortical glia. To determine the fate of transduced cells, immunohistochemical analyses have been performed. More specifically, given prior knowledge on the effect of ASCL1 phosphorylation *in vivo* during *Xenopus* and mouse neural development, it was hypothesised that the wild type protein would induce neurogenesis (left side), while the phospho-deficient protein would induce increased neurogenesis (middle). Conversely, the working hypothesis for the function of the phospho-mimetic mutant in glia-to-neuron conversion was that it would induce a non-neuronal, i.e. glial fate (right side).

Knowing whether the phosphorylation of ASCL1 modulates the neurogenic ability during *in vivo* cell fate-switch can help improving forced conversion efficiency.

Besides investigating the role of post-translational modifications, I adapted a tool used for *in vivo* clonal labelling, called StarTrack, to be used for conversion of postnatal cortical astrocytes into neurons. The StarTrack system allows clonal labelling of cells via *in utero* electroporation of plasmids encoding for different fluorophores. These plasmids encode the transgenes within transposons of the *PiggyBAC* transposase which, after injection in the lateral ventricle and electroporation, get randomly internalised in neural progenitors and randomly integrated by a hyperactive form of the *PiggyBAC* transposase (called hyPBase) in the genome of the host cell. This randomised integration of the fluorophores results in the acquisition of a specific colour-barcode of the cells (García-Marqués & López-Mascaraque 2013; García-Marqués et al. 2014). The StarTrack system offers the advantage of exploiting different

promoters for the expression of the transgenes, thus allowing tracking of cells from different lineages (Figueres-Oñate et al. 2016; García-Marqués & López-Mascaraque 2013; García-Marqués et al. 2014). By electroporating a plasmid mix containing plasmids encoding for the proneural factors *Neurog2* and *Ascl1* and plasmids encoding for the fluorophores in E14 embryos, it is possible to combine forced conversion of astrocytes into neurons in the postnatal uninjured cortex with clonal analysis of induced neurons (Fig.2.18). The investigation of the clonal origin of induced neurons will allow to study the starting cell population and to determine whether the heterogeneity of astroglia influences the outcome of forced neurogenesis. This knowledge will help determining why different subpopulations of astroglia expressing the transcription factors fail or succeed to reprogram into neurons and, consequently, to improve strategies to force cortical astroglia to change lineage *in vivo*.

2 Results

2.1 Influence of phosphorylation on ASCL1-mediated direct glia-to-neuron conversion

2.1.1 *In vitro* conversion of postnatal cortical astrocytes into neurons by exogenous expression of differentially phosphorylated forms of ASCL1

The use of Moloney Murine Leukaemia Virus (MoMLV)-based retroviral vectors to exogenously express proneural transcription factors is an established tool for direct conversion of cortical glia into neurons (Heinrich et al. 2010; Heinrich et al. 2011). Thus, in order to assess the influence of the phosphorylation state of ASCL1 on its ability to force fate-switch of cortical glia, I cloned retroviral constructs for exogenous expression of three forms of mouse *Ascl1* encoding for proteins with different phosphorylation states (all together: pASCL1). The ASCL1 protein contains in fact six Serine/Proline (SP) sites that are phosphorylated by kinases of the RAS/ERK signalling pathway (Li et al. 2014). In the wild type form (Ascl1 wt), the SP residues are not mutated and therefore possible phosphorylation targets. In the phospho-deficient mutant (Ascl1SA6), a S>A mutation is present at all six sites, thus hindering the attachment of a phosphoryl group. Conversely, in the phospho-mimetic mutant (Ascl1SD6), there is a S>D mutation that mimics constitutive phosphorylation due to the presence of a negative charge (Fig.2.1 and Fig. 4.1).

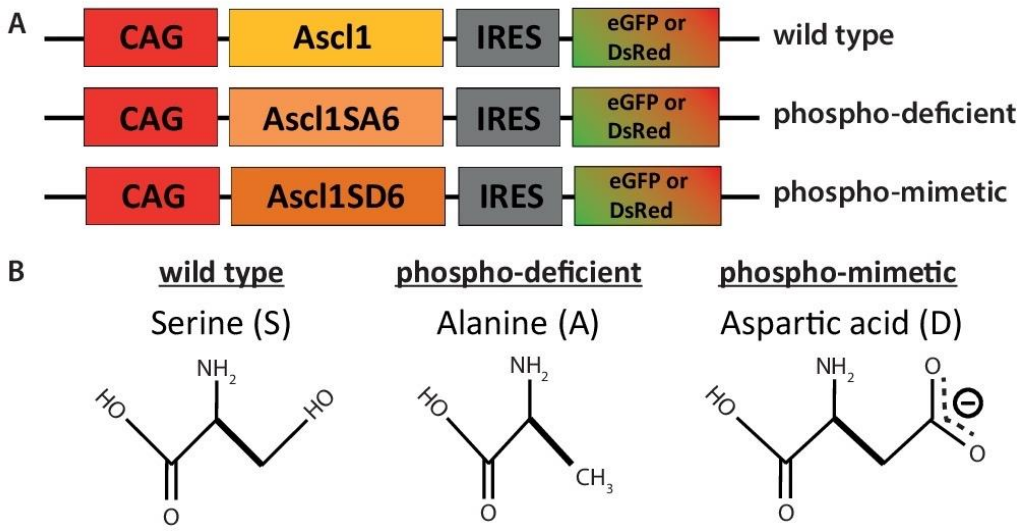

Fig.2.1 Retroviral vectors for the exogenous expression of *pAscl1*. A, Schematic of the retroviral constructs cloned for mammalian expression of the *pAscl1* genes. B, Structure of the amino acids present at the phosphorylation sites in the wild type and phospho-mutant constructs.

After cloning the constructs for the production of retroviruses, I assessed their ability to force cell fate-switch of astrocytes *in vitro* in a preliminary study via lipofection. Thus, I transfected postnatal day 5-7 (P5-7) cortical astrocytes 24 hours (24h) after seeding the cells on PDL-coated coverslips, as previously described (Heinrich et al. 2011). One day after transfection, the medium was gradually switched to a differentiation medium without serum, to support induced neurons (Fig.2.2A). I analysed the astrocyte-to-neuron conversion rate one week after transfection, namely at 8 days *in vitro* (div), via immunostaining for the immature neuronal marker doublecortin (DCX) (Fig.2.2B-B''). Surprisingly, the analyses revealed that all three phosphorylation states of ASCL1 are capable of converting astrocytes into DCX-positive immature neurons (Ascl1 wt 57.3±9.9%; Ascl1SA6 79.3±8.9%; Ascl1SD6 36.8±10.4%). However, the phospho-mimetic construct exhibited a significantly lower direct conversion efficiency compared to the phospho-deficient one (Fig.2.2C).

These experiments show that the three *pAscl1* constructs can all convert astrocytes into neurons *in vitro*. However, transfection has higher variability and lower efficiency than retroviral transduction. Thus, retroviral particles for the expression of all three exogenous genes were produced with the aim of further studying *pAscl1*-mediated direct neuronal reprogramming. I therefore transduced postnatal cortical astrocytes and analysed the expression of the pan-neuronal marker beta III-tubulin (bIIItub) at 7div (Fig.2.3B-B'''). As a control I used a virus expressing only a fluorescent reporter (pCAG-IRES-eGFP). Given the ability of MoMLV-based retroviruses to transduce only cells that are proliferating, due to the requirement of the breakdown of the nuclear envelope to access the nucleus (Roe et al. 1993), astrocytes were maintained in culture with mitotic factors inducing gliogenesis, namely EGF and FGF-2 until 24h post transduction, when the medium was completely switched to medium for the support of induced neurons (Fig.2.3A). As expected, no induction of neurons was observed in cells transduced with the control retrovirus (Fig.2.3B). Consistently with previously published results (Berninger et al. 2007; Heinrich et al. 2010), the wild type form of *Ascl1* converted astrocytes into neurons. In addition to this, both phospho-mutants successfully induced neuronal fate-switch of astrocytes (Fig.2.3C) and the phospho-deficient mutant had the highest conversion efficiency (Ctrl 0.1±0.1%; Ascl1 wt 27.3±3.8%; Ascl1SA6 51.1±7.0%; Ascl1SD6 37.2±3.6%).

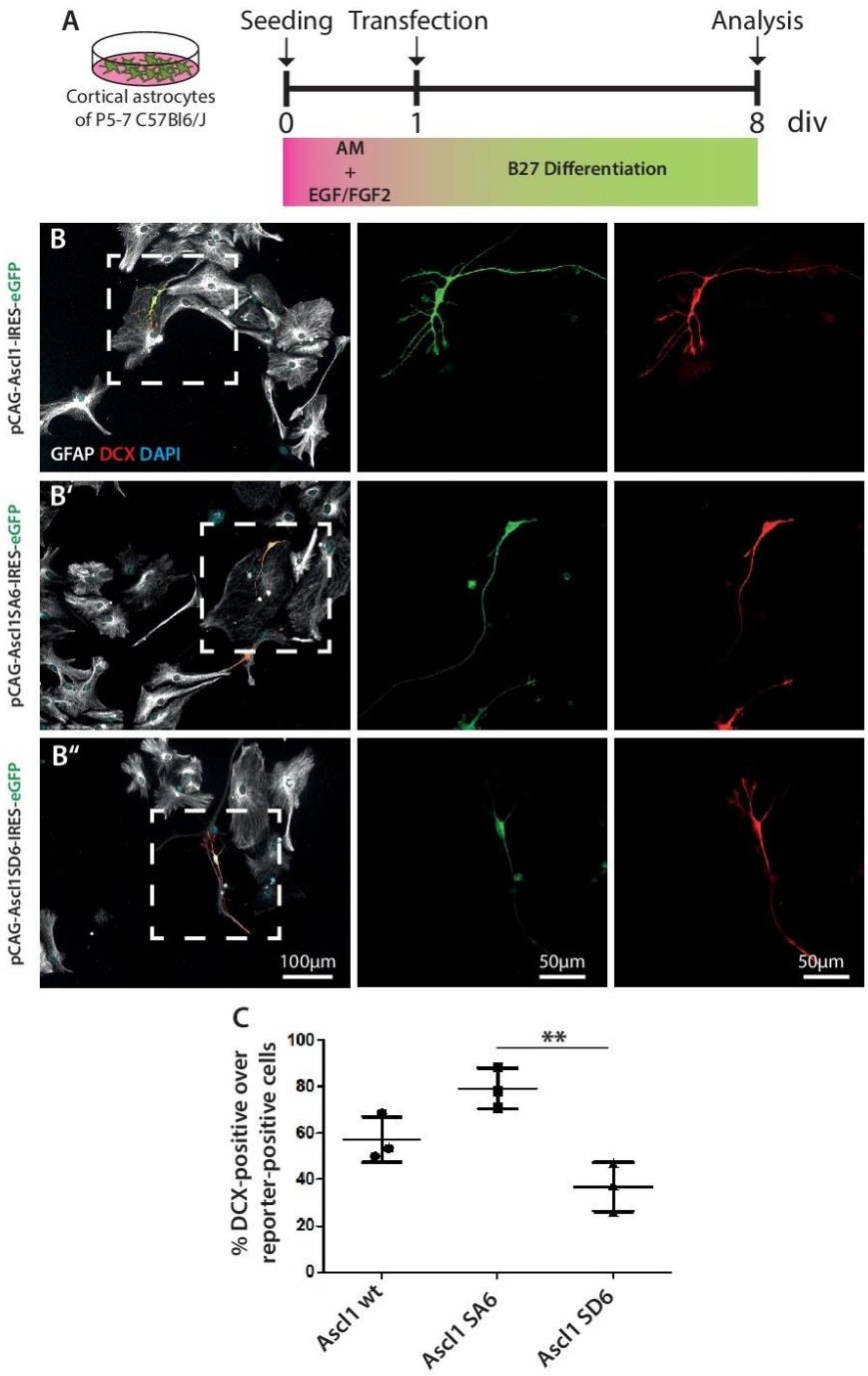

Fig.2.2 Exogenous expression of *pAscl1* converts astrocytes into neurons *in vitro*. A, Experimental design. Cells were cultured in a medium supporting astroglial proliferation until the day of transfection. Subsequently, it was gradually switched to a medium for the support of induced neurons. B-B'', Microscopy pictures illustrating cells transfected with *pAscl1* (green) expressing the immature neuronal marker DCX (red). Cultured cortical astrocytes express GFAP (white). C, Percentage of DCX-positive cells among transfected cells at 8div. p=0.005 (One-Way ANOVA for all quantifications of section 2.1); n=3. Means±SD. For numbers of cells quantified and all p-values see Appendix III and IV. AM=Astromedium.

In summary, my results show that, independently on its phosphorylation state, ASCL1 can convert astrocytes into neurons *in vitro*. Nonetheless, they also hint at a role of phosphorylation in modulating neurogenesis, as revealed by the higher conversion rate achieved by the phospho-deficient mutant.

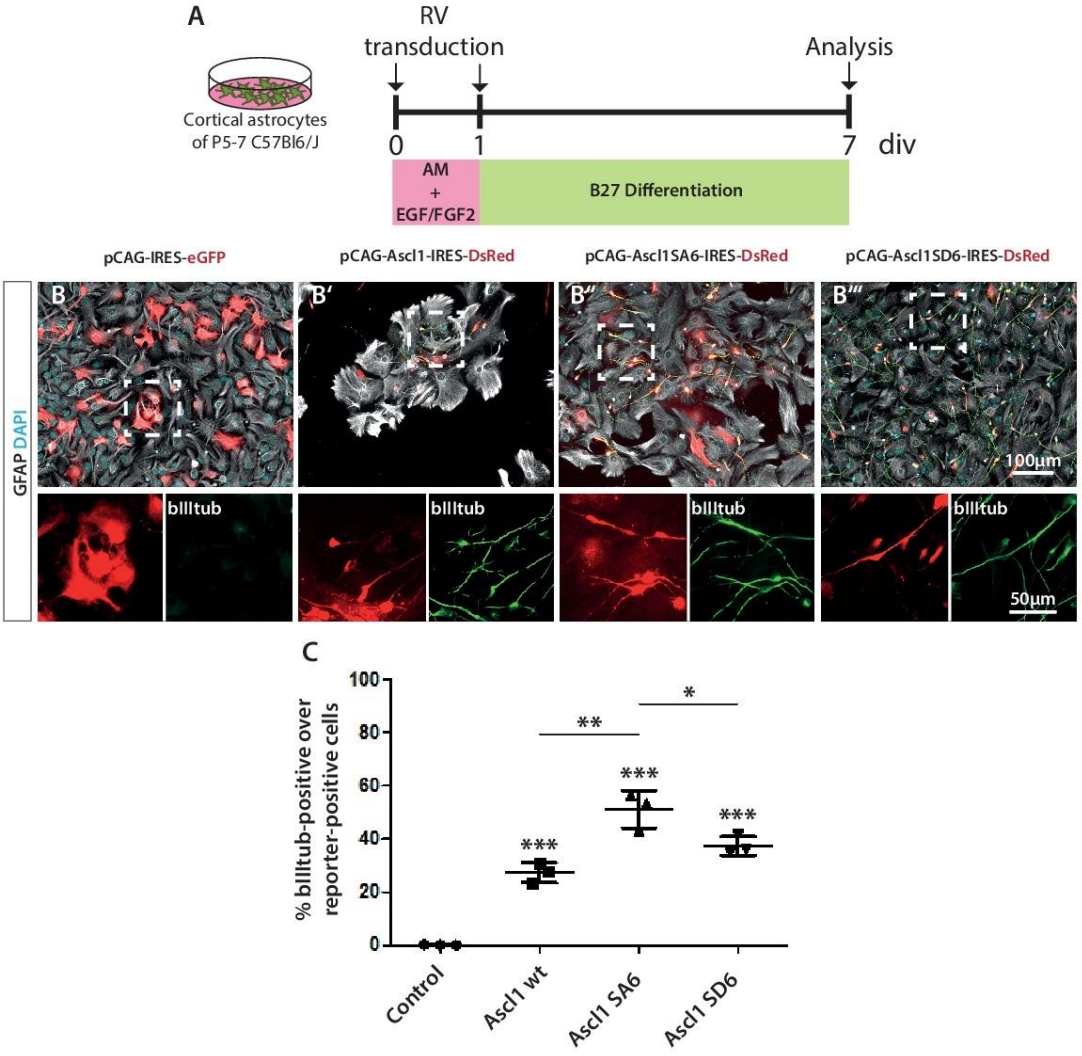

Fig.2.3 Retroviral expression of *pAscl1* converts astrocytes into neurons *in vitro*. A, Experimental design. B-B''', Microscopy illustrations of cultures of postnatal cortical astrocytes (GFAP, white). Transduced cells (red) were converted into beta III-tubulin (green) positive neurons upon exogenous expression of pASCL1. C, Percentage of converted neurons at 7div. $p<0.001$; n=3. Means±SD. For numbers of cells quantified and all p-values see Appendix III and IV. AM=Astromedium. RV=Retrovirus.

2.1.2 *In vivo* direct reprogramming of postnatal cortical glia: identification of cell populations transduced by the retroviruses and validation of pASCL1 expression

In order to investigate whether the phosphorylation state of ASCL1 has a role in forced neurogenesis *in vivo*, the postnatal murine cerebral cortex was transduced with the three retroviruses validated during *in vitro* experiments. Injections were performed in P5 mice, when neurogenesis is over but gliogenesis is occurring and astrocytes are locally proliferating (reviewed in Miller & Gauthier 2007; Ge et al. 2013). This means that glial cells at P5 are susceptible to transduction by retroviruses.

It has been proposed that a viral injection itself can be considered as an injury leading to astrogliosis in the adult mouse cortex (Guo et al. 2014). In order to determine whether the retroviral injection performed on P5 mice induced a reactive phenotype of cortical glia, I analysed cells transduced with a control retrovirus encoding for the fluorophore DsRed (pCAG-IRES-DsRed) (Fig.2.5A-A'). I performed immunohistochemistry for GFAP and SOX10 at 3 days post-injection (dpi). Cells transduced with the pCAG-IRES-DsRed retrovirus do not exhibit hyperregulation of GFAP expression and hypertrophy at 3dpi as compared to the contralateral, non-injected, hemisphere (Fig.2.4), thus excluding reactive astrogliosis.

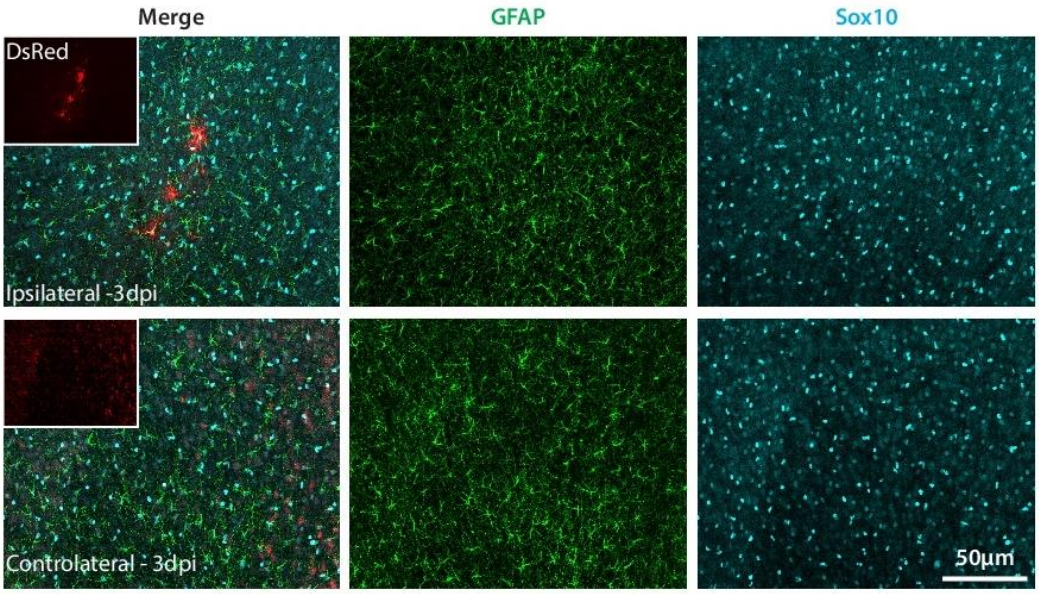

Fig.2.4 No signs of hypertrophy of GFAP-positive cells and reactive gliosis in the injected cortex at 3dpi. Immunohistochemistry analysis of cortices 3 days after transduction with the control retrovirus pCAG-IRES-DsRed illustrate that there are no evident signs of reactive gliosis ongoing in the injected area. GFAP-positive astrocytes in the injected (ipsilateral) cortex are not hypertrophic and do not show signs of reactive astrogliosis, as compared to the non-injected (contralateral) cortex. Immunohistochemistry for SOX10, does not illustrate an increase in OPCs in the ipsilateral cortex, as compared to the contralateral one.

Subsequently, to determine the identity of cortical cells transduced by the MoMLV-derived retroviruses in vivo, I first performed immunohistochemistry for glial and neuronal markers on cells transduced with the control retrovirus at 3dpi and then analysed their expression (Fig.2.5B-B'', C-C''). A large number of reporter-positive cells were found throughout the cortex, as expected (Fig.2.5A'). The vast majority of them were GFAP-positive astrocytes and SOX10-positive cells of the oligodendroglial lineage (62.8±8.1% and 32.2±6.1%, respectively) (Fig.2.5B-B'', D). A limited fraction of cells were Iba1-positive microglial cells (1.0±0.9%) and, importantly, no DCX-positive neurons were detected (Fig.2.5C-C'', D).

To test the ability of *pAscl1* to convert cortical glia into neurons in vivo, *pAscl1*-encoding retroviruses were injected together with a control retrovirus at P5 and the cell fate-switch success was analysed at 12dpi. I first determined whether cells transduced with *pAscl1*-encoding retroviruses were indeed exogenously expressing the proneural factor *in vivo*. To do this, I performed immunohistochemistry with a monoclonal antibody against ASCL1 (Fig.2.6A). ASCL1 was successfully detected in cells transduced with *pAscl1* (Fig.2.6D'-D'''). Conversely, cells transduced with the control virus did not express it (Fig.2.6D).

In conclusion, I confirmed that retroviruses can very efficiently and specifically target glial cells, predominantly astrocytes, and that the retroviral vectors encoding for *pAscl1* were successfully inducing expression of exogenous ASCL1 in the cells.

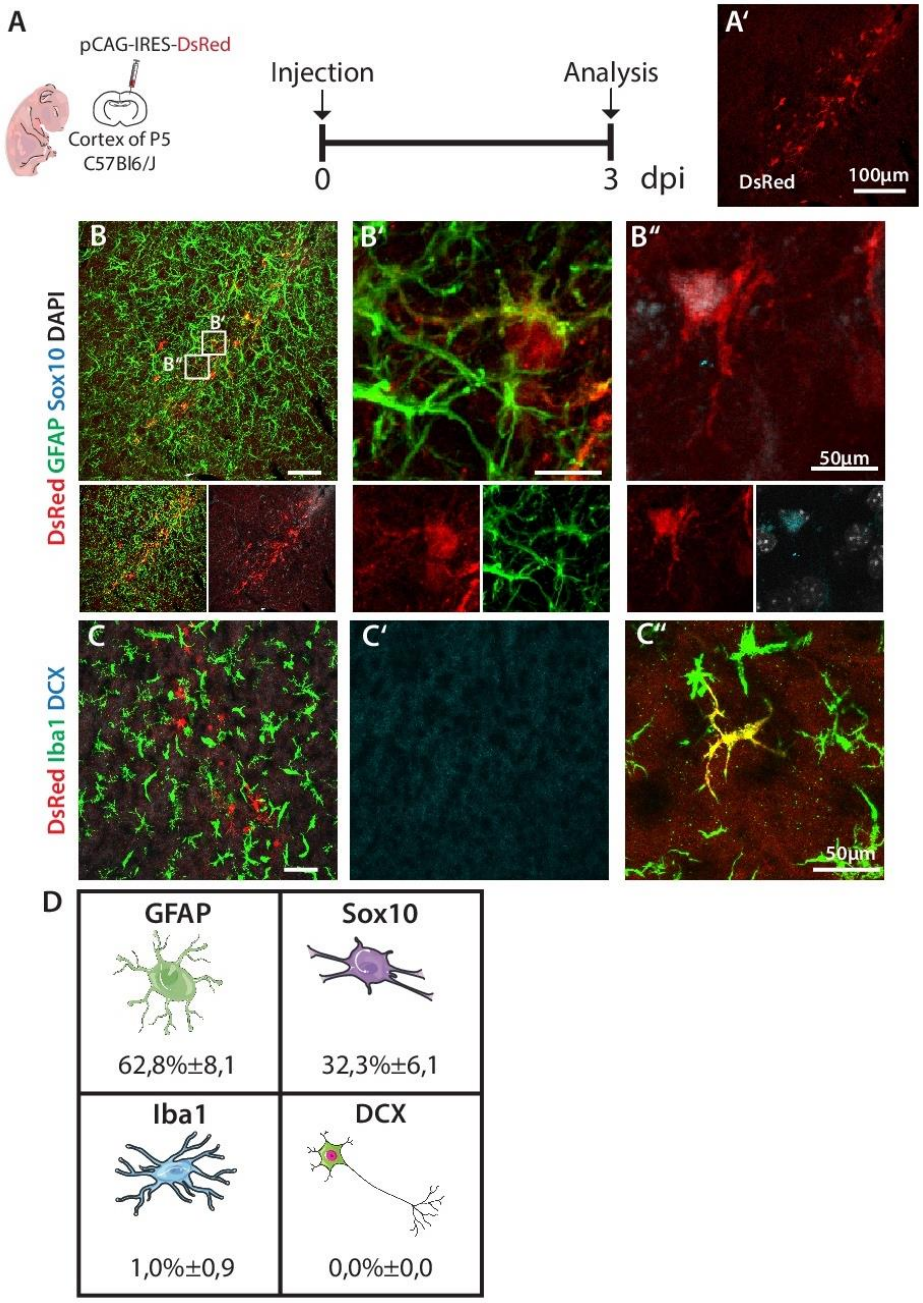

Fig.2.5 Analyses at 3dpi in the postnatal mouse cortex reveal that glial cells are specifically targeted by a control retrovirus. A, Experimental scheme. A' Transduced cells detected in the cortex. B-B''', Confocal microscopy pictures showing that GFAP-positive astrocytes (green) and SOX10-positive oligodendroglial cells (cyan) are targeted by the pCAG-IRES-DsRed retrovirus at 3dpi. C-C''', DCX-positive neuronal cells (cyan) were never detected. Very rare Iba1-positive microglial cells (green) were found. D, Percentage of cells among transduced cells targeted by the retroviral vectors. n=3. Means±SD. For numbers of cells quantified see Appendix III.

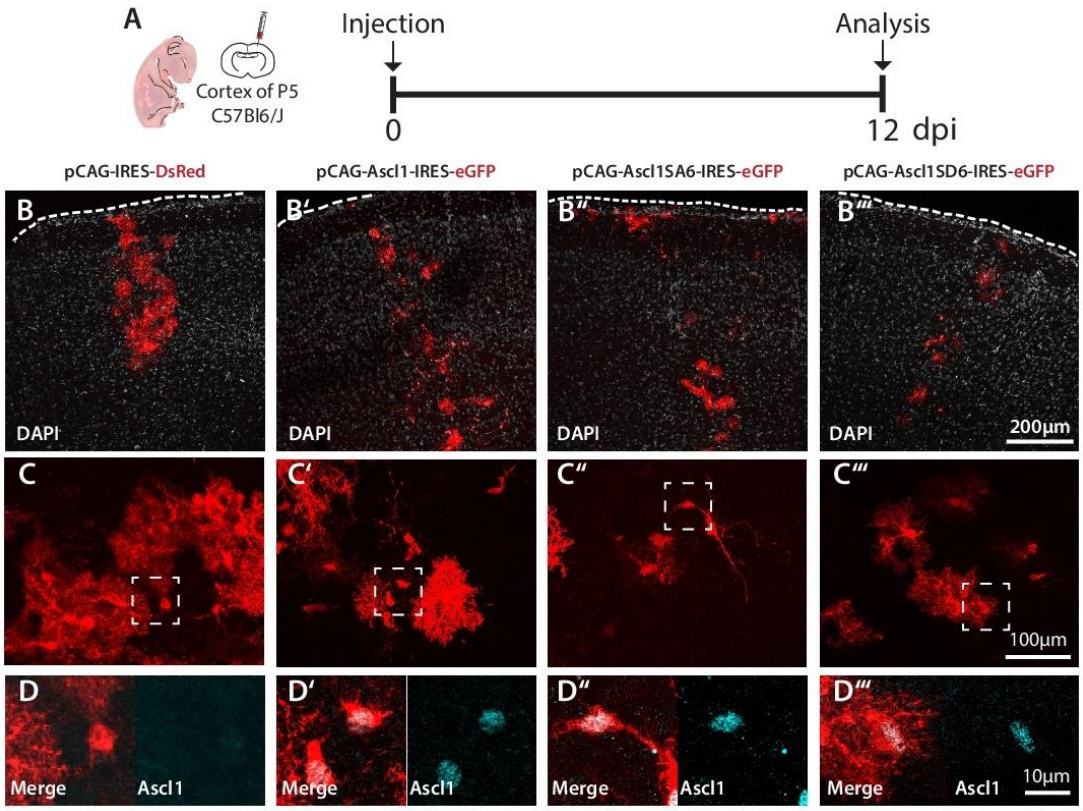

Fig.2.6 Exogenous expression of *pAscl1* in transduced cells at 12dpi. A, Experimental scheme. B-B''', Confocal microscopy pictures depicting the injection site in the cortex at 12dpi for the control retrovirus (B) and the *pAscl1*-encoding retroviruses (B'-B'''). C-C''', High magnification of transduced cells (red) showing their glial morphology. D-D''', Magnifications of cells transduced with *pAscl1* in C'-C''' revealing they express exogenous ASCL1. Conversely, ASCL1 expression was not detected in control conditions.

2.1.3 *In vivo* direct reprogramming of postnatal cortical glia: effect of different phosphorylation states of ASCL1

To investigate whether pASCL1 proteins (namely Ascl1 wt, Ascl1SA6 and Ascl1SD6) have an influence on forced neuronal fate-switch of glial cells *in vivo*, I analysed the fate of transduced cells 12 days after injection of *pAscl1*-encoding retroviruses (Fig.2.6A) via immunohistochemistry for the immature neuronal marker DCX (Fig.2.7). While no emergence of DCX-positive induced neurons was detected in control conditions, I found sporadic DCX-positive cells after exogenous expression of *pAscl1* (Ctrl 0.0±0.0%; Ascl1 wt 4.9±1.6%; Ascl1SA6 6.8±0.1%; Ascl1SD6 4.0±0.2%) (Fig.2.7C). In any case, although significantly different to control and higher with the phospho-deficient mutant than with the phospho-mimetic one, the direct conversion efficiency was very low as compared to the *in vitro* results (Fig.2.3C and 2.7C). Moreover, the level of DCX expression was low and the morphology of most of the DCX-positive cells was not convincingly resembling immature neurons (Fig.2.7D).

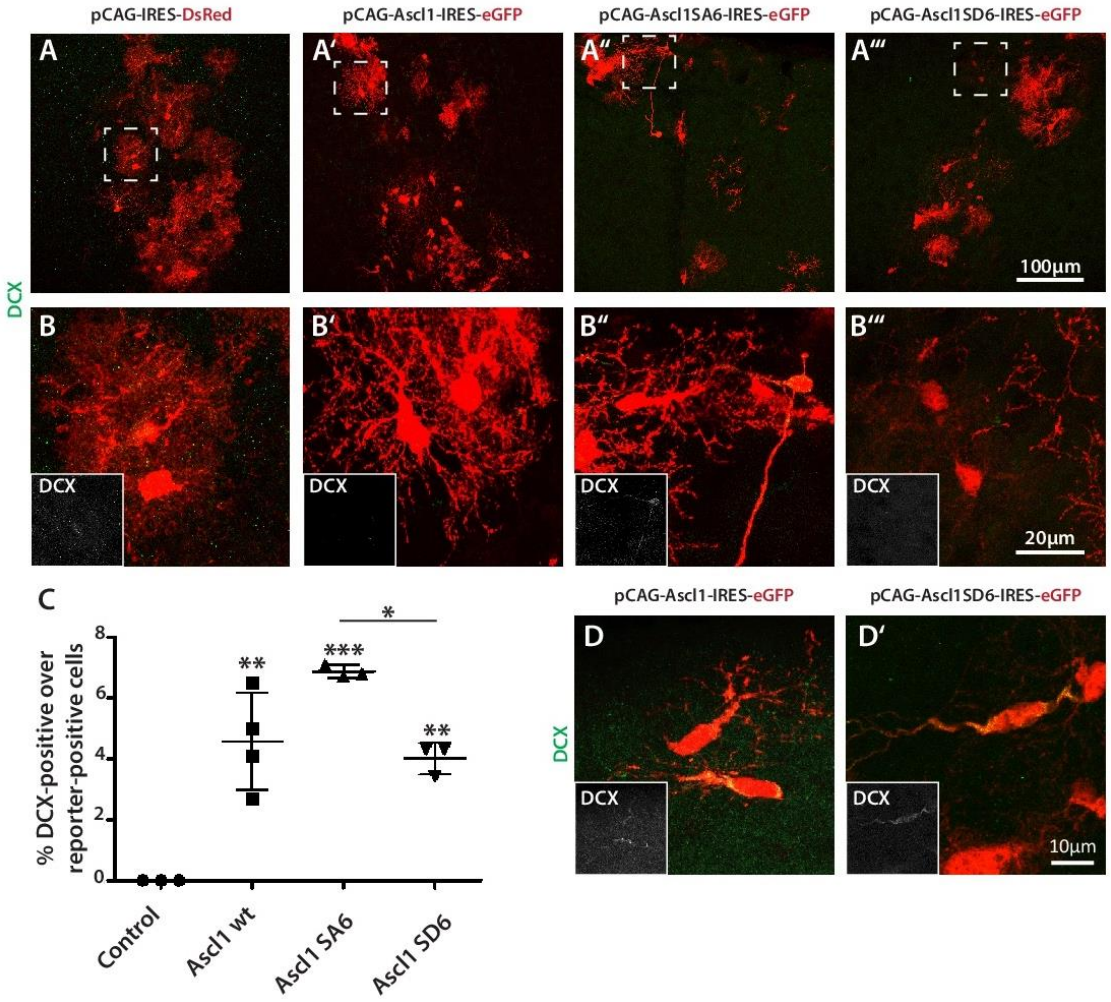

Fig.2.7 Inefficient formation of neurons upon exogenous expression of *pAscl1 in vivo*. A-A''', Transduced cells (red) at 12dpi. B-B''', Few DCX-positive cells were found among Ascl1SA6 expressing cells and only in this condition they changed their morphology and looked like neuroblasts. Insets illustrate the DCX staining alone (white). C, Percentage of DCX-positive cells among transduced cells at 12dpi. D-D', Examples of rare DCX-positive cells (white in the insets) detected among Ascl1 wt and Ascl1SD6 expressing cells and do not exhibit a striking neuroblast-like morphology. P<0.001; n=3-4. Means±SD. For numbers of cells quantified and all p-values see Appendix III and IV.

Given this overall unsuccessful glia-to-neuron fate-switch, I checked if *Ascl1* was involved in inducing an alternative, non-neuronal, fate-switch *in vivo*. Thus, I performed immunohistochemistry for the two macroglial populations targeted by the retroviruses. More precisely, I verified if there was a change in the proportion of astrocytes and oligodendroglial cells by performing a co-immunostaining for GFAP and for the pan-oligo marker SOX10 (Fig.2.8). Surprisingly, exogenous expression of pASCL1 led to a consistent decrease of astrocytes, as revealed by the three-times lower percentage of cells expressing only GFAP compared to control (Ctrl 63.9±12.1%; Ascl1 wt 18.7±3.1%; Ascl1SA6 19.5±6.1%; Ascl1SD6 23.1±6.3%) (Fig.2.8C). This decrease in GFAP-only expressing cells was accompanied by an increase of the percentage of cells expressing only SOX10 upon expression of wild type *Ascl1*, but not of the phospho-mutants (Ctrl 34.9±11.3%; Ascl1 wt 69.9±7.7%; Ascl1SA6 51.1±3.1%; Ascl1SD6 49.3±4.7%) (Fig.2.8C').

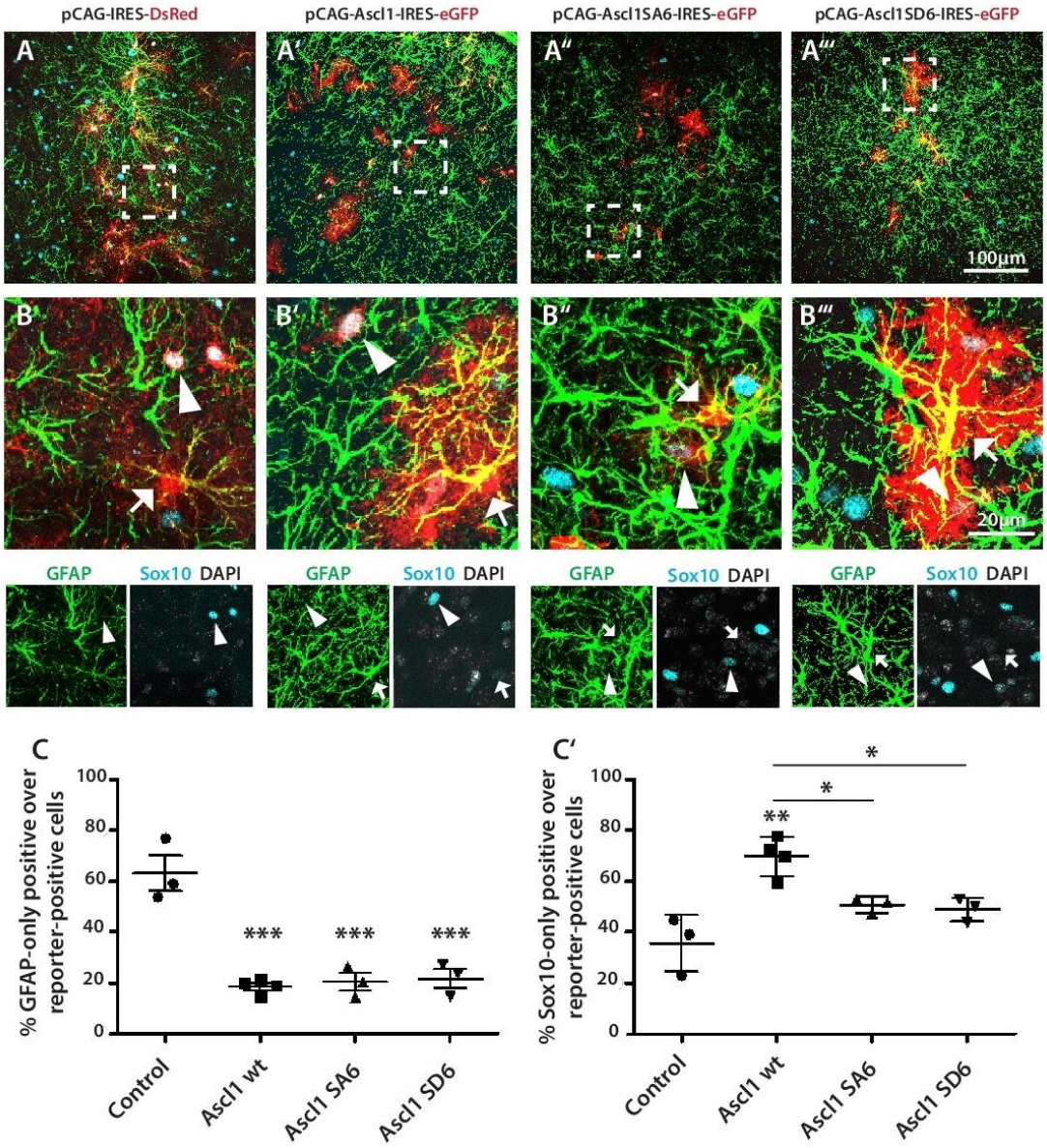

Fig.2.8 *pAscl1* expression decreases the proportion of astrocytes and increases the oligodendroglial population.
(See page before) A-A''', Overview of cells transduced with *pAscl1* and control vector (red) at 12dpi in brain sections following co-immunohistochemistry for GFAP and SOX10. B-B''', Magnifications illustrating transduced cells expressing GFAP (green, arrows) or SOX10 (cyan, arrowheads). Insets show single channels; p=0.000. C, Percentage of transduced cells expressing only GFAP. C', Percentage of transduced cells expressing only SOX10; p=0.001. n=3-4. Means±SD. For numbers of cells quantified and all p-values see Appendix III and IV.

Intriguingly, in cells transduced with *pAscl1* I also detected a subpopulation that was not present in control conditions, namely cells co-expressing GFAP and SOX10 (Fig.2.9), suggesting a state of transition between the two lineages. Despite the fact that all three phosphorylation states induced the presence of these double-labelled cells, the two phospho-mutants (Ascl1SA6 and Ascl1SD6) yielded a higher proportion of them (Ctrl 0.1±0.1%; Ascl1 wt 4.5±2.6%; Ascl1SA6 17.6±6.0%; Ascl1SD6 11.9±3.4%) (Fig.2.9B), suggesting a role in increasing oligodendrogenesis.

In light of these findings, I determined to investigate if, within the oligodendroglial population, there was a change in the proportion of oligodendrocyte progenitor cells (OPCs) and mature oligodendrocytes. To assess this and to identify these two subpopulations, I performed co-immunohistochemistry for the pan-oligo marker SOX10 and for the oligodendrocyte-specific marker APC (Fig.2.10). I quantified as oligodendrocytes cells that were co-expressing SOX10 and APC and as OPCs cells that were expressing only SOX10. As in my former analyses (Fig.2.8C'), the proportion of cells expressing only SOX10 was affected by the wild type form of ASCL1 but not by the mutants (Ctrl 36.8±5.5%; Ascl1 wt 56.3±3.3%; Ascl1SA6 33.5±3.4%; Ascl1SD6 44.3±6.5%) (Fig.2.10C). Interestingly, albeit not influencing the progenitors' fraction (Fig. 2.10C), the phospho-mutants increased the oligodendrocytes' fraction compared to the wild type (Ctrl 15.2±5.5%; Ascl1 wt 9.1±3.3%; Ascl1SA6 19.4±3.4%; Ascl1SD6 20.3±6.5%) (Fig.2.10C'), suggesting a possible role in oligodendrocyte differentiation. Moreover, ASCL1 seems to slightly reduce the fraction of oligodendrocytes, even though the decrease was not significant (Fig.2.10C').

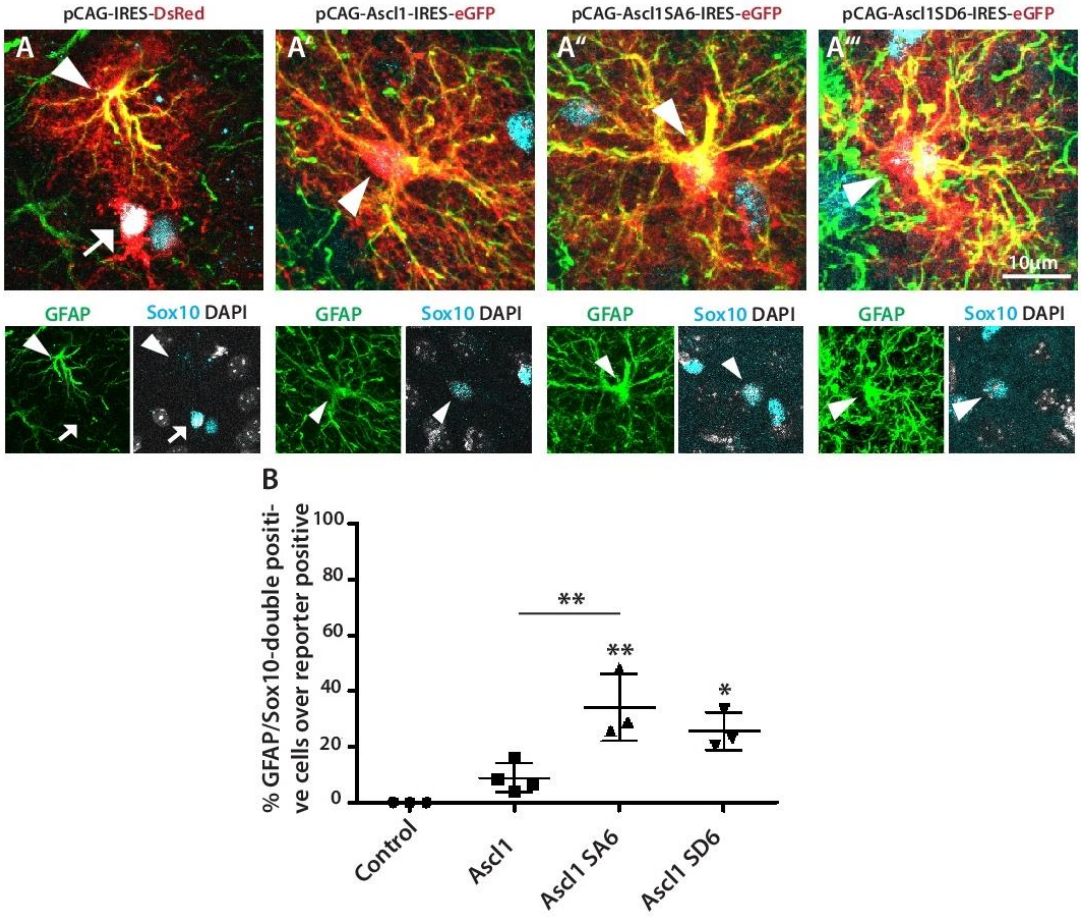

Fig.2.9 Some *pAscl1*-transduced cells co-express astroglial and oligodendroglial markers. A-A''', Confocal images of transduced cells (red) at 12dpi co-expressing GFAP (green, arrowhead in A) and SOX10 (cyan, arrow in A). B, Percentage of cells co-expressing macroglial markers among transduced cells (arrowheads in A'-A'''). p=0.001; n=3-4. Means±SD. For numbers of cells quantified and all p-values see Appendix III and IV.

Taken together, my results reveal that the exogenous expression of pASCL1 in the mouse postnatal cortex, independently on its phosphorylation state, is not capable of efficiently converting glia into neurons. They also hint at a role of *Ascl1* in the maturation of cells within the oligodendroglial lineage, as highlighted by the higher percentage of OPCs detected upon expression of wild type ASCL1 and different maturation levels upon expression of the phospho-mutants.

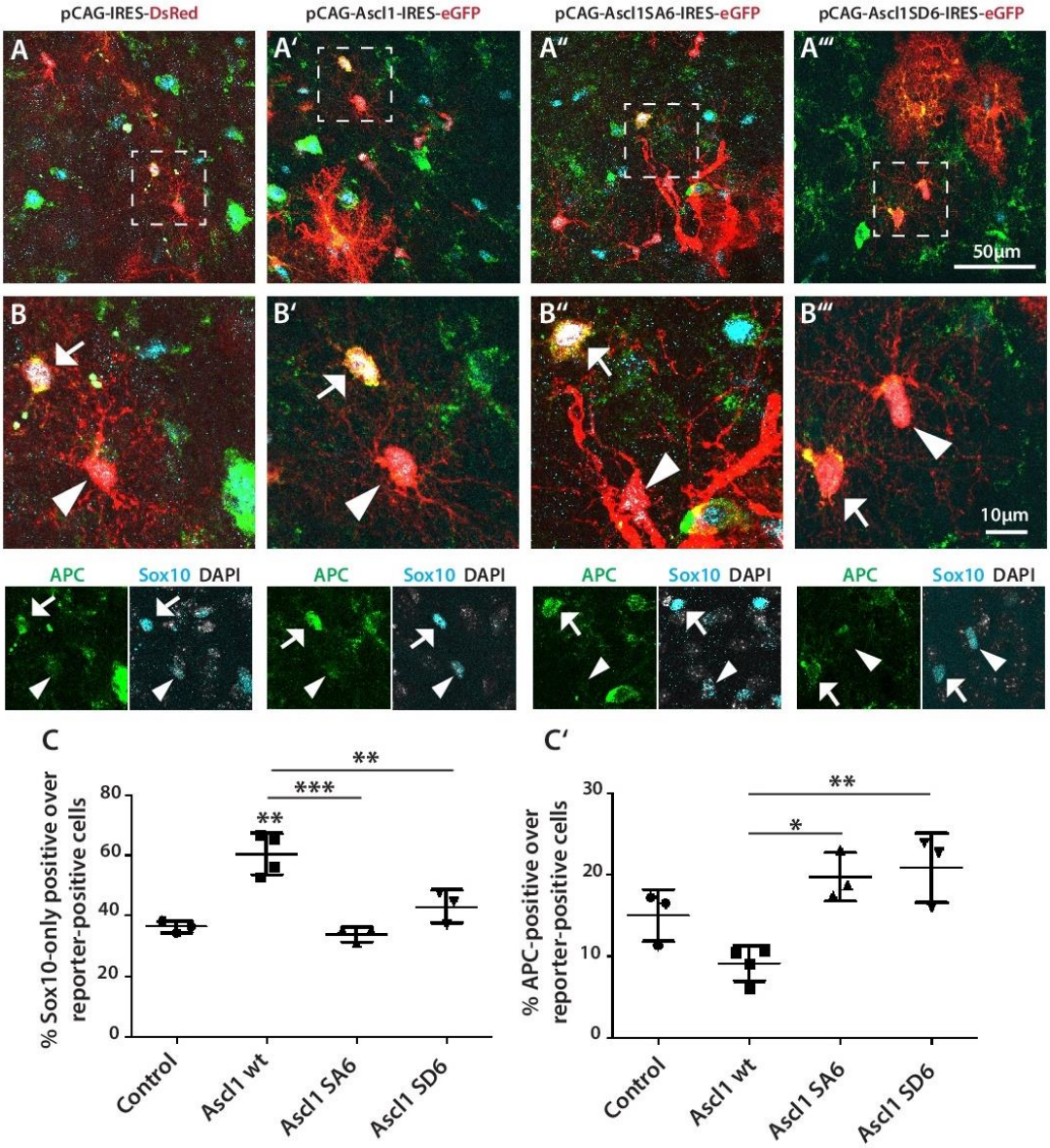

Fig.2.10 The phospho-mutants yields more mature oligodendrocytes than ASCL1 wt. A-A''', Confocal images of transduced cells (red) expressing APC (green) and SOX10 (cyan). B-B''', Magnifications illustrating oligodendrocyte progenitors (arrowheads) and oligodendrocytes (arrows). Insets show single channels. C, Percentage of oligodendrocyte progenitors expressing only SOX10 among transduced cells at 12dpi; p<0.001. C', Percentage of oligodendrocytes co-expressing SOX10 and APC among transduced cells; p=0.003. n=3-4. Means±SD. For numbers of cells quantified and all p-values see Appendix III and IV.

2.1.4 *In vivo* direct reprogramming of postnatal cortical glia: co-transduction of *pAscl1* and *Bcl2* in the mouse postnatal cortex

Due to the low glia-to-neuron conversion rate achieved upon exogenous expression of pASCL1 alone *in vivo*, it was not possible to determine whether phosphorylation of this proneural transcription factor is involved in the modulation of forced neurogenesis. Recently, it has been demonstrated that co-transduction of the proneural factor *Neurog2* with *Bcl2* greatly increases the direct conversion of cortical glia into neurons in the adult lesioned cortex *in vivo* (Gascón et al. 2016). I therefore evaluated whether *Bcl2* would similarly improve the neuronal fate-switch rate in postnatal cortical glia and analysed cells transduced with two retroviruses encoding for *Bcl2-GFP* and *pAscl1-DsRed*, respectively, at 12dpi (Fig.2.11A). With all three forms of *Ascl1* (*pAscl1*), I observed several co-transduced cells which, with great surprise, had neuronal morphology (Fig.2.11B-B''). Moreover, single transduced cells seemed to retain glial morphology (Fig.2.11B-B''), confirming my previous observation that *pAscl1* alone does not convert cortical glia into neurons and indicating that *Bcl2* alone does not do it either.

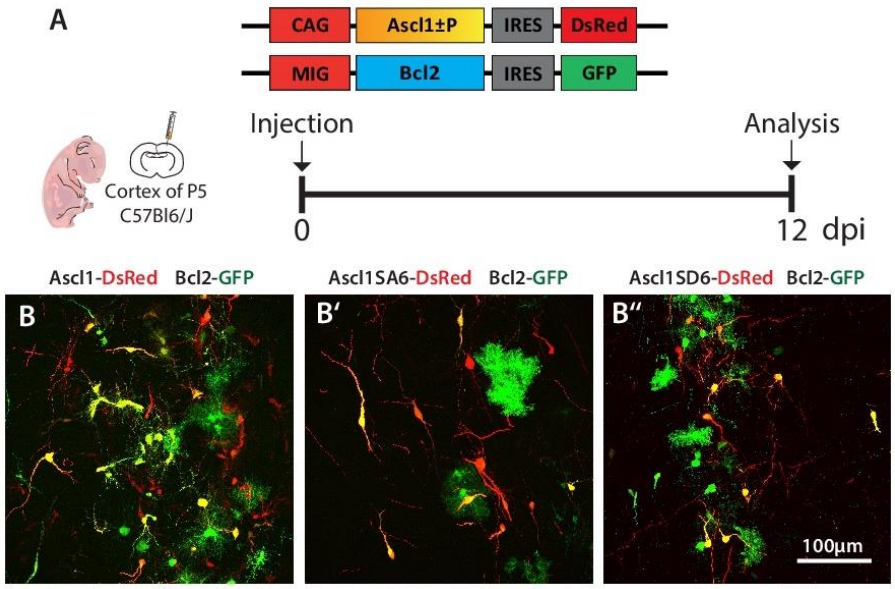

Fig.2.11 Co-transduction of *pAscl1* and *Bcl2*. A, Schematic of the retroviral vectors used and of the experiment. B-B'', Confocal images of cells co-transduced with *pAscl1* (red) and *Bcl2* (green), showing that while single transduced cells retain glial morphology, a majority of double-transduced cells (yellow) drastically change morphology and resemble neuronal cells.

I therefore determined whether phosphorylation of ASCL1 would modulate the level of forced neurogenesis in the context of *Bcl2*-facilitated direct reprogramming. For this purpose, I analysed the expression of the immature and mature neuronal markers DCX and NeuN, respectively, after co-immunohistochemistry (Fig.2.12, 2.13). No *Bcl2*-only transduced cells and, in accordance with my previous results (Fig.2.7C), rare *pAscl1*-only transduced cells expressed DCX (Fig.2.12D). On the contrary, many co-transduced cells acquired expression of neuronal markers (Fig.2.12D and 2.13D), in line with the morphological alteration described above. Interestingly, while expression of either the wild type or phospho-deficient protein gave a similar abundance of DCX-only positive cells, the phospho-mimetic protein yielded a slightly but significantly higher proportion of immature neurons (Ascl1 wt 26.9±2.6%; Ascl1SA6 23.0±5.5%; Ascl1SD6 38.8±6.0%) (Fig.2.12D). In contrast, the induction of NeuN-only positive neurons was more prominent when expressing the phospho-deficient protein (Ascl1 wt 5.8±3.0%; Ascl1SA6 27.5±3.9%; Ascl1SD6 13.1±4.7%) (Fig.2.13D). Notably, some cells expressing only the fluorescent reporter DsRed presented neuronal morphology and expressed NeuN (Fig.2.13D), an observation that was never made upon *pAscl1*-only transduction (Fig.2.7). Rather than suggesting the ability of *pAscl1* alone to generate mature neurons from glia, this may result from non-detectable levels of transgene (*Bcl2-gfp*) expression and may suggest that low levels of *Bcl2* expression are sufficient to promote *Ascl1*-mediated glia-to-neuron conversion.

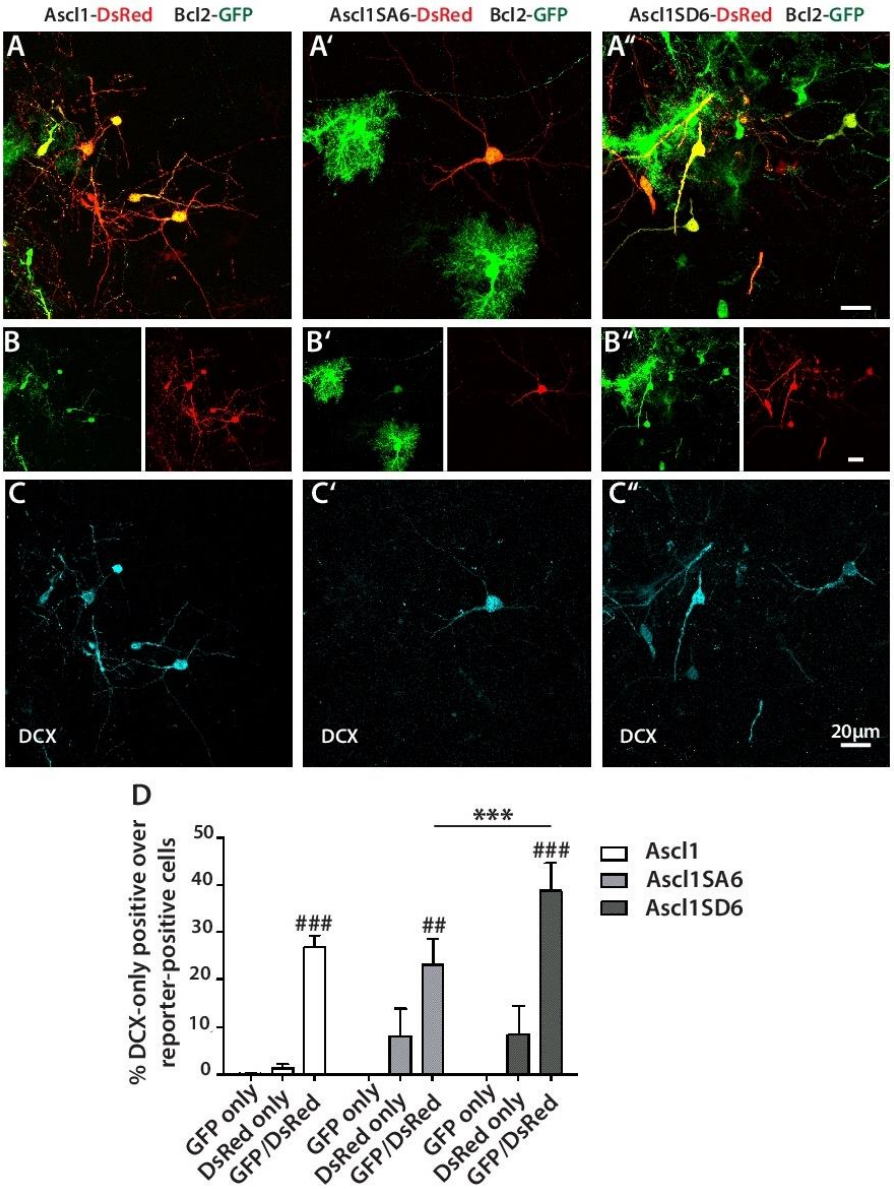

Fig.2.12 Successful forced neuronal fate induction in cells co-transduced with *pAscl1* and *Bcl2*. A-A''', Confocal illustrations of co-transduced cells. B-B'', Insets show single channels for the retroviral reporters of *pAscl1* (red) and *Bcl2* (green). C-C'', Single channel images revealing that co-transduced cells in B-B'' are also expressing the immature neuronal marker DCX (cyan). D, Percentage of cells expressing DCX among transduced cells. $p<0.001$; n=3. Means±SD. Hashtags indicate significance of the percentage of co-transduced cells compared to cells transduced with *pAscl1* only. Asterisks compare double-transduced conditions. For numbers of cells quantified and all p-values see Appendix III and IV.

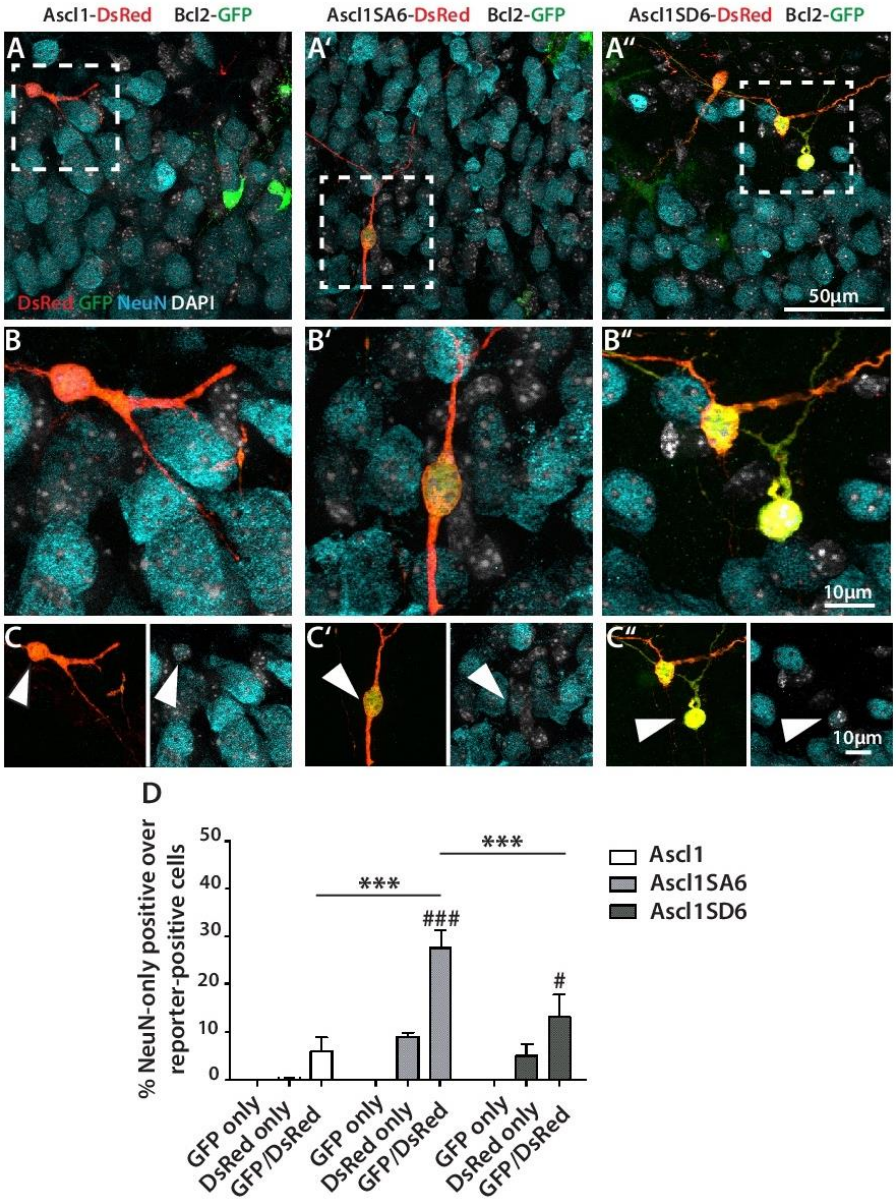

Fig.2.13 Forced cell fate-switch mediated by *pAscl1* and *Bcl2* leads to mature neurons. A-A'', Confocal images show an overview of the injected area with NeuN-positive cells (cyan). B-B'', Magnifications illustrating double-transduced cells expressing NeuN. C-C'', Single channel images of cells in B-B'' (arrowheads). D, Percentage of cells expressing NeuN among transduced cells. $p<0.001$; n=3. Means±SD. Hashtags indicate significance of the percentage of co-transduced cells compared to cells transduced with *pAscl1* only. For numbers of cells quantified and all p-values see Appendix III and IV.

Transient expression of DCX in newly generated neurons in the hippocampus of two months old rats is rapidly downregulated around one week after emergence of the cells; simultaneously, NeuN expression starts being upregulated, indicating the transition of the cells to a more mature stage (Brown et al. 2003). The expression of these two markers between day 7 and day 21 overlaps (Brown et al. 2003). Interestingly, further analyses of co-stainings for DCX and NeuN at 12dpi (Fig.2.14) revealed that a proportion of cells co-transduced by *pAscl1* and *Bcl2* were expressing both neuronal markers (Ascl1 wt 12.7±3.6%; Ascl1SA6 23.2±4.4%; Ascl1SD6 18.3±2.5%) (Fig.2.14D), indicating the presence of cells in

transition between their immature stage and a more mature one. Of note, the phospho-deficient mutant induced a percentage of DCX/NeuN-double positive cells higher than wild type ASCL1 (Fig.2.14D).

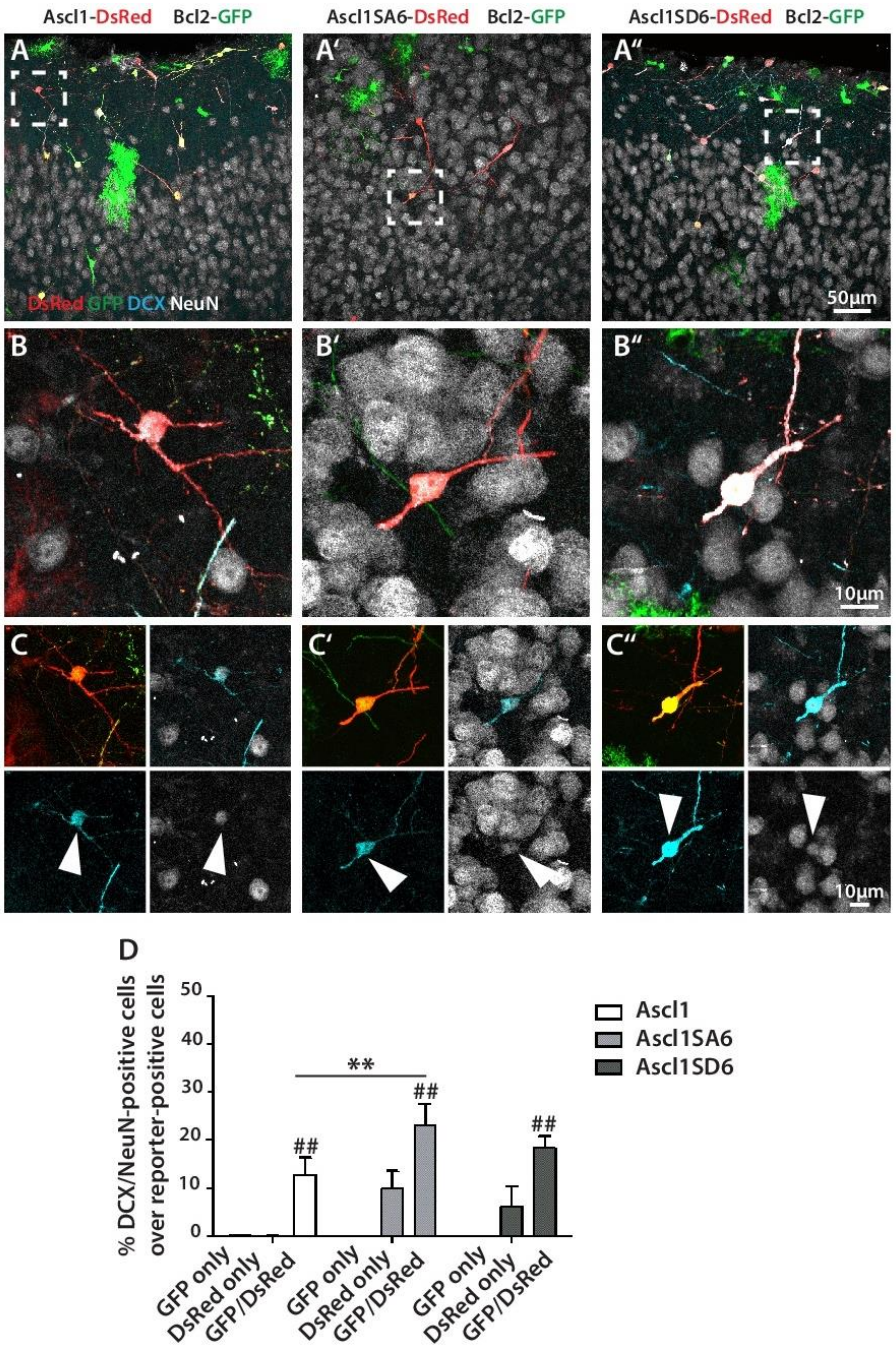

Fig.2.14 Some converted neurons co-express DCX and NeuN. A-A'', Confocal images show an overview of the injected area with DCX-positive (cyan) and NeuN-positive cells (white). B-B'', Magnifications illustrating double-transduced cells co-expressing DCX and NeuN. C-C'', Single channels of insets in B-B'' (arrowheads). D, Percentage of cells expressing NeuN among transduced cells. $p<0.001$; n=3. Means±SD. Hashtags indicate significance of the percentage of cells co-transduced by *pAscl1* and *Bcl2* compared to cells transduced with *pAscl1* only. For numbers of cells quantified and all p-values see Appendix III and IV.

To summarise, I have here demonstrated that co-transduction of *pAscl1* and *Bcl2* promotes pASCL1-mediated glia-to-neuron fate-switch, thus allowing the investigation of the influence of phosphorylation of ASCL1 on its ability to induce neuronal fate conversion in cortical glia. Moreover, the collected results highlight an overall higher glia-to-neuron conversion rate upon expression of the phospho-deficient or phospho-mimetic mutants (Table 2.1). In particular, mimicking constitutive phosphorylation yielded more immature neurons at 12dpi, while a deficiency in phosphorylation resulted in a higher percentage of mature neurons (Fig.2.12, 2.13, 2.14). Interestingly, the overall neurogenic potential of the two phospho-mimetic mutants was similarly higher compared to the wild type protein, as revealed by the sum of the percentage of double-reporter positive cells expressing neuronal markers (Ascl1 wt 45.5±9.1%; Ascl1SA6 73.7±2.6%; Ascl1SD6 70.3±6.5%) (Table 2.1).

Table 2.1 Total percentage of neuronal cells among cells co-transduced with *pAscl1* and *Bcl2*. The mean values for each subpopulation quantified were considered.

	Ascl1 wt + Bcl2	Ascl1SA6 + Bcl2	Ascl1SD6 + Bcl2
DCX	26.9 ± 2.6%	23.0 ± 5.5%	38.8 ± 6.0%
NeuN	5.8 ± 3.0%	27.5 ± 3.9%	13.1 ± 4.7%
DCX/NeuN	12.7 ± 3.6%	23.2 ± 4.4%	18.3 ± 2.5%
Total	45.5 ± 9.1%	73.7 ± 2.6%	70.3 ± 6.5%

Ascl1 regulates the specification of GABAergic interneurons during development (Casarosa et al., 1999). Neuronal cells derived from *Ascl1*-mediated conversion of *in vitro*-expanded adult neural stem cells (Berninger et al. 2007) or from *Dlx2*-mediated conversion of astrocytes *in vitro* (Heinrich et al. 2010) were shown to express GABA or the GABAergic transporter vGaT, respectively, which confirmed their interneuronal identity. I therefore investigated whether neurons derived from *pAscl1*/*Bcl2*-mediated fate-switch *in vivo* were expressing interneuronal markers. Given the fact that a considerable proportion of neurons induced by *pAscl1* and *Bcl2* already expresses the maturation marker NeuN (Fig.2.13 and 2.14), I sought to determine whether they were also expressing GABA via immunohistochemistry. Even though some co-transduced cells were already expressing GABA, only a small proportion was positive at 12dpi (Ascl1 wt 1.2±0.1%; Ascl1SA6 9.2±2.4%; Ascl1SD6 3.0±0.4%) (Fig.2.15). The phospho-mutants exhibited more GABA-positive co-transduced cells and the phospho-deficient, which was also promoting the highest fraction of NeuN-positive cells (Fig.2.13D), induced three times more neurotransmitter-positive cells (Fig.2.15). This suggests that *pAscl1/Bcl2*-induced neurons might not yet be functionally mature, despite the expression of the mature neuronal marker NeuN.

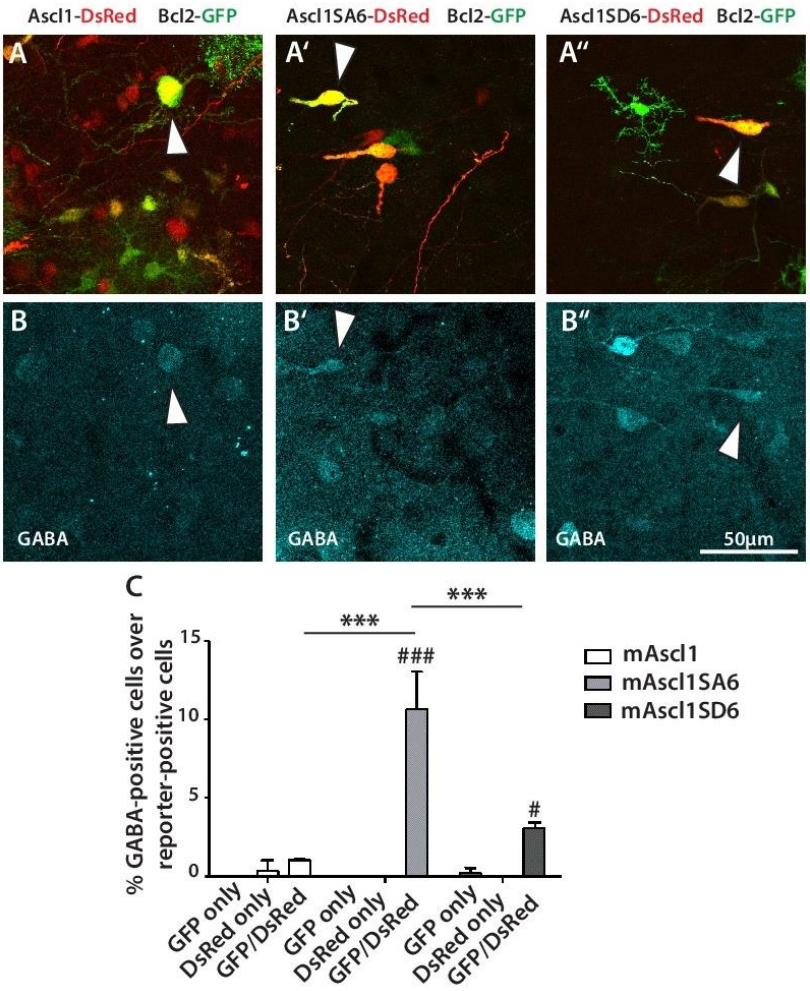

Fig.2.15 Some converted neurons express GABA. A-A'', Confocal images showing cells transduced by *pAscl1* (red) and *Bcl2* (green). B-B'', Single channels illustrating GABA expression of some co-transduced cells (arrowheads). C, Percentage of cells expressing GABA among transduced cells. $p<0.001$; n=3. Means±SD. Hashtags indicate significance of the percentage of cells co-transduced by *pAscl1* and *Bcl2* compared to cells transduced with *pAscl1* only. For numbers of cells quantified and all p-values see Appendix III and IV.

Co-expression of ASCL1 and SOX2 in the adult injured cortex induces direct conversion of OPCs into neurons expressing DCX at 10dpi, some of which further mature into NeuN-expressing neurons and by 24dpi exhibit electrophysiological properties similar to immature neuronal phenotypes (Heinrich et al. 2014). While the morphology of *pAscl1*/*Bcl2*-induced neurons at 12dpi (Fig.2.11) and the markers they expressed (Fig.2.13, 2.14, 2.15) suggest that the majority of reprogrammed cells become mature neurons, these elements are not proof of their functional maturation and integration in the cortical networks. Thus, in order to determine whether *pAscl1*/*Bcl2*-induced neurons were functional and to determine their degree of maturation, whole-cell patch-clamp electrophysiological recordings were performed on acute brain slices at 4 weeks post injection (wpi) (Fig.2.16A). Given the finding that co-

expression at 12dpi of *Bcl2* in cells expressing the phospho-deficient protein ASCL1SA6 induces the highest percentage of cells positive for neuronal markers (Table 2.1) and for the neurotransmitter GABA (Fig.2.15), a first set of experiments were performed to determine the functional properties and maturation of *Ascl1SA6*/*Bcl2*-induced neurons at 4wpi (Fig.2.16B). Current-clamp recordings showed that some co-transduced cells had the ability to generate high-frequency repetitive action potential in response to a depolarising current pulse (Fig.2.16C), resembling the functional phenotype of fast-spiking cortical interneurons (Kepecs and Fishell 2014). Moreover, sustained depolarising current steps (5 seconds long) showed that induced neurons were able to maintain their high firing frequency (Fig.2.16D), suggesting that these cells have acquired a substantial degree of functional maturation. Subsequently, voltage-clamp recordings were performed to determine whether *Ascl1SA6*/*Bcl2*-induced neurons integrated in the cortical circuitry and received synaptic inputs from surrounding neurons. Interestingly, five over six recorded cells exhibited spontaneous synaptic inputs (Fig.2.16E), suggesting a certain level of integration in the local pre-existing neuronal circuitry. Taken together, electrophysiological recordings of *Ascl1SA6*/*Bcl2*-induced neurons at 4wpi suggest that these cells become mature functional neurons resembling interneurons with high firing frequency and that they receive synaptic inputs, which indicates their integration in the postnatal cortical circuitry.

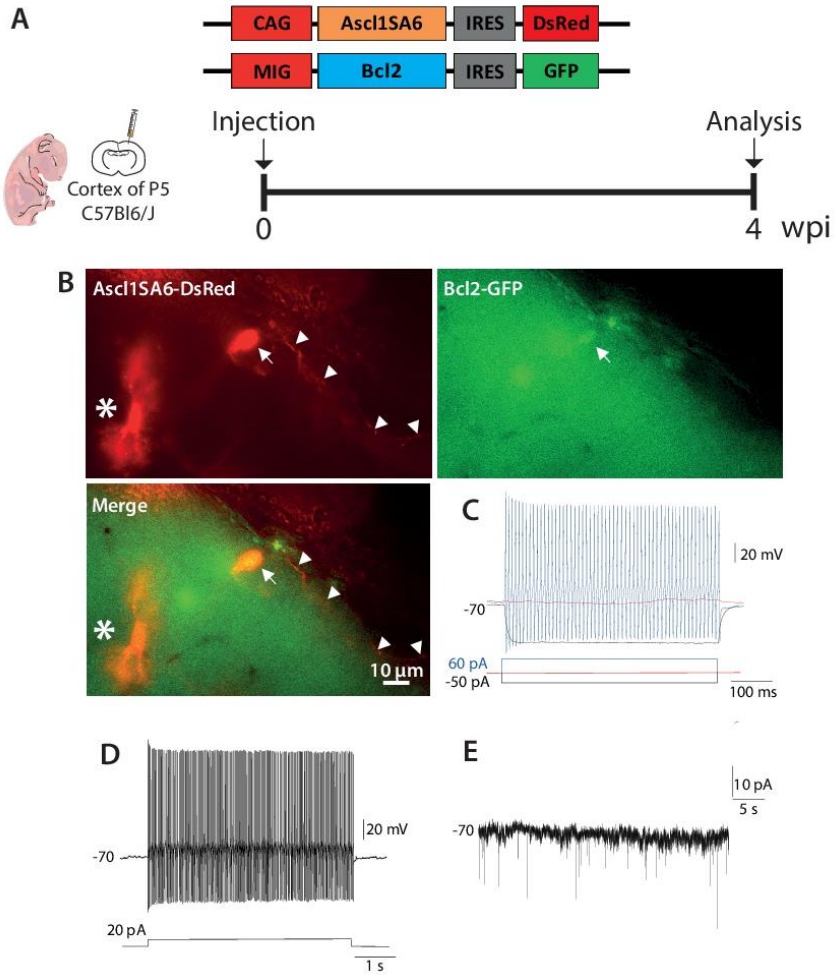

Fig.2.16 *ASCL1SA6/Bcl2*-expressing cells mature into high-frequency firing neurons. A, Experimental scheme. B, Epifluorescent pictures of an *ex vivo* cortical slice showing a cell transduced by *Ascl1SA6* (red) and *Bcl2* (green) (arrow). Arrowheads indicate the process of the cell. Notably, a cell transduced only with Ascl1SA6 (red, asterisk) retains glial morphology. C, Current-clamp recording of co-transduced cell shown in B. A depolarising current step of 60pA and a hyperpolarising step current of -50pA were applied for 500ms. Interestingly, the recorded cell exhibits high firing frequency (114Hz). D, Current-clamp recording after applying a 20pA depolarising current for 5s show that the cells maintains a high firing frequency for long time. E, Voltage-clamp recordings revealed the presence of spontaneous synaptic inputs in induced neurons. n=3. For numbers of cells quantified see Appendix III.

2.2 Development of a novel paradigm for clonal analysis of astrocytes converted into neurons *in vivo*

2.2.1 Cloning of constructs for *in vivo* exogenous expression of proneural transcription factors via a transposable system

Astrocytes are known to be heterogeneous in terms of morphology and function (reviewed in Farmer and Murai 2017). However, it is still unknown to what extent the heterogeneity of cortical astrocytes influences the outcome of forced fate-switch. Thus, to investigate the role of astroglia heterogeneity in direct reprogramming, I adapted a transposition- and *in utero* electroporation-based technique that was developed at the Instituto Cajal (Madrid, Spain) – the StarTrack clonal labelling system (see also section 1.5.2).

The StarTrack system exploits transposable elements to stably integrate them into the host cell's genome. Such transposons are administered to the cells as plasmids via *in utero* electroporation and contain the operons for the expression of genes of interest (promoter, genes, transcription termination sequences). Their transposition is catalysed by a hyperactive version of the *PiggyBAC* transposase, called hyPBase (Fig.4.6).

In order to study the clonal origin of induced neurons, I adapted to my purpose the plasmids of the original version of the StarTrack system, developed for clonal labelling of astroglia. I therefore subcloned tamoxifen-dependent forms of the proneural transcription factors *Neurog2* and *Ascl1* (*Neurog2ERT2* and *Ascl1ERT2*, respectively) in transposons with the human GFAP (hGFAP, in the constructs referred to as GFAP) promoter, thus to ensure the induction of cell fate-switch at the desired timepoint and specifically in astrocytes, respectively (Fig.2.17). To be able to detect the subpopulation of astrocytes electroporated with the plasmids for expression of the proneural factors, I subcloned in the transposon also the coding sequence of a fluorescent reporter preceded by an Internal Ribosome Entry Sequence (IRES) for enhanced transcription. Given the prior knowledge that *Neurog2*-mediated and *Ascl1*-mediated cell fate-switch *in vivo* both greatly improve upon co-expression of *Bcl2* and *Sox2*, respectively (Gascón et al. 2016; Heinrich et al. 2014), I subcloned in transposons also the genes for these two factors, again under the control of the hGFAP promoter (Fig.2.17). In light of the results I presented in section 2.1, combination of *Ascl1* and *Bcl2* is currently planned.

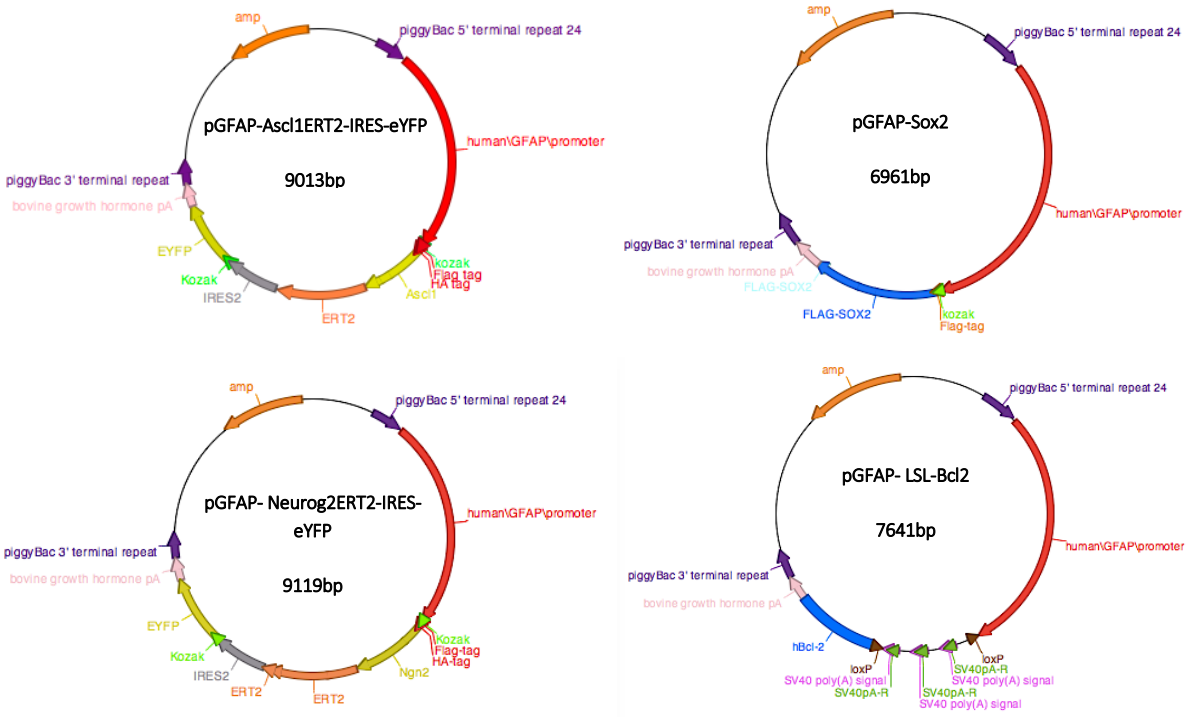

Fig. 2.17 Maps of the transposable constructs for direct conversion of astrocytes into neurons *in vivo*. The four constructs I cloned contain the tamoxifen-dependent genes for astrocyte-to-neuron conversion (Ascl1ERT2 and Neurog2ERT2) within the transposon. To avoid effects of constitutive expression of *Bcl2*, an antiapoptotic factor, and make it strictly dependent on tamoxifen, I subcloned upstream to the gene a loxed STOP cassette (LSL).

As explained in section 1.5.2, the StarTrack system allows clonal labelling of cells thanks to six fluorescent reporters: mTSapphire, mCerulean, eGFP, eYFP, mKO, mCherry. Each fluorescent reporter is expressed by a different plasmid and has either cytoplasmic or nuclear localisation (due to the fusion with the *Histone 2B* (*H2B*) gene) (Fig.4.5). Thus, there are in total twelve constructs, which greatly increases the resolution power for clonal labelling. For the purpose of achieving clonal labelling of electroporated cells even if they are not reprogrammed, I use the ubiquitous StarTrack system, with the human Ubiquitin promoter (Figueres-Onãte et al. 2016). Since each of the six fluorophores has a different intensity and frequency of presence in the clonal labels (Figueres-Oñate et al. 2016), I opted to maintain the clonal labelling system as powerful as possible and to use one of the least represented fluorescent proteins in the clonal labels, namely eYFP, as a fluorescent reporter for the plasmids expressing *Ascl1ERT2* and *Neurog2ERT2*. Thus, the clonal labelling plasmids with ubiquitous promoter used in this study are ten instead of twelve.

To determine the role of astroglial heterogeneity in astrocyte-to-neuron conversion, I performed *in utero* electroporations. I therefore injected embryonic stage 14 (E14) embryos with a mix containing: plasmids for the expression of tamoxifen-dependent versions of proneural factors; plasmids for the expression of their cofactors; plasmids of the ubiquitous StarTrack clonal labelling system, including one for transposase's expression and one for Cre recombinase expression. To electroporate cells, I applied positive electric current. After birth I treated electroporated animals with tamoxifen, which ensured removal of the episomal copies of the ubiquitous StarTrack (Figueres-Oñate et al. 2015), activation of the proneural factors and activation of the transcription of *Bcl2*. On one hand, transcriptional activation of the targets of either NEUROG2 or ASCL1 is aimed at forcing direct conversion of astrocytes into neurons. On the other hand, labelling with the ubiquitous StarTrack plasmids allows clonal analysis of induced neurons, even after they have lost eYFP labelling due to inactivation of the hGFAP promoter (Fig.2.18).

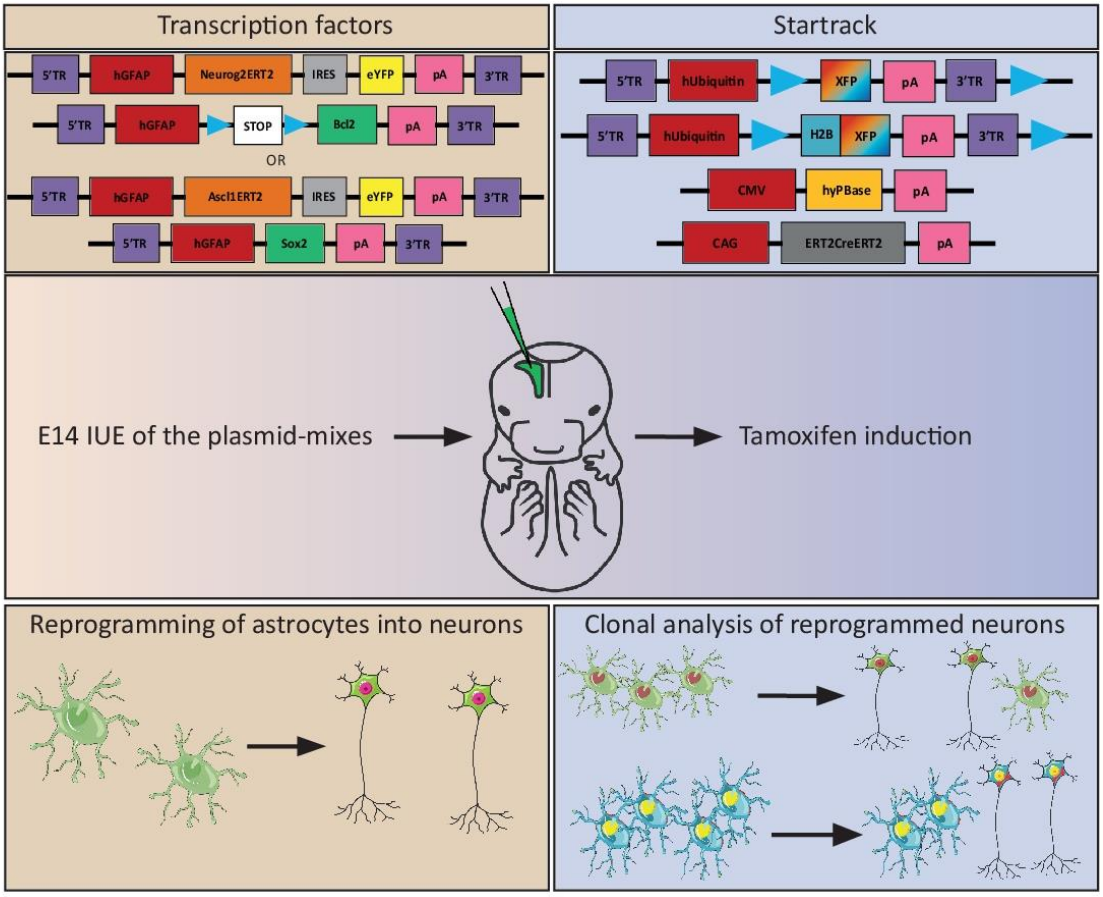

Fig.2.18 Graphical abstract of the project. A plasmid mixture containing both the transcription factors for cell fate-switch and the StarTrack system for integration of the plasmids and clonal analysis is injected in the lateral ventricles of E14 embryos. In order to internalise the plasmids in the neural progenitors lining the ventricle, I electroporated them. After birth, I induced activation of the factors for astrocyte-to-neuron conversion via tamoxifen administration. At the collection of the brains I can analyse the success of the cell fate-switch as well as the clonal origin of the induced neurons. XFP= Fluorescent protein.

2.2.2. Confocal detection of cloned constructs after *in utero* electroporation

The first step to determine the success of this method was to assess whether the constructs I cloned for exogenous expression of *Ascl1ERT2* and *Neurog2ERT2* can be detected. Thus, I first co-electroporated the pGFAP-Ascl1ERT2-IRES-eYFP plasmid and the ubiquitous construct pUbq-LoxP-H2BmKO-LoxP, to ensure correct identification of the electroporated area. I analysed the expression of the fluorophores via confocal imaging shortly after *in utero* electroporation, at E18 (Fig.2.19A). Upon detection, the eYFP signal appeared to be localised only in the soma despite the lack of the *H2B*-fusion for nuclear localisation (Fig.2.19B-B').

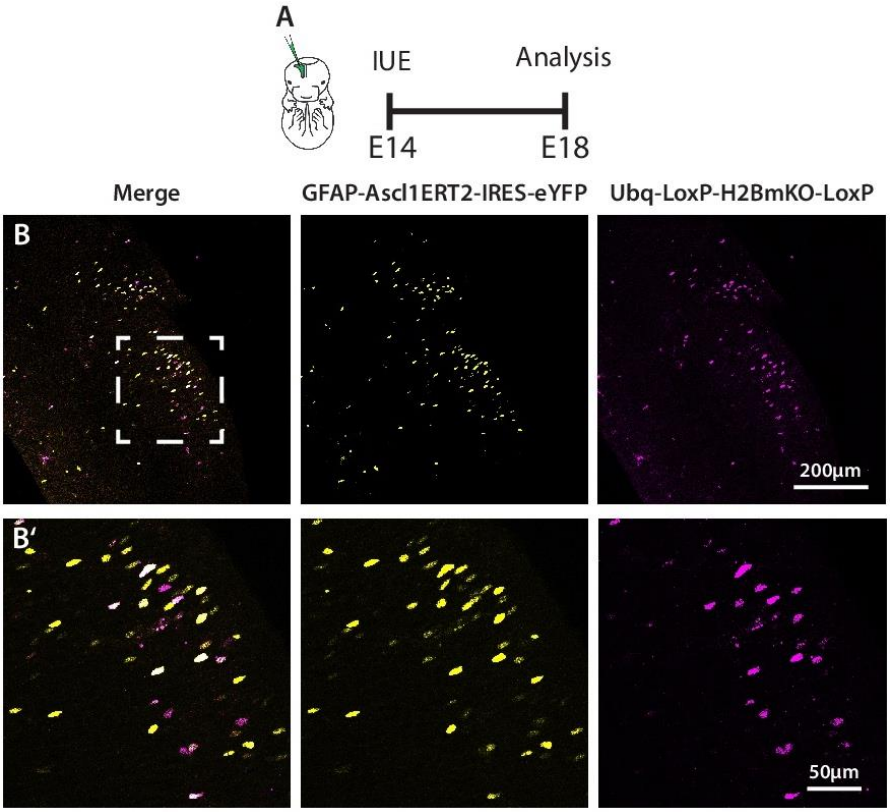

Fig.2.19 Detection of the plasmid for the exogenous expression of *Ascl1ERT2*. A, Experimental scheme. B, Confocal picture depicting cells electroporated in the cortex at E18. B', Magnification of the inset shown in B. The signal of the mKO is nuclear, due to the fusion with the H2B protein. The plasmid mix included the hyPBase-encoding plasmid.

Subsequently, I analysed the brains of animals electroporated with the pGFAP-Neurog2ERT2-IRES-eYFP plasmid and the ubiquitous construct pUbq-LoxP-mCherry-LoxP (Fig.2.20B-B'). This time, the electroporation was performed on newborn pups at P0 and the expression of fluorophores was analysed at P6 (Fig.2.20A). I could detect eYFP signal at the lateral ventricle, even though at a low level (Fig.2.20B-B').

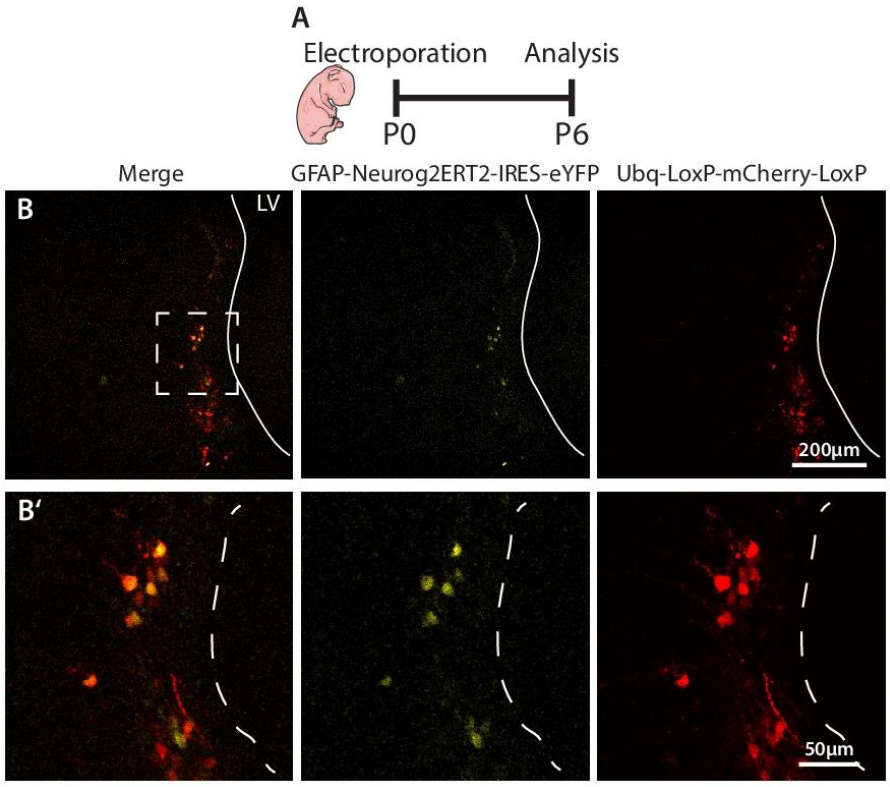

Fig.2.20 Detection of the plasmid for the exogenous expression of *Neurog2ERT2*. A, Experimental scheme. This electroporation was performed in collaboration with the Instituto Cajal (Madrid, Spain). B, Confocal picture depicting cells electroporated in the cortex at P6. B', Magnification of the inset shown in B. The signal of the eYFP is quite low, as opposed to the one of mCherry. The plasmid mix included the hyPBase-encoding plasmid.

The expression of the YFP reporter after *in utero* electroporation of the pGFAP-Neurog2ERT2-IRES-eYFP and the pGFAP-Ascl1ERT2-IRES-eYFP plasmids (Fig.2.19 and 2.20) is different to the expression pattern detected in cells electroporated with the control plasmid pPB-hGFAP-eYFP (Fig.2.21). In fact, confocal imaging of cells electroporated with the control plasmid and analysed at E18 shows that many cells have internalised the plasmid and some of them express eYFP also in their radial processes (Fig.2.21).

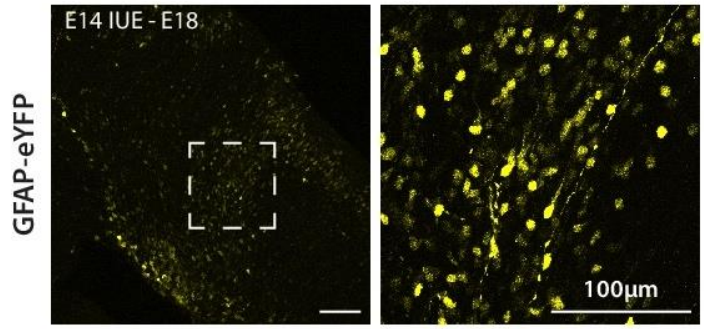

Fig.2.21 Morphology of cells electroporated with the pPB-hGFAP-eYFP plasmid. Cells electroporated at E14 with a control plasmid (pPB-hGFAP-eYFP), express a higher amount of fluorescent protein at E18 (right), as compared to cells electroporated with plasmids encoding for Ascl1ERT2-IRES-eYFP (Fig.2.19) and Neurog2ERT2-IRES-eYFP (Fig.2.20). Moreover, it is possible to observe their radial processes directed towards the pial surface (left).

During these preliminary experiments to find whether the pGFAP-Ascl1ERT2-IRES-eYFP and pGFAP-Neurog2ERT2-IRES-eYFP constructs can be detected (Fig.2.19 and 2.20), the plasmids encoding for the tamoxifen-inducible proneural factors, the plasmid encoding for the hyPBase and the ubiquitous StarTrack-plasmid used to detect the electroporated area were present in the mix with a 1:1:1 proportion. In order to determine whether a higher concentration of plasmids encoding for the transcription factors will give a stronger expression of eYFP, thus allowing a better identification of electroporated cells, a test has been performed in newborn mice. P1 mice were electroporated with a mix containing the plasmid encoding for *Neurog2ERT2* (pPB-hGFAP-Neurog2ERT2-IRES-eYFP), one plasmid from the ubiquitous StarTrack system (pPB-Ubq-mCherry) and the hyPBase. The hyPBase constituted one-third of the mix; the remaining two-thirds contained GFAP-Neurog2ERT2-IRES-eYFP and Ubq-mCerry in different proportions (Fig.2.22). Confocal analysis to detect the fluorescent proteins was performed at P6. Cells electroporated with two times more *Neurog2ERT2* than *mCherry* expression plasmid (2:1:1 dilution) (Fig.2.22, left) have higher levels of fluorescence than cells electroporated with a 1:1:1 proportion of plasmids (Fig.2.20, for comparison). Thus, for future experiments, a higher concentration of the plasmids encoding for the transcription factors will be used, hoping to achieve a higher expression of the reporter eYFP and therefore to better identify cells expressing them. Interestingly, cells electroporated with five times more *Neurog2ERT2*- than *mCherry*-expressing plasmids (5:1:1 dilution) have a lower level of fluorescence (Fig.2.22, right), suggesting that a too high concentration of the plasmid might not improve the expression efficiency.

In summary, I could detect the eYFP reporter signal of the plasmids that express *Ascl1ERT2* and *Neurog2ERT2*. Nevertheless, they both displayed unsatisfactory signal levels. The late embryonic-stage expression of pGFAP-Ascl1ERT2-IRES-eYFP is restricted to the soma, despite the fact that the fluorescent

protein should be localised in the cytoplasm thereby labelling the whole cell (Fig.2.19B-B'). Similarly, the postnatal expression level of pGFAP-Neurog2ERT2-IRES-eYFP is very low and does not highlight the processes of the radial glia-like cells targeted, as opposed to the mCherry signal (Fig.2.20B-B') and to the expression of eYFP from a control plasmid (Fig.2.21).

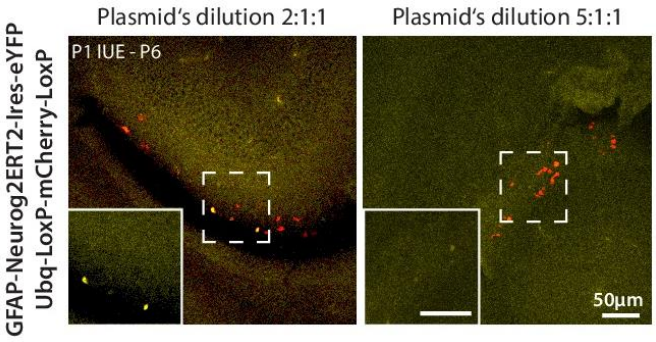

Fig.2.22 Cells electroporated with different dilutions of the *Neurog2ERT2*-encoding plasmid. The electroporation was performed at P1 with the GFAP-Neurog2ERT2-IRES-eYFP, the Ubq-LoxP-mCherry-LoxP and the CMV-hyPBase plasmids with, respectively, 2:1:1 or 5:1:1 dilution. At P6, cells containing double the amount of Neurog2ERT2-encoding plasmid compared to the mCherry encoding one (left) express a higher level of eYFP than cells containing five times the amount of Neurog2ERT2-encoding plasmid compared to the mCherry-encoding one (right). The quantity of the hyPBase in the plasmid mix is the same one as the quantity of the mCherry-encoding plasmid. The electroporations and the confocal imaging were performed in collaboration with the Instituto Cajal (Madrid, Spain).

2.2.3 *In utero* electroporation for the clonal analysis of induced neurons

In order to convert postnatal cortical astrocytes into neurons for their subsequent clonal analysis *in vivo*, I performed *in utero* electroporation at E14, when radial glia is targeted by the plasmid mixture. Exogenous expression of *Ascl1* alone fails to reprogram adult cortical glia into neurons after injury *in vivo*, but co-expression of *Ascl1* with *Sox2* induced cell fate-switch of adult OPCs into DCX-positive neurons (Heinrich et al. 2014). Thus, I co-electroporated the plasmid encoding for *Ascl1ERT2*, the plasmid encoding for *Sox2* and the StarTrack plasmids (Fig.2.23A). The proneural factors fused to the ERT2 protein are able to induce cell fate-switch *in vitro* only when activated by tamoxifen administration (Masserdotti et al. 2015). Thus, starting at P5 I treated the newborn pups with tamoxifen for 5 consecutive days and analysed the cell fate-switch 10 days after the end of tamoxifen administration (Fig.2.23A'). A successful electroporation should result in random internalisation of the plasmids in the cells and integration in the genome (Fig.2.23B). This implies that cells might not express all fluorescent reporters, and that they might express different levels of each reporter due to a different number of copies integrated (Figueres-Oñate et al. 2016). As a consequence of this, the number of possible labelling combinations to be analysed, is greatly increased. Moreover, I confirmed that it is possible to

perform immunohistochemistry for the detection of DCX-positive induced neurons without losing the fluorescent signal of the six reporters (Fig.2.23B'-B''). With great disappointment I was not able to detect DCX-positive induced neurons labelled with the StarTrack system, but this may be related to the low levels of expression presented in section 2.2.2.

To conclude, I have adapted a clonal labelling system to be used for direct conversion of astroglia into neurons. After cloning the vectors for the expression of transcription factor-mediated cell fate-switch, I performed preliminary experiments *in vivo* to determine whether electroporated cells can be easily detected. Even though such experiments have not yet allowed conversion of astrocytes into neurons and clonal analysis of induced neurons, they highlighted limitations of the technique as of now, which will be discussed in section 3.2. This will serve as basis for the further improvement of the system and successful completion of the project.

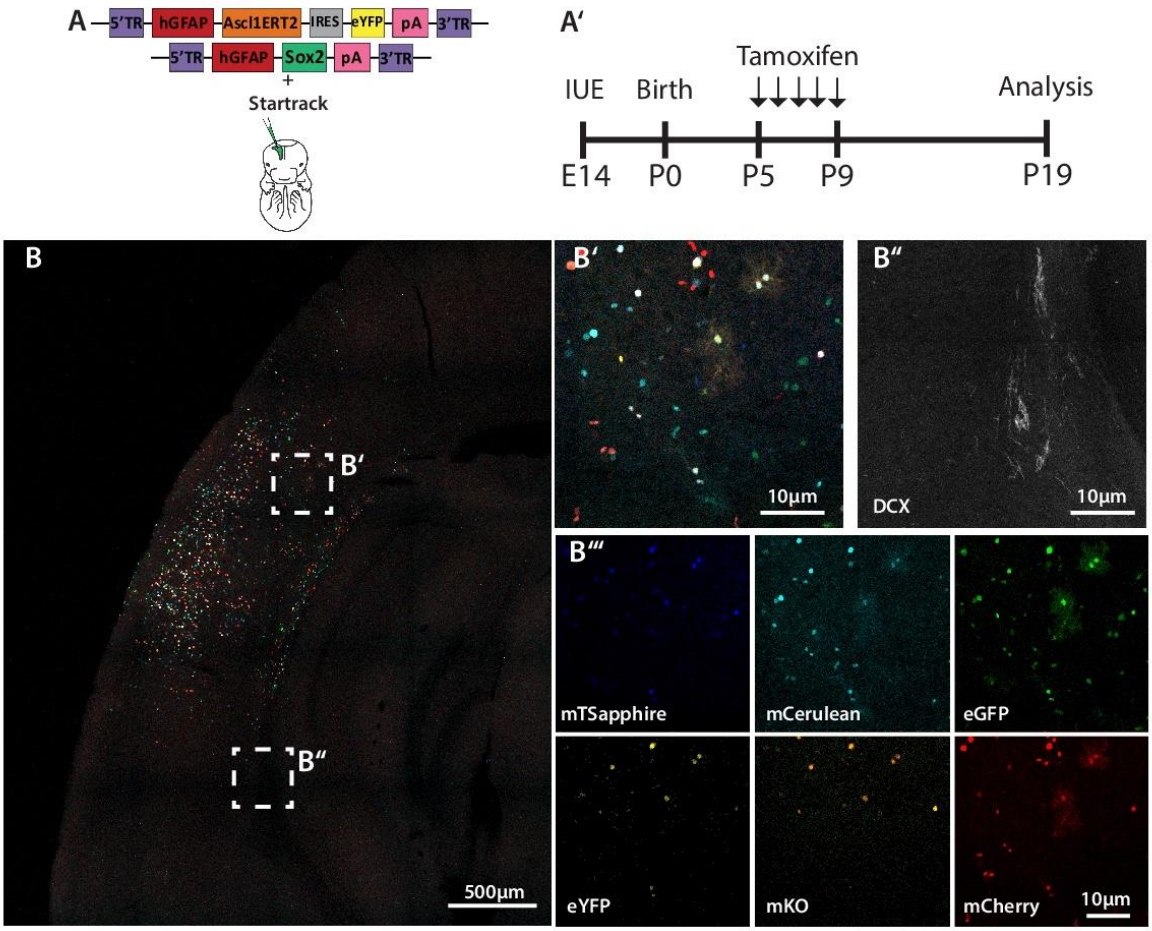

Fig.2.23 Example of *in utero* electroporation for clonal analysis of induced neurons. A, Experimental scheme. The proneural factor *Ascl1ERT2* and *Sox2* were co-electroporated, in addition to the ubiquitous StarTrack. Astrocyte-to-neuron conversion was initiated at P5, with daily tamoxifen injections until P9. Analysis were performed at P19, 10 days after the end of tamoxifen administration. B, Confocal overview of an electroporated cortex. B', Magnification of the inset shown in B. B'', DCX-positive cells in the striatum, where there are no electroporated cells, serve as a control for DCX immunohistochemistry. B''', Micrographs illustrating single channels of the inset shown in B'.

3 Discussion and outlook

3.1 Cell extrinsic and cell intrinsic factors in direct cell fate-switch

In this study, I have investigated the role of cell extrinsic and cell intrinsic factors in determining competence for direct glia-to-neuron conversion in the postnatal murine brain (Fig.3.1).

First, I studied the role that signalling pathways leading to phosphorylation of transcription factors have on direct reprogramming. In recent years, it has been shown that RAS/ERK signalling controls *Ascl*1 proneural function through the phosphorylation of ASCL1, thereby controlling developmental neural cell fate selection (Li et al. 2014). This opens the question of whether such kind of cell extrinsic control directed by signalling pathways can influence the outcome of direct cell fate-switch in the postnatal brain. The role of the phosphorylation of ASCL1 in forced cell fate-switch *in vivo* was investigated via exogenous expression of coding sequences encoding for the ASCL1 protein with three different states of phosphorylation (all together, pASCL1): wild type ASCL1 (ASCL1 wt or ASCL1), which can phosphorylated at six serine/proline (S/P) sites (Fig.4.3); phospho-deficient ASCL1 (ASCL1SA6 mutant), which cannot be phosphorylated due to S>A mutation of the S/P sites; phospho-mimetic ASCL1 (ASCL1SD6 mutant), which mimics constitutive phosphorylation due to S>D mutation of the S/P sites (Fig.2.1).

Second, I investigated the influence that the heterogeneity of the starting cell population has on direct astrocyte-to-neuron conversion. The cell population of origin (e.g. mouse cortical astrocytes, human brain pericytes, mouse cortical OPCs) is indeed an intrinsic factor playing an important role in the promotion of forced neurogenesis (reviewed in Falk and Karow 2018) (see sections 1.3.2 and 1.3.3). Astrocytes constitute an heterogeneous population in terms of morphology, transcriptome and function (reviewed in Farmer and Murai 2017). Moreover, Karow and colleagues recently published a study in which they identified subpopulations of pericytes with different competence for neuronal reprogramming (Karow et al. 2018). It is therefore of interest to understand whether an intrinsic factor, such as the heterogeneity of mouse cortical astrocytes, is associated to different outcomes of forced neurogenesis. This knowledge will provide fundamental information that might help improving direct astrocyte-to-neuron conversion strategies *in vivo*. In order to determine whether the heterogeneity of astroglia (reviewed in Khakh and Sofroniew 2015, Sofroniew 2009) influences the susceptibility of astrocytes to neuronal fate-switch, I have adapted an *in utero* electroporation-based clonal analysis system to suit the needs of *in vivo* direct conversion of cortical astrocytes into neurons.

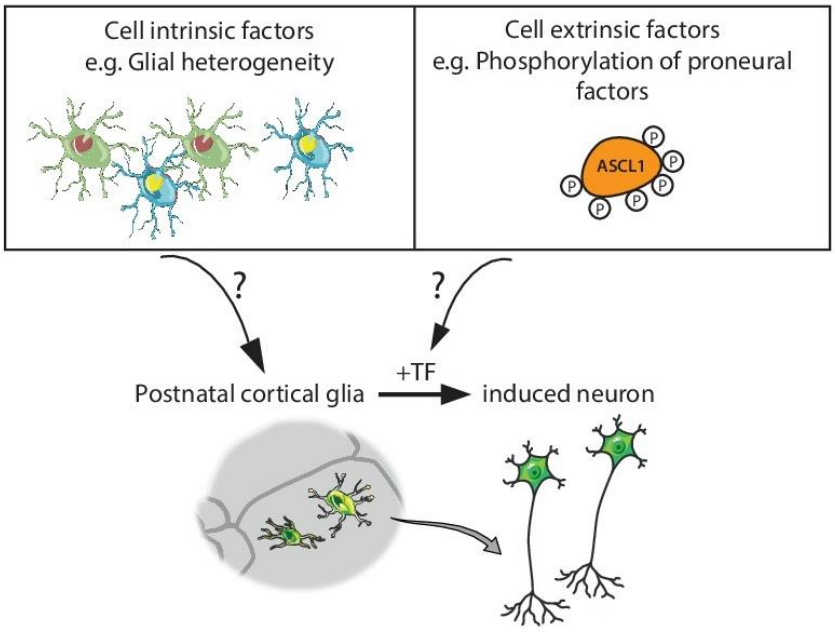

Fig.3.1 Cell intrinsic and cell extrinsic factors in direct glia-to-neuron conversion. The role of cell extrinsic factors, such as the phosphorylation status of proneural transcription factors exogenously expressed to induce cell fate-switch (right side), and cell intrinsic factors, such as the heterogeneity of the starting cell population (left side), in direct reprogramming of mouse postnatal cortical glia into neurons *in vivo* has been investigated in this study. TF= Transcription Factor.

3.2 Role of the phosphorylation state of ASCL1 in directing glia-to-neuron reprogramming

3.2.1 *pAscl1* converts postnatal cortical glia into neurons *in vitro* but not *in vivo*

First, I determined whether the pASCL1 proteins had different ability to induce forced cell fate-switch *in vitro*. In the past decade, it has been shown that retroviral-mediated or lipofection-mediated forced expression of the proneural gene *Ascl1* in cultured astrocytes isolated from the cortex of P5-7 mice successfully induced conversion into neurons (Berninger et al. 2007; Heinrich et al. 2010, 2011; Masserdotti et al. 2015). Consistent with these data, I observed about 30% of induced neurons generated after transduction of cortical postnatal astrocytes with a retroviral vector encoding for the wild type *Ascl1* gene (Fig.2.3C). Moreover, the phospho-deficient mutant yielded a higher proportion of induced neuronal cells among transduced cells (circa 51%, Fig.2.3C) compared to wild type *Ascl1*, thus highlighting a more efficient forced neurogenic effect *in vitro*. Increased neurogenesis upon expression of the *Ascl1SA6* mutated gene was already observed during embryonic development, first in *Xenopus* after injections of lentiviruses in the oocyte, and then in the embryonic cortex of mice after *in utero* electroporation (Li et al. 2014; Ali et al. 2014). The phospho-deficient mutant was also found to have a higher forced-conversion efficiency of human fibroblasts into neurons *in vitro* when co-expressed with

Neurog2 or *Brn2* and *Myt1l* (Ali et al. 2014). Interestingly, the phospho-mimetic mutant yields lower forced neurogenesis compared to the phospho-deficient one (37% of induced neurons among transduced cells, Fig.2.3C). A more pronounced difference in neurogenesis induced by phospho-mutant proneural proteins was observed by Quan and colleagues, who mutated a residue within the bHLH motif of mouse *Neurog2*, which is target of phosphorylation, either into an alanine (A) or into an aspartic acid (D) residue. They found that the phospho-deficient mutant induces neurogenesis, while the phospho-mimetic functions as a strong loss of function allele (Quan et al. 2016). This seems to be due to the fact that the location of the residue in the protein influences its DNA binding abilities, introducing a repulsion between the transcription factor and the DNA in presence of the negatively charged aspartic acid (Quan et al. 2016). However, the six S/P residues targeted in the *Ascl1*-expressing plasmids used in this study are located outside of the bHLH domain, thus hinting at a possible different mechanism, as will be discussed in more detail later.

Surprisingly, the overall efficiency of direct glia-to-neuron conversion was higher in transfection experiments than in transduction ones, but was also accompanied by a higher dispersion of the data values upon transfection (Fig.2.2D and 2.3D). The reason for this higher percentage of induced neurons quantified in transfected cultures could be due to the fact that transfection is less efficient and gives a less stable reporter-signal. In fact, plasmids internalised by the cell via lipofection need to enter the nucleus for transcription (Dean et al. 1999). Once in the nucleus, they can undergo nuclear exclusion upon cell proliferation and be relocated in the cytoplasm of daughter cells, where the exogenous genes cannot be transcribed (Ludtke et al. 2002). Moreover, cell proliferation leads to a dilution of the copy-number per cells (Ludtke et al. 2002; Dean et al. 1999), which means that daughter cells of proliferating cells will express less fluorescent reporter protein. Transfected cultures will therefore tend to give an overestimate of the number of induced neurons, which don't proliferate, versus the number of astrocytes, which proliferate and can lose fluorescent signal. Conversely, the retroviral vector used for this study integrates its DNA in the genome of the host cell (Naviaux et al. 1996), thus leading to stable and inheritable expression of the inserted genes.

After determining that the pASCL1 proteins can induce astrocyte-to-neuron conversion *in vitro*, I transduced cortical glia of P5 mouse cortices with *pAscl1*-expressing retroviruses and the outcome was analysed at 12 days post injection (dpi) (Fig.2.6A). Exogenous pASCL1 expression resulted in very low percentage of induced neurons among transduced cells (Fig.2.7C). The unsuccessful neuronal cell fate-switch might be due to the lack of injury in the experimental paradigm. In fact, transcription factors-mediated direct conversion of adult cortical glia into neurons *in vivo* has been so far achieved in the presence of a pre-existing injury, such as a stab wound, or degeneration, such as Alzheimer's Disease (Fig. 1.5) (Gascón et al. 2016; Guo et al. 2014; Heinrich et al. 2014). Cells around the injury site react to the stimulus by assuming a so called "reactive" phenotype (reviewed in Robel et al. 2011, Sofroniew

2009) and acquire characteristics typical of neural stem cells (Buffo et al. 2008). Three days after stab wound injury, cortical astroglia upregulates the expression of GFAP (Buffo et al. 2008) and by day 7 some resident astrocytes around the injury site start to proliferate (Bardehle et al. 2013; Buffo et al. 2008). GFAP-positive cells isolated from the injured cortex are able to form multipotent neurospheres (Buffo et al. 2008), a property typical of neural stem cells (Morshead et al. 2003), while cells derived from the uninjured cortex do not. Thus, reactive astrocytes acquire a progenitor-like state that allows them to change their lineage fate (reviewed in Robel et al. 2011). Even though Guo and colleagues proposed that the viral injection itself can be considered as an injury in the adult mouse cortex (Guo et al. 2014), immunohistochemistry for GFAP shows that cells transduced with the pCAG-IRES-DsRed control retrovirus do not exhibit signs of hypertrophy at 3dpi as compared to the non-injected hemisphere (Fig.2.4). This is in contrast to what observed by Heinrich and colleagues, who detected reactive astrogliosis in the ipsilateral adult cortex after stab wound injury (Heinrich et al. 2014). The pool of cells becoming "reactivated" has been identified with genetic fate mapping as quiescent astrocytes (Buffo et al. 2008). However, postnatal cortical astrocytes proliferate (Ge et al. 2013), thus pointing at a possible partial lack of reactive astrogliosis in the postnatal brain. Moreover, as described in section 2.1.4, *pAscl1* does not require reactive astrogliosis to convert cortical glia into neurons.

Noteworthy, direct reprogramming of cortical glia into neurons seems to be context-dependent. In fact, *Ascl1* alone fails to convert glia into neurons in the injured adult cortex, while it successfully does it when co-expressed with *Sox2* (Heinrich et al. 2014). In the absence of injury, striatal astrocytes can be converted into neurons through expression of *Sox2* only (Niu et al. 2015, 2013) and hippocampal glial neural progenitors can be converted into oligodendrocytes through expression of *Ascl1* (Braun et al. 2015; Jessberger et al. 2008). In the postnatal cortex, as opposed to the adult one, astrocytes are still actively proliferating (Ge et al. 2013). Thus, the cortical postnatal environment is different from the adult one and proliferating postnatal astroglia differs from the quiescent adult one, which might lead to a different neurogenic response. Nevertheless, there might be other barriers hampering forced cell fate-switch in the postnatal cortex, and the fact that local astrocytes proliferate until P21 (Ge et al. 2013) seems to not be sufficient to induce p*Ascl1*-mediated glia-to-neuron conversion.

3.2.2 *pAscl1*-induced change in the proportion of OPCs and oligodendrocytes *in vivo*

Despite the lack of conversion into neurons, cells transduced with *pAscl1* exhibited a change of phenotype within the glial lineages, as revealed by four observations. Firstly, all three proteins induced a sharp reduction in the proportion of cells expressing GFAP (from 63.9% with a *DsRed*-expressing vector, to about 20% with each of the *pAscl1*-expressing vectors, Fig.2.8C). Secondly, some cells expressing the phospho-mutants co-express the astroglial marker GFAP and the pan-oligodendroglial marker SOX10 (Fig.2.9B). The lower proportion of GFAP-positive astrocytes and higher proportion of

oligodendroglial cells (Fig.2.8C-C') could be due to cell fate-switch of astrocytes into cells of the oligodendroglial lineage. The surprising emergence of GFAP/SOX10-double positive cells upon expression of *pAscl1*, a population that is absent in controls (Fig.2.9C), would also point to astrocyte-to-OPCs conversion. Notably, retrovirus-mediated expression of *Ascl1* in the dentate gyrus of adult mice demonstrated a capacity of *Ascl1* in forced oligodendrogenesis. At 4 weeks after transduction, cells expressing exogenous ASCL1 protein were located in the hilus of the uninjured dentate gyrus, have glial morphology and express markers typical of OPCs and mature oligodendrocytes (Braun et al. 2015; Jessberger et al. 2008). The expression of *Ascl1* exhibited also a much higher conversion rate of hippocampal neuronal progenitors into OPCs than *Olig2* or *Sox10*, it induced formation of mature myelinating oligodendrocytes and rescued hilar myelination in a demyelination model (Braun et al. 2015). However, despite this published evidence of the forced conversion of glial neural progenitors into OPCs by *Ascl1*, it is not possible to establish yet the identity of the cell population influenced by the exogenous expression of *pAscl1*. In fact, the two main cell populations I found to be transduced by the MoMLV-derived retrovirus are GFAP-positive astrocytes and SOX10-positive oligodendroglial cells (Fig. 2.4D), which both proliferate at this stage of cortical development (Ge et al. 2013; Nakatani et al. 2013) and are therefore susceptible to transduction with the retroviral vector used (Roe et al. 1993). Heinrich and colleagues showed by means of lineage tracing that the cell population they converted into neurons by co-expression of *Sox2* and *Ascl1* was NG2-positive glia, namely OPCs, rather than reactive astrocytes (Heinrich et al. 2014). Thus, lineage tracing experiments will help to determine whether *pAscl1*-induced oligodendroglial cells derive from direct conversion of astrocytes. Knowing if the oligodendroglial cells quantified at 12dpi derive from astrocytes or from OPCs will be of importance, to understand if *pAscl1* indeed induces astrocyte-to-OPC conversion.

Thirdly, there is an increase in the proportion of SOX10-positive cells of the oligodendroglial lineage when transduced cells express the pASCL1 proteins (Fig.2.8C'). Fourthly, the wt ASCL1 protein induces an increase in the proportion of SOX10-positive OPCs (Fig.2.10C), while expression of the phospho-mutants increases the proportion of APC-positive oligodendrocytes (Fig.2.10C'). An alternative explanation to the astrocyte-to-oligodendrocyte conversion interpretation for the changes in the proportion of glial cells in *pAscl1*-transduced cell population is that pASCL1 could have an effect on proliferation and differentiation, given the higher proportion of OPCs and of oligodendrocytes induced by ASCL1 wt and the phospho-mutants, respectively (Fig.2.9C-C'). In fact, it is known that *Ascl1* is expressed in a subset of OPCs during mouse cortical embryonic development and after birth (Parras et al. 2007; Parras et al. 2004). However, the presence of ASCL1 is required only for the generation of the first wave of OPCs, around E12.5 (Parras et al. 2007), while at later stages it is not necessary, perhaps due to the expression of other genes mediating oligodendrogenesis (Li et al. 2014; Parras et al. 2007). Interestingly, tamoxifen-induced ablation of *Ascl1* at P5 or P8-9 showed that after 7 days, OPCs of the

subependymal zone proliferate more, and asymmetric divisions generating one OPC and one oligodendrocyte (OPC/OL) are reduced in favour of symmetric divisions generating two OPCs (OPC/OPC) (Nakatani et al. 2013). Interestingly, the rate of symmetric divisions generating two oligodendrocytes is not affected by loss of *Ascl1* (Nakatani et al. 2013). Thus, *Ascl1* controls proliferation and differentiation of OPCs, favouring asymmetric divisions at the expense of symmetric OPC/OPC divisions. Such control of proliferative events would be expected to result in more reporter-positive OPCs and oligodendrocytes upon expression of wild type *Ascl1*. However, the effect of ASCL1 on cortical cells at 12dpi illustrated in this study leads to an increase only in the proportion of OPCs among transduced cells (Fig.2.10C), suggesting a possible increase in symmetric OPC/OPC divisions. This different proportion of oligodendroglial cells might depend on other mechanisms compensating in the long term the *Ascl1*-mediated effect, as suggested by a return to proportions of OPCs and oligodendrocytes similar to wild type conditions in *Ascl1-/-* mice at 28dpi (Nakatani et al. 2013) or on the fact that cortical OPCs behave differently than their counterparts in the subependymal zone. It could also be that *Ascl1* increases the survival of transduced OPCs. Lineage tracing experiments with a GLAST::CreERT2 (Buffo et al. 2008) and a Sox10-iCreERT2 (Simon et al. 2012) are required to determine whether *pAscl1*-induced oligodendroglial cells derive from direct conversion of astrocytes or from OPCs, respectively, and the use of BrdU/EdU paradigms could aid to unravel the proliferative behaviour of cells transduced with *pAscl1*-expressing retroviruses.

3.2.3 Role of ASCL1 phosphorylation in the induction of OPCs and oligodendrocytes

Immunohistochemical analysis of brains 12 days after injecting the *pAscl1*-expressing retroviruses revealed that the ASCL1-mediated effect on cells of the oligodendroglial lineage appears to be phosphorylation-dependent (Fig.3.2). First, the phospho-mutants do not increase the proportion of SOX10-positive cells compared to a control expressing only the fluorescent reporter DsRed (Fig.2.9C' and 2.10C). Recent work demonstrated that the RAS/ERK signalling pathway modulates the decision between gliogenesis and neurogenesis by directly phosphorylating ASCL1 during mouse development (Li et al. 2014). The wild type protein has gliogenic potential when RAS/ERK signalling is activated at high levels, inducing predominantly oligodendrogenic fate, while at low levels of RAS/ERK signalling ASCL1 transactivates the *Dlx1/2* genes (Li et al. 2014), hinting that high levels of ASCL1 phosphorylation are driving formation of OPCs while lower levels drive neurogenesis. The observation that wild type ASCL1 induces higher OPCs formation compared to control-injected postnatal brains (Fig.2.10C), suggests that the niche environment allows phosphorylation of ASCL1. However, this would not explain why the phospho-mutants increased the proportion of oligodendroglial cells (Fig.2.8C', 2.10C'). Expression of the phospho-deficient ASCL1SA6 protein in the mouse embryonic brain at E12.5 or in the oocytes of *Xenopus* resulted in increased neurogenesis (Ali et al. 2014; Li et al. 2014) and showed that the lack of

phosphorylation on ASCL1 has a neurogenic effect in a *Dlx*-independent manner (Li et al. 2014). However, constitutively active RAS is able to induce in *Ascl1-/-* embryos a proportion OLIG2-positive cells similar to the one induced in wild type embryos (Li et al. 2014). Thus, it is possible that if the niche conditions are supporting high RAS/ERK activity, the high level of RAS pathway activity are compensating for the lack of phosphorylation of ASCL1 and determine an oligodendrogenic fate. The fact that between P15 and P18 the levels of phosphorylated ERK (pERK) are elevated (Galabova-Kovacs et al. 2008) supports this interpretation.

Second, the phospho-mutants induce a higher proportion of APC-positive oligodendrocytes compared to wild type ASCL1 (Fig.2.10C'). Third, the phospho-mimetic mutant had an effect similar to the one of the phospho-deficient (Fig.2.8C-C', 2.9C and 2.10C-C'). Co-expression of ASCL1SA6 in human fibroblasts with either NEUROG2 or BRN2/MYT1L resulted higher maturation of induced neurons, as compared to expression of wild type ASCL1 (Ali et al. 2014). Moreover, exogenous expression of *Ascl1* has already been shown to induce gradual maturation of *Ascl1*-derived oligodendroglia in the adult hippocampus (Jessberger et al. 2008). Thus, it is possible that loss of phosphorylation leads to increased maturation of the oligodendroglial cells transduced by a *pAscl1*-expressing retrovirus. Notably, rather than having a loss-of-function effect like the phospho-mimetic mutant of mouse NEUROG2 (Quan et al. 2016), ASCL1SD6 had an effect similar to the one of the phospho-deficient mutant, inducing an increase in the proportion of oligodendrocyte (Fig.2.10C'). It is possible that, despite mimicking the presence of negatively charged phosphorylation-moieties, the six aspartic acid residues on ASCL1SD6 modify the binding of the proneural factor to DNA target sites or co-factors, thus leading to the activation of different pathways downstream of *Ascl1*. A bHLH transcription factor that is not classified as a proneural factor but is expressed in oligodendroglial cells, OLIG2, is phosphorylated at S147 during embryonic development of the spinal cord, thus forming homodimers and leaving NEUROG2 available for binding to E47 and induction of motor neuron formation. However, when oligodendrogenesis begins it is de-phosphorylated and binds preferentially to other bHLH transcription factors, consequently inducing OPCs generation (Li et al. 2011). The role of the zinc-finger protein ZFP24 in proliferation and differentiation of OPCs is regulated by phosphorylation too. When the transcription factor is de-phosphorylated, it binds target genes that specify OPCs, while upon phosphorylation it binds to target genes specifying oligodendrocyte maturation (Elbaz et al. 2018). These studies point to a phosphorylation-dependent choice of dimerization partners and DNA binding for transcription factors, as described for OLIG2 and ZFP24. This raises the possibility that, despite mimicking the constitutive presence of phosphorylation, the conformation of the ASCL1SD6 protein is modifying its binding abilities hampering binding to the targets of wt phosphorylated ASCL1. Moreover, the elevated levels of pERK in the postnatal murine brain (Galabova-Kovacs et al. 2008) could be determining an oligodendrogenic fate also in cells expressing the phospho-mimetic mutant. Further experiments to determine the DNA-

binding abilities of the pASCL1 proteins, or their preference of binding partner will help understanding the mechanisms underpinning their role in postnatal cortical glia.

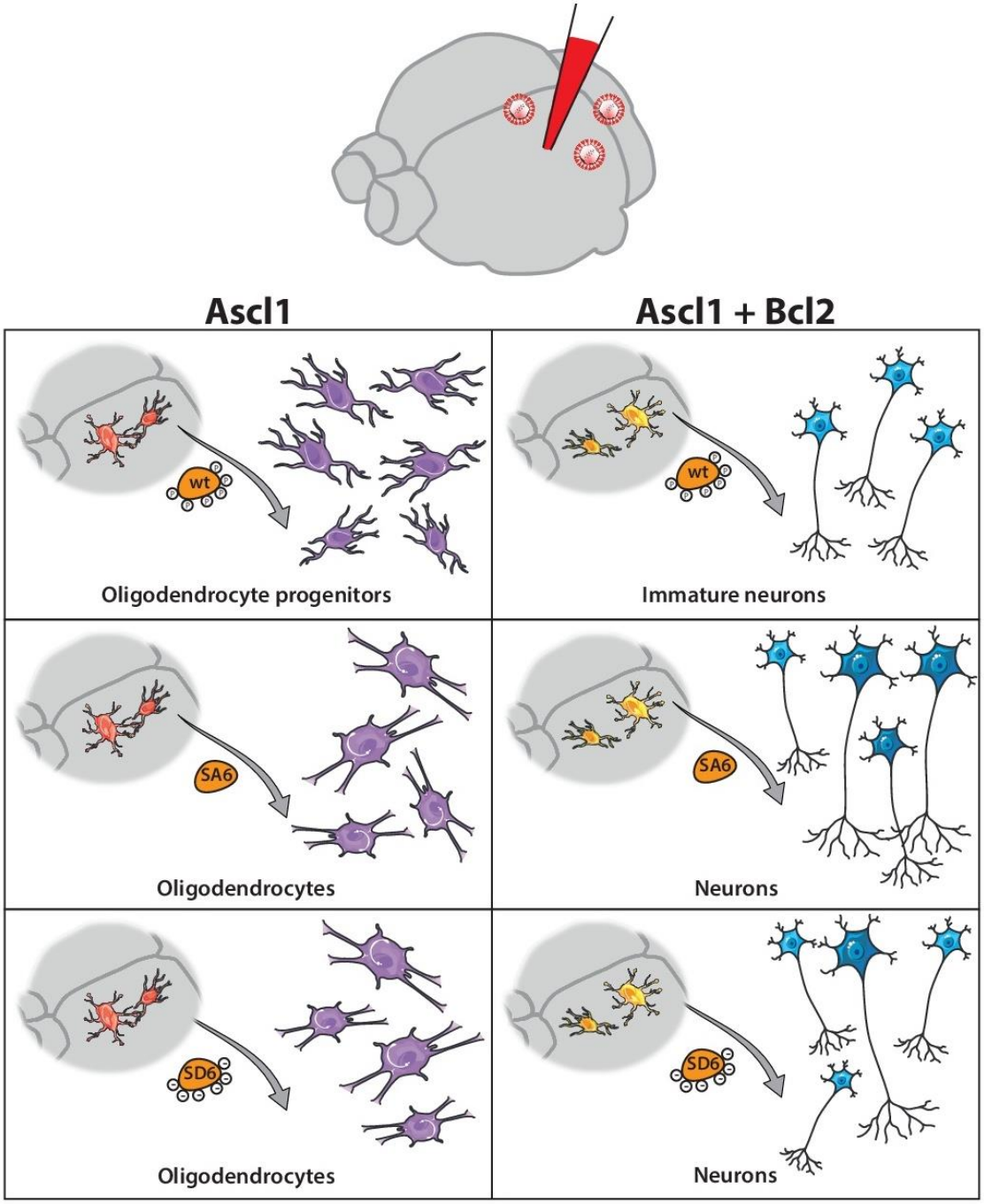

Fig.3.2 pASCL1-mediated cell fate-switch: graphical abstract. Cortical glia of P5 mice transduced with retroviruses encoding for *pAscl1* (left panel, red) or for *pAscl1* and *Bcl2* (right panel, yellow). Exogenous expression of pASCL1 only affects the glial population. The wild type protein (wt) increases the proportion of OPCs, while the phospho-deficient (SA6) and phospho-mimetic (SD6) mutants favour oligodendrocytes production. When co-expressed with *Bcl2*, *pAscl1* successfully converts cortical glia into neurons. ASCL1 wt expression results in production of a lower percentage of DCX-positive immature neurons (Table2.1), compared to the phospho-mutants. The two mutant ASCL1 proteins result in high efficiency of neuronal conversion but also higher maturation of induced neurons.

3.2.4 Role of ASCL1 phosphorylation in the *pAscl1/Bcl2*-mediated neuronal conversion of postnatal cortical glia

Co-expression of *Bcl2* with the proneural transcription factor *Neurog2* successfully converts adult cortical glia into neurons in the presence of injury (Gascón et al. 2016). In order to investigate whether *Bcl2* has a role in *pAscl1*-induced cell fate-switch in the postnatal uninjured cortex, I have analysed cells co-transduced with *pAscl1*- and *Bcl2*-expressing retroviruses at 12dpi (Fig.2.11). Immunohistochemistry for the neuronal markers DCX and NeuN showed abundant generation of induced neurons in cells co-transduced with *pAscl1*- and *Bcl2*-expressing retroviruses (Fig.2.12 and 2.13, Table 2.1). Notably, upon co-expression of wild type *Ascl1* and *Bcl2* I have quantified at 12dpi about 26% of DCX-positive immature neurons (Fig.2.12D) and about 5% of NeuN-positive mature neurons (Fig.2.13D). Interestingly, I have observed also about 12% of cells co-expressing DCX and NeuN among reporter-positive ones (Fig.2.14D), indicating the presence of neuronal cells undergoing maturation (Brown et al. 2003). The ability of ASCL1 to force direct conversion of postnatal cortical glia co-expressing *Bcl2* into neurons seems to be phosphorylation-dependent.

Firstly, the phospho-mutants exhibit a direct cell fate-switch rate of circa 70% when co-expressed with *Bcl2*, as compared to circa 45% for wild type *Ascl1* (Table 2.1). The higher neurogenic ability of the phospho-deficient mutant confirms previous findings obtained upon ectopic expression of ASCL1SA6 *in vivo,* in which it increased neurogenesis during *Xenopus* and mouse development (Ali et al. 2014; Li et al. 2014). Moreover, *in vitro* conversion of human fibroblasts into neurons led to increased neuronal conversion of ASCL1/NEUROG2- or BAM-induced neurons upon *Ascl1SA6* exogenous expression (Ali et al. 2014). Notably, the work of Li and colleagues demonstrated that ASCL1 phosphorylation in the murine embryonic cortex is mediated by RAS/ERK signalling in a dosage-dependent way (Li et al. 2014). By placing *Ras* gene under the control of the EF1-*alpha* promoter, the level of activation of *Ras* is low and RAS has reduced ability to induce phosphorylation of ERK (Li et al. 2014). Upon low level of *Ras* activation, *Ascl1* induces GABAergic neurogenesis, while upon constitutive activation of *Ras* (achieved by exogenous expression of the constitutively active protein RASV12 in a pCIG2 vector) *Ascl1* induces gliogenesis (Li et al. 2014). Thus, it is likely that ASCL1 is less successful in inducing forced neurogenesis than ASCL1SA6 because of the presence of increasing RAS/ERK signalling in the postnatal brain between P5 and P10, that would phosphorylate ASCL1. The potential involvement of signalling mechanisms in *pAscl1*-mediated glia-to-neuron conversion are discussed more in depth in session 3.2.5.

Secondly, the SD6 mutation induces an intermediate phenotype between that of the wild type protein and that of the phospho-deficient protein, exhibiting higher levels of forced neurogenesis than ASCL1 wt (Table 2.1). The levels of neurogenesis induced by ASCL1SD6 could be linked to a higher resistance to NOTCH-mediated lateral inhibition of the phospho-mimetic mutant. In fact, *Ascl1* is sensitive to lateral inhibition and its expression in the *Xenopus* oocyte fails to induce neurogenesis (Ali et al. 2014).

However, loss of phosphorylation in the SA6 mutant results in resistance to NOTCH-mediated lateral inhibition and induction of neuronal differentiation (Ali et al. 2014). Lateral inhibition is involved in the oscillatory expression of *Ascl1* and *Hes1* in neural progenitors: high and low levels of *Ascl1* expression correspond to low and high levels of *Hes1* expression, respectively, in a negative-feedback loop of gene regulation (Imayoshi et al. 2013). When neural progenitors differentiate into neurons, ASCL1 protein is expressed in a sustained manner (Imayoshi et al. 2013). If the SD6 mutation confers ASCL1SD6 binding properties different than the ones of ASCL1, it could be resistant to NOTCH-mediated lateral inhibition, thereby inducing neuronal differentiation (Ali et al. 2014). It would be interesting to determine whether the three pASCL1 proteins are actually binding different co-factors, via pull-down assays. Another possible explanation for the phenotype of *Ascl1SD6/Bcl2*-transduced cells might be that the binding affinity of ASCL1SD6 is not the same one of the wild type ASCL1 protein, whereby the mutant protein cannot bind the same targets of phosphorylated ASCL1. It would be thus interesting to investigate the DNA-binding ability of the pASCL1 proteins via ChIP-sequencing (ChIP-seq) experiments. In ChIP-seq, after the creation of protein-protein and DNA-protein cross-links, the DNA is sonicated and then immunoprecipitated (Milne et al. 2009). The analysis of the precipitated DNA allows the identification of histone modifications and DNA binding sites for proteins (Milne et al. 2009). This would help elucidating the transcriptional programs initiated by pASCL1 and whether they differ in the specification or maturation of neurons. A study involving ChIP-seq of BAM-expressing and ASCL1-expressing fibroblasts revealed that ASCL1 binds in both cases the same targets on the genome, without needing cooperation with BRN2 and MYT1L, thereby acting as a "pioneer factor" (Wapinski et al. 2013). Interestingly, upon *Ascl1*-mediated direct reprogramming, the genomic region of *Brn2* gene becomes accessible around 5 days after *Ascl1* induction (Wapinski et al. 2017). In fact, ASCL1 induces rapid chromatin changes after binding to its targets, opening chromatin at neuronal genes-associated regions and increasing chromatin accessibility within 12 hours after induction of the proneural gene, thus leading to a cascade of transcription factors' activation that, by day 5, transitions to late neuronal programs (Wapinski et al. 2017). Thus, given the role of ASCL1 as pioneer factor and in inducing chromatin accessibility during cell fate-switch, it will be interesting to determine whether the phospho-mutants induce the same chromatin-remodelling events and activate the same transcription factor cascades as the wild type protein. Another possible difference in the phenotype of *Ascl1/Bcl2* and *Ascl1SD6/Bcl2*-transduced cells could be that the phospho-mimetic mutant is less susceptible to ubiquitination. Noteworthy, phosphorylation can function as a signal for ubiquitination (Hunter 2007). It has been recently demonstrated that chromatin-bound ASCL1 is post-translationally modified by addition of short ubiquitin chains that confer lower susceptibility to proteasomal degradation, while cytoplasmic ASCL1 carries long ubiquitin chains (Gillotin et al. 2018). The different type of ubiquitination results in about double half-life of chromatin-bound ASCL1 (Gillotin et al. 2018). In case of involvement

of phosphorylation in the ubiquitination of the protein it is possible that the phospho-mimetic construct exhibits lower susceptibility to the degradation-mechanism, thus remaining for longer time in the cell nucleus. Further experiments to determine the half-life of the phospho-mutants and their ubiquitination state will help understanding whether the phosphorylation of ASCL1 has an impact on its degradation.

Thirdly, the phospho-deficient mutant induced a higher percentage of NeuN-positive and DCX/NeuN-positive cells, as compared to the phospho-mimetic (Table 2.1). Fibroblast-derived neurons induced by ASCL1SA6/NEUROG2 or BAM factors containing ASCL1SA6 showed also a higher level of maturation, with increased branching and neurite length, than the ones induced by ASCL1 (Ali et al. 2014), thus indicating that loss of phosphorylation on ASCL1 could promote neuronal maturation. Notably, the expression of the interneuronal marker GABA I observed at 12dpi is barely detectable or at low levels in cells transduced with *pAscl1/Bcl2* (Fig.2.15), thus indicating that while cells expressing the phospho-mutants reach morphological maturation (Fig.2.13A'-A'') and show increased expression of the mature neuronal marker NeuN (Fig.2.13D, Table 2.1), they might not yet be functionally mature or might acquire an alternative neuronal fate. It has recently been shown that pericytes-derived neurons induced by forced expression of *Ascl1*, *Sox2* and *Dlx1* (ASD) first transition to a neural stem cell-like state and then bifurcate into two alternative lineages: the majority of reprogrammed cells express interneuronal genes, while a smaller set of cells expresses genes of the glutamatergic specification program (Karow et al. 2018). Interestingly, one of the genes induced during ASD-mediated reprogramming is *Myt1* (Karow et al. 2018), which acts downstream of *Ascl1* to repress Notch signalling and the progenitor state of the cells, thus promoting neuronal differentiation (Vasconcelos et al. 2016). MYT1L, a transcription factor related to MYT1 and used in the combination of factors BAM (*Brn2*, *Ascl1*, *Myt1l*) to induce direct conversion of fibroblasts into neurons, represses many somatic lineage programs, except the neuronal one, during reprogramming (Mall et al. 2017). Moreover, the transcriptional repressor REST competes with NEUROG2 for binding on the regulatory regions of NEUROG2 targets, making them no longer accessible and thereby hampering the unravelling of the alternative non-astrocytic lineage program (Masserdotti et al. 2015). Thus, the fact that direct neuronal reprogramming requires silencing of alternative lineage programs to promote neuronal differentiation, and that induced neurons can acquire alternative transmitter identities, points to the possibility that *pAscl1/Bcl2*-induced neurons could acquire a glutamatergic rather than GABAergic identity. The finding that some *pAscl1/Bcl2*-induced neurons express the mature neuronal marker NeuN at 12dpi suggests that these reprogrammed cells could reach functional maturation at later time points. Heinrich and colleagues showed in 2014 that adult cortical OPCs co-expressing *Sox2* and *Ascl1* can be converted into neurons after stab-wound injury. By 24dpi, some of these induced neurons exhibit action potential-like spikes in response to injected depolarising currents and received some spontaneous synaptic inputs (Heinrich et al. 2014), indicating that they acquired neuronal functional properties but remained rather immature after almost one

month from the retroviral transduction. However, *Ascl1SA6/Bcl2*-transduced cells exhibit high-frequency firing pattern and spontaneous synaptic inputs at 4wpi (Fig.2.16), pointing out that co-expression of *Bcl2* and the phospho-deficient mutant induces the reprogramming of cortical glia into neurons that can functionally mature and integrate in the cortical circuitry. Interestingly, the higher firing frequency recorded in current-clamp (Fig.2.16C, Heinrich et al. 2014 for comparison), indicates that *Ascl1SA6/Bcl2*-induced neurons reach a higher level of functional maturation than *Sox2/Ascl1*-induced neurons, which show instead functional features typical of immature neurons. Additional electrophysiological recordings at 4wpi will help determining whether *Ascl1/Bcl2*- and *Ascl1SD6/Bcl2*-induced neurons can reach a functional maturation similar to the one of *Ascl1SA6/Bcl2*-induced neurons.

The *in situ* formation of induced neurons in the murine cortex, together with the transplantation of induced neurons, is an emerging strategy that could help in the future to replenish the pool of neuronal cells lost and to ameliorate circuits disfunctions during neurodegenerative diseases, e.g. epilepsy or Parkinson Disease (reviewed in Heinrich et al. 2015, Dehorter et al. 2017). To this purpose, it will be important also to specify different subtypes of interneurons. To date, the formation of specific interneuronal subtypes via direct reprogramming of cortical glia *in vivo* has not yet been achieved (reviewed in Dehorter et al. 2017). However, cell fate-switch of OPCs into neurons via *Ascl1/Lmx1a/Nurr1* in the striatum yielded induced neurons that reached functional maturation by 12wpi (Pereira et al. 2017). The majority of these induced neurons became fast-spiking parvalbumin (PV)-positive interneurons (Pereira et al. 2017). Similarly, neurons derived by conversion of fibroblasts with *Ascl1/Sox2/FoxG1/Dlx5/Lhx6 in vitro* mature and become express PV by 21div (Colasante et al. 2015). Interestingly, the majority of these induced neurons die after transplantation in the adult murine hippocampus and the surviving cells express GABA but not PV; the surviving neurons successfully integrated in the host circuitry and exhibited inhibitory activity of endogenous granule neurons (Colasante et al. 2015). It is possible that the cortical circuitry maintains the homeostasis of the network and limits the survival of transplanted or reprogrammed interneurons, for instance by controlling their integration and survival in an activity-dependent manner (reviewed in Dehorter et al. 2017; Wong et al. 2018). It will be interesting to determine whether *Ascl1SA6/Bcl2*-induced neurons that exhibit high firing frequency at 4wpi become PV-expressing interneurons, and whether other subtypes of interneurons are specified by *Ascl1* in the postnatal cortex.

3.2.5 Pathways potentially involved in pASCL1-mediated glia-to-neuron reprogramming

Given the role of *pAscl1* in forced cell fate-switch illustrated in this study, it will be interesting to understand which signalling pathways are taking place in the postnatal brain and mediating *pAscl1*-induction of neurogenesis. Phosphorylation of ASCL1 has been described to be mediated by CDK2 in the *Xenopus* oocyte (Ali et al. 2014), or by RAS/ERK signalling in mouse embryonic cortical development (Li et al. 2014) (Fig. 3.3). RAS/ERK signalling activates cell proliferation-related programs and, in the postnatal brain, is required for oligodendrocyte differentiation (Galabova-Kovacs et al. 2008; reviewed in Molina and Adjei 2006), while CDK2 is required for the S/G2 transition of the cell cycle (Rosenblatt e al. 1992).

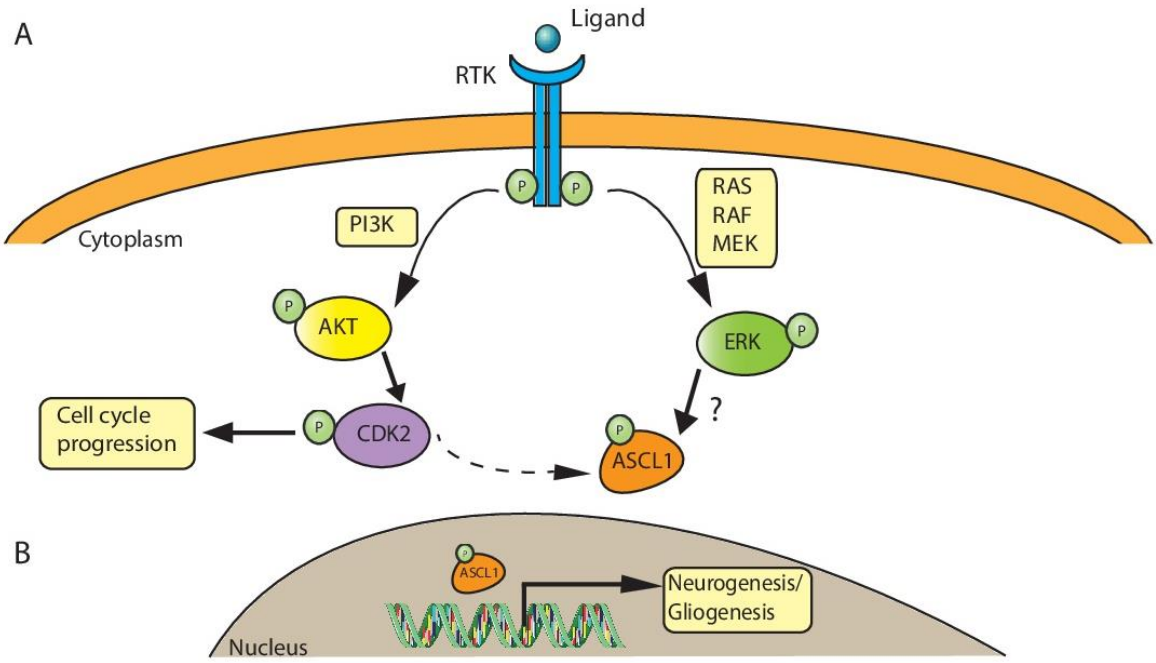

Fig. 3.3 Signalling pathways potentially involved in pASCL1-mediated glia-to-neuron conversion. A, The phosphorylation of ASCL1 has so far been described to be mediated by RAS/ERK pathway (Li et al. 2014) and CDK2 (Ali et al. 2014). Activation of RTKs by their ligands, lead to phosphorylation of ERK or AKT (Li et al. 2014; Maddika et al. 2008). Active RAS/ERK signalling leads to phosphorylation of ASCL1 in the mouse embryonic cortex (Li et al. 2014). AKT phosphorylates and activates CDK2 (Maddika et al. 2008), which has been implied in the regulation of ASCL1 phosphorylation in *Xenopus* oocyte (Ali et al. 2014). However, it is not known what is the role of CDK2 in ASCL1 phosphorylation. B, In the nucleus, ASCL1 exerts its activity of transcriptional control. Depending on the level of activity of RAS/ERK pathway, ASCL1 activates a gliogenic or a neurogenic program during embryonic cortical development (Li et al. 2014). RTK= Receptor Tyrosine Kinase.

CDK2 is phosphorylated and thereby activated by AKT, in a signalling cascade activated by EGF (Maddika et al. 2008). However, exogenous expression of an active form of *Akt* revealed that AKT does not induce phosphorylation of ERK (Li et al. 2014), an effector of the RAS/ERK pathway (Li et al. 2014; reviewed in Molina and Adjei 2006), and confirmed that the RAS/ERK pathway, but not AKT, is mediating ASCL1 phosphorylation in the embryonic murine cortex (Li et al. 2014).

The increase of phosphorylated ERK (pERK) between P5 and P15 in the mouse brain (Galabova-Kovacs et al. 2008) introduces the intriguing possibility that RAS/ERK signalling could have a role in the *pAscl1*-induced effects described in this study. *B-Raf* is the main effector of RAS/ERK signalling in the postnatal brain, and its genetic ablation leads to loss of pERK, dismyelination, and reduced oligodendrocyte differentiation (Galabova-Kovacs et al. 2008), thus indicating a role for the RAS/ERK signalling pathway in the differentiation of myelinating oligodendrocytes in the postnatal brain. Interestingly, *Ras* activation levels influence the neurogenic activity of *Ascl1*: when *Ras* is constitutively expressed and there is high pERK, *Ascl1* induces gliogenesis; when the *Ras* gene has low activity and there is low phosphorylation of ERK, *Ascl1* induces GABAergic neurogenesis (Li et al. 2014). It is possible that the wild type ASCL1 protein is phosphorylated by RAS/ERK signalling in the postnatal cortex, thus leading to the observed increase in the percentage of SOX10-positive OPCs (Fig. 2.10C), as suggested by the pro-gliogenic effect of high RAS/ERK activity and the fact that exogenous expression of *Ascl1* increases expression of *Dll* and *Sox9*, markers of proliferating progenitors and glial progenitors, respectively (Li et al. 2014). Interestingly, exogenous expression of *Ascl1SA6* induces higher proportion of OPCs (Fig. 2.10C'), which is in contrast with the role described for RAS/ERK signalling in promoting oligodendrocyte differentiation in the postnatal brain (Galabova-Kovacs et al. 2008). Thus, it is likely that other mechanisms are involved in mediating the differentiation of oligodendrocytes upon *pAscl1* expression. Remarkably, *Ascl1SA6/Bcl2* co-expression successfully induces forced neurogenesis in transduced cells (Table 2.1). The fact that ASCL1SA6 seems to mediate oligodendrogenesis rather than neurogenesis when expressed alone, could be due to the fact that the lack of *Bcl2* effect in promoting neuronal reprogramming (discussed in section 3.2.6) leads to occupation by pASCL1 of genomic regions regulating gliogenesis. Alternatively, it could be that in the absence of *Bcl2* neurons do not survive during cell fate-switch, thus making it possible to detect only glial cells via immunohistochemistry.

The RAS/ERK pathway is activated by receptor tyrosine kinases (RTKs), a family of transmembrane receptors with a cytoplasmic tyrosine kinase domain and an extracellular ligand-binding domain (reviewed in Lemmon and Schlessinger 2010). Among the family of RTKs there are the ErbB receptors and EGFR, whose ligand is EGF, and FGF receptors (FGFR), whose ligand is FGF (reviewed in Lemmon and Schlessinger 2010). EGF and FGF have been described to activate RAS/ERK pathway and induce pERK both in the embryonic cortex (Li et al. 2014) and in the postnatal brain (Galabova-Kovacs et al. 2008), thus making them likely candidates for the activation of RAS/ERK signalling and subsequent

induction of *pAscl1*-mediated effects described in this study. Intriguingly, EGF and FGF-2 are used to treat postnatal cortical astrocytes *in vitro* and induce gliogenesis in culture (Heinrich et al. 2011; reviewed in Oliveira et al. 2013). Thus, it would be interesting to determine whether withdrawal of the mitogens from the culture changes the reprogramming efficiency of *pAscl1 in vitro*. This, united with experiments in which the receptors activated by EGF and FGF are inhibited (reviewed in Lemmon and Schlessinger 2010) could help shed light on the mechanism leading to phosphorylation of ASCL1 in the postnatal brain during forced neurogenesis.

3.2.6 Role of *Bcl2* in direct glia-to-neuron reprogramming

The role of *Bcl2* in facilitating *Neurog2*-mediated conversion of cortical glia into neurons was shown to be exerted through alleviation of the excess of reactive oxygen species (ROS) produced during cell fate-conversion, rather than being mediated by its anti-apoptotic function (Gascón et al. 2016). In fact, the process of direct cell fate-switch forces the cells to change their metabolic state from glycolysis to oxidative phosphorylation (OxPhos) (Gascón et al. 2016; Kim et al. 2018), thereby inducing mitochondrial defects typical of cellular aging and loss of ATP to almost half in converted neurons, due to the increased workload (Kim et al. 2018). Moreover, forced neurogenesis induces high levels of ROS, which can be attenuated by administration of anti-oxidants, such as vitamin E, calcitriol and *alpha*-tocopherol, or by *Bcl2* expression (Gascón et al. 2016). This increase in the presence of ROS in cells undergoing lineage conversion is due to a mechanism of programmed cell death called ferroptosis (Gascón et al. 2016; Dixon et al. 2012), which is iron-dependent and doesn't have the same morphological and molecular features of apoptosis, autophagy, necrosis and other known cell death pathways (Dixon et al. 2012; reviewed in Xie et al. 2016). During ferroptosis, mitochondria appear smaller than usual, have higher membrane density and intracellular ATP is depleted (Dixon et al. 2012). Ferroptosis induces accumulation of ROS, which can be reverted by iron chelators (Dixon et al. 2012; Yu et al. 2015). Accumulation of high levels of ROS eventually leads to cell death (Dixon et al. 2012). Exogenous expression of *Bcl2* or vitamin E treatment reduce the levels of lipid peroxidation in cultured postnatal astrocytes undergoing *Ascl1*-mediated cell fate-switch (Gascón et al. 2016), which might promote the survival of induced neurons. It is likely that the role of *Bcl2* in the direct conversion of *pAscl1*-transduced cortical glia into neurons is similar to the one described by Gascón and colleagues.

An interesting perspective into the role of *Bcl2* in facilitating neuronal reprogramming comes from the recent finding that the phosphatase PTEN is involved in the programmed cell death of GABAergic interneurons between P5 and P10, thus sculpting the cortical neuronal network composition (Wong et al. 2018). The mechanism is mediated by the activity of pyramidal neurons, which inhibit – in a non-cell-autonomous manner – PTEN in GABAergic interneurons (Wong et al. 2018). Inhibition of PTEN results in activation of the kinase AKT and subsequent inhibition of apoptosis (Stambolic et al. 1998; Wong et

al. 2018). Thus, given the heterogeneous activity pattern of pyramidal neurons, and the fact that PTEN is active in sparse cells around the cortex at P5-10, there is a wave of programmed cell death of GABAergic interneurons sculpting the cortical circuit (Wong et al. 2018). The presence of active RAS/ERK signalling in the postnatal brain at P5-10 (Galabova-Kovacs et al. 2008) and the fact that RAS kinase activates also the PIP3/AKT pathway (Zalckvar et al. 2009), united with the fact that in my experiments co-transduction with *pAscl1* and *Bcl2* was performed at P5, suggests that *pAscl1/Bcl2*-induced neurons might undergo a similar PTEN-mediated regulation, assuming they are specified into GABAergic interneurons. However, induced neurons positively selected during this wave of programmed cell death could later succumb to ferroptosis-induced accumulation of ROS, and the exogenous expression of *Bcl2* could likely promote their survival. Interestingly, 75% of *Neurog2*/*Bcl2*-induced neurons among co-transduced cells were NeuN-positive cells as early as 10dpi (Gascón et al. 2016). It could be that the anti-oxidant effect accelerates the maturation of induced neurons, through increased cell survival (Gascón et al. 2016).

Interestingly, the function of BCL2 can also be regulated by phosphorylation. In fact, the non-phosphorylated BCL2 protein can bind to BECLIN1 or its activators, thus inhibiting the autophagic process, while phosphorylation of BCL2 disrupts the BECLIN1:BCL2 complex and allows BECLIN1-mediated initiation of autophagy (reviewed in Marquez and Xu 2012; Wei et al. 2008). Upon prolonged phosphorylation of BCL2, the cell eventually undergoes apoptosis mediated by caspase 3 (reviewed in Marquez and Xu 2012; Wei et al. 2008). The main kinase responsible for phosphorylation of BCL2 at the endoplasmic reticulum is JNK1; phospho-deficient and phospho-mimetic BCL2-mutants exhibit lower anti-apoptotic and autophagic effect, and higher anti-apoptotic and autophagic effect, respectively (Wei et al. 2008). Moreover, such mutated constructs revealed that a lack of phosphorylation of BCL2 induces more *Neurog2*-mediated conversion of glia into neurons (Gascón et al. 2016). Given that ROS are generated during forced conversion of astrocytes into neurons (Gascón et al. 2016), and that ROS are an activator of JNK signalling (reviewed in Marquez and Xu 2012; Wei et al. 2008), it is possible that during *Ascl1/Bcl2*-mediate cell fate-switch BCL2 is phosphorylated.

Thus, the role of BCL2 seems to be related to protection of cells from ROS generated during forced lineage conversion via ferroptosis, and might be related to its phosphorylated status. It would be interesting to determine whether there is phosphorylation of BCL2 undergoing in transduced cells, and if so, whether it is key determinant of the success of pASCL1-mediated direct neuronal reprogramming and of the maturation of induced neurons.

3.3 Clonal analysis of induced neurons: establishment of a system for the study of forced cell fate-switch in the context of astroglial heterogeneity

3.3.1 An *in utero* electroporation system to study the role of astroglial heterogeneity in direct reprogramming

In order to determine whether the heterogeneity of astroglia (reviewed in Khakh and Sofroniew 201, Sofroniew 2009) influences the susceptibility of astrocytes to neuronal fate-switch, I have adapted an *in utero* electroporation-based clonal analysis system to suit the needs of *in vivo* direct conversion of cortical astrocytes into neurons. Such system, called StarTrack, has been developed as an *in vivo* clonal labelling system (García-Marqués and López-Mascaraque 2013). It holds different advantages:

- Cell type-specific conditional activation of the transcription factors: the factors used to induce astrocyte-to-neuron conversion were subcloned in plasmids with the hGFAP promoter (Fig. 2.17), thus restricting their expression in astrocytes (García-Marqués and López-Mascaraque 2013). Upon electroporation, the plasmids are internalised by the neural stem cells and neural progenitors of the VZ/SVZ, which can give rise to both glial and neuronal populations (Figueres-Onãte et al. 2016; Fuentealba et al. 2015; Kriegstein & Alvarez-Buylla 2009). Thus, the presence of the hGFAP promoter will allow to restrict cell fate-switch only in one postnatal cortical cell population, namely astrocytes.
- Temporal conditional activation of NEUROG2ERT2 and ASCL1ERT2: the proneural factors NEUROG2 and ASCL1 are fused to a modified version of the oestrogen receptor (Fig.2.17), which allows their activation only upon treatment with tamoxifen (Littlewood et al. 1995; Masserdotti et al. 2015).
- Integration into the genome of the host cell: the StarTrack system exploits transposons of the *PiggyBAC* transposase, which can stably integrate in the host genome (García-Marqués and López-Mascaraque 2013).
- Pairing to a clonal labelling system: the StarTrack system allows clonal labelling of cells *in vivo* (García-Marqués and López-Mascaraque 2013). More specifically, I was using the ubiquitous StarTrack for clonal labelling, which labels cells of every lineage because the fluorophores are under the control of the hUbiquitin promoter (Figueres-Onãte et al. 2016).

To establish this new method for direct reprogramming, I have first subcloned tamoxifen-inducible forms of NEUROG2 and ASCL1 (NEUROG2ERT2 and ASCL1ERT2, respectively) (Masserdotti et al. 2015) in plasmids containing the transposons of the *PiggyBAC* transposase (Fig.2.17). Some issues arose during preliminary *in utero* electroporation experiments.

First, the eYFP reporter of the pPB-hGFAP-NEUROG2ERT2-IRES-eYFP and pPB-hGFAP-ASCL1ERT2-IRES-eYFP plasmids was expressed at very low level and seemed to be mostly localised at the soma of the cells (Fig.2.19 and 2.20). This could be due to the fact that the quantity of plasmid electroporated is too low to reach sufficient signal to detect the processes of cells. It is also important to consider that the plasmids expressing the factors for direct reprogramming do not contain LoxP sites; they thereby remain in the nucleus or cytoplasm of the cells when they are not integrated in the host cell's genome, as explained in section 1.5.2 (Figueres-Oñate et al. 2015). Episomal copies are diluted within the progeny of proliferating astrocytes and, as a consequence of the lower number of copies in the daughter cells, their transgenes' expression is also lower (Figueres-Oñate et al. 2015; Ludtke et al. 2002). Interestingly, cells electroporated with a control plasmid exhibit radial morphology, with processes that are directed towards the pial surface (Fig.2.21).

Second, I have not detected DCX-positive cells among the progeny of *Ascl1ERT2/Sox2* co-electroporated cells to date (Fig.2.23). The too low concentration, possible dilution and nuclear exclusion of episomes could be factors leading to low transgene expression and therefore lack of reprogramming. In fact, the amount of proneural factor required to induce astrocyte-to-neuron conversion might not be adequate in the current experimental setting. Alternatively, in the light of the finding that co-expression of *Ascl1* and *Bcl2* in the postnatal cortex induces forced neurogenesis, it is possible that the absence of *Bcl2* leave induced cells to succumb to the effects of ferroptosis, which hinders direct reprogramming (Gascón et al. 2016). Thus, in the future *Bcl2* will be co-electroporated with both proneural factors. It is also not known for how long the transcription factors should be expressed in order to induce direct conversion of astrocytes into neurons. The induction of astrocyte-to-neuron conversion mediated by *Ascl1ERT2* and *Neurog2ERT2 in vitro* was possible via a transient activation of the proneural factors (Masserdotti et al. 2015). In fact, four days of tamoxifen treatment were sufficient to promote direct reprogramming (Masserdotti et al. 2015). So far, I have treated pups with tamoxifen for five consecutive days, but such a short treatment might not be sufficient *in vivo*. The levels of tamoxifen administered via intraperitoneal injection are strongly decreased after 24h (Wilson et al. 2014), thus the need for multiple applications to maintain relatively stable levels of the compound in the system of the animal. Even though a longer duration of activation of the proneural factors might be necessary, it is yet to be determined for how long the factors should remain active in the cells in order to induce direct neuronal reprogramming and if a transient expression is sufficient, as opposed to a prolonged one. Noteworthy, when using retroviral vectors for the exogenous expression of factors under the control of a strong ubiquitous CAG promoter to induce cell fate-switch, the expression is maintained active throughout the whole experiment, while with a hGFAP promoter the expression would be lost upon downregulation of the promoter in case of successful lineage conversion. Moreover, the proneural factors are co-injected with co-factors that have been previously shown to increase the glia-to-neuron conversion efficiency,

namely *Sox2* and *Bcl2* (Heinrich et al. 2014; Gascón et al. 2016). The possibility of remaining in the cytoplasm of the cell as an episome applies to them too.

To improve the strategy and its success chances, an "all-in-one" construct is under preparation (Fig.3.4). Such construct contains multiple elements within the terminal repeats:

- hGFAP promoter, for expression of the transgenes specifically in GFAP-expressing astrocytes.
- Tamoxifen-inducible Cre-recombinase, fused to the modified oestrogen receptor domain. The recombinase is located upstream of a floxed Stop-cassette.
- Internal Ribosomal Entry Site (IRES), followed by the coding sequence of *Neurog2* or *Ascl1*. Notably, the coding sequences of the proneural factors in this construct won't be tamoxifen-inducible.
- pA, for termination of transcription.

This construct can be electroporated in a transgenic mouse line, such as the Ai3 line (Rosa-CAG-LSL-eYFP-WPRE, The Jackson Laboratory). The Ai3 mouse line contains in the *Rosa26* locus the eYFP transgene downstream of a floxed Stop cassette (LSL). The Cre-recombinase of the all-in-one construct will be expressed upon tamoxifen treatment only in electroporated astrocytes. Its activation will ensure excision of the Stop-cassettes present in the transposon and in the *Rosa26* genomic locus, thus allowing consequent transcriptional activation of the transcription factor and of the eYFP reporter, respectively. The expression of the eYFP fluorescent reporter will be stable and inheritable in the progeny of electroporated cells. Moreover, the expression of eYFP will be active also in induced neurons, because the transgenes in the *Rosa26* locus are under the control of the ubiquitous CAG promoter. The use of the Ai3 mouse line with the all-in-one construct (Fig.3.4) would also limit the tamoxifen treatment to just one injection and yield stable expression of the proneural factors until cell fate-switch.

Fig.3.4 All-in-one plasmid for the electroporation in a transgenic mouse line. TF=transcription factor, here indicating *Neurog2* or *Ascl1*.

The co-expression of transcription factors and ubiquitously expressed fluorophores to label electroporated cells allows clonal analysis of induced neurons based on their colour barcoding (Fig.2.18) and on their proximity to the astroglial clone from which they originated. In fact, sibling astrocytes belonging to the same clone detected through ubiquitous StarTrack labelling are closed to each other and occupy tight domains (Figueres-Oñate et al. 2016). Conversely, neurons belonging to a mixed neuronal and glial clone derived from the same ventricular progenitor during cortical development are

located in different domains one week after electroporation, distant from the sibling astrocytes (Figueres-Onãte et al. 2016). Thus, in mixed clones containing induced DCX-positive neurons, we expect to detect induced neurons as sibling cells closely related to the other cells of the clone rather than located in distant cortical regions.

3.3.2 Role of astroglial heterogeneity in direct reprogramming

Direct reprogramming seems to be influenced by the heterogeneity of reprogrammed cells. First of all, there is heterogeneity of response within the same population. A recent study showed that pericytes, brain-resident cells of mesodermal origin, constitute an heterogeneous population of cells that do not reprogram and cells that reprogram into neurons (Karow et al. 2018). Moreover, pericytes undergoing *Ascl1/Sox2*-mediated direct conversion *in vitro* bifurcate in two different neuronal lineages during differentiation: a subset of cells expresses genes of the glutamatergic program, while another subset expresses genes of the GABAergic program (Karow et al. 2018). This, together with the fact that cells undergoing neuronal reprogramming activate non-neuronal programs that are silenced to allow neuronal differentiation (Mall et al. 2017), suggests that cells belonging to the same population might respond to the induction of cell fate-switch in different ways. Second, transcription factors inducing neuronal reprogramming might elicit different differentiation programs in different cell populations. *Ascl1* exogenous expression in neural stem cells isolated from the subependymal zone *in vitro* induces neuronal differentiation in GABAergic interneurons (Berninger e al. 2007), while pericytes induced by *Ascl1/Sox2* induce an intermediate stem cell-like state that precedes neuronal differentiation in GABAergic or glutamatergic neurons (Karow et al. 2018). Third, the same cell type might have different reactions to *in vivo* reprogramming: OPCs in the adult murine cortex do not respond to *Ascl1/Sox2*-induction, but they reprogram into DCX-positive neurons upon cortical injury (Heinrich et al. 2014); conversely, striatal OPCs are susceptible to reprogramming also in the absence of injury (Pereira et al. 2017). Moreover, the presence of cortical injury and subsequent reactive gliosis does not guarantee that a cell type will be reprogrammed. In fact, *Ascl1/Sox2*-induction does not convert adult cortical reactive astrocytes into neurons, but rather converts OPCs (Heinrich et al. 2014). Reactive gliosis seems also to not be necessary for direct conversion of cortical glia into neurons at postnatal stages, as described in this study.

Given the multitude of heterogeneous responses of cells to forced cell fate-switch, it is of interest to understand whether the heterogeneity of mouse cortical astrocytes is associated to different outcomes of forced neurogenesis. This knowledge will provide fundamental information that might help improving direct astrocyte-to-neuron conversion strategies *in vivo*. Coupling direct conversion of astrocytes into neurons with clonal analysis of induced neurons will help elucidating whether the outcome of direct reprogramming *in vivo* is influenced by the heterogeneity of astrocytes. Many factors contribute to

astroglial heterogeneity. The variety of different morphological and functional properties of astrocytes (reviewed in Khakh and Sofroniew 2015) might hint at a different cell plasticity during fate-conversion. Various aspects can be thus investigated in mixed clones containing astrocytes and neurons. Firstly, it will be interesting to determine whether clones containing induced neurons are located in specific areas of the cortex. In fact, cortical astrocytes are generated in a columnar way (Magavi et al. 2012) and have layer-specific properties, including cell orientation, arborisation and volume occupied by the cell (Lanjakornsiripan et al. 2018). Besides being reflected by different morphology, layer distribution of astrocytes hints at different functional properties, as astrocytes of layer II/III contact a higher fraction of synaptic axon-dendrite surface than astrocytes of layer VI (Lanjakornsiripan et al. 2018).

Second, astrocytes exhibit different Ca^{2+} signalling activity, thus mediating a variety of functions, including contribution to neuromodulation, uptake of electrolytes and neurotransmitters, coordination of neuronal synchronisation and control of vasodilation and vasoconstriction among others (reviewed in Khakh and Sofroniew 2015, Mishra 2017; Sasaki et al. 2014). Available genetic tools encoding for fluorescent Ca^{2+} indicators (reviewed in Khakh and Sofroniew 2015, Mishra 2017; Sasaki et al. 2014) can help dissecting the functions of Ca^{2+} signalling in astrocytes, and perhaps to determine whether the type of Ca^{2+} signalling exhibited by astroglia is peculiar to cells successfully (or unsuccessfully) converting into neurons or to the induction of neurons with different functional properties.

Third, given the requirement to induce reactive astrogliosis in most direct neuronal conversion paradigms (Gascón et al. 2016; Guo et al. 2014; Heinrich et al. 2014; reviewed in Heinrich et al. 2015), the size of clones is another factor that can be analysed, to determine whether proliferation of astroglia is a prerequisite for direct neuronal conversion.

Fourth, it would be of interest to analyse the proximity of astrocytes to the vasculature. Neurovascular coupling, which is the coupling between neuronal activity and cerebral blood flow, is in fact an important aspect of astroglial function (reviewed in Mishra 2017, Khakh and Sofroniew 2015) because the blood flow and astrocytes are the two sources of energy in the brain (reviewed in Mishra 2017). Astrocytes control the resting tone of cerebral vasculature in a mechanism mediated by the Ca^{2+}-channel TRPV4, which is expressed by astrocytes and modulates the intracellular concentration of Ca^{2+}, thus modulating the extracellular concentration of ATP (Kim et al. 2015; reviewed in Mishra 2017). These changes in intracellular Ca^{2+} concentration mediated by TRPV4 are triggered by changes in the pressure and flow of arterioles (Kim et al. 2015; reviewed in Mishra 2017).

Fifth, changes in intracellular Ca^{2+} concentration in astrocytes influence neuronal function (Araque et al. 2014). In fact, besides blood flow and pressure astrocytes can sense pH and Na^{+} concentration and can release gliotransmitters upon Ca^{2+}-dependent signalling (Araque et al. 2014; reviewed in Mishra 2017). The release of gliotransmitters modulates neuronal activity (Araque et al. 2014). This Ca^{2+}-regulated

astrocyte-mediated control on neuronal function might have an impact on the control of interneuronal cell death orchestrated by pyramidal neurons during postnatal cortical development (Wong et al. 2018). Sixth, storage of glycogen granules in the cytoplasm of astrocytes is not only linked to their function in providing energy to the brain, but also to their metabolic state (reviewed in Khakh and Sofroniew 2015; Zhang et al. 2014). A transcriptomic analysis performed on brain cells revealed that glycolytic components are enriched in astrocytes, while neurons rely predominantly on OxPhosph (Zhang et al. 2014). This provides evidence for the fact that astrocytes transitioning to a neuronal fate undergo a series of forced metabolic changes, which can eventually hamper the conversion into neurons (Gascón et al. 2016; Kim et al. 2018). Thus, it would be interesting to find whether the amount of glycogen storage in the starting cells influences direct neuronal conversion, provided it is homogeneous among cells of the same clone.

Another interesting aspect of astroglial heterogeneity is raised by the work of Morel and colleagues, who determined the transcriptional profile of astrocytes isolated from different brain regions (Morel et al. 2017). Surprisingly, astrocytes exhibit a dorso-ventral gradient of transcribed mRNA in the mouse brain (Morel et al. 2017), suggesting not only different function, but also possible different chromatin states at genomic loci targeted by factors for direct lineage conversion. Supporting the existence of heterogeneous chromatin states in astroglia, the work of Tiwari and colleagues demonstrated that, during the process of astroglial differentiation *in vitro*, different genetic programs underlie different stages of astrogliogenesis (Tiwari et al. 2018). At an early stage of differentiation, astrocytes express genes involved in nervous system development, while at a late stage of differentiation, corresponding to mature astrocytes, astroglial cells express genes involved in signalling and cytokine response (Tiwari et al. 2018). Interestingly, for each stage of astroglial differentiation there is a specific profile of chromatin activation, with enrichment of H3K27ac at stage-specific distal regulatory regions (Tiwari et al. 2018). These sites are primed by presence of H3K4me1 before their stage-specific acquisition of H3K27ac and transcriptional activation (Tiwari et al. 2018). Notably, two main effectors of early astrogliogenesis have been identified, namely *Nfia* and *Atf3*, which are likely responsible for repression of the neurogenic program and promotion of cell cycle exit, respectively (Tiwari et al. 2018). *Runx2* has instead been identified as a gene involved in late astrogliogenesis, likely through repression of the acquisition of a reactive phenotype (Tiwari et al. 2018). Binding of these transcription factors to their primed stage-specific target elements is required for the acquisition of H3K27ac and the increase of chromatin accessibility on the targets (Tiwari et al. 2018). Knowing that astrocytes exhibit stage-specific transcriptional and epigenetic signatures, with unique priming and activation at regulatory elements is a first step towards understanding the heterogeneity of astroglia at a genomic level. In the future, transcriptome analysis and ChIP-seq data of cells electroporated and expressing the proneural factors

will help understanding if targeted astrocytes exhibit expression profiles and chromatin states favouring or disfavouring direct neuronal conversion.

3.4 Conclusive remarks and future perspectives

The direct conversion of cortical glia into neurons *in vivo* is of great importance as a potential brain repair strategy, to replenish the neuronal population depleted after traumatic brain injury or in the presence of neurodegeneration (reviewed in Heinrich et al. 2015). However, researchers face many challenges in order to find the best design for cell fate-switch, exhibiting high efficiency of conversion and integration of induced neurons in the pre-existing circuitry. In fact, different aspects are determining whether cells will be converted and which neuronal subtype will be generated, such as the choice of transcription factors exogenously expressed, the starting cell population targeted and its susceptibility to reprogramming. Moreover, cells undergoing forced cell fate-switch face several constraints both during lineage conversion and after, when induced neurons have to integrate in the circuitry. Thus, it is important to understand the mechanisms underpinning direct neuronal reprogramming in order to design more efficient strategies. In this section I will give a brief overview of the aspects that I find of greatest interest when it comes to finding new experimental designs for the improvement of the efficiency and efficacy of direct reprogramming *in vivo*.

Cells that exogenously express transcription factors to induce neuronal fate-switch are subjected to both intrinsic and extrinsic influences determining the outcome of reprogramming. Among the most important intrinsic ones are the mechanisms triggered by forced expression of transcription factors and the heterogeneity of the starting cell population, which determines its susceptibility to reprogramming. ChIP sequencing experiments show on which targets the transcription factors are binding (Milne et al. 2009), while RNA sequencing studies are providing insights into the transcriptional programs triggered by the expression of transcription factors, such as the presence of alternative fates (non-neuronal ones or inducing different neuronal subtypes) or the activation of possible cytotoxic pathways (Gascón et al. 2016; Karow et al. 2018). Knowing the genome-wide binding of transcription factors and the difference between the transcriptional state of cells undergoing forced lineage conversion at different timepoints could help identifying subpopulations of cells susceptible and cells refractory to neuronal reprogramming. This could allow the sorting of cell populations that are productively reprogramming (Karow et al. 2018), thus increasing the reprogramming success. Moreover, the information on the genome accessibility in cells undergoing cell fate-switch, which can be provided by FAIRE sequencing (Giresi et al. 2007) or the more recent ATAC sequencing (Buenrostro et al. 2016), would be another important cue on the heterogeneity of the starting population. Such knowledge will help determining the proper choice of transcription factors, to be expressed alone or in combination with other transcription factors, for the induction of a specific type or subtype of neurons. It will also allow the

strategic design for the improvement of direct conversion efficiency by the development of ways to increase susceptibility to neuronal reprogramming, e.g. through increased chromatin accessibility at specific loci. The locus-specific induction of chromatin accessibility could be achieved thanks to the use of the CRISPR/dCas9 system, which increases accessibility at the genomic sites surrounding the sgRNA thus altering local transcription factor binding (Barkal et al. 2016).

Noteworthy, the discovery that posttranslational modifications are modulating the neurogenic capacity of some proneural factors should pave the way to the identification of the modifications that induce glia-to-neuron conversion more efficiently *in vivo*. Given the finding reported in section 2.1.4 that, despite all having neurogenic potential, mutants of the ASCL1 protein with different states of phosphorylation induce different levels of neuronal maturation, it is important also to identify a combination of transcription factors which yields mature neurons. So far, *in vivo* glia-to-neuron conversion resulted in the generation of mostly DCX-positive neurons, with few NeuN-positive mature neurons. However, the co-expression of *Neurog2* with *Bcl2* not only induced a proportion of induced neurons among co-transduced cells higher than 90%, but also yielded about 70% of NeuN-positive neurons when coupled to anti-oxidant treatments (Gascón et al. 2016). Similarly, treatment with valproic acid and BDNF in the striatum and in the spinal cord induced maturation of the DCX-positive neurons induced by exogenous expression of *Sox2* (Niu et al. 2015; Su et al. 2014). This suggests that a boosted maturation of induced neurons can be achieved via additional treatments aimed at counteracting constraints to neuronal maturation. As mentioned above, identification of transcriptional programs triggered during forced cell fate-switch will be of advantage in the determination of the stimuli repressing maturation of induced neurons.

Besides intrinsic influences, there are also extrinsic ones involved in the modulation of susceptibility of cells to reprogramming and in the functional integration of induced neurons in the neuronal network. Among such stimuli are signals derived from the niche and the intercellular communication of cells undergoing reprogramming with other cell types. Astrocytes are one of the cell types used as a starting population for direct neuronal conversion, together with OPCs. Astrocytes maintain contacts with both neurons and blood vessels, consequently mediating neurovascular coupling (reviewed in Mishra 2017). Two-photon calcium imaging allows the monitoring of networks activity through recordings of Ca^{2+} transients (Stosiek et al. 2003; Wang et al. 2009). Neuronal activity corresponds to increased blood flow (Girouard et al. 2009; reviewed in Mishra 2017). In the future, it will be of interest to exploit the blood flow-dependent regulation of astrocytic Ca^{2+} transients to determine whether there is a correlation between the regulation of neuronal activity and the susceptibility to lineage conversion. Moreover, neuronal activity might have an important role in the modulation of the integration of induced neurons. As recently reported, the activity of pyramidal neurons in the postnatal cortex modulates a PTEN-mediated mechanism of regulated cell death of newborn GABAergic interneurons (Wong et al. 2018).

Thus, it will be important to determine if cortical activity exerts such regulatory activity also in induced neurons, thereby determining their chance of surviving and consequently integrating in the pre-existing cortical circuitry. The high efficiency of direct conversion into neurons, achieved for instance via co-expression of *pAscl1* and *Bcl2*, coupled to the use of chemogenetic tools like DREADDS (reviewed in Roth 2017), could help determining whether the postnatal cortical environment is indeed modulating survival and integration of induced neurons.

Another aspect to not be overlooked is concerning the possibility that transduced cells expressing neuronal markers might not derive from direct reprogramming of cortical glia into neurons. In fact, oligodendrocytes and astrocytes are both secreting extracellular vesicles called exosomes (Goetzl et al. 2016; Krämer-Albers et al. 2007; Willis et al. 2017), which mediate glia-neuron communication (Frühbeis et al. 2013; Krämer-Albers et al. 2007; reviewed in White and Krämer-Albers 2014). Exosomes contain small cytoplasmic molecules, lipids, proteins, mRNAs and miRNAs (Krämer-Albers et al. 2007; Frühbeis et al. 2013; Valadi et al. 2007). Neurons can uptake exosomes released by glial cells and internalise their content, which can in turn support neuronal metabolism during oxidative stress (Frühbeis et al. 2013). Thus, in the future it will be interesting to determine whether neuronal cells expressing the reporter gene actually derive from cell fate-switch or from exosome-mediated internalisation of transcripts transferred from transduced cortical glia.

4 Methods

4.1 *In vitro* methods

4.1.1 Preparation of postnatal cortical astrocytes' cultures

Postnatal cortical astrocytes were isolated from cortices of 5-7 days old C57Bl6/J mice (stage P5-7). After decapitating the mice, brains were transferred in a 6cm dish containing ice cold 1xPBS (Phosphate Buffer Saline) for dissection. The two hemispheres were separated and hippocampus, cerebellum and midbrain were removed. The meninges were then carefully removed using fine Dumont #5 Fine Forceps (FST). Finally, hindbrain structures and the developing white matter were eliminated under a stereotactic dissection microscope, to avoid contaminations of the culture from oligodendroglial progenitors. The frontal cortex was thereby isolated and kept in 15ml tubes with ice cold 1xPBS until further treatment. Dissected cortices were mechanically dissociated using a P1000 pipette and the homogenised tissue was spun down at 150xg/5min at 4°C. After carefully removing the supernatant, cells were resuspended with a serological pipette in 5ml of Astromedium (see Table 4.3) supplemented with 10ng/µl Epidermal Growth Factor (EGF) and 10ng/µl basic-Fibroblast Growth Factor (FGF-2). Cells were kept in culture and expanded to 7-10 days in a T25 flask, incubated at 37°C with 5% CO_2.

4.1.2 Passaging postnatal cortical astrocytes for experiments

Cells were prepared for passaging when they reached 70-80% confluency (after ca. 1 week from preparation). One day before passaging the cells, the necessary amount of 24-well plates with glass coverslips (12mm, Menzel-Gläser) were prepared. To favour the attachment of induced neurons, the glass surface was coated with Poly-D-Lysine hydrobromide (PDL) (Sigma) dissolved in sterile dH_2O at the concentration of 1mg/ml (PDL 1:100). Coverslips were incubated 4h at room temperature (RT) with the PDL solution and washed 3 times with sterile dH_2O. The plates were then let to dry overnight.
Cells were trypsinised with trypsin 0.05% for 5min at 37°C. Trypsinisation was stopped by adding Astromedium. The cell suspension was spun down at 150xg/5min at 4°C and resuspended with Astromedium. To count cells, cell suspension and Trypan Blue were mixed at a 1:1 ratio. 10µl of the mix was used to count the number of cells in an improved Neubauer chamber (VWR). Dead cells were not considered. Cells were seeded at a density of 50000-80000 cells/well in 500µl Astromedium supplemented with EGF and FGF-2. Before any other treatment, they were incubated for at least 4h so that they could attach to the surface of the coverslips.

4.1.3 Transfection of postnatal cortical astrocytes

To prepare cells for transfection, conditioned medium was substituted with 300µl of Transfection Medium (TM) (see Table 4.3) 24h after seeding. The collected conditioned medium and cells in TM were equilibrated in the incubator at 37°C with 5% CO_2 for at least 1h.

Cells were transfected by lipofection with 0.5µg plasmid DNA and 0.7µl Lipofectamine™2000 in TM, according to manufacturer's instructions. The mix of DNA and Lipofectamine™2000 was added dropwise to the cultured cells. Cells undergoing transfection were left in the incubator for 4h, during which the lipofection took place. Briefly, the positively charged lipids of Lipofectamine™2000 bind the negatively charged backbone of DNA, forming vesicles that can merge with the phospholipid bilayer of the cell membrane. This leads to internalisation of the exogenous DNA in the cell.

After 4h, the Transfection Medium was removed and substituted with new pre-warmed Astromedium supplemented with EGF and FGF-2. Cells were moved to incubation with 8%CO_2. One day after transfection, half of the conditioned medium was replaced with an equal volume of B27 Differentiation Medium (see Table 4.3), which supports the growth of induced neurons. The next day the whole medium was substituted with 1ml of new pre-warmed B27 Differentiation Medium. Cells were kept in culture up to 8 days *in vitro* starting from the day of seeding.

For immunocytochemical analyses, cells were fixed with ice cold 4% Paraformaldehyde (PFA) for 10-15min and washed with 1xPBS three times. Fixed cells were stored at 4°C with 1xPBS until further analyses.

4.1.4 Transduction of postnatal cortical astrocytes

After seeding the cells and letting them attach for 4h in the incubator, cells were transduced with retroviruses. In order to maximise the resuspension of the retrovirus in the medium and to avoid possible toxicity effects, retroviral particles were not directly applied to the cells. Instead, half of the volume of Astromedium was collected from each well in separate 2ml tubes and each tube received 1µl of retrovirus per well. The mixture was resuspended and the treated conditioned medium was gently added to the cells. The incubation conditions were changed to 37°C with 8% CO_2. The day after, the treated Astromedium was removed and substituted with pre-warmed B27 Differentiation Medium, that was already inoculated and mixed with 1µl/well of retrovirus. On the third day, the culture volume was brought to 1ml/well with fresh B27 Differentiation Medium. Cells were kept in culture for a total of 7days *in vitro* and fixed for immunocytochemical analyses with 4% PFA, as described in section 4.1.3.

4.1.5 Preparation of 4% Paraformaldehyde (PFA)

To prepare 4% PFA, a volume of milliQ H_2O corresponding to one fourth of the final volume of the solution was heated up. Once it reached 65°C, 4% PFA (w/v) was added and stirred for about 5min until partial dissolution of the powder, carefully checking that it would not boil. To allow full dissolution of the Paraformaldehyde, the pH of the solution was slowly raised with 5M Sodium Hydroxide to approximately 6.9, when the appearance of the solution became completely clear. At this point a volume of 0,4M Phosphate Buffer (see Table 4.3) was added while the solution was still stirring. Final volume was reached with millQ H_2O. To remove microcrystals of undissolved powder, the 4% PFA was filtered with Whatman paper filters.
For fixation of cells in culture, the solution was aliquoted and stored at -20°C until use. For perfusion of animals, 4% PFA was prepared fresh and maintained on ice until the end of the tissue's fixation.

4.1.6 Immunocytochemistry

Since antibodies might weakly bind to non-antigen proteins mimicking their binding epitope, which causes higher background or unspecific signal, cells were treated with a Blocking Solution containing 3% Bovine Serum Albumin in 1xPBS. Moreover, the Blocking Solution was supplemented with 0.5% Triton X-100 to permeabilise membranes and allow penetration of the antibodies in the cells. Coverslips were thereby covered with Blocking Solution and incubated 1h at RT. Meanwhile, primary antibodies were diluted in Blocking Solution and stored at 4°C. After the blocking step, cells were incubated with the primary antibodies' solution for 2-3h at RT. After washing 3 times with 1xPBS, cells were incubated with fresh secondary antibodies' solution prepared in Blocking Solution for 1h at RT at the dark. In order to be able to visualise cell nuclei, cells were treated with DAPI diluted in Blocking Solution for 5min at RT. Finally, cells were washed 3 times in 1xPBS and mounted with Aqua Polymount (Polysciences). The mounting medium was left to dry for at least 24h before imaging.

4.2 Molecular Cloning

4.2.1 Cloning of retroviral vectors: Gateway® cloning system

The retroviral vectors used for this study are based on Moloney Murine Leukemia Virus (Mo-MLV) and were originally obtained in the laboratory of Inder Verma (Naviaux et al. 1996). They contain the following elements (Fig.4.1):

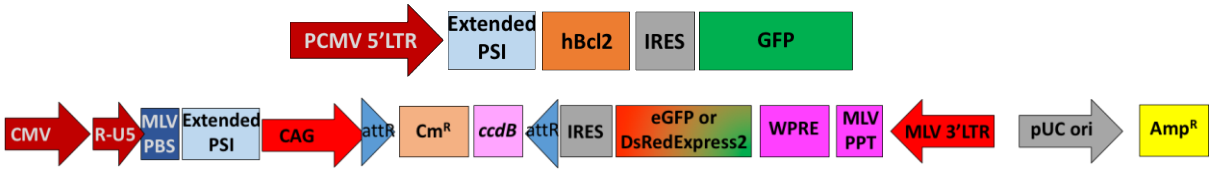

Fig.4.1 Schematic of the retroviral backbones used for mammalian exogenous expression in this study.

CMV: cytomegalovirus early-immediate enhancer;

R-U5: Moloney Murine Sarcoma Virus fused to the U3 region, a viral transcriptional enhancer;

MLV-PBS: Mo-MLV primer binding site, a target of retroviral repression after integration in the host genome;

Extended PSI: retroviral packaging signal;

CAG: ubiquitous strong promoter for mammalian expression;

IRES: internal ribosome entry site, to enhance the translation of the fluorescent reporter;

eGFP or DsRed Express2: fluorescent reporters, derived from *Aequorea victoria* or *Discosoma* respectively. DsRedExpress2 will be indicated in this manuscript as DsRed;

WPRE: Woodchuck Hepatitis Virus Post-translational Regulatory Element, to enhance viral gene expression;

MLV PPT: Mo-MLV Poly-Purine Tract, a primer for DNA synthesis during reverse transcription;

MLV 3'LTR: Mo-MLV 3' Long Terminal Repeat, for integration in the genome of the host cell;

pUC ori: bacterial origin of replication, for synthesis of the plasmid DNA;

Amp^R: gene encoding for β-lactamase, which confers resistance to the antibiotic ampicillin, for positive selection of bacterial clones.

Additionally, the vectors contain the following elements required for molecular cloning:

attR1 and *attR2* sites: recombination sites, to perform LR recombination with the Gateway® kit (Invitrogen);

Cm^R-*ccdB* cassette: dual selection cassette containing the chloramphenicol acetyltranspherase, an effector of the resistance to chloramphenicol in bacteria, and the *ccdB* gene, encoding for a protein toxic to bacteria.

The retroviral plasmids were cloned using the Gateway® kit (Invitrogen®). It consists of a series of plasmids containing specific recombination sites, called *att* sites, deriving from the Lambda phage mechanism of integration in the host genome.

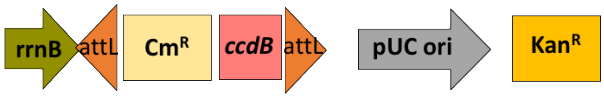

Fig. 4.2 Schematic of the main features of the plasmid pENTRY1A Dual Selection.

The general cloning strategy consists of sub-cloning the insert in the multiple cloning site of the pENTRY1A Dual Selection, thus generating the so-called donor vector. This plasmid contains *attL* and *attB* sites, which allow the recombination with the retroviral destination vectors. The use of appropriate restriction enzymes consents the excision of the Cm^R-*ccdB* cassette and the ligation with the insert of interest. After generation of this intermediate construct (pENTR-, the donor vector), an LR recombination catalysed by the LR Clonase® II was performed between the pENTR- construct and the destination vector (in this case the retroviral plasmid depicted in Fig.4.1). This resulted in the excision of the Cm^R-*ccdB* cassette present in the destination vector and the subsequent insertion of the gene of interest.

The retroviral construct for the expression of human *Bcl2* (pMIG-hBcl2-IRES-GFP) was a kind gift of the Gascón lab (Universidad Complutense, Madrid) and contains a 5'LTR that functions as a strong promoter for the gene of interest (Fig.4.1).

4.2.2 Cloning of retroviral vectors: Plasmids generated

In order to investigate the role of phosphorylation of ASCL1 on the modulation on forced neurogenesis, I cloned three retroviral constructs for the exogenous expression of *pAscl1*. The three genes I used were encoding respectively for the following proteins (Fig.4.3, see also Fig.2.1):

- Wild type form of mouse ASCL1: contains six SP residues, which are targeted by phosphorylation;
- Phospho-deficient form of mouse ASCL1: six S>A mutations had been inserted at the SP sites, to hamper phosphorylation due to the presence of alanine;
- Phospho-mimetic form of mouse ASCL1: six S>D mutations had been inserted, to mimic constitutive phosphorylation via the negative charge of aspartate.

Fig.4.3 Alignment of the secondary structure of the proteins encoded by the three forms of *Ascl1*. The nucleotide sequences were translated with Ape (A Plasmid Editor, by M. Wayne Davies). The alignment's analysis of the three proteins was performed online with Clustal Omega (EBL-EBI), using a Multiple Sequence Alignment. Results were manually aligned for visual representation. Asterisks indicate multiple alignment. Mismatches, corresponding to the S>A and S>D mutations, are highlighted in orange. mAscl1= mouse Ascl1.

The coding sequences were originally inserted in the pCIG2 vector and kindly provided by Carol Schuurmans (Sunnybrook Research Institute, Toronto, ON, Canada). In order to sub-clone them into the pENTRY1A Dual Selection vector, I excided all three coding sequences via XhoI/SalI double restriction and inserted them into the intermediate backbone previously opened via SalI single restriction. I thereby generated the donor constructs pENTR-Ascl1, pENTR-Ascl1SA6 and pENTR-Ascl1SD6. Each of these intermediate constructs was recombined with the destination vector, to generate the final retroviral plasmids for exogenous expression of *Ascl1* in mammalian cells (Fig.4.4). For all coding sequences were cloned: one expression vector with eGFP fluorescent reporter; one expression vector with DsRedExpress2 reporter. All plasmids were sequenced at GATC Biotech GmbH.

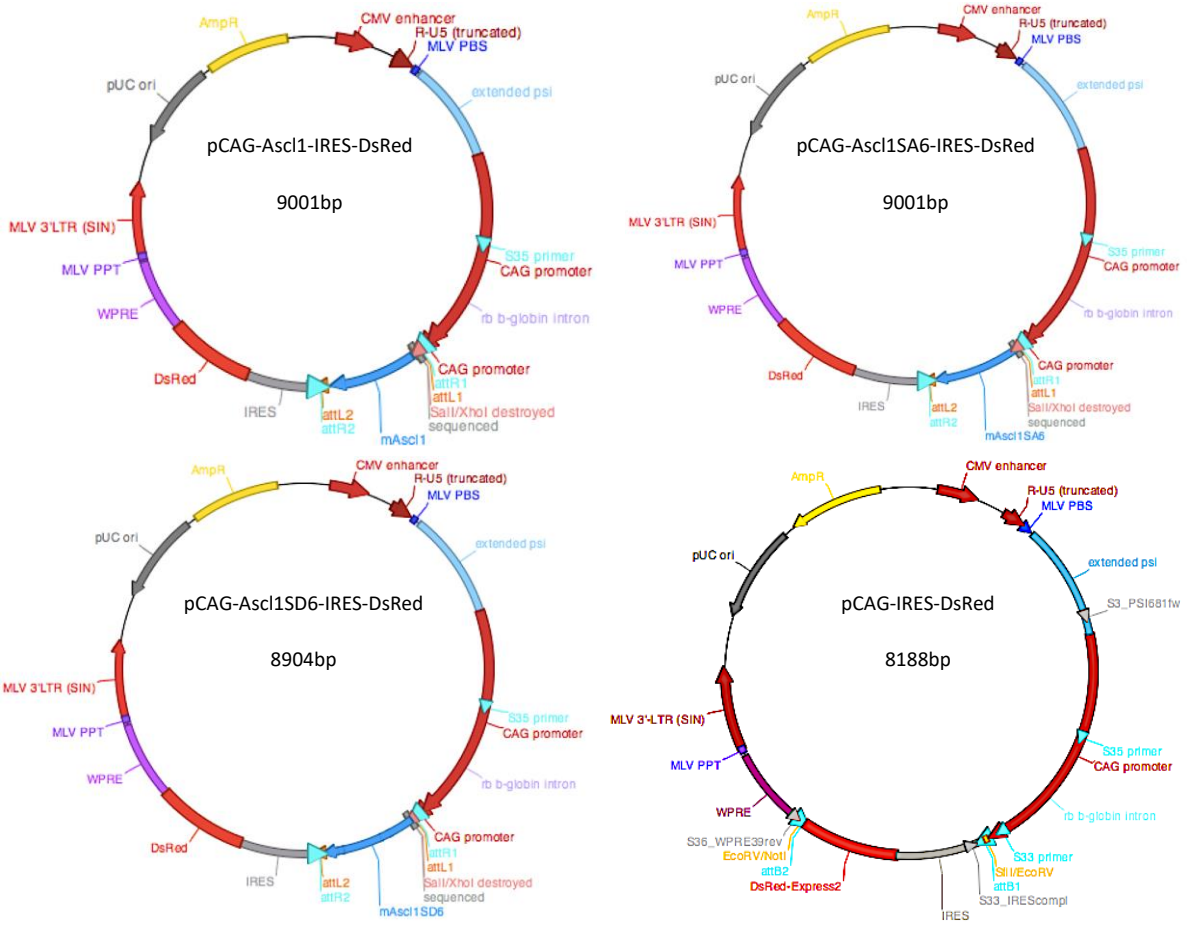

Fig.4.4 Maps of the retroviral constructs cloned for the exogenous expression of *Ascl1*. *(see next page)* The maps illustrate location, proportional size and directionality of the elements present in the retroviral plasmids I cloned. The fourth map depicts the control retroviral plasmid encoding only for the fluorescent reporter DsRed, pCAG-IRES-DsRed. This construct, together with the pCAG-IRES-eGFP, was already available in the lab. While these maps are showing only the construction of the plasmids with DsRed as fluorescent reporter, they all have been cloned with the green fluorescent reporter eGFP too.

4.2.3 Cloning of transposon-based constructs

To perform *in utero* electroporation experiments, I obtained the plasmids of the StarTrack clonal labelling system from the Instituto Cajal (Madrid, Spain) in the frame of a collaboration. The StarTrack system exploits *PiggyBAC*-transposition to stably integrate transposons into the host cell's genome. Transposons are flanked by Terminal Repeats at the 5' and 3' sides (5'TR and 3'TR). The vectors containing transposons have the following elements (Fig.4.5):

hUbc: human Ubiquitin promoter, for expression in every cell type;

5'TR and 3'TR: Terminal Repeats, elements that are recognised by the *PiggyBAC* transposase and determine the integration site in the genome of the host cell.

LoxP: recombination sites that are recognised by the Cre recombinase.

pA: bovine growth hormone polyadenylation sequence, for termination of transcription;

pUC ori: bacterial origin of replication, for synthesis of the plasmid DNA;

Amp^R: gene encoding for β-lactamase, which confers resistance to the antibiotic ampicillin, for positive selection of bacterial clones.

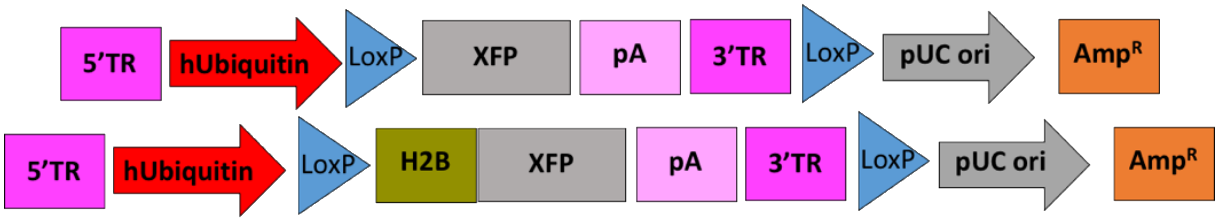

Fig.4.5 Schematic of the main features of the plasmids for expression of the StarTrack fluorescent proteins. The transposon, namely the part of the plasmid that is integrated in the host cell via retrotransposition, is flanked by the 5'TR and the 3'TR.

A hyperactive form of the *PiggyBAC* transposase (hyPBase) is expressed by an additional plasmid with CMV promoter (Fig.4.6). In addition to these constructs, it is necessary to have another one to express the Cre recombinase fused to the oestrogen receptor element (ERT2) for tamoxifen-dependent activation (Fig.4.6). The presence of active Cre recombinase is in fact necessary to induce recombination of the LoxP sites for removal of episomal copies of the plasmids (see section 1.5.2).

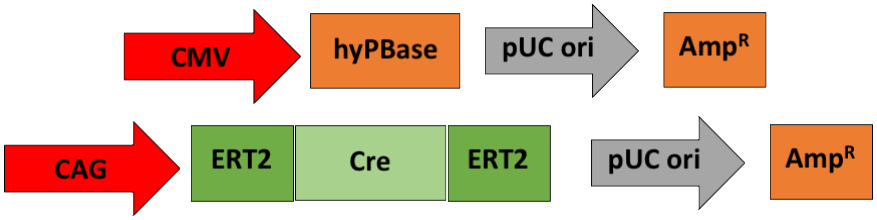

Fig.4.6 Schematic of the main features of the plasmids for expression of the transposase and of the Cre recombinase. The Cre recombinase is fused both upstream and downstream to the ERT2 element, for tamoxifen-dependent activation.

To exogenously express proneural transcription factors for forced fate-switch of electroporated astrocytes into neurons, I subcloned the coding sequences of tamoxifen-dependent NEUROG2 and ASCL1 into the transposon of a plasmid with human GFAP promoter (Fig.4.7). Tamoxifen-dependent activation is ensured by the fusion of the proneural genes with the *ERT2* gene. The original fused coding sequences were previously cloned at the LMU Munich (Masserdotti et al. 2015). To insert the coding sequence of *Ascl1ERT2*, the pGFAP-eGFP vector was opened via EcoRI restriction and blunted. *Ascl1ERT2* was obtained via PCR and subcloned via blunted ClaI-ends.

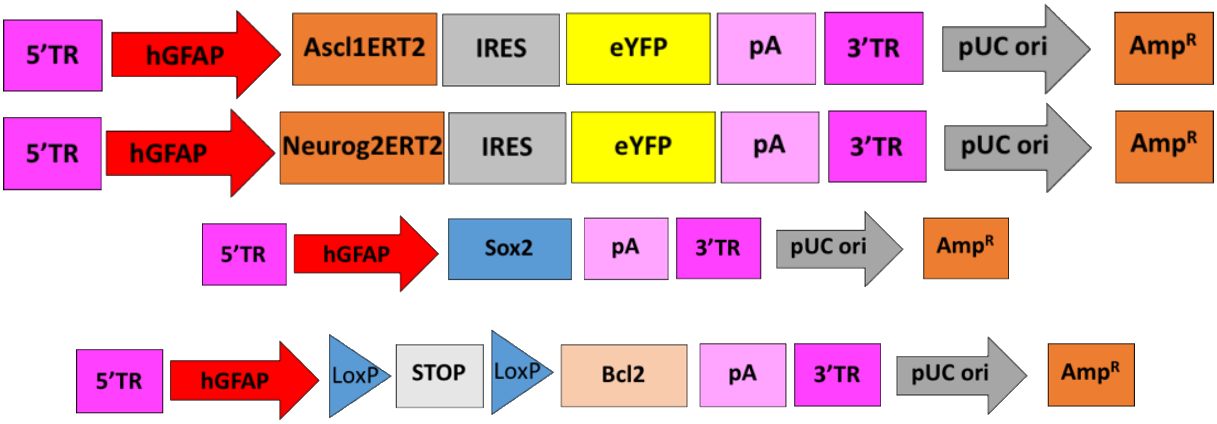

Fig.4.7 Schematic of the main features of the plasmids for expression of the proneural factors and of their cofactors. The STOP cassette consists in a series of repeated SV40 polyA sequences.

To insert *Neurog2ERT2*, I opened the vector via EcoRI and BamHI restriction and blunted the EcoRI end. *Neurog2ERT2* was obtained via PCR and subcloned via ClaI+blunting and BamHI restriction. Similarly, to subclone *Sox2* I prepared the vector via EcoRI/BamHI double-restriction and blunted both ends. The insert with the coding sequence for *Sox2* was obtained via PCR and inserter via blunted BamHI-ends.
For the expression of BCL2, an antiapoptotic protein, it was necessary to add upstream of the gene a STOP cassette flanked by LoxP sites, to induce transcriptional activation only upon tamoxifen-dependent Cre recombination (Fig.4.7 and 2.17). Thus, I first prepared an intermediate construct containing only the STOP cassette and then subcloned *Bcl2*. For this purpose, I opened the pGFAP-eGFP vector via BamHI and EcoRI restriction and I blunted only the BamHI ends. The loxed STOP cassette was inserted via AccI blunted end and EcoRI end. To finally add the *Bcl2* coding sequence, I linearized the intermediate construct (pPB-GFAP-LSL) via EcoRI; *Bcl2* was obtained via PCR and inserted via EcoRI.
All plasmids were sequenced at GATC GmbH.

4.2.4 Preparation of DNA for retroviral production and for *in utero* electroporation

To prepare DNA for experiments, plasmids generated via ligation or recombination were first transformed into a competent strain of *Escherichia coli*, called DH5*alpha*, for amplification. Positive transformants were inoculated in liquid Luria Bertani medium containing Ampicillin and expanded for 12-16h at 37°C, shaking at 210rpm.
To isolate the expression plasmids, bacterial suspensions were first pelleted by centrifugation 20min/4500xg at RT. Subsequently, the DNA plasmids were extracted and purified via anion-exchange column chromatography using commercial kits, according to the manufacturers' instructions. They were finally resuspended in Tris-EDTA pH8.0.

For transfections and for the production of retroviral particles, I used the PureLink™ HiPure Plasmid DNA Maxiprep kit (Invitrogen™), which allows the preparation of high-quality and high-purity DNA. Nevertheless, this kit yields a DNA preparation with an endotoxin content of 0.1-1.5EU/µg Plasmid DNA. Endotoxins, namely lipopolysaccharides, are present in the inner membrane of the wall of the *E.coli* strain used to amplify the plasmids. For some applications, such as *in utero* electroporation, in which the plasmids are directly injected in the organism of the experimental animal, their presence can be unwanted and even harmful, with potential toxic or inflammatory effects. Thus, in order to purify DNA for *in utero* electroporation, I used the NucleoBond® Xtra Maxi EF kit (Macherey-Nagel). This kit is an anionic-exchange chromatography kit that yields DNA preparations containing an endotoxin level of less than 0.05EU/µg Plasmid DNA. Plasmids were resuspended in endotoxin free Tris-EDTA pH8.0.

For *in utero* electroporation experiments, the plasmid mix was prepared by mixing all plasmids at a concentration of 1µg/µl. The relative proportion of plasmids was thus divided:

- one third of the total amount in micrograms: factors for direct conversion of astrocytes into neurons (Fig. 4.7), transposase and Cre recombinase (Fig.4.6);
- two thirds of the total amount in micrograms: ubiquitous StarTrack (Fig.4.5).

In order to be able to see the plasmid mix during ventricular injections, I added about 1µl of FastGreen (Sigma) diluted at 1mg/ml in milliQ H_2O.

4.3 Production of retroviruses

4.3.1 Cells

Retroviruses were produced using 1F8 cells, a monoclonal line derived from a batch of 293GPG cells (Ory et al., 1996). These cells are derived from HEK293T cells modified via Adenoviruses-5 to stably express the retroviral *gag-pol* polycistronic element. This sequence encodes for the VSV-G protein, which is toxic for HEK cells. In order to avoid cytotoxicity, the system is maintained under the control of a Tetracycline-repressed (tetO) minimal promoter and a Tetracycline-responsive (tetR)/VP16. The genomic composition of this cell line allows the production of VSVG-pseudotyped retroviruses with a single transfection.

1F8 cells were cultured in Growth Medium (see Table 4.3) supplemented with antibiotics: 2µg/ml Puromycin for selection of the integrated VSVG gene and the transactivator tetR/VP16; 0.3 mg/ml G418 Sulfate (Geneticin) for selection of the MLV genome *(gag-pol*); 2µg/ml Tetracyclin for inhibition of the VSVG gene. Cells were kept in culture at 37°C with 5%CO2 and passaged via trypsinisation and resuspension when at 70-80% confluency.

4.3.2 Retroviral packaging

In order to prepare cells for transfection, they were gently washed with 1xPBS and trypsinised with 0.05% Trypsine-EDTA. Trypsinisation was stopped with pre-warmed Plating Medium (see Table 4.3) and cells were plated on 10cm dishes at a density of about $1x10^5$-$1x10^7$ cells/dish. Cells were transfected when they reached 70-80% confluency. Briefly, a DNA mix and a reagent mix were prepared in Transfection Medium (DMEM; 1x Glutamine). Usually, 6x10cm dishes per each construct were transfected with 150µg plasmid DNA and the reagent mix with 250µl of GenJet Plus or with 1mg/µg of PEI. While incubating the transfection mix, Plating Medium was removed from the cells and substituted with Packaging Medium (see Table 4.3). At this point, because of the Tetracycline withdrawal, the VSVG expression is induced. The transfection mixture was then added dropwise to the cells. One day later, cells were washed with Packaging Medium and fed with 10ml of new Packaging medium.

4.3.3 Retroviral harvesting and titering

To harvest the viral particles released by transfected cells, supernatants were collected 3 days after transfection and spun 15min/350xg at 4C° to pellet cell debris. Cleared supernatants were filtered with a 0.44µm PVDF filter and transferred on SW28 tubes for ultracentrifuge. A cushion of 300µl Opti-PREP was added at the bottom of each tube and viral supernatants were centrifuged in pre-cooled ultracentrifuge with pre-cooled SW28 rotor 2h/24000rpm at 4°C. Supernatants were carefully removed and the Opti-PREP embedded pellet was washed with circa 30ml sterile ice-cold TBS-5 buffer (see Table 4.3). Viral pellets were ultracentrifuged again 2h/24000rpm at 4°C. The supernatant was removed and the viral pellet was resuspended in 50µl TBS-5 buffer. The viral suspension was kept on ice until the next day and aliquoted for storage at -80°C. Three rounds of viral harvests were performed, each at 2 days from the previous one. First and second harvest were usually mixed together and used for *in vitro* experiments.

Each harvest of each production was tested and titered using HEK293 cells. Briefly, HEK293 cells were trypsinised with 0.05% Trypsin-EDTA when they reached 70-80% confluence and seeded at a density of 50000-80000 cells per well of a 24-well plate. 4-12h after seeding them, cells were transduced with the following dilutions: 1µl virus/well; 10^{-3}µl virus/well; 10^{-5}µ virus/well.

The day after transduction, cells were fixed with 4% Paraformaldehyde and analysed via immunocytochemistry. Six random pictures of each coverslip were taken at the 20x objective at an AxioVision fluorescent microscope (Zeiss). The reporter-positive cells were counted over the total number of cells, indicated by DAPI-positive nuclei. The viral titer was calculate as it follows:

$$viral\ titer = \frac{(reporter\ positive\ cells)x100}{DAPI\ positive\ cells}$$

Viral titers of 5-9x10^7 were considered suitable for viral injections *in vivo*.

4.4 Animal experiments

4.4.1 Animals

All animal procedures were conducted in accordance to Policies on the Use of Animals and Humans in Neuroscience Research, revised and approved by the Society for Neuroscience and the state of Rheinland-Pfalz under licence number 23 177 07-G15-1-031 and licence number 23 177 07-G17-1-067, and carried on under the supervision of the licence holder (University Medical Center Mainz, Germany). For *in vitro* cultures, C57Bl6/J at the age of P5-7 were kindly provided by the Institute of Microscopy and Microscopic Anatomy (University Medical Center Mainz, Germany). All *in vivo* experiments were performed on C57Bl6/J mice obtained from Janvier. For retroviral injections, P5 mice were ordered with the mother, to ensure their survival until the end of the experiment. Retroviral injections were performed by the licence holder. For *in utero* electroporation experiments, timed pregnant mice (ordered from Janvier) at the E14 stage were operated. The day of detection of vaginal plug was considered day zero. Postnatal electroporations at P0 and P1 were performed by our collaborator at the Instituto Cajal (Madrid, Spain).

4.4.2 Retroviral injections

Before surgery, P5 pups were treated with analgesia (Rimadyl® 4mg/Kg of body weight in 0.9% NaCl). Anaesthesia was administered via intraperitoneal injection of 0.5mg/Kg body weight Medetomidin + 5mg/Kg body weight Midazolam + 0.025mg/Kg body weight Fentanyl. Reflexes were checked and once mice were in deep anaesthesia, viruses were injected in the cerebral cortex using borosilicate glass capillaries (0.8-0.9mm diameter, World precision Instruments Inc.) pulled with a micropipette puller to have a tip diameter of about 20µm. Briefly, a small incision was made on the skin with a surgical blade and the skull was carefully opened with a needle. Each pup received a volume of 0.5-1µl of retroviral suspension injected in the cortex. After injection the wound was closed with surgical glue and anaesthesia was antagonised via intraperitoneal injection of 2.5mg/k body weight Atipamezol + 0.5mg/Kg body weight Flumazenil + 0.1mg/Kg body weight Buprenorphin. Pups were left on a hot plate at 37°C to recover before reuniting them to the mother. The recovery state was daily checked for one week after the operation.

4.4.3 *In utero* electroporation and tamoxifen administration

Timed pregnant mothers were operated as previously described (Baumgart and Grebe 2015). Half an hour before surgery, mice were analgesized subcutaneously with Rimadyl® (5mg/Kg of body weight in 0.9% NaCl). To perform surgery, they were initially anesthetised per inhalation with 2.5% Isoflurane in pure O_2. After fixing the limbs on the operation table and checking that mice were in full anaesthesia, the Isoflurane level at the inhalation mask was reduced to 2%. The abdomen was cleaned with a sterile gauze with 0.9% NaCl containing the bacteriostatic benzyl alcohol (0.9%), and with 70% Ethanol. The surgical area was surrounded by sterile gauze and the abdominal cavity was opened with a 2-2.5cm wide incision at the skin and a slightly smaller one at the muscle. The uterine horns were carefully extracted using ring loops (FST) and the area of the incision was kept moist with the solution of 0.9% NaCl and benzyl alcohol for the whole procedure.

The plasmid mix was injected in the lateral ventricles of the embryos with borosilicate glass capillaries (0.8-0.9mm diameter, World Precision Instruments Inc.) pulled with a micropipette puller to have a tip diameter of about 20µm. The lateral ventricles were filled with 1-1.5µl plasmid mix (prepared as described in section 4.2.4), namely until when the ventricular cavity looked filled by the coloured dye Fast Green. Five electric current pulses (30mV, 50ms cycles length, 950ms interval pause) were applied via platinum electrodes (3mm diameter, Nepagene) connected to an electroporator. After electroporation, the uterine horns were carefully put back into the abdomen with ring loops. The muscle was sutured with surgical 5-0 PermaHand Silk (Ethicon) and the skin was sutured with 4/0 Safil® self-resorbing silk (Braun). If necessary, mice were analgesized again the day after surgery (5mg/Kg body weight Rimadyl®, subcutaneous). Mice were visually controlled until they woke up. The recovery state was checked daily for one week after the surgery. The day of delivery was considered postnatal day zero (P0).

Beginning at the age of P5, pups were injected intraperitoneally with 25mg/Kg body weight of Tamoxifen (Sigma) diluted in corn oil for five consecutive days.

4.4.4 Fixation and preparation of tissue

Prior to sacrifice, animals were lethally anesthetised with Ketamine (120mg/Kg body weight) and Xylazine (16mg/Kg body weight). Reflexes were checked and once animals reached the state of deep anaesthesia their limbs were fixed and their thoracic cavity was opened to expose the heart. They were transcardiacally perfused with pre-warmed 0.9% NaCl supplemented with heparin (1000U/ml), papaverine (4mg/ml) and polyvinylpyrrolidon (2.5%), to remove the blood from the vessels. Then, they were perfused with freshly prepared, ice-cold 4% PFA to fix the tissues. After fixation, the brains were taken out and post-fixed overnight in 4% PFA at 4°C.

The next day, brains were washed in 1xPBS and prepared for vibratome sectioning. The brains were coronally sliced with a thickness of 40µm for retrovirus-injected brains and 50µm for electroporated brains. Slices were separated into six series per each brain, each series containing one slice every six. Thus, one series is a representative sample of the brain along the rostro-caudal axis every 240 or 300µm. Brain slices were put in cryoprotective solution (see Table 4.3) and stored at -20°C.

4.4.5 Immunohistochemistry

For immunohistochemistry, one series obtained as in section 4.4.5 was stained as it follows. To remove the cryoprotective solution, slices were first washed three times for 15min with filtered 0.1M TBS, pH7.6 (hereafter, 1xTBS). Subsequently they were incubated for 1,5h in blocking solution (5% Donkey Serum; 0.1-0.3% Triton X-100 in 1xTBS). After the blocking step, slices incubated with the primary antibodies diluted in blocking solution for 2-3h at RT, followed by an overnight incubation at 4°C. After washing three times with 1xTBS, they were incubated with the secondary antibodies diluted blocking solution for 1h at RT. Slices were washed twice with 1xTBS and incubated with DAPI dissolved in 1xTBS for 5min at RT. Every excess of DAPI was removed by washing three times with 1xTBS. Before mounting, slices were washed two times with 0.1M Phospate Buffer, pH7.4.
To mount them, slices were disposed on Superfrost™ (Thermo Fisher Scientific) microscope slides and allowed to dry. For retroviral-injected brains, slices were further dehydrated with toluene and covered with cover-glasses mounted with DPX mounting medium. For electroporated samples, slices were covered with cover-glasses mounted with Mowiol® 40-88 (Sigma).

4.4.6 Electrophysiology

To perform patch-clamp recordings on *ex vivo* brain slices, C57Bl/6J mice were injected with retroviruses at P5 as described in section 4.4.2 and analysed at 4 weeks post injection.
Mice were terminally anaesthetised with CO_2 and decapitated. The brain was dissected out in ice-cold modified artificial cerebro-spinal fluid (ACSF) solution (see Table 4.3) saturated with 5% CO2 and 95% O2, pH7.4. Dissected brains were cut in 300µm thick coronal slices at the vibratome (Leica VT12005) and transferred to standard ACSF prepared as described above but containing 2mM $CaCl_2$ and 1mM $MgCl_2$ (see Table 4.3). After equilibration at RT for at least 1h, the slices were placed in a recording chamber, superfused with 1ml/min of standard ACSF and mounted on a Zeiss Axio Imager 2 epifluorescent microscope. Cells were visualized with a 40x objective (0.75 NA). Patch-clamp whole-cell recordings were performed at RT with electrodes filled with a fluorescent dye-containing solution to allow morphological analysis of the cells: 125mM K-Gluconate; 5mM NaCl; 2mM Na_2-ATP; 2mM $MgCl_2$; 10mM EGTA; 10mM HEPES; 10mM Biocytin; 0.2mM Alexa 488/594 hydrazide (Invitrogen), pH7.4. Current-clamp recordings were obtained using an Axopatch 200B amplifier (Molecular Devices). Current

steps were triggered with the pClamp10 software (Molecular Devices), which was also used for further analysis. Seal resistances were between 4 and 18 GΩ. Series resistance and whole-cell capacitance were not compensated.

4.5 Image acquisition and analysis

4.5.1 Epifluorescent and confocal microscopy

Pictures of *in vitro* experiments were taken with an upright Axio Imager.M2 epifluorescent microscope equipped with an ApoTome.2 system (Zeiss GmbH). Images were acquired with the 20x dry objective (NA 0.5) or the 40x dry objective (NA 0.75) in epifluorescent mode.

For the quantification of *in vivo* experiments, pictures were taken at the Axio Imager.M2 in ApoTome mode. For illustrations of result from *in vivo* experiments of section 2.1 and for Fig.2.19, the image acquisition was performed at the TCS SP5 Confocal Laser Scanning inverted microscope (Leica) of the Institute of Molecular Biology (IMB, Mainz, Germany). This confocal microscope is equipped with four PMTs, four lasers (405 Diode, Argon, HeNe 543, HeNe 633) and a fast-resonant scanner. Pictures were taken with the 20x dry objective (NA 0.7) or with the 40x oil objective (NA 1.3). Serial Z-stacks of 0.4µm (Fig.2.17) and 0.8µm were acquired to image the whole thickness of the slices. For Fig.2.6C-C'''/D-D''' and Fig.2.13, pictures were acquired at the Axio Imager.M2 in ApoTome mode with 63x oil objective (NA 1.25). Serial Z-stacks of 0.3µm were taken. For Fig.2.4, images were acquired at the Axio Imager.M2 in ApoTome mode with the 20x dry objective. Serial Z-Stacks of 1.2µm were taken.

For the other *in utero* electroporation illustrations, acquisition was performed at the TCS SP5 Confocal Laser Scanning inverted microscope (Leica) of the Microscopy and Scientific Imaging Unit (Instituto Cajal, Madrid, Spain). Tile scans were taken at the 20x oil objective (NA 0.7), with serial Z-stacks of 3µm.

4.5.2 Image analyses and cell counting

For quantifications of *in vitro* experiments, biological triplicates obtained by independent cultures from three different brains were performed. For each biological replicate, technical duplicates of every experimental condition were analysed and the mean of their results was considered. From Fig.2.2, six random pictures of each coverslip were acquired at the 20x objective. For Fig.2.3, a 4x4 tile scan of each coverslip was acquired at the 20x objective. Cell counting was performed by quantifying the number of marker-positive cells among the transduced population (eGFP- or DsRed-positive cells).

For quantifications of *in vivo* experiments, tile scans of the areas containing transduced cells were taken at the Axio Imager.M2 in ApoTome mode, with a serial Z-stack of 1.25µm. Cells were quantified, after collapsing the Z-stacks via maximum intensity projection, by counting the marker-positive cells among transduced or double-transduced cells.

For illustrations, images were exported in TIFF format at the Zen Blue Light software (Zeiss GmbH) or with FIJI (National Institutes of Health), and the colour balance of each channel was uniformly adjusted with Photoshop (Adobe). If necessary, Lookup Tables were changed to maintain uniformity of colour coding among the same figure and noise was filtered via removal of outlier pixels in FIJI. To obtain some of the insets showing magnifications, as indicated by dashed squares, pictures were cropped in Photoshop. The final organisation of figures was performed in Illustrator (Adobe).

4.5.3 Workflow for clonal analysis of StarTrack-electroporated cells

The clonal analysis of cells electroporated with the StarTrack labelling system will be performed by mean of macros in Fiji that were developed at the Instituto Cajal (Madrid, Spain). The macros recognise only the original file of the confocal microscope's software (LASX, Leica). After collecting all maximum intensity projections of confocal images obtained from one brain's series, it is necessary to manually set thresholds for the minimum size of a cells and the minimum intensity level of each fluorescent signal. The main functions of the macros are (Fig.4.8):

- identification of all electroporated cells in each image, according to the threshold for cells' size manually set;
- creation of the galleries' folder, containing micrographs of each cell in each channel;
- assignment of the barcodes, namely binary codes identifying the labelling pattern of a specific cell according to the thresholds for fluorescent intensity manually set;
- merging and organisation of data derived from the thresholds' analyses.

One limitation of the macros is that they allow only the setting of a mean threshold of fluorescent intensity among all the channels, rather than the setting of one threshold value for each fluorophore. Thus, it is important to perform manual check and editing of the readout of the macros, so that each cell identified receives its real barcode.

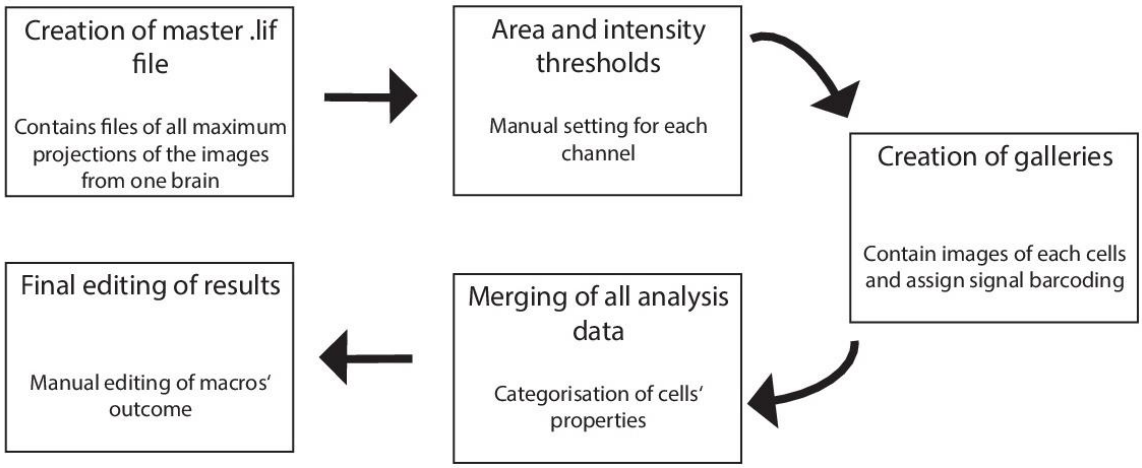

Fig.4.8 Workflow of clonal analysis of brains electroporated with the StarTrack clonal labelling system.

4.6 Statistical analysis

All results of quantifications are represented as means ± standard deviations (SD) and the statistical significance was analysed with One-Way ANOVA after checking normality in SPSS Statistics 23 V5 (IBM). Multiple comparisons were tested for significance with the Bonferroni post-hoc test in SPSS. Graphical representations of results were obtained in GraphPad Prism 5 (GraphPad).

4.7 Materials

4.7.1 Primary antibodies

Table 4.1 List of primary antibodies. If necessary to specify, it is indicated if the antibody has been used for immunocytochemistry (ICC) or immunohistochemistry (IHC).

Antigen	Host species	Dilution	Company	Cell types stained
Adenomatous Polyposic Coli (APC)	Mouse IgG2b	1:100	Calbiochem (OP80-100UG)	Mature oligodendrocytes
Achete Scute-like 1 (Ascl1)	Mouse IgG1	1:400 ICC 1:100 IHC	BD Pahrmingen (550644)	Cells expressing ASCL1
Beta III tubuline (bIIItub)	Mouse IgG2b	1:1000	Sigma (T8660)	Neurons
Doublecortin (DCX)	Guinea pig	1:400 ICC	Millipore (AB2253)	Immature neurons
Doublecortin (DCX)	Goat	1:250 IHC	Santa Cruz Biotechnology (sc-8066)	Immature neurons
γ-aminobutyric acid (GABA)	Rabbit	1:300	Sigma (A2052)	Interneurons
Green Fluorescent Protein (GFP)	Chicken	1:300 ICC 1:1000 IHC	AvesLab (GFP-1020)	GFP- and eGFP-labelled cells
Glial Fibrillar Acidic Protein (GFAP)	Rabbit	1:1000 ICC 1:300 IHC	Dako (Z0334 – 29-2)	Astrocytes
Ionized calcium-binding adapter molecule 1 (IBA1)	Rabbit	1:800	Wako (019-19741)	Microglia
Cherry DsRed (mCherry)	Chicken	1:300 IHC	EnCor Biotechnology (CPCA-mCherry)	DsRed-labelled cells
Neuronal Nuclei (NeuN)	Mouse IgG1	1:500	Millipore (MAB377)	Mature neurons
Red Fluorescent Protein (RFP)	Rabbit	1:500 IHC	Biomol (6004013795)	DsRed-labelled cells
Red Fluorescent Protein (RFP)	Rat	1:400	Chromotek (5F8)	DsRed-labelled cells
SRY-Box 10 (Sox10)	Goat	1:100	Santa Cruz Biotechnology (sc-17342)	OPCs, pre-OPCs and oligodendrocytes

4.7.2 Secondary antibodies

Table 4.2 List of secondary antibodies. It is specified if the antibody has been used for immunocytochemistry (ICC) or immunohistochemistry (IHC).

Species specificity	Fluorescent label	Dilution	Company
Donkey α-Chicken	Alexa 488	1:1000 ICC 1:200 IHC	Jackson Immunoresearch (703-545-155)
Donkey α-Chicken	Cy3	1:500 IHC	Dianova (703-165-155)
Donkey α-Goat	Cy3	1:500 IHC	Dianova (705-165-147)
Donkey α-Goat	Cy5	1:1000 ICC 1:500 IHC	Dianova (705-155-147)
Donkey α-Guinea pig	Cy3	1:1000 ICC	Dianova (706-166-148)
Donkey α-Mouse	Alexa 405	1:200 IHC	Jackson Immunoresearch (715-475-151)
Donkey α-Mouse	Alexa 488	1:1000 ICC	Invitrogen (A21202)
Goat α-Mouse	Cy3	1:1000 ICC	Dianova (115-165-166)
Donkey α-Mouse	Alexa 647	1:500 IHC	Invitrogen (A31571)
Donkey α-Rabbit	Cy3	1:1000 ICC	Dianova (711-165-152)
Donkey α-Rabbit	A647	1:500 IHC	Invitrogen (A31573)
Goat α-Rabbit	Cy5	1:1000 ICC	Dianova (115-155-144)
Goat α-Rat	Cy3	1:1000 ICC	Dianova (112-165-167)

4.7.3 List of solutions

Table 4.3 List of media and solutions.

Solution	Composition	Storage
1xPBS	137mM NaCl; 100mM Na_2HPO_4; 18mM KH_2PO_4: 2.7mM KCl; pH7.4	RT
Astromedium	DMEM/F12; 10%FBS; 5% Horse Serum; 1x PenStrep; 1xGlutaMax; 1x B27 Supplement	4°C up to one month
PDL 1:100	1mg/ml PDL in sterile dH_2O	4°C

Transfection Medium	OptmiMEM; 1x GlutaMAX; 1xPenStrep; 10ng/µl EGF; 10ng/µl FGF-2	4°C up to one month
B27 Differentiation Medium	DMEM/F12; 1xPenStrep; 1xGlutaMAX; 1x B27 Supplement	4°C up to one month
0.4M Phosphate Buffer	117mM $Na_2HPO_4 \cdot 12H_2O$; 128mM $NaH_2PO_4 \cdot 2H_2O$; pH7.4	RT
4% PFA	4%w/v PFA; 0,4M Phosphate Buffer; up to volume in millQ H_2O	-20°C
Blocking Solution ICC	3% Bovine Serum Albumin; 0.5% Triton X-100; up to volume in 1x PBS	-20°C
Luria Bertani	10% Trypton; 5% Yeast Extract; 10% NaCl; up to volume in dH_2O ; pH7.4 with NAOH	RT
Growth Medium	DMEM/F12; 1xGlutamine; 10% FCS; 2µg/ml Puromycin; 0.3 mg/ml G418 Sulfate; 2µg/ml Tetracyclin	4°C up to one month
Plating Medium	DMEM; 10% FCS; 1xGlutaMAX; 1xNEAA; 1xNa-Pyruvate; 0.5 µg/ml Tetracycline	4°C up to one month
Transfection Medium (1F8)	DMEM; 1x Glutamine	4°C up to one month
Packaging Medium	DMEM; 10% FCS; 1xGlutaMAX; 1xNEAA; 1xNa-Pyruvate	4°C up to one month
TBS-5	1M Tris/HCl, pH7.8; 5M NaCl; 1M KCl; 1M Mg2Cl	4°C
Cryoprotective Solution	20% Glucose + 40% Ethylene Glycol + 0.025% Sodium Azide + 0.05M Phosphate Buffer pH7.4	RT
Blocking Solution IHC	5% Donkey Serum; 0.1-0.3% Triton X-100 in 1xTBS	4°C up to two days
Standard ACSF	125mM NaCl; 2.5mM KCl; 25mM $NaHCO_3$; 2mM $CaCl_2$; 1mM $MgCl_2$; 1.25mM NaH_2PO_4; 25mM Glucose	RT
Modified ACSF	125mM NaCl; 2.5mM KCl; 25mM $NaHCO_3$; 0.5mM $CaCl_2$; 4mM $MgCl_2$; 1.25mM NaH_2PO_4; 25mM Glucose	RT
Fluorescent solution	125mM K-Gluconate; 5mM NaCl; 2mM Na_2-ATP; 2mM $MgCl_2$; 10mM EGTA; 10mM HEPES; 10mM Biocytin; 0.2mM Alexa 488/594 hydrazide, pH7.4	RT

4.7.4 List of reagents

Table 4.4 List of reagents. Includes reagents and commercially available kits used.

Reagent	Company	Catalog number/Identifier
1 Kb ladder	NEB	N3232S
100 bp ladder	NEB	N3231S
100x GlutaMax	Invitrogen	35050-0380
10x Antractic Phos run Buffer	NEB	B0389 S
1M Hydrochloric acid	Applichem	A1434.1000
2-Propanol	Sigma	I9516-500ML
4-hydroxy-tamoxifen	Sigma	H7904
Acetic Acid Glacial	Sigma	ARK2183
Agar	Merck	1119251000
Agarose	Lonza	98200-100
Alexa 488 hydrazide	Life Technologies	A10436
Alexa 633 hydrazide	Life Technologies	A30634
Alzane® 5mg/ml (Atipamezol)	Pfizer	PZN 11283538
Ampicillin Sodium Salt	AppliChem	4G017739
Antarctic Phosphase	NEB	M0289S
Aqua-polymount	Polysciences Inc.	18606-20
ATP disodium salt hydrate	Sigma	A26209
B27 supplement	Life Technologies	17504-044
Bepanthen® Augen und Nasesalbe 5g	Bepanthen	PZN 01578675
Biocytin	Sigma	B4261E
BSA	Sigma	A9418-50 g
DAPI	Sigma	D9542
DMEM	Gibco	21969-035
DMEM-F12	Gibco	21331-020
Donkey serum	Merck Milipore	S30-100ml
Dorbene vet® (Medetomidin)	Pfizer	PZN 07725752
DPX mountant for histology	Sigma	06522
Calcium Chloride dihydrate	VWR	437053L
Corn Oil	Sigma	C8267
DH5α Competent Cells	Invitrogen	18265017
dNTP mix	NEB	N0447S

EGF	PeproTech	AF-100-15-1 mg
Ethanol absolute	Sigma	34923
Ethidium bromide	Sigma	46065
Ethylene glycol	Sigma	324558
Ethylenediamine tetraacetic acid Disodiumsalt (EDTA)	Calbiochem	15576-028/324503
ethylene glycol tetraacetic acid (EGTA)	Sigma	E0396
Fast Green FCF	Sigma	F7252
FBS	Invitrogen	10270-106
Fentadon® 50µg/ml (Fentanyl)	Albrecht	PZN 00094716
FGF-2	PeproTech	100-18B-100 ug
Flumazenil 0.1mg/ml	Hameln	PZN 9611975
G418 sulphate	InVivoGen	ant-gn-5
GenJet Plus	Tebu-bio	SL100499
Glucose	Sigma	G8270-1KG
Glycerol 99%	Sigma	G5516-500ML
Hepes 1M	Sigma	H0877-100ML
Horse serum	Invitrogen	16050-130
Invivo jetPEI transfection reagent	VWR	201-10
Forene 100v/v (Isoflurane)	Baxter	PZN: 06497131
Kanamycin sulfate	Sigma	60615-5 g
Ketaset® 100mg/ml (Ketamin)	Zoetis	PZN 12467849
L-Glutamax	Invitrogen	35050-0380
L-glutamine	Gibco	25030081
Lipofectamine™2000	Invitrogen	11668-019
LR Clonase™ II Enzyme Mix	Invitrogen	11791-020
Magnesium chloride anhydrous	Sigma	M8266
Midazolam 5mg/ml	Hameln	PZN 3760906
Mowiol® 40-88	Sigma	324590
Non-essential amino acids	Gibco	1140-035
NucleoBond® Xtra Maxi EF kit	Macherey-Nagel	740424.50
NucleoSpin® Plasmid EasyPure	Macherey-Nagel	740727.250
NucleoSpin® Gel and PCR Clean-up	Macherey-Nagel	740609.50

One Shot™ TOP10 Chemically Competent *E. coli*	Invitrogen	C404010
OptiMEM™	Gibco	31985-047
OptiPrep™ 60% (Iodixanol)	Sigma	D1556
Paraformaldehyde	Merck	8.18715.1000
PBS pH 7.2 (10x)	500 ml	70013-016
Pen/Strep, 10000u/ml	Invitrogen	15140122
pENTR™ 1A Dual Selection Vector	Invitrogen	A10462
Platinum™ Pfx DNA Polymerase	Invitrogen	11708-013
Poly-D-Lysine	Sigma	P6407
Potassium chloride	Fluka	60129
Potassium gluconate	Sigma	P1847
Potassium hydroxide, granular	Merck	1050330500
Potassium Phosphate monobasic (KH_2PO_4)	Calbiochem	529568
PureLink™ HiPure Plasmid Filter Maxiprep Kit	Invitrogen	K210017
Puromycin	Sigma	P9620
Purple loading dye	NEB	B7024 S
Quick Ligation™ kit	NEB	M2200S
Rimadyl® 50mg/ml (Carprofen)	Zoetis	2209276
Rompun® 2% (Xylazine)	Bayer	PZN 1320422
0.5 % Trypsin-EDTA	Gibco	15400-054
Sodium azide	Sigma	S2202
Sodium bicarbonate	Applichem	A0384
Sodium chloride	Amresco	0241-1KG
Sodium chloride 0.9% with benzylalcohol 0.9%	Prepared in house by the Pharmacy of the University Medical Center Mainz	
Sodium phosphate dibasic (Na_2HPO_4) dodecahydrate	Merck	106579
Sodium dihydrogen phosphate (NaH_2PO_4) dihydrate	Gen-Apex	33616.262
Sodium hydroxide	VWR	28244295
Sodium Pyruvate	Sigma	P2256
T4 DNA Ligase	NEB	M0202S

T4 DNA Ligase Buffer	NEB	B0202S
T4 DNA polymerase	NEB	M0203S
Tamoxifen	Sigma	T5648
Temgesic® (Buprenorphin)	RB Pharmaceuticals	PZN 0912306
Tetracyclin	Sigma	T660
Tris Ultrapure	Invitrogen	15504-020
Tris-Hydrochloride	CalBiochem	648317
Triton x 100	Sigma	X100-1L
Trypan blue	Gibco	15250-061
Trypsin-EDTA, 0.5 %	Life Technologies	15400054
Tryptone	Sigma (Fluka)	T9410-250 g
Tween 20	Sigma	P1379-500ML
Yeast extract	Sigma	Y1625

4.7.5 List of recombinant DNA and organisms modified

Table 4.5 List of recombinant DNA and organisms modified. Includes all constructs and organisms used in this study.

Plasmid	Original study/Origin
pCAG-Ascl1-IRES-eGFP	This study
pCAG-Ascl1SA6-IRES-eGFP	This study
pCAG-Ascl1SD6-IRES-eGFP	This study
pCAG-Ascl1-IRES-DsRed	This study
pCAG-Ascl1SA6-IRES-DsRed	This study
pCAG-Ascl1SD6-IRES-DsRed	This study
pCAG-IRES-DsRed	Heinrich et al. 2010
pMIG-Bcl2-IRES-GFP	Cheng et al. 2001 (Addgene 8793)
pGFAP-Ascl1ERT2-IRES-eYFP	This study
pGFAP-Ngn2ERT2-IRES-eYFP	This study
pGFAP-eYFP	García-Marqués e López-Mascaraque 2013

pGFAP-LSL-Bcl2	This study
pGFAP-Sox2	This study
pCMV-hyPBase	García-Marqués e López-Mascaraque 2013
pCAG-ERT2-Cre-ERT2	Figueres-Oñate et al. 2016
pUbc-loxP-eGFP-loxP	Figueres-Oñate et al. 2016
pUbc-loxP-mCherry-loxP	Figueres-Oñate et al. 2016
pUbc-loxP-mKO-loxP	Figueres-Oñate et al. 2016
pUbc-loxP-mCerulean-loxP	Figueres-Oñate et al. 2016
pUbc-loxP-mTSapphire-loxP	Figueres-Oñate et al. 2016
pUbc-loxP-H2BeGFP-loxP	Figueres-Oñate et al. 2016
pUbc-loxP-H2BmCherry-loxP	Figueres-Oñate et al. 2016
pUbc-loxP-H2BmKO-loxP	Figueres-Oñate et al. 2016
pUbc-loxP-H2BmCerulean-loxP	Figueres-Oñate et al. 2016
pUbc-loxP-H2BmTSapphire-loxP	Figueres-Oñate et al. 2016
HEK293	RRID:CVCL_0045
C57Bl6/J (*Mus musculus*)	RRID:IMSR_JAX:000664

4.7.6 List of primers

Table 4.6 List of primers. fw=forward primer (sequencing); rev=reverse primer (sequencing); F=forward primer (cloning); R=reverse primer (cloning). Underlined nucleotides on cloning primers indicate annealing to target DNA.

Primer	Sequence	Length (base pairs)	Target
E1fw	CGTTTCTACAAACTCTTCCTGTT	23	pENTR 1ADS
E1rev	AACATCAGAGATTTTGAGACAC	22	pENTR 1ADS
pUbc_fw	GGTTTTGAACTATGCGCTC	19	Human ubiquitin promoter, 3‘ end
hGFAP1970_fw	TGCCCAGGAAGCTCTGC	17	Human GFAP promoter, 3’ end

BGHpolyA_rev	AACTAGAAGGCACAGTCG	18	BGH polyA, 3'end
ERT2rev	TTGATCATGAGCGGGCTTGG	20	ERT2, 5' end
polyA_rev	CCAGCCACCACCTTCTGAT	19	PolyA, 5' end
Cre_fw	CAAAATTTGCCTGCATTACC	22	Cre recombinase, 5' end
Sox2117_rev	CGTTCATGGGCCTCTTGAC	19	Sox2, 5' end
hBcl2_rev	CTGCGACAGCTTATAATG	18	hBcl2, 5' end
IRES555fw	CGATGATAATATGGCCACAACC	19	IRES, 3' end
CAG477fw	CGTGTGACCGGCGGCTCTA	19	CAG promoter, 3' end
IREScompl	CACCGGCCTTATTCCAAGC	19	IRES, 5' end
40Fb_BamHI-kozak-HA	ATTCGGATCCAGCCACCATGTACCCATACGATGTTCCAG	39	Neurog2ERT2, N-terminus
40R_IRES-BamHI	AGATCGGATCCTTCATCGTGTTTTTCAAAGG	31	IRES, C-terminus
41F_BamHI-ClaI-IRES	ATTAGGATCCCTATCGATATCGACGGTACAAACGATCC	38	IRES, N-terminus
42F_ClaI-Ascl1ERT2	ATTAATCGATACCCGCACCATGGACTACAAG	30	Ascl1ERT2, N-terminus
42R_ERT2-ClaI	AGATCATCGATGAGACTCGAGTCAAGCTGTGG	32	ERT2, C-terminus
52F_BglII-ClaI-kozak-hBcl2	ATTAAGATCTAATCGATTCCACCATGGCGCACG	33	hBcl2, N-terminus
52R_IRES-BglII	TGATAGATCTTAGTGGCATATTATCATCGTG	31	IRES, C-terminus
53F_BamHI-Sox2	ATTAGGATCCGGACCATGGACTACAAGGACG	31	Sox2, N-terminus
53R_Sox2-BamHI	TGATGGATCCCGACTTACATGTGCGACAGG	30	Sox2, C-terminus

4.7.7 List of software and algorithms

Table 4.7 List of software and algorithms.

Software or algorithm	Company/Origin	Identifier
Image J (FIJI)	NIH	RRID:SCR_003070
ZEN	Carl Zeiss Microscopy	RRID:SCR_013672
SPSS	IBM	RRID:SCR_002865
Graphpad Prism 5	Graphpad	RRID:SCR_005375
Ape (A Plasmid Editor)	By M. Wayne Davis	RRID:SCR_014266
LASX	Leica	RRID:SCR_013673
pClamp10	Molecular Devices	RRID:SCR_011323
Clustal Omega	EBL-EBI	RRID:SCR_001591

5 Appendix

Appendix I - List of abbreviations (including genes and proteins mentioned in this manuscript)

°C	Celsius degrees
3'-OH	Hydroxy group left exposed at the 3' of a nicked DNA filament
3D	3 dimensional
A	Alanine
AKT	Protein Kinase B
AM	Astromedium
ANOVA	Analysis of variance
APC	Adenomatous polyposis coli
AQP4	Aquaporin 4
ASCL1	*Achaete Scute*-Like 1
Atf3	Activating transcription factor 3
ATOH1	Atonal bHLH Transcription Factor 1
ATOH7	Atonal bHLH Transcription Factor 7
BAM	Brn2+Ascl1+Myt1l
BCL2	B-cell lymphoma 2
bHLH	basic Helix-Loop-Helix
bIIItub	Beta III tubulin
BMP	Bone Morphogenetic Protein
BrdU	Bromodeoxyuridine
BRN2	POU class 3-Homeobox 2
BSA	Bovine serum albumin
c-Myc	Myc proto-oncogene c
Ca^{2+}	Calcium ion
CAG	Chicken b-actin
CANNTG	Cytosine-Alanine-any base-any base-Thymidine-Guanine
CBP	CREB-binding protein

CDK	Cyclin-dependent kinase
CENPJ	Centromere protein J
ChIP	Chromatin immunoprecipitation
cm	Centimetre
CMV	Cytomegalovirus
CRISPR	Clustered regularly interspaced short palindromic repeats
Ctrl	Control
D	Aspartic acid
DAPI	4′,6-diamidino-2-phenylindole
dCas9	Endonuclease deficient CRISPR associated protein 9
DCX	Doublecortin
DDE/D	Domain containing Aspartate-Aspartate-Glutamate/Aspartate
dH_2O	Distilled water
div	Days *in vitro*
DLX	Distal-less homeobox
DLX1/2	DLX1 and DLX2
DNA	Deoxyribonucleic acid
dpi	Days post injection
DREADDs	Designer Receptors Exclusively Activated by Designer Drugs
Drosophila	*Drosophila melanogaster*
DsRed	*Discosoma* red fluorescent protein
E	Embryonic day
E. coli	*Escherichia coli*
E47	E protein 47
EDTA	Ethylenediaminetetraacetic acid
EdU	5-Ethynyl-2′-deoxyuridine
EF	Endotoxin free
EGF	Epidermal growth factor
eGFP	Enhanced green fluorescent protein

Ephb2	Ephrin-type B receptor 2
ERK	Extracellular signal-regulated kinase
ERT2	Modified ligand-binding domain of the oestrogen receptor
eXFP	Enhanced fluorescent protein
FAIRE	Formaldehyde-assisted isolation of regulatory elements
FEZF2	Forebrain Embryonic Zinc Finger-like Protein 2
FGF	Fibroblast Growth factor
g	Gravity acceleration
GΩ	Giga Ohm
GABA	Gamma-Aminobutyric acid
GABAergic	That releases the neurotransmitter GABA
gag	Group-specific antigen
Gata4	GATA binding protein 4
GC-rich	Rich in Guanosine and Cytosine
GFAP	Glial fibrillar acidic protein
GFP	Green fluorescent protein
GLAST	Glutamate aspartate transporter
GLT-1	Glutamate transporter 1
GSK3	Glycogen synthase kinase 3
GTP	Guanosine-5'-Triphosphate
h	hours
H2B	Histone 2B
H3K4me1	Monomethylation of Lysine 4 on Histone 3
H3K4me3	Trimethylation of Lysine 4 on Histone 3
H4K20me3	Trimethylation of Lysine 20 on Histone 4
H3K27ac	Acethylation of Lysine 27 on Histone 4
HEK	Human embryonic kidney
HES	Hairy and enhancer of split
hGFAP	Human GFAP promoter

hiPSCs	Human induced pluripotent stem cells
HUWE1	HECT, UBA and WWE domain-containing protein 1
hyPBase	Hyperactive form of the *PiggyBAC* transposase
Hz	Hertz
Iba1	Ionized calcium-binding adapter molecule 1
ID	Inhibitor of DNA binding
IRES	Internal ribosome entry
JAK	Janus Kinase
Kb	Kilobases (=1000 base pairs)
Kir4.1	ATP-sensitive inward rectifier potassium channel 10
Klf4	Kruppel-like factor 4
miR/miRNA	micro-RNA
mKO	Monomeric Kusabira orange
LGE	Lateral ganglionic eminence
Lox (LoxP)	Locus of X over P1
m	mouse
Mef2c	Myocyte enhancer factor 2C
MEK	Mitogen-activated protein-kinase
MGE	Medial ganglionic eminence
min	Minutes
miRNA	microRNA
ml	Millilitre
mM	millimolar
MoMLV	Moloney-Murine Laeukemia Virus
mXFP	Monomeric fluorescent protein
MYOD	Myogenic differentiation 1
Myt1l	Myelin transcription factor 1-like
n	Number of biological replicates

ND4	Neuro D4
NeuN	Neuronal nuclei antigen
NFIA	Nuclear factor 1A-type
NG2	Chondroitin sulfate proteloglycan 4
NEUROG1	Neurogenin 1
NEUROG1/2	Neurogenin 1 and Neurogenin 2
NEUROG2	Neurogenin 2
NFIA	Nuclear factor 1 A-type
NSC	Neural stem cell
Oct4	Octamer-binding transcription factor 4
OLIG2	Oligodendrocyte lineage transcription factor 2
OPC	Oligodendrocyte progenitor cell
P	Postnatal day
p300	Protein p300
pASCL1	Collectively, wild type ASCL1, phospho-deficient ASCL1 and phospho-mutant ASCL1
PAX6	Paired box6
PBS	Phosphate buffer saline
PDGFR	Platelet-derived growth factor-alpha
PDL	Poly-D-Lysine hydrobromide
PI3K	Phosphoinositide 3 kinase
pol	DNA polymerase
polyA	Polyadenylation
PTEN	Phosphatase and tensin homolog
PVDF	Polyvinylidene fluorid
PZN	Pharmazentralnummer
RAF	Raf-1 proto-oncogene
RAS	RAS GTPase
RBPJ	Recombination signal binding protein for immunoglobulin kappa J region
REST	RE1-silencing transcription factor

RFP	Red fluorescent protein
RG	Radial glia
RGC	Radial glial cell
RNA	Ribonucleic acid
Rnd2	Rho family GTPase 2
ROS	Reactive oxygen species
RT	Room temperature
RTK	Receptor tyrosine kinase
Runx2	Runt-related transcription factor 2
RV	Retrovirus
SA	Serine>Alanine mutation
SA6	Serine>Alanine mutation at all six SP sites present in the protein
SD	Serine>aspartate mutation
SD	Standard deviation
SD6	Serine>aspartate mutation at all six SP sites present in the protein
SEZ	Subependymal zone
S/G2	Synthesis/Gap2
sgRNA	Small guide RNA
Shh	Sonic hedgehog
Sox	Sex-detemining region Y-box
SP (S/P)	Serine/Proline
STAT	Signal Transducer and Activator of Transcription proteins
SVZ	Subventricular zone
TA-rich	Rich in Thymidine and Alanine
TBS	Tris-buffered saline
Tbx	T-box
tetO/tetR	Tetracycline-repressed/Tetracycline responsive
TF	Transcription factor
TIR (TR)	Terminal inverted repeat (Terminal repeat)

Tlx	Nuclear receptor TLX
TM	Transfection medium
TP (T/P)	Threonine/Proline
U	unit
Ubq	Ubiquitin promoter
VP16	Transactivating tegument protein VP16
VSV-G	Vesicular stomatitis virus G-protein
VZ	Ventricular zone
Wnt	Wingless type MMTV integration site
wpi	Weeks post injection
wt	Wild type
Xaenopus	Xaenopus laevis
xg	Relative centrifugal force
Y	Thyrosine
YFP	Yellow fluorescent protein
ZBTB20	Zinc finger and BTB domain-containing protein 20
ZFP24	Zinc finger protein 24
µg	Microgram
µl	Microliter

Appendix II - List of figures and tables

Appendix III - Number of cells quantified for each experiment of section 2.2. Total number of cells analysed. The n of each experiment indicates the number of independent experiments (biological replicates).

Experiment	Figure - Experimental condition; staining quantified	Number of animals (n)	Total number of cells
Transfection - *in vitro*	Fig. 2.2 - Ascl1 wt; DCX	3	625
	Fig. 2.2 - Ascl1SA6; DCX	3	904
	Fig. 2.2 - Ascl1SD6; DCX	3	515
Transduction - *in vitro*	Fig. 2.3 – Ctrl; bIIItub	3	1398
	Fig. 2.3 - Ascl1 wt; bIIItub	3	3061
	Fig. 2.3 - Ascl1SA6; bIIItub	3	3462
	Fig. 2.3 - Ascl1SD6; bIIItub	3	4376
Injection - 3dpi	Fig. 2.4 - Ctrl; Iba1/DCX	3	578
	Fig. 2.4 - Ctrl; GFAP/Sox10	3	753
Injection - 12dpi	Fig. 2.6 - Ctrl; DCX	3	2157
	Fig. 2.6 - Ascl1 wt; DCX	4	720
	Fig. 2.6 - Ascl1SA6; DCX	3	409
	Fig. 2.6 - Ascl1SD6; DCX	3	286
	Fig. 2.7, 2.8 - Ctrl; GFAP/Sox10	3	1885
	Fig. 2.7, 2.8 - Ascl1 wt; GFAP/Sox10	4	848
	Fig. 2.7, 2.8 - Ascl1SA6; GFAP/Sox10	3	573
	Fig. 2.7, 2.8 - Ascl1SD6; GFAP/Sox10	3	286
	Fig. 2.9 - Ctrl; Sox10/APC	3	1830
	Fig. 2.9 - Ascl1 wt; Sox10/APC	4	1654
	Fig. 2.9 - Ascl1SA6; Sox10/APC	3	690
	Fig. 2.9 - Ascl1SD6; Sox10/APC	3	237
Injection + Bcl2 - 12dpi	Fig. 2.11, 2.12, 2.13 - Ascl1 wt, DCX/NeuN	3	2380
	Fig. 2.11, 2.12, 2.13 - Ascl1SA6, DCX/NeuN	3	836
	Fig. 2.11, 2.12, 2.13 - Ascl1SD6, DCX/NeuN	3	734
	Fig. 2.14 - Ascl1 wt, GABA	3	2258
	Fig. 2.14 - Ascl1SA6, GABA	3	556
	Fig. 2.14 - Ascl1SD6, GABA	3	643
	Fig. 2.15 - Ascl1SA6, electrophysiology	3	6

Appendix IV - List of p-values for all comparisons represented in section 2.2. *(see next page)* Statistical analyses were run as One-Way ANOVA. Multiple comparisons were performed with Bonferroni post-hoc.

Figure number	One-Way ANOVA p-value	Comparison	Bonferroni p-value	Symbol
Fig. 2.2	0.005	Ascl1SA6 vs Ascl1SD6	0,005	**

Fig. 2.3	<0.001	Ascl1 wt vs Ctrl	<0.001	***
		Ascl1SA6 vs Ctrl	<0.001	***
		Ascl1SD6 vs Ctrl	<0.001	***
		Ascl1 wt vs Ascl1SA6	0,001	**
		Ascl1SD6 vs Ascl1SA6	0,028	*
Fig. 2.6	<0.001	Ascl1 wt vs Ctrl	0,001	**
		Ascl1SA6 vs Ctrl	<0.001	***
		Ascl1SD6 vs Ctrl	0,004	**
		Ascl1SD6 vs Ascl1SA6	0,031	*
Fig. 2.7C	<0.001	Ascl1 wt vs Ctrl	<0.001	***
		Ascl1SA6 vs Ctrl	<0.001	***
		Ascl1SD6 vs Ctrl	<0.001	***
Fig. 2.7C'	0.001	Ascl1 wt vs Ctrl	0,001	**
		Ascl1 wt vs Ascl1SA6	0,033	*
		Ascl1 wt vs Ascl1SD6	0,021	*
Fig. 2.8	0.001	Ascl1SA6 vs Ctrl	0,002	**
		Ascl1SD6 vs Ctrl	0,011	*
		Ascl1 wt vs Ascl1SA6	0,008	**
Fig. 2.9C	<0.001	Ascl1 wt vs Ctrl	0,001	**
		Ascl1 wt vs Ascl1SA6	<0.001	***
		Ascl1 wt vs Ascl1SD6	0,007	**
Fig. 2.9C'	0.003	Ascl1 wt vs Ascl1SA6	0,010	*
		Ascl1 wt vs Ascl1SD6	0,005	**
Fig. 2.11	<0.001	Ascl1 wt GFP/RFP vs Ascl1 t RFP-only	<0.001	###
		Ascl1SA6 GFP/RFP vs Ascl1SA6 RFP-only	0,008	##
		Ascl1SD6 GFP/RFP vs Ascl1SD6 RFP-only	<0.001	###
		Ascl1SA6 GFP/RFP vs Ascl1SD6 GFP/ RFP	0,005	**
Fig. 2.12	<0.001	Ascl1SA6 GFP/RFP vs Ascl1SA6 RFP-only	<0.001	###
		Ascl1SD6 GFP/RFP vs Ascl1SD6 RFP-only	0,023	#
		Ascl1 wt GFP/RFP vs Ascl1SA6 GFP/ RFP	<0.001	***
		Ascl1SA6 GFP/RFP vs Ascl1SD6 GFP/ RFP	<0.001	***
Fig. 2.13	<0.001	Ascl1 wt GFP/RFP vs Ascl1 wt RFP-only	0,001	##
		Ascl1SA6 GFP/RFP vs Ascl1SA6 RFP-only	0,001	##
		Ascl1SD6 GFP/RFP vs Ascl1SD6 RFP-only	0,002	##
		Ascl1 wt GFP/RFP vs Ascl1SA6 GFP/ RFP	0,008	**
Fig. 2.14	<0.001	Ascl1SA6 GFP/RFP vs Ascl1SA6 RFP-only	<0.001	###
		Ascl1SD6 GFP/RFP vs Ascl1SD6 RFP-only	0,022	#
		Ascl1 wt GFP/RFP vs Ascl1SA6 GFP/ RFP	<0.001	***
		Ascl1SA6 GFP/RFP vs Ascl1SD6 GFP/ RFP	<0.001	***

Bibliography

Abernathy, D. G., W. K. Kim, M. J. McCoy, A. M. Lake, R. Ouwenga, S. W. Lee, X. Xing, et al. 2017. "MicroRNAs Induce a Permissive Chromatin Environment That Enables Neuronal Subtype-Specific Reprogramming of Adult Human Fibroblasts." *Cell Stem Cell* 21 (3): 332–348.e9. https://doi.org/10.1016/j.stem.2017.08.002.

Ali, F., C. Hindley, G. McDowell, R. Deibler, A. Jones, M. Kirschner, F. Guillemot, and A. Philpott. 2011. "Cell Cycle-Regulated Multi-Site Phosphorylation of Neurogenin 2 Coordinates Cell Cycling with Differentiation during Neurogenesis." *Development* 138 (19): 4267–77. https://doi.org/10.1242/dev.067900.

Ali, F. R., K. Cheng, P. Kirwan, S. Metcalfe, F. J. Livesey, R. A. Barker, and A. Philpott. 2014. "The Phosphorylation Status of Ascl1 Is a Key Determinant of Neuronal Differentiation and Maturation in Vivo and in Vitro." *Development* 141 (11): 2216–24. https://doi.org/10.1242/dev.106377.

Amamoto, R., and P. Arlotta. 2014. "Development-Inspired Reprogramming of the Mammalian Central Nervous System." *Science* 343. https://doi.org/10.1126/science.1239882.

Andersen, J., N. Urba, A. Achimastou, A. Ito, M. Simic, K. Ullom, B. Martynoga, C. Goeritz, M. Nakafuku, and F. Guillemot. 2014. "A Transcriptional Mechanism Integrating Inputs from Extracellular Signals to Activate Hippocampal Stem Cells." *Neuron* 83: 1085–97. https://doi.org/10.1016/j.neuron.2014.08.004.

Anderson, M. A., J. E. Burda, Y. Ren, Y. Ao, T. M. O'Shea, R. Kawaguchi, G. Coppola, B. S. Khakh, T. J. Deming, and M. V. Sofroniew. 2016. "Astrocyte Scar Formation Aids Central Nervous System Axon Regeneration." *Nature* 532 (7598): 195–200. https://doi.org/10.1038/nature17623.

Araque, A., G. Carmignoto, P. G. Haydon, S. H.R. Oliet, R. Robitaille, and A. Volterra. 2014. "Gliotransmitters Travel in Time and Space." *Neuron* 81 (4): 728–39. https://doi.org/10.1016/j.neuron.2014.02.007.

Bardehle, S., M. Krüger, F. Buggenthin, J. Schwausch, J. Ninkovic, H Clevers, H. J. Snippert, et al. 2013. "Live Imaging of Astrocyte Responses to Acute Injury Reveals Selective Juxtavascular Proliferation." *Nature Neuroscience* 16 (5): 580–86. https://doi.org/10.1038/nn.3371.

Barkal, A. A., S. Srinivasan, T. Hashimoto, D. K. Gifford, and R. I. Sherwood. 2016. "Cas9 Functionally Opens Chromatin." *PLoS ONE* 11 (3): 1–8. https://doi.org/10.1371/journal.pone.0152683.

Barry, D., and H. McDermott. 2005. "Differentiation of Radial Glia from Radial Precursor Cells and Transformation into Astrocytes in the Developing Rat Spinal Cord." *Glia* 50 (3): 187–97. https://doi.org/10.1002/glia.20166.

Baumgart, J., and N. Grebe. 2015. "C57BL/6-Specific Conditions for Efficient in Utero Electroporation of the Central Nervous System." *Journal of Neuroscience Methods* 240: 116–24. https://doi.org/10.1016/j.jneumeth.2014.11.004.

Ben-Arie, N., H. J. Bellen, D. L. Armstrong, A. E. McCall, P. R. Gordadze, Q. Guo, M. M. Matzuk, and H. Y. Zoghbi. 1997. "Math1 Is Essential for Genesis of Cerebellar Granule Neurons." *Nature* 390: 169–72.

Berninger, B., M. R. Costa, U. Koch, T. Schroeder, B. Sutor, B. Grothe, and M. Götz. 2007. "Functional Properties of Neurons Derived from In Vitro Reprogrammed Postnatal Astroglia." *Journal of Neuroscience* 27 (32): 8654–64. https://doi.org/10.1523/JNEUROSCI.1615-07.2007.

Berninger, B., F. Guillemot, and M. Götz. 2007. "Directing Neurotransmitter Identity of Neurones Derived from Expanded Adult Neural Stem Cells." *European Journal of Neuroscience* 25 (November 2006): 2581–90. https://doi.org/10.1111/j.1460-9568.2007.05509.x.

Bertrand, N., D. S. Castro, and F. Guillemot. 2002. "Proneural Genes and the Specification of Neural Cell Types." *Nature Reviews Neuroscience* 3 (7): 517–30. https://doi.org/10.1038/nrn874.

Bluske, K. K., T. Y. Vue, Y. Kawakami, M. M. Taketo, K. Yoshikawa, J. E. Johnson, and Y. Nakagawa. 2012. "Beta-Catenin Signaling Specifies Progenitor Cell Identity in Parallel with Shh Signaling in the Developing Mammalian Thalamus." *Development* 2702: 2692–2702. https://doi.org/10.1242/dev.072314.

Borromeo, M. D., D. M. Meredith, D. S. Castro, J. C. Chang, K. Tung, F. Guillemot, and J. E. Johnson. 2017. "A Transcription Factor Network Specifying Inhibitory versus Excitatory Neurons in the Dorsal Spinal Cord." *Development* 144: 2803–12. https://doi.org/10.1242/dev.155986.

Braun, S. M. G., G. A. Pilz, R. A. C. Machado, J. Moss, B. Becher, N. Toni, and S. Jessberger. 2015. "Programming Hippocampal Neural Stem/Progenitor Cells into Oligodendrocytes Enhances Remyelination in the Adult Brain after Injury." *Cell Reports* 11 (11): 1679–85. https://doi.org/10.1016/j.celrep.2015.05.024.

Brown, J. P., S. Couillard-Després, C. M. Cooper-Kuhn, J. Winkler, L. Aigner, and H. G. Kuhn. 2003. "Transient Expression of Doublecortin during Adult Neurogenesis." *Journal of Comparative Neurology* 467 (1): 1–10. https://doi.org/10.1002/cne.10874.

Brown, N. L., S. L. Dagenais, C. M. Chen, and T. Glaser. 2002. "Molecular Characterization and Mapping of ATOH7, a Human Atonal Homolog with a Predicted Role in Retinal Ganglion Cell Development." *Mammalian Genome* 13 (2): 95–101. https://doi.org/10.1007/s00335-001-2101-3.

Buenrostro, J., B. Wu, H. Chang, and W. Greenleaf. 2016. "ATAC-Seq: A Method for Assaying Chromatin Accessibility Genome-Wide." *Current Protocols in Molecular Biology* 109: 1–10. https://doi.org/10.1002/0471142727.mb2129s109.

Buffo, A., I. Rite, P. Tripathi, A. Lepier, D. Colak, A.-P. Horn, T. Mori, and M. GATAC-seq: A Method for Assaying Chromatin Accessibility Genome-Widetz. 2008. "Origin and Progeny of Reactive Gliosis: A Source of Multipotent Cells in the Injured Brain." *Proceedings of the National Academy of Sciences* 105 (9): 3581–86. https://doi.org/10.1073/pnas.0709002105.

Bushong, E. A., M. E. Martone, Y. Z. Jones, and M. H. Ellisman. 2002. "Protoplasmic Astrocytes in CA1 Stratum Radiatum Occupy Separate Anatomical Domains." *The Journal of Neuroscience* 22 (1): 183–92. https://doi.org/https://doi.org/10.1523/JNEUROSCI.22-01-00183.2002.

Cadiñanos, J., and A. Bradley. 2007. "Generation of an Inducible and Optimized PiggyBac Transposon Systemy." *Nucleic Acids Research* 35 (12): e87. https://doi.org/10.1093/nar/gkm446.

Cai, L., E. M. Morrow, and C. L. Cepko. 2000. "Misexpression of Basic Helix-Loop-Helix Genes in the Murine Cerebral Cortex Affects Cell Fate Choices and Neuronal Survival." *Development (Cambridge, England)* 127 (14): 3021–30.

Caiazzo, M., M. T. Dell'Anno, E. Dvoretskova, D. Lazarevic, S. Taverna, D. Leo, T. D. Sotnikova, et al. 2011. "Direct Generation of Functional Dopaminergic Neurons from Mouse and Human Fibroblasts." *Nature* 476 (7359): 224–27. https://doi.org/10.1038/nature10284.

Caiazzo, M., S. Giannelli, P. Valente, G. Lignani, A. Carissimo, A. Sessa, G. Colasante, et al. 2015. "Direct Conversion of Fibroblasts into Functional Astrocytes by Defined Transcription Factors." *Stem Cell Reports* 4 (1): 25–36. https://doi.org/10.1016/j.stemcr.2014.12.002.

Camp, J. G., F. Badsha, M. Florio, S. Kanton, T. Gerber, M. Wilsch-Bräuninger, E. Lewitus, et al. 2015. "Human Cerebral Organoids Recapitulate Gene Expression Programs of Fetal Neocortex Development." *Proceedings of the National Academy of Sciences* 112 (51): 201520760. https://doi.org/10.1073/pnas.1520760112.

Casarosa, S., C. Fode, and F. Guillemot. 1999. "Mash1 Regulates Neurogenesis in the Ventral

Telencephalon." *Development (Cambridge, England)* 126: 525–34. https://doi.org/10.1371/journal.pcbi.0020117.

Castro, D. S., B. Martynoga, C. Parras, V. Ramesh, E. Pacary, L. G. Garcia, C. Johnston, et al. 2011. "A Novel Function of the Proneural Factor Ascl1 in Progenitor Proliferation Identified by Genome-Wide Characterization of Its Targets." *Genes and Development* 25: 930–45. https://doi.org/10.1101/gad.627811.6.

Castro, D. S., D. Skowronska-Krawczyk, O. Armant, I. J. Donaldson, C. Parras, C. Hunt, J. A. Critchley, et al. 2006. "Proneural BHLH and Brn Proteins Coregulate a Neurogenic Program through Cooperative Binding to a Conserved DNA Motif." *Developmental Cell* 11 (6): 831–44. https://doi.org/10.1016/j.devcel.2006.10.006.

Cataldo, A. M., and R. D. Broadwell. 1986. "Cytochemical Identification of Cerebral Glycogen and Glucose-6-Phosphatase Activity under Normal and Experimental Conditions . II . Choroid Plexus and Ependymal Epithelia , Endothelia and Pericytes." *Journal of Neurocytology* 524: 511–24. https://doi.org/https://doi.org/10.1007/BF01611733.

Chai, H., B. Diaz-Castro, E. Shigetomi, E. Monte, J. C. Octeau, X. Yu, W. Cohn, et al. 2017. "Neural Circuit-Specialized Astrocytes: Transcriptomic, Proteomic, Morphological, and Functional Evidence." *Neuron* 95 (3): 531–549.e9. https://doi.org/10.1016/j.neuron.2017.06.029.

Chen, H., A. Thiagalingam, H. Chopra, M. W. Borges, J. N. Feder, B. D. Nelkin, S. B. Baylin, and D. W. Ball. 1997. "Conservation of the Drosophila Lateral Inhibition Pathway in Human Lung Cancer: A Hairy-Related Protein (HES-1) Directly Represses Achaete-Scute Homolog-1 Expression." *Proceedings of the National Academy of Sciences of the United States of America* 94 (10): 5355–60. https://doi.org/10.1073/pnas.94.10.5355.

Cheng, E. H. A., M. C. Wei, S. Weiler, R. A. Flavell, T. K. Mak, T. Lindsten, S. J. Korsmeyer, and N. Haven. 2001. "BCL-2 , BCL-X L Sequester BH3 Domain-Only Molecules Preventing BAX- and BAK-Mediated Mitochondrial Apoptosis." *Molecular Cell* 8: 705–11. https://doi.org/https://doi.org/10.1016/S1097-2765(01)00320-3.

Cheng, P. Y., Y. P. Lin, Y. L. Chen, Y. C. Lee, C. C. Tai, Y. T. Wang, Y. J. Chen, C. F. Kao, and J. Yu. 2011. "Interplay between SIN3A and STAT3 Mediates Chromatin Conformational Changes and GFAP Expression during Cellular Differentiation." *PLoS ONE* 6 (7): 1–15. https://doi.org/10.1371/journal.pone.0022018.

Chien, C.-t., C.-D. Hsiao, L. Y. Jan, and Y. N. Jan. 1996. "Neuronal Type Information Encoded in the Basic-Helix-Loop-Helix Domain of Proneural Genes." *Proceedings of the National Academy of Sciences* 93 (23): 13239–44. https://doi.org/10.1073/pnas.93.23.13239.

Clements, J. D., R. A. J. Lestert, G. Tong, C. E. Jahr, and G. L. Westbrook. 1992. "The Time Course of Glutamate in the Synaptic Cleft." *Science* 258: 1498–1501. https://doi.org/10.1126/science.1359647.

Colasante, G., G. Lignani, A. Rubio, L. Medrihan, L. Yekhlef, A. Sessa, L. Massimino, et al. 2015. "Rapid Conversion of Fibroblasts into Functional Forebrain GABAergic Interneurons by Direct Genetic Reprogramming." *Cell Stem Cell* 17 (6): 719–34. https://doi.org/10.1016/j.stem.2015.09.002.

Cornell-Bell, A. H., S. M. Finkbeiner, M. S. Cooper, and S. J. Smith. 1989. "Glutamate Induces Clacium Waves in Cultures Astrocytes: Long-Range Glial Signaling." *Science* 247 (24): 470–73. https://doi.org/10.1126/science.1967852.

Culican, S. M., N. L. Baumrind, M. Yamamoto, and A. L. Pearlman. 1990. "Cortical Radial Glia: Identification in Tissue Culture and Evidence for Their Transformation to Astrocytes." *The Journal of Neuroscience* 10 (February): 684–92.

Dean, D. A., B. S. Dean, S. Muller, and L. C. Smith. 1999. "Sequence Requirements for Plasmid Nuclear Import." *Experimental Cell Research* 253 (2): 713–22. https://doi.org/10.1006/excr.1999.4716.

Dehorter, N., N. Marichal, O. Marín, and B. Berninger. 2017. "Tuning Neural Circuits by Turning the Interneuron Knob." *Current Opinion in Neurobiology* 42: 144–51. https://doi.org/10.1016/j.conb.2016.12.009.

Dennis, D. J., S. Han, and C. Schuurmans. 2018. "BHLH Transcription Factors in Neural Development, Disease, and Reprogramming." *Brain Research*. https://doi.org/10.1016/j.brainres.2018.03.013.

Dimou, L., and M. Gotz. 2014. "Glial Cells as Progenitors and Stem Cells: New Roles in the Healthy and Diseased Brain." *Physiological Reviews* 94 (3): 709–37. https://doi.org/10.1152/physrev.00036.2013.

Dixit, R., G. Wilkinson, G. I. Cancino, T. Shaker, L. Adnani, S. Li, D. Dennis, et al. 2014. "Neurog1 and Neurog2 Control Two Waves of Neuronal Differentiation in the Piriform Cortex." *Journal of Neuroscience* 34 (2): 539–53. https://doi.org/10.1523/JNEUROSCI.0614-13.2014.

Dixon, S. J., K. M. Lemberg, M. R. Lamprecht, R. Skouta, E. M. Zaitsev, C. E. Gleason, D. N. Patel, et al. 2012. "Ferroptosis: An Iron-Dependent Form of Nonapoptotic Cell Death." *Cell* 149 (5): 1060–72. https://doi.org/10.1016/j.cell.2012.03.042.

Elbaz, B., J. D. Aaker, S. Isaac, A. Kolarzyk, P. Brugarolas, A. Eden, and B. Popko. 2018. "Phosphorylation State of ZFP24 Controls Oligodendrocyte Differentiation." *Cell Reports* 23 (8): 2254–63. https://doi.org/10.1016/j.celrep.2018.04.089.

Encinas, J. M., and C. P. Fitzsimons. 2017. "Gene Regulation in Adult Neural Stem Cells. Current Challenges and Possible Applications." *Advanced Drug Delivery Reviews* 120: 118–32. https://doi.org/10.1016/j.addr.2017.07.016.

Espuny-Camacho, I., K. A. Michelsen, D. Gall, D. Linaro, A. Hasche, J. Bonnefont, C. Bali, et al. 2013. "Pyramidal Neurons Derived from Human Pluripotent Stem Cells Integrate Efficiently into Mouse Brain Circuits In Vivo." *Neuron* 77 (3): 440–56. https://doi.org/10.1016/j.neuron.2012.12.011.

Faiz, M., N. Sachewsky, S. Gascón, K. W. A. Bang, C. M. Morshead, and A. Nagy. 2015. "Adult Neural Stem Cells from the Subventricular Zone Give Rise to Reactive Astrocytes in the Cortex after Stroke." *Cell Stem Cell* 17 (5): 624–34. https://doi.org/10.1016/j.stem.2015.08.002.

Falk, S., and M. Karow. 2018. "Natural and Forced Neurogenesis: Similar and yet Different?" *Cell and Tissue Research* 371 (1): 181–87. https://doi.org/10.1007/s00441-017-2690-0.

Farmer, W. T., T. Abrahamsson, S. Chierzi, C. Lui, C. Zaelzer, E. V. Jones, B. Ponroy Bally, et al. 2016. "Neurons Diversify Astrocytes Int He Adult Brain through Sonic Hedgehog Signaling." *Science* 351 (6275): 849–54. https://doi.org/10.1126/science.aab3103.

Farmer, W. T., and K. Murai. 2017. "Resolving Astrocyte Heterogeneity in the CNS." *Frontiers in Cellular Neuroscience* 11 (September): 1–7. https://doi.org/10.3389/fncel.2017.00300.

Ferré-D'Amaré, A. R., G. C. Prendergast, E. B. Ziff, and S. K. Burley. 1993. "Recognition by Max of Its Cognate DNA through a Dimeric b/HLH/Z Domain." *Nature* 363 (6424): 38–45. https://doi.org/10.1038/363038a0.

Figueres-Onãte, M., J. Garciá-Marqués, and L. López-Mascaraque. 2016. "UbC-StarTrack, a Clonal Method to Target the Entire Progeny of Individual Progenitors." *Scientific Reports* 6: 1–13. https://doi.org/10.1038/srep33896.

Figueres-Oñate, M., J. García-Marqués, M. Pedraza, J. A. De Carlos, and L. López-Mascaraque. 2015. "Spatiotemporal Analyses of Neural Lineages after Embryonic and Postnatal Progenitor Targeting Combining Different Reporters." *Frontiers in Neuroscience* 9 (MAR): 1–11. https://doi.org/10.3389/fnins.2015.00087.

Figueres-Onãte, Mariá, J. Garciá-Marqués, and L. López-Mascaraque. n.d. "UbC-StarTrack, a Clonal Method to Target the Entire Progeny of Individual Progenitors." *Scientific Reports* 6 (May): 1–13. https://doi.org/10.1038/srep33896.

Fode, C., G. Gradwohl, X. Morin, A. Dierich, M. LeMeur, C. Goridis, and F Guillemot. 1998. "The BHLH Protein NEUROGENIN 2 Is a Determination Factor for Epibranchial Placode-Derived Sensory Neurons." *Neuron* 20 (3): 483–94. https://doi.org/10.1016/S0896-6273(00)80989-7.

Fode, C., Q. Ma, S. Casarosa, S. L. Ang, D. J. Anderson, and F. Guillemot. 2000. "A Role for Neural Determination Genes in Specifying the Dorsoventral Identity of Telencephalic Neurons." *Genes and Development* 14 (1): 67–80. https://doi.org/10.1101/gad.14.1.67.

Fraser, M., J. S. Brusca, G. Smith, and M. D. Summers. 1985. *Transposon-Mediated Mutagenesis of a Baculovirus*. *Virology*. Vol. 145. https://doi.org/10.1016/0042-6822(85)90172-2.

Frühbeis, C., D. Fröhlich, W. P. Kuo, J. Amphornrat, S. Thilemann, A. S. Saab, F. Kirchhoff, et al. 2013. "Neurotransmitter-Triggered Transfer of Exosomes Mediates Oligodendrocyte-Neuron Communication." *PLoS Biology* 11 (7): e1001604. https://doi.org/10.1371/journal.pbio.1001604.

Fuentealba, L. C., S. B. Rompani, J. I. Parraguez, K. Obernier, R. Romero, C. L. Cepko, and A. Alvarez-Buylla. 2015. "Embryonic Origin of Postnatal Neural Stem Cells." *Cell* 161 (7): 1644–55. https://doi.org/10.1016/j.cell.2015.05.041.

Furutachi, S., H. Miya, T. Watanabe, H. Kawai, N. Yamasaki, Y. Harada, I. Imayoshi, et al. 2015. "Slowly Dividing Neural Progenitors Are an Embryonic Origin of Adult Neural Stem Cells." *Nature Neuroscience* 18 (5): 657–65. https://doi.org/10.1038/nn.3989.

Galabova-Kovacs, G., F. Catalanotti, D. Matzen, G. X. Reyes, J. Zezula, R. Herbst, A. Silva, I. Walter, and M. Baccarini. 2008. "Essential Role of B-Raf in Oligodendrocyte Maturation and Myelination during Postnatal Central Nervous System Development." *Journal of Cell Biology* 180 (5): 947–55. https://doi.org/10.1083/jcb.200709069.

Garcez, P. P., J. Diaz-alonso, I. Crespo-enriquez, D. Castro, and D. Bell. 2015. "Cenpj/CPAP Regulates Progenitor Divisions and Neuronal Migration in the Cerebral Cortext Downstream of Ascl1." *Nature Communications* 6:6474. https://doi.org/10.1038/ncomms7474.

García-Marqués, J., and L. López-Mascaraque. 2013. "Clonal Identity Determines Astrocyte Cortical Heterogeneity." *Cerebral Cortex* 23 (6): 1463–72. https://doi.org/10.1093/cercor/bhs134.

García-Marqués, J., R. Núñez-Llaves, and L. López-Mascaraque. 2014. "NG2-Glia from Pallial Progenitors Produce the Largest Clonal Clusters of the Brain: Time Frame of Clonal Generation in Cortex and Olfactory Bulb." *Journal of Neuroscience* 34 (6): 2305–13. https://doi.org/10.1523/JNEUROSCI.3060-13.2014.

Gascón, S., E. Murenu, G. Masserdotti, F. Ortega, G. L. Russo, D. Petrik, A. Deshpande, et al. 2016. "Identification and Successful Negotiation of a Metabolic Checkpoint in Direct Neuronal Reprogramming." *Cell Stem Cell* 18 (3): 396–409. https://doi.org/10.1016/j.stem.2015.12.003.

Ge, W. P., A. Miyawaki, F. H. Gage, Y. N. Jan, and L.Y. Jan. 2013. "Local Generation of Glia Is a Major Astrocyte Source in Postnatal Cortex." *Nature* 484 (7394): 376–80. https://doi.org/10.1038/nature10959.Local.

Gillotin, S., J. D. Davies, and A. Philpott. 2018. "Subcellular Localisation Modulates Ubiquitylation and Degradation of Ascl1." *Scientific Reports* 8 (1): 1–13. https://doi.org/10.1038/s41598-018-23056-4.

Giresi, P.G., J. Kim, R. M. McDaniell, V. R. Iyer, and J. D. Lieb. 2007. "FAIRE (Formaldehyde-Assisted Isolation of Regulatory Elements) Isolates Active Regulatory Elements from Human Chromatin." *Genome Research* 17 (6): 877–85. https://doi.org/10.1101/gr.5533506.

Girouard, H., A. D. Bonev, R. M. Hannah, A. Meredith, R. W. Aldrich, and M. T. Nelson. 2009. "Astrocytic Endfoot Ca2+ and BK Channels Determine Both Arteriolar Dilation and Constriction." *Proceedings of the National Academy of Sciences* 107 (8): 3811–16. https://doi.org/10.1073/pnas.0914722107.

Goetzl, E. J., M. Mustapic, D. Kapogiannis, E. Eitan, I. V. Lobach, L. Goetzl, J. B. Schwartz, and B. L. Miller. 2016. "Cargo Proteins of Plasma Astrocyte-Derived Exosomes in Alzheimer's Disease." *The FASEB Journal* 30: 3853–59. https://doi.org/https://doi.org/10.1096/fj.201600756R.

Göritz, C., D. O. Dias, N. Tomilin, M. Barbacid, O. Shupliakov, and J. Frisén. 2011. "A Pericyte Origin of Spinal Cord Scar Tissue." *Science* 333 (July): 238–43. https://doi.org/10.1126/science.1203165.

Gross, R. E., M. F. Mehler, P. C. Mabie, Z. Zang, L. Santschi, and J. A. Kessler. 1996. "Bone Morphogenetic Proteins Promote Astroglial Lineage Commitment by Mammalian Subventricular Zone Progenitor Cells." *Neuron* 17 (4): 595–606. https://doi.org/10.1016/S0896-6273(00)80193-2.

Guillemot, F., and B. A. Hassan. 2017. "Beyond Proneural: Emerging Functions and Regulations of Proneural Proteins." *Current Opinion in Neurobiology* 42: 93–101. https://doi.org/10.1016/j.conb.2016.11.011.

Guillemot, F., and A. L. Joyner. 1993. "Dynamic Expression of the Murine Achaete-Scute Homologue Mash-1 in the Developing Nervous System." *Mechanisms of Development* 42: 171–85.

Guillemot, F., L. C. Lo, J. E. Johnson, A. Auerbach, D. J. Anderson, and A. L. Joyner. 1993. "Mammalian Achaete-Scute Homolog 1 Is Required for the Early Development of Olfactory and Autonomic Neurons." *Cell* 75 (3): 463–76. https://doi.org/10.1016/0092-8674(93)90381-Y.

Guo, Z., L. Zhang, Z. Wu, Y. Chen, F. Wang, and G. Chen. 2014. "In Vivo Direct Reprogramming of Reactive Glial Cells into Functional Neurons after Brain Injury and in an Alzheimer's Disease Model." *Cell Stem Cell* 14 (2): 188–202. https://doi.org/10.1016/j.stem.2013.12.001.

Gurdon, J. B. 1962. "Adult Frogs Derived from the Nuclei of Single Somatic Cells." *Developmental Biology* 4 (2): 256–73. https://doi.org/10.1016/0012-1606(62)90043-X.

Hand, R., D. Bortone, P. Mattar, L. Nguyen, J. I. T. Heng, S. Guerrier, E. Boutt, et al. 2005. "Phosphorylation of Neurogenin2 Specifies the Migration Properties and the Dendritic Morphology of Pyramidal Neurons in the Neocortex." *Neuron* 48 (1): 45–62. https://doi.org/10.1016/j.neuron.2005.08.032.

Hardwick, L. J.A., and A. Philpott. 2015. "Multi-Site Phosphorylation Regulates NeuroD4 Activity during Primary Neurogenesis: A Conserved Mechanism amongst Proneural Proteins." *Neural Development* 10 (1): 1–18. https://doi.org/10.1186/s13064-015-0044-8.

He, F., W. Ge, K. Martinowich, S. Becker-Catania, V. Coskun, W. Zhu, Hao Wu, et al. 2005. "A Positive Autoregulatory Loop of Jak-STAT Signaling Controls the Onset of Astrogliogenesis." *Nature Neuroscience* 8 (5): 616–25. https://doi.org/10.1038/nn1440.

Heinrich, C., M. Bergami, S. Gascón, A. Lepier, F. Viganò, L. Dimou, B. Sutor, B. Berninger, and M. Götz. 2014. "Sox2-Mediated Conversion of NG2 Glia into Induced Neurons in the Injured Adult Cerebral Cortex." *Stem Cell Reports* 3 (6): 1000–1014. https://doi.org/10.1016/j.stemcr.2014.10.007.

Heinrich, C., R. Blum, S. Gascón, G. Masserdotti, P. Tripathi, R. Sánchez, S. Tiedt, T. Schroeder, M. Götz, and Benedikt Berninger. 2010. "Directing Astroglia from the Cerebral Cortex into Subtype Specific Functional Neurons." *PLoS Biology* 8 (5). https://doi.org/10.1371/journal.pbio.1000373.

Heinrich, C., S. Gascón, G. Masserdotti, A. Lepier, R. Sanchez, T. Simon-Ebert, T. Schroeder, M. Götz, and B. Berninger. 2011. "Generation of Subtype-Specific Neurons from Postnatal Astroglia of the Mouse Cerebral Cortex." *Nature Protocols* 6 (2): 214–28. https://doi.org/10.1038/nprot.2010.188.

Heinrich, C., F. M. Spagnoli, and B. Berninger. 2015. "In Vivo Reprogramming for Tissue Repair." *Nature Cell Biology* 17 (3): 204–11. https://doi.org/10.1038/ncb3108.

Heinrich, C., M. Bergami, S. Gascón, A. Lepier, F. Viganò, L. Dimou, B. Suto, B. Berninger, and M. Götz.

2014. “Sox2-Mediated Conversion of NG2 Glia into Induced Neurons in the Injured Adult Cerebral Cortex.” *Stem Cell Reports* 3 (6): 1000–1014. https://doi.org/10.1016/j.stemcr.2014.10.007.

Heins, N., P. Malatesta, F. Cecconi, M. Nakafuku, K. L. Tucker, M. A. Hack, P. Chapouton, Y. A. Barde, and M. Goötz. 2002. “Glial Cells Generate Neurons: The Role of the Transcription Factor Pax6.” *Nature Neuroscience* 5 (4): 308–15. https://doi.org/10.1038/nn828.

Heng, J. I. T., L. Nguyen, D. S. Castro, C. Zimmer, H. Wildner, O. Armant, D. Skowronska-Krawczyk, et al. 2008. “Neurogenin 2 Controls Cortical Neuron Migration through Regulation of Rnd2.” *Nature* 455 (7209): 114–18. https://doi.org/10.1038/nature07198.

Herrmann, J. E., T. Imura, B. Song, J. Qi, Y. Ao, T. K. Nguyen, R. A. Korsak, K. Takeda, S. Akira, and M. V. Sofroniew. 2008. “STAT3 Is a Critical Regulator of Astrogliosis and Scar Formation after Spinal Cord Injury.” *The Journal of Neuroscience* 28 (28): 7231–43. https://doi.org/10.1523/JNEUROSCI.1709-08.2008.

Higashi, K., A. Fujita, A. Inanobe, M. Tanemoto, K. Doi, T. Kubo, and Y. Kurachi. 2001. “An Inwardly Rectifying K+ Channel , Kir4.1 , Expressed in Astrocytes Surrounds Synapses and Blood Vessels in Brain.” *American Journal of Phyiology and Cellular Physiology* 281: 922–31. https://doi.org/10.1152/ajpcell.2001.281.3.C922.

Hindley, C., F. Ali, G. McDowell, K. Cheng, A. Jones, F. Guillemot, and A. Philpott. 2012. “Post-Translational Modification of Ngn2 Differentially Affects Transcription of Distinct Targets to Regulate the Balance between Progenitor Maintenance and Differentiation.” *Development* 139 (10): 1718–23. https://doi.org/10.1242/dev.077552.

Hinz, U., B. Giebel, and J. A. Campos-Ortega. 1994. “The Basic-Helix-Loop-Helix Domain of Drosophila Lethal of Scute Protein Is Sufficient for Proneural Function and Activates Neurogenic Genes.” *Cell* 76 (1): 77–87. https://doi.org/10.1016/0092-8674(94)90174-0.

Ho, B. C., E. Epping, K. Wang, N. C. Andreasen, A. Librant, and T. H. Wassink. 2008. “Basic Helix-Loop-Helix Transcription Factor NEUROG1 and Schizophrenia: Effects on Illness Susceptibility, MRI Brain Morphometry and Cognitive Abilities.” *Schizophrenia Research* 106 (2–3): 192–99. https://doi.org/10.1016/j.schres.2008.08.009.

Houades, V., A. Koulakoff, P. Ezan, I. Seif, and C. Giaume. 2008. “Gap Junction-Mediated Astrocytic Networks in the Mouse Barrel Cortex.” *Journal of Neuroscience* 28 (20): 5207–17. https://doi.org/10.1523/JNEUROSCI.5100-07.2008.

Hu, X., Y. Yuan, D. Wang, and Z. Su. 2016. “Heterogeneous Astrocytes: Active Players in CNS.” *Brain Research Bulletin* 125: 1–18. https://doi.org/10.1016/j.brainresbull.2016.03.017.

Huang, L., F. Hu, L. Feng, X. J. Luo, G. Liang, X. Y. Zeng, J. L. Yi, and L. Gan. 2014. “Bhlhb5 Is Required for the Subtype Development of Retinal Amacrine and Bipolar Cells in Mice.” *Developmental Dynamics* 243 (2): 279–89. https://doi.org/10.1002/dvdy.24067.

Hunter, T. 2007. “The Age of Crosstalk: Phosphorylation, Ubiquitination, and Beyond.” *Molecular Cell* 28 (5): 730–38. https://doi.org/10.1016/j.molcel.2007.11.019.

Imayoshi, I., A. Isomura, Y. Harima, K. Kawaguchi, H. Kori, H. Miyachi, T. Fujiwara, F. Ishidate, and R. Kageyama. 2013. “Oscillatory Control of Factors Determining Multipotency and Fate in Mouse Neural Progenitors.” *Science* 342 (6163): 1203–8. https://doi.org/10.1126/science.1242366.

Inoue, T., M. Hojo, Y. Bessho, Y. Tano, J. E. Lee, and R. Kageyama. 2002. “Math3 and NeuroD Regulate Amacrine Cell Fate Specification in the Retina.” *Development* 129 (4): 831–42. https://doi.org/9806930.

Jessberger, S., N. Toni, G. D. Clemenson, J. Ray, and F. H. Gage. 2008. “Directed Differentiation of Hippocampal Stem/Progenitor Cells in the Adult Brain.” *Nature Neuroscience* 11 (8): 888–93.

https://doi.org/10.1038/nn.2148.

Kanski, R., M. E. Van Strien, P. Van Tijn, and E. M. Hol. 2014. "A Star Is Born: New Insights into the Mechanism of Astrogenesis." *Cellular and Molecular Life Sciences* 71 (3): 433–47. https://doi.org/10.1007/s00018-013-1435-9.

Karow, M., J. G. Camp, S. Falk, T. Gerber, A. Pataskar, M. Gac-Santel, J. Kageyama, et al. 2018. "Direct Pericyte-to-Neuron Reprogramming via Unfolding of a Neural Stem Cell-like Program." *Nature Neuroscience* 21 (July): 932–40. https://doi.org/10.1038/s41593-018-0168-3.

Karow, M., R. Sánchez, C. Schichor, G. Masserdotti, F. Ortega, C. Heinrich, S. Gascón, et al. 2012. "Reprogramming of Pericyte-Derived Cells of the Adult Human Brain into Induced Neuronal Cells." *Cell Stem Cell* 11 (4): 471–76. https://doi.org/10.1016/j.stem.2012.07.007.

Kele, J., N. Simplicio, A. L. M. Ferri, H. Mira, F. Guillemot, E. Arenas, and S. L. Ang. 2004. "Neurogenin 2 Is Required for the Development of Ventral Midbrain Dopaminergic Neurons." *Development* 133: 495–505. https://doi.org/10.1242/dev.02223.

Kelenis, D. P., E. Hart, M. Edwards-Fligner, J. E. Johnson, and T. Y. Vue. 2018. "ASCL1 Regulates Proliferation of NG2-Glia in the Embryonic and Adult Spinal Cord." *Glia* 66 (9): 1–19. https://doi.org/10.1002/glia.23344.

Kepecs, A., and G. Fishell. 2014. "Interneuron Cell Types Are Fit to Function." *Nature* 505 (7483): 318–26. https://doi.org/10.1038/nature12983.

Khakh, B. S., and M.V. Sofroniew. 2015. "Diversity of Astrocyte Functions and Phenotypes in Neural Circuits." *Nature Neuroscience* 18 (7): 942–52. https://doi.org/10.1038/nn.4043.

Kim, K. J., J. A. Iddings, J. E. Stern, V. M. Blanco, D. Croom, S. A. Kirov, and J. A. Filosa. 2015. "Astrocyte Contributions to Flow/Pressure-Evoked Parenchymal Arteriole Vasoconstriction." *Journal of Neuroscience* 35 (21): 8245–57. https://doi.org/10.1523/JNEUROSCI.4486-14.2015.

Kim, Y., X. Zheng, Z. Ansari, M. C. Bunnell, J. R. Herdy, L. Traxler, Hyungjun Lee, et al. 2018. "Mitochondrial Aging Defects Emerge in Directly Reprogrammed Human Neurons Due to Their Metabolic Profile." *Cell Reports* 23 (9): 2550–58. https://doi.org/10.1016/j.celrep.2018.04.105.

Kohyama, J., T. Sanosaka, A. Tokunaga, E. Takatsuka, K. Tsujimura, H. Okano, and K. Nakashima. 2010. "BMP-Induced REST Regulates the Establishment and Maintenance of Astrocytic Identity." *Journal of Cell Biology* 189 (1): 159–70. https://doi.org/10.1083/jcb.200908048.

Koyano-Nakagawa, N., J. Kim, D. Anderson, and C. Kintner. 2000. "Hes6 Acts in a Positive Feedback Loop with the Neurogenins to Promote Neuronal Differentiation." *Development (Cambridge, England)* 127: 4203–16.

Krämer-Albers, E. M., N. Bretz, S. Tenzer, C. Winterstein, W. Möbius, H. Berger, K. A. Nave, H. Schild, and J. Trotter. 2007. "Oligodendrocytes Secrete Exosomes Containing Major Myelin and Stress-Protective Proteins: Trophic Support for Axons?" *Proteomics - Clinical Applications* 1 (11): 1446–61. https://doi.org/10.1002/prca.200700522.

Kriegstein, A., and A. Alvarez-Buylla. 2009. "The Glial Nature of Embryonic and Adult Neural Stem Cells." *Annual Review of Neuroscience* 32 (1): 149–84. https://doi.org/10.1146/annurev.neuro.051508.135600.

Kuwabara, T., J. Hsieh, A. Muotri, G. Yeo, M. Warashina, D. C. Lie, L. Moore, K. Nakashima, M. Asashima, and F. H. Gage. 2009. "Wnt-Mediated Activation of NeuroD1 and Retro-Elements during Adult Neurogenesis." *Nature Neuroscience* 12 (9): 1097–1105. https://doi.org/10.1038/nn.2360.

Ladewig, J., P. Koch, and O. Brüstle. 2013. "Leveling Waddington: The Emergence of Direct Programming and the Loss of Cell Fate Hierarchies." *Nature Reviews Molecular Cell Biology* 14 (March): 225. https://doi.org/10.1038/nrm3543.

Lancaster, M. A., M. Renner, C. A. Martin, D. Wenzel, L. S. Bicknell, M. E. Hurles, T. Homfray, J. M. Penninger, A. P. Jackson, and J. A. Knoblich. 2013. "Cerebral Organoids Model Human Brain Development and Microcephaly." *Nature* 501 (7467): 373–79. https://doi.org/10.1038/nature12517.

Lanjakornsiripan, D., B. J. Pior, D. Kawaguchi, S. Furutachi, T. Tahara, Y. Katsuyama, Y. Suzuki, Y. Fukazawa, and Y. Gotoh. 2018. "Layer-Specific Morphological and Molecular Differences in Neocortical Astrocytes and Their Dependence on Neuronal Layers." *Nature Communications* 9 (1). https://doi.org/10.1038/s41467-018-03940-3.

Le Dréau, G., R. Escalona, R. Fueyo, A. Herrera, J. D. Martínez, S. Usieto, A. Menendez, S. Pons, M. A. Martinez-Balbas, and E. Marti. 2018. "E Proteins Differentially Co-Operate with Proneural BHLH Transcription Factors to Sharpen Neurogenesis." *BioRxiv*, 301093. https://doi.org/10.1101/301093.

Lee, S. K., B. Lee, E. C. Ruiz, and S. L. Pfaff. 2005. "Olig2 and Ngn2 Function in Opposition to Modulate Gene Expression in Motor Neuron Progenitor Cells." *Genes and Development* 19: 282–94. https://doi.org/10.1101/gad.1257105.to.

Lee, S. W., Y. M. Oh, Y. L. Lu, W. K. Kim, and A. S. Yoo. 2018. "MicroRNAs Overcome Cell Fate Barrier by Reducing EZH2-Controlled REST Stability during Neuronal Conversion of Human Adult Fibroblasts." *Developmental Cell* 46 (1): 73–84.e7. https://doi.org/10.1016/j.devcel.2018.06.007.

Lehre, K. P., L. M. Levy, J. Storm-Mathisen, O. P. Ottersen, and N. C. Danbolt. 1995. "Differential Expression Rat Brain : Quantitative of Two Glial Glutamate and Lmmunocytochemical Transporters in the Observations." *The Journal of Neuroscience* 15 (3): 1835–53. https://doi.org/https://doi.org/10.1523/JNEUROSCI.15-03-01835.1995.

Lemmon, M. A., and J. Schlessinger. 2010. "Cell Signaling by Receptor Tyrosine Kinases." *Cell* 141 (7): 1117–34. https://doi.org/10.1016/j.cell.2010.06.011.

Levitt, P., M. L. Cooper, and P. Rakic. 1981. "COEXISTENCE OF NEURONAL AND GLIAL PRECURSOR CELLS IN THE CEREBRAL VENTRICULAR ZONE OF THE FETAL MONKEY: AN ULTRASTRUCTURAL IMMUNOPEROXIDASE ANALYSIS." *The Journal of Neuroscience* 1 (1): 27–39. https://doi.org/https://doi.org/10.1523/JNEUROSCI.01-01-00027.1981.

Levitt, P., M. L. Cooper, and P. Rakic. 1983. "Early Divergence and Changing Proportions of Neuronal and Glial Precursor Cells in the Primate Cerebral Ventricular Zone." *Developmental Biology* 484: 472–84. https://doi.org/10.1016/0012-1606(83)90184-7.

Li, H., J. Paes de Faria, P. Andrew, J. Nitarska, and W. D. Richardson. 2011. "Phosphorylation Regulates OLIG2 Cofactor Choice and the Motor Neuron-Oligodendrocyte Fate Switch." *Neuron* 69 (5): 918–29. https://doi.org/10.1016/j.neuron.2011.01.030.

Li, M. A., S. J. Pettitt, S. Eckert, Z. Ning, S. Rice, J. Cadinanos, K. Yusa, N. Conte, and A. Bradley. 2013. "The PiggyBac Transposon Displays Local and Distant Reintegration Preferences and Can Cause Mutations at Noncanonical Integration Sites." *Molecular and Cellular Biology* 33 (7): 1317–30. https://doi.org/10.1128/MCB.00670-12.

Li, M. A., D. J. Turner, Z. Ning, K. Yusa, Q. Liang, S. Eckert, L. Rad, T. W. Fitzgerald, N. L. Craig, and A. Bradley. 2011. "Mobilization of Giant PiggyBac Transposons in the Mouse Genome." *Nucleic Acids Research* 39 (22): e148. https://doi.org/10.1093/nar/gkr764.

Li, S., P. Mattar, R. Dixit, S. O. Lawn, G. Wilkinson, C. Kinch, D. Eisenstat, D. M. Kurrasch, J. A. Chan, and C. Schuurmans. 2014. "RAS/ERK Signaling Controls Proneural Genetic Programs in Cortical Development and Gliomagenesis." *Journal of Neuroscience* 34 (6): 2169–90. https://doi.org/10.1523/JNEUROSCI.4077-13.2014.

Li, S., P. Mattar, D. Zinyk, K. Singh, C.-P. Chaturvedi, C. Kovach, R. Dixit, et al. 2012. "GSK3 Temporally Regulates Neurogenin 2 Proneural Activity in the Neocortex." *Journal of Neuroscience* 32 (23):

7791–7805. https://doi.org/10.1523/JNEUROSCI.1309-12.2012.

Li, X., X. Zuo, J. Jing, Y. Ma, J. Wang, D. Liu, J. Zhu, et al. 2015. "Small-Molecule-Driven Direct Reprogramming of Mouse Fibroblasts into Functional Neurons." *Cell Stem Cell* 17 (2): 195–203. https://doi.org/10.1016/j.stem.2015.06.003.

Liddelow, S. A., K. A. Guttenplan, L. E. Clarke, F. C. Bennett, C. J. Bohlen, L. Schirmer, M. L. Bennett, et al. 2017. "Neurotoxic Reactive Astrocytes Are Induced by Activated Microglia." *Nature* 541 (7638): 481–87. https://doi.org/10.1038/nature21029.

Littlewood, T. D., D. C. Hancock, P. S. Danielianl, and M. G. Parker. 1995. "A Modified Oestrogen Receptor Ligand-Binding Domain as an Improved Switch for the Regulation of Heterologous Proteins." *Methods* 23 (27): 1686–90.

Liu, Y. H., J. W. Tsai, J. L. Chen, W. S. Yang, P. C. Chang, P. L. Cheng, D. L. Turner, Y. Yanagawa, T. W. Wang, and J. Y. Yu. 2017. "Ascl1 Promotes Tangential Migration and Confines Migratory Routes by Induction of Ephb2 in the Telencephalon." *Scientific Reports* 7: 1–17. https://doi.org/10.1038/srep42895.

Liu, Y., Q. Miao, J. Yuan, S. Han, P. Zhang, S. Li, Z. Rao, et al. 2015. "Ascl1 Converts Dorsal Midbrain Astrocytes into Functional Neurons In Vivo." *Journal of Neuroscience* 35 (25): 9336–55. https://doi.org/10.1523/JNEUROSCI.3975-14.2015.

Livet, J., T. A. Weissman, H. Kang, R. W. Draft, J. Lu, R. A. Bennis, J. R. Sanes, and J. W. Lichtman. 2007. "Transgenic Strategies for Combinatorial Expression of Fluorescent Proteins in the Nervous System." *Nature* 450 (7166): 56–62. https://doi.org/10.1038/nature06293.

Lo, L. C., J. E. Johnson, W. W. Carol, T. Saito, and J. A. David. 1991. "Mammalian Achaete-Scute Homolog 1 Is Transiently Expressed by Spatially Restricted Subsets of Early Neuroepithehal and Neural Crest Cells." *Genes and Development* 47: 1524–37.

Lo, L., E. Dormand, A. Greenwood, and D. J. Anderson. 2002. "Comparison of the Generic Neuronal Differentiation and Neuron Subtype Specification Functions of Mammalian Achaete-Scute and Atonal Homologs in Cultured Neural Progenitor Cells." *Development (Cambridge, England)* 129: 1553–67.

Ludtke, J. J., M. G. Sebestyén, and J. A. Wolff. 2002. "The Effect of Cell Division on the Cellular Dynamics of Microinjected DNA and Dextran." *Molecular Therapy* 5 (5 I): 579–88. https://doi.org/10.1006/mthe.2002.0581.

Ma, Q., C. Fode, F. Guillemot, and D. J. Anderson. 1999. "NEUROGENIN1 and NEUROGENIN2 Control Two Distinct Waves of Neurogenesis in Developing Dorsal Root Ganglia." *Genes and Development* 13 (13): 1717–28. https://doi.org/10.1101/gad.13.13.1717.

Ma, Q., C. Kintner, and D. J. Anderson. 1996. "Identification of Neurogenin, a Vertebrate Neuronal Determination Gene." *Cell* 87 (1): 43–52. https://doi.org/10.1016/S0092-8674(00)81321-5.

Ma, Y. C., Mi. R. Song, J. P. Park, H.Y. Henry Ho, L. Hu, M. V. Kurtev, J. Zieg, Q. Ma, S. L. Pfaff, and M. E. Greenberg. 2008. "Regulation of Motor Neuron Specification by Phosphorylation of Neurogenin 2." *Neuron* 58 (1): 65–77. https://doi.org/10.1016/j.neuron.2008.01.037.

Ma, Z., T. Stork, D. E. Bergles, and M. R. Freeman. 2016. "Neuromodulators Signal through Astrocytes to Alter Neural Circuit Activity and Behaviour." *Nature* 539 (7629): 428–32. https://doi.org/10.1038/nature20145.

Maddika, S., S. R. Ande, E. Wiechec, L. L. Hansen, S. Wesselborg, and M. Los. 2008. "Akt-Mediated Phosphorylation of CDK2 Regulates Its Dual Role in Cell Cycle Progression and Apoptosis." *Journal of Cell Science* 121 (7): 979–88. https://doi.org/10.1242/jcs.009530.

Magavi, S., D. Friedmann, G. Banks, A. Stolfi, and C. Lois. 2012. "Coincident Generation of Pyramidal Neurons and Protoplasmic Astrocytes in Neocortical Columns." *Journal of Neuroscience* 32 (14):

4762–72. https://doi.org/10.1523/JNEUROSCI.3560-11.2012.

Magnusson, J. P., C. Goeritz, J. Tatarishvili, D. O. Dias, E. M. K. Smith, O. Linvall, Z. Kokaia, and J. Fisén. 2014. "A Latent Neurogenic Program in Astrocytes Regulated by Notch Signaling in the Mouse." *Science* 346 (6206): 237–42. https://doi.org/10.1126/science.346.6206.237.

Mall, M., M. S. Kareta, S. Chanda, H. Ahlenius, N. Perotti, B. Zhou, S. D. Grieder, et al. 2017. "Myt1l Safeguards Neuronal Identity by Actively Repressing Many Non-Neuronal Fates." *Nature* 544 (7649): 245–49. https://doi.org/10.1038/nature21722.

Marquez, R. T., and L. Xu. 2012. "Bcl-2:Beclin 1 Complex: Multiple , Mechanisms Regulating Autophagy/Apoptosis Toggle Switch." *Cancer Research* 2 (2): 214–21.

Martinez-Ferre, A., C. Lloret-Quesada, N. Prakash, W. Wurst, J. L.R. Rubenstein, and S. Martinez. 2016. "Fgf15 Regulates Thalamic Development by Controlling the Expression of Proneural Genes." *Brain Structure and Function* 221 (6): 3095–3109. https://doi.org/10.1007/s00429-015-1089-5.

Massari, M. E., and C. Murre. 2000. "Helix-Loop-Helix Proteins: Regulators of Transcription in Eucaryotic Organisms." *Molecular and Cellular Biology* 20 (2): 429–40. https://doi.org/10.1128/MCB.20.2.429-440.2000.

Masserdotti, G., S. Gascón, and M. Götz. 2016. "Direct Neuronal Reprogramming: Learning from and for Development." *Development* 143 (14): 2494–2510. https://doi.org/10.1242/dev.092163.

Masserdotti, G., S. Gillotin, B. Sutor, D. Drechsel, M. Irmler, H. F. Jørgensen, S. Sass, et al. 2015. "Transcriptional Mechanisms of Proneural Factors and REST in Regulating Neuronal Reprogramming of Astrocytes." *Cell Stem Cell* 17 (1): 74–88. https://doi.org/10.1016/j.stem.2015.05.014.

Masserdotti, Giacomo, Sergio Gascón, and Magdalena Götz. 2016. "Direct Neuronal Reprogramming: Learning from and for Development." *Development* 143 (14): 2494–2510. https://doi.org/10.1242/dev.092163.

Miller, Fr.D., and A. S. Gauthier. 2007. "Timing Is Everything: Making Neurons versus Glia in the Developing Cortex." *Neuron* 54 (3): 357–69. https://doi.org/10.1016/j.neuron.2007.04.019.

Milne, T. A., K. Zhao, and J. L. Hess. 2009. "Chromatin Immunoprecipitation (ChIP) for Analysis of Histone Modifications and Chromatin-Associated Proteins Thomas." *Methods Mol Biol.* 538: 409–23. https://doi.org/10.1007/978-1-59745-418-6.

Mishra, A. 2017. "Binaural Blood Flow Control by Astrocytes: Listening to Synapses and the Vasculature." *Journal of Physiology* 595 (6): 1885–1902. https://doi.org/10.1113/JP270979.

Mitra, R., J. Fain-thornton, and N. L. Craig. 2008. "PiggyBac Can Bypass DNA Synthesis during Cut and Paste Transposition." *The EMBO Journal* 27 (7): 1097–1109. https://doi.org/10.1038/emboj.2008.41.

Molina, J. R., and A. A. Adjei. 2006. "The Ras/Raf/MAPK Pathway." *Journal of Thoracic Oncology* 1 (1): 7–9. https://doi.org/10.1097/01243894-200601000-00004.

Morel, L., M. S. R. Chiang, H. Higashimori, T. Shoneye, L. K. Iyer, J. Yelick, A. Tai, and Y. Yang. 2017. "Molecular and Functional Properties of Regional Astrocytes in the Adult Brain." *The Journal of Neuroscience* 37 (36): 3956–16. https://doi.org/10.1523/JNEUROSCI.3956-16.2017.

Morshead, C. M., A. D. Garcia, M. V. Sofroniew, and D. Van Der Kooy. 2003. "The Ablation of Glial Fibrillary Acidic Protein-Positive Cells from the Adult Central Nervous System Results in the Loss of Forebrain Neural Stem Cells but Not Retinal Stem Cells." *European Journal of Neuroscience* 18 (1): 76–84. https://doi.org/10.1046/j.1460-9568.2003.02727.x.

Nagao, M., T. Ogata, Y. Sawada, and Y. Gotoh. 2016. "Zbtb20 Promotes Astrocytogenesis during Neocortical Development." *Nature Communications* 7: 1–14. https://doi.org/10.1038/ncomms11102.

Nagy, J. I., D. Patel, P. A.Y. Ochalski, and G. L. Stelmack. 1999. "Connexin30 in Rodent, Cat and Human Brain: Selective Expression in Gray Matter Astrocytes, Co-Localization with Connexin43 at Gap Junction and Late Developmental Appearance." *Neuroscience* 88 (2): 447–68. https://doi.org/10.1016/S0306-4522(98)00191-2.

Nagy, J. I., and J. E. Rash. 2007. "Astrocyte and Oligodendrocyte Connexins of the Glial Syncytium in Relation to Astrocyte Anatomical Domains and Spatial Buffering." *Cell Commun Adhes.* 10 (1): 401–6. https://doi.org/10.1080/15419060390263191.

Nakatani, H., E. Martin, H. Hassani, A. Clavairoly, C. L. Maire, A. Viadieu, C. Kerninon, et al. 2013. "Ascl1/Mash1 Promotes Brain Oligodendrogenesis during Myelination and Remyelination." *Journal of Neuroscience* 33 (23): 9752–68. https://doi.org/10.1523/JNEUROSCI.0805-13.2013.

Namihira, M., J. Kohyama, K. Semi, T. Sanosaka, B. Deneen, T. Taga, and K. Nakashima. 2009. "Committed Neuronal Precursors Confer Astrocytic Potential on Residual Neural Precursor Cells." *Developmental Cell* 16 (2): 245–55. https://doi.org/10.1016/j.devcel.2008.12.014.

Nato, G., A. Caramello, S. Trova, V. Avataneo, C. Rolando, V. Taylor, A. Buffo, P. Peretto, and F. Luzzati. 2015. "Striatal Astrocytes Produce Neuroblasts in an Excitotoxic Model of Huntington's Disease." *Development* 142 (5): 840–45. https://doi.org/10.1242/dev.116657.

Naviaux, R. K., E. Costanzi, M. Haas, and I. M. Verma. 1996. "The PCL Vector System: Rapid Production of Helper-Free, High-Titer, Recombinant Retroviruses." *J Virol* 70 (8): 5701–5. http://www.ncbi.nlm.nih.gov/pubmed/8764092.

Nieto, M., C. Schuurmans, O. Britz, and F. Guillemot. 2001. "Neural BHLH Genes Control the Neuronal versus Glial Fate Decision in Cortical Progenitors." *Neuron* 29 (2): 401–13. https://doi.org/10.1016/S0896-6273(01)00214-8.

Niu, W., T. Zang, D. K. Smith, T. Y. Vue, Y. Zou, R. Bachoo, J. E. Johnson, and C. L. Zhang. 2015. "SOX2 Reprograms Resident Astrocytes into Neural Progenitors in the Adult Brain." *Stem Cell Reports* 4 (5): 780–94. https://doi.org/10.1016/j.stemcr.2015.03.006.

Niu, W., T. Zang, Y. Zou, S. Fang, D. K. Smith, R. Bachoo, and C. L. Zhang. 2013. "In Vivo Reprogramming of Astrocytes to Neuroblasts in the Adult Brain." *Nature Cell Biology* 15 (10): 1164–75. https://doi.org/10.1038/ncb2843.

Norenberg, M. D., and A. Martinez-Hernandez. 1979. "Fine Structural Localization of Glutamine Synthetase in Astrocytes of Rat Brain." *Brain Research* 161: 303–10. https://doi.org/10.1016/0006-8993(79)90071-4.

Oliveira, S. L. B, M. M. Pillat, A. Cheffer, C. Lameu, T. T. Schwindt, and H. Ulrich. 2013. "Function of Neurotrophins and Growth Factors in Neurogenesis and Brain Repair." *Cytometry* 83A: 76–89. https://doi.org/10.1002/cyto.a.22161.

Ory, D. S., B. A. Neugeboren, and R. C. Mulligan. 1996. "A Stable Human-Derived Packaging Cell Line for Production of High Titer Retrovirus/Vesicular Stomatitis Virus G Pseudotypes." *Proceedings of the National Academy of Sciences of the United States of America* 93 (21): 11400–406. https://doi.org/10.1073/pnas.93.21.11400.

Pappalardo, L. W., O. A. Samad, J. A. Black, and S. G. Waxman. 2015. "Voltage-Gated Sodium Channel Nav1.5 Vontributes to Astrogliosis in an in Vitro Model of Glial Injury via Reverse Na+/Ca2+ Exchange." *Glia* 62 (7): 1162–75. https://doi.org/10.1002/glia.22671.

Parras, C. M., R. Galli, O. Britz, S. Soares, C. Galichet, J. Battiste, J. E Johnson, M. Nakafaku, A. Vescovi, and F. Guillemot. 2004. "Mash1 Specifies Neurons and Oligodendrocytes in the Postnatal Brain." *EMBO Journal* 23 (22): 4495–4505. https://doi.org/10.1038/sj.emboj.7600447.

Parras, C. M., C. Hunt, M. Sugimori, M. Nakafuku, D. Rowitch, and F. Guillemot. 2007. "The Proneural Gene Mash1 Specifies an Early Population of Telencephalic Oligodendrocytes." *Journal of*

Neuroscience 27 (16): 4233–42. https://doi.org/10.1523/JNEUROSCI.0126-07.2007.

Parras, C. M., C. Schuurmans, R. Scardigli, J. Kim, D. J. Anderson, and F. Guillemot. 2002. "Divergent Functions of the Proneural Genes Mash1 and Ngn2 in the Specification of Neuronal Subtype Identity." *Genes and Development* 16 (3): 324–38. https://doi.org/10.1101/gad.940902.

Pereira, M., M. Birtele, S. Shrigley, J. A. Benitez, E. Hedlund, M. Parmar, and D. R. Ottosson. 2017. "Direct Reprogramming of Resident NG2 Glia into Neurons with Properties of Fast-Spiking Parvalbumin-Containing Interneurons." *Stem Cell Reports* 9 (3): 742–51. https://doi.org/10.1016/j.stemcr.2017.07.023.

Péron, S., L. M. Miyakoshi, M. S. Brill, F. Ortega, M. Karow, S. Gascón, and B. Berninger. 2017. "Programming of Neural Progenitors of the Adult Subependymal Zone towards a Glutamatergic Identity By." *BioRxiv*.

Poopalasundaram, S., C. Knott, O. G. Shamotienko, P. G. Foran, J. O. Dolly, C. A. Ghiani, V. Gallo, and G. P. Wilkin. 2000. "Glial Heterogeneity in Expression of the Inwardly Rectifying K+ Channel, Kir4.1, in Adult Rat CNS." *Glia* 372 (November 1999): 362–72. https://doi.org/https://doi.org/10.1002/(SICI)1098-1136(200006)30:4<362::AID-GLIA50>3.0.CO;2-4.

Porteus, M. H., A. Bulfone, J. K. Liu, L. Puelles, L. C. Lo, and J. L. R. Rubenstein. 1994. "DLX-2 , MASH-l , and MAP-2 Expression and Bromodeoxyuridine Lncorpkation Define Molecularly Distinct Cell Population in the Embryonic Mouse Forebrain." *The Journal of Neuroscience : The Official Journal of the Society for Neuroscience* 14 (11): 6370–83.

Powell, E. M., and H. M. Geller. 1999. "Dissection of Astrocyte-Mediated Cues in Neuronal Guidance and Process Extension." *Glia* 26 (1): 73–83. https://doi.org/10.1002/(SICI)1098-1136(199903)26:1<73::AID-GLIA8>3.0.CO;2-S.

Qian, L., Y. Huang, C. I. Spencer, A. Foley, V. Vedantham, L. Liu, S. J. Conway, J. D. Fu, and D. Srivastava. 2012. "In Vivo Reprogramming of Murine Cardiac Fibroblasts into Induced Cardiomyocytes." *Nature* 485 (7400): 593–98. https://doi.org/10.1038/nature11044.

Quadrato, G., T. Nguyen, E. Z. Macosko, J. L. Sherwood, S. M. Yang, D. R. Berger, N. Maria, et al. 2017. "Cell Diversity and Network Dynamics in Photosensitive Human Brain Organoids." *Nature* 545 (7652): 48–53. https://doi.org/10.1038/nature22047.

Quan, X. J., L. Yuan, L. Tiberi, A. Claeys, N. De Geest, J. Yan, R. Van Der Kant, et al. 2016. "Post-Translational Control of the Temporal Dynamics of Transcription Factor Activity Regulates Neurogenesis." *Cell* 164 (3): 460–75. https://doi.org/10.1016/j.cell.2015.12.048.

Raposo, A. A. S. F., F. F. Vasconcelos, D. Drechsel, C. Marie, and C. Johnston. 2015. "Ascl1 Coordinately Regulates Gene Expression and the Chromatin Landscape during Neurogenesis Article Ascl1 Coordinately Regulates Gene Expression and the Chromatin Landscape during Neurogenesis." *Cell Reports* 10: 1544–56. https://doi.org/10.1016/j.celrep.2015.02.025.

Robel, S., B. Berninger, and M. Götz. 2011. "The Stem Cell Potential of Glia: Lessons from Reactive Gliosis." *Nature Reviews Neuroscience* 12 (2): 88–104. https://doi.org/10.1038/nrn2978.

Roe, T, T C Reynolds, G Yu, and P O Brown. 1993. "Integration of Murine Leukemia Virus DNA Depends on Mitosis." *The EMBO Journal* 12 (5): 2099–2108.

Rosenblatt, J., Y. Gu, and D.O. Morgan. 1992. "Human Cyclin-Dependent Kinase 2 Is Activated during the S and G2 Phases of the Cell Cycle and Associates with Cyclin A." *Proceedings of the National Academy of Sciences of the United States of America* 89 (7): 2824–28. https://doi.org/10.1073/pnas.89.7.2824.

Roth, B. L. 2017. "DREADDs for Neuroscientists." *Neuron* 89 (4): 683–94. https://doi.org/10.1016/j.neuron.2016.01.040.DREADDs.

Rouaux, C., and P. Arlotta. 2010. "Fezf2 Directs the Differentiation of Corticofugal Neurons from Striatal Progenitors in Vivo." *Nature Neuroscience* 13 (11): 1345–47. https://doi.org/10.1038/nn.2658.

Rouaux, C., and P. Arlotta. 2013. "Direct Lineage Reprogramming of Post-Mitotic Callosal Neurons into Corticofugal Neurons in Vivo." *Nature Cell Biology* 15 (2): 214–21. https://doi.org/10.1038/ncb2660.

Samanta, J., and John A. Kessler. 2004. "Interactions between ID and OLIG Proteins Mediate the Inhibitory Effects of BMP4 on Oligodendroglial Differentiation." *Development* 131 (17): 4131–42. https://doi.org/10.1242/dev.01273.

Sasaki, T., T. Ishikawa, R. Abe, R. Nakayama, A. Asada, N. Matsuki, and Y. Ikegaya. 2014. "Astrocyte Calcium Signalling Orchestrates Neuronal Synchronization in Organotypic Hippocampal Slices." *Journal of Physiology* 592 (13): 2771–83. https://doi.org/10.1113/jphysiol.2014.272864.

Schummers, J., H. Yo, and M. Sur. 2008. "Tuned Responses of Astrocytes and Their Influence on Hemodynamic Signals in the Visual Cortex." *Science* 320 (June): 1638–44. https://doi.org/10.1126/science.1156120.

Schuurmans, C., O. Armant, M. Nieto, J. M. Stenman, O. Britz, N. Klenin, C. Brown, et al. 2004. "Sequential Phases of Cortical Specification Involve Neurogenin-Dependent and -Independent Pathways." *EMBO Journal* 23 (14): 2892–2902. https://doi.org/10.1038/sj.emboj.7600278.

Segklia, A., E. Seuntjens, M. Elkouris, S. Tsalavos, E. Stappers, T. A. Mitsiadis, D. Huylebroeck, E. Remboutsika, and D. Graf. 2012. "Bmp7 Regulates the Survival, Proliferation, and Neurogenic Properties of Neural Progenitor Cells during Corticogenesis in the Mouse." *PLoS ONE* 7 (3): e34088. https://doi.org/10.1371/journal.pone.0034088.

Simon, C., H. Lickert, M. Götz, and L. Dimou. 2012. "Sox10-ICreER T2: A Mouse Line to Inducibly Trace the Neural Crest and Oligodendrocyte Lineage." *Genesis* 50 (6): 506–15. https://doi.org/10.1002/dvg.22003.

Sirko, S., G. Behrendt, P. A. Johansson, P. Tripathi, M. Costa, S. Bek, C. Heinrich, et al. 2013. "Reactive Glia in the Injured Brain Acquire Stem Cell Properties in Response to Sonic Hedgehog Glia." *Cell Stem Cell* 12 (4): 426–39. https://doi.org/10.1016/j.stem.2013.01.019.

Sofroniew, M. V. 2009. "Molecular Dissection of Reactive Astrogliosis and Glial Scar Formation." *Trends in Neurosciences* 32 (12): 638–47. https://doi.org/10.1016/j.tins.2009.08.002.

Sofroniew, M. V., and H.V. Vinters. 2010. "Astrocytes: Biology and Pathology." *Acta Neuropathologica* 119 (1): 7–35. https://doi.org/10.1007/s00401-009-0619-8.

Sommer, L., Q. Ma, and D. J. Anderson. 1996. "Neurogenins, a Novel Family of Atonal-Related BHLH Transcription Factors, Are Putative Mammalian Neuronal Determination Genes That Reveal Progenitor Cell Heterogeneity in the Developing CNS and PNS." *Molecular and Cellular Neurosciences* 8 (4): 221–41. https://doi.org/10.1006/mcne.1996.0060.

Son, E.Y., J. K. Ichida, B. J. Wainger, J. S. Toma, V. F. Rafuse, C. J. Woolf, and K. Eggan. 2011. "Conversion of Mouse and Human Fibroblasts into Functional Spinal Motor Neurons." *Cell Stem Cell* 9 (3): 205–18. https://doi.org/10.1016/j.stem.2011.07.014.

Stambolic, V., A. Suzuki, J. L. DelaPompa, G. M. Brothers, C. Mirtsos, T. Sasaki, J. Ruland, J. M. Penninger, D. P. Siderovski, and T. W. Mak. 1998. "Negative Regulation of PKB/Akt-Dependent Cell Survival by the Tumor Repressor PTEN." *Cell* 95: 29–39.

Stosiek, C., O. Garaschuk, K. Holthoff, and A. Konnerth. 2003. "In Vivo Two-Photon Calcium Imaging of Neuronal Networks." *Proceedings of the National Academy of Sciences of the United States of America* 100 (12): 7319–24. https://doi.org/10.1073/pnas.1232232100.

Su, Z., W. Niu, M. L. Liu, Y. Zou, and C. L. Zhang. 2014. "In Vivo Conversion of Astrocytes to Neurons in

the Injured Adult Spinal Cord." *Nature Communications* 5: 1–15. https://doi.org/10.1038/ncomms4338.

Su, Zhida, Wenze Niu, Meng Lu Liu, Yuhua Zou, and Chun Li Zhang. 2014. "In Vivo Conversion of Astrocytes to Neurons in the Injured Adult Spinal Cord." *Nature Communications* 5: 1–15. https://doi.org/10.1038/ncomms4338.

Sun, Y., M. Nadal-vicens, S. Misono, M. Z. Lin, A. Zubiaga, X. Hua, G. Fan, M. E. Greenberg, and P. Vasco. 2001. "Neurogenin Promotes Neurogenesis and Inhibits Glial Differentiation by Independent Mechanisms." *Cell* 104: 365–76.

Takahashi, K., and S. Yamanaka. 2006. "Induction of Pluripotent Stem Cells from Mouse Embryonic and Adult Fibroblast Cultures by Defined Factors." *Cell* 126 (4): 663–76. https://doi.org/10.1016/j.cell.2006.07.024.

Tapscott, S. J., R. L. Davis, M. J. Thayer, P. F. Cheng, H. Weintraub, and A. B. Lassar. 1988. "MyoD1: A Nuclear Phosphoprotein Requiring a Myc Homology Region to Convert Fibroblasts to Myoblasts." *Science* 242 (4877): 405–11. https://doi.org/10.1126/science.3175662.

Tiwari, N., A. Pataskar, S. Péron, S. Thakurela, S. K. Sahu, M. Figueres-Oñate, N. Marichal, L. Lopez-Mascaraque, V. K. Tiwari, and B. Berninger. 2018. "Stage-Specific Transcription Factors Drive Astrogliogenesis by Remodeling Gene Regulatory Article." *Cell Stem Cell* 23: 557–71. https://doi.org/10.1016/j.stem.2018.09.008.

Tomita, K., K. Moriyoshi, S. Nakanishi, F. Guillemot, and R. Kageyama. 2000. "Mammalian Achaete-Scute and Atonal Homologs Regulate Neuronal versus Glial Fate Determination in the Central Nervous System." *The EMBO Journal* 19 (20): 5460–72. https://doi.org/10.1093/emboj/19.20.5460.

Tong, X., Y. Ao, G. C. Faas, S. E. Nwaobi, J. Xu, M. D. Haustein, M. A. Anderson, et al. 2014. "Astrocyte Kir4.1 Ion Channel Deficits Contribute to Neuronal Dysfunction in Huntington's Disease Model Mice." *Nature Neuroscience* 17 (5): 694–703. https://doi.org/10.1038/nn.3691.

Torper, O., U. Pfisterer, D. A. Wolf, M. Pereira, S. Lau, J. Jakobsson, A. Bjorklund, S. Grealish, and M. Parmar. 2013. "Generation of Induced Neurons via Direct Conversion in Vivo." *Proceedings of the National Academy of Sciences* 110 (17): 7038–43. https://doi.org/10.1073/pnas.1303829110.

Treutlein, B., Q. Y. Lee, J. G. Camp, M. Mall, W. Koh, S. A. M. Shariati, S. Sim, et al. 2016. "Dissecting Direct Reprogramming from Fibroblast to Neuron Using Single-Cell RNA-Seq." *Nature* 534 (7607): 391–95. https://doi.org/10.1038/nature18323.

Valadi, H., K. Ekstrom, B. Apostolos, M. Siostrand, J. L. Lee, and J. O. Lotvall. 2007. "Exosome-Mediated Transfer of MRNAs and MicroRNAs Is a Novel Mechanism of Genetic Exchange between Cells." *Nature Cell Biology* 9 (6): 654–59. https://doi.org/https://doi.org/10.1038/ncb1596.

Vasconcelos, F. F., A. Sessa, J. Muhr, V. Broccoli, and D. S. Castro. 2016. "MyT1 Counteracts the Neural Progenitor Program to Promote Vertebrate Neurogenesis Article MyT1 Counteracts the Neural Progenitor Program to Promote Vertebrate Neurogenesis." *Cell Reports* 17: 469–83. https://doi.org/10.1016/j.celrep.2016.09.024.

Victor, M. B., M. Richner, T. O. Hermanstyne, J. L. Ransdell, C. Sobieski, P. Y. Deng, V. A. Klyachko, J. M. Nerbonne, and A. S. Yoo. 2014. "Generation of Human Striatal Neurons by MicroRNA-Dependent Direct Conversion of Fibroblasts." *Neuron* 84 (2): 311–23. https://doi.org/10.1016/j.neuron.2014.10.016.

Vierbuchen, T., A. Ostermeier, Z. P. Pang, Y. Kokubu, T. C. Südhof, and M. Wernig. 2010. "Direct Conversion of Fibroblasts to Functional Neurons by Defined Factors." *Nature* 463 (7284): 1035–41. https://doi.org/10.1038/nature08797.

Villares, R., and C. V. Cabrera. 1987. "The Achaete-Scute Gene Complex of D. Melanogaster:

Conserved Domains in a Subset of Genes Required for Neurogenesis and Their Homology to Myc." *Cell* 50 (3): 415–24. https://doi.org/10.1016/0092-8674(87)90495-8.

Viñals, F., J. Reiriz, S. Ambrosio, R. Bartrons, J. L. Rosa, and F. Ventura. 2004. "BMP-2 Decreases Mash1 Stability by Increasing Id1 Expression." *EMBO Journal* 23 (17): 3527–37. https://doi.org/10.1038/sj.emboj.7600360.

Waddington, C. H. 1957. *The Strategy of the Genes. A Discussion of Some Aspects of Theoretical Biology*. London: George Allen & Unwin, Ltd.

Wang, L. H., and N. E. Baker. 2015. "Salvador-Warts-Hippo Pathway in a Developmental Checkpoint Monitoring Helix-Loop-Helix Proteins." *Developmental Cell* 32 (2): 191–202. https://doi.org/10.1016/j.devcel.2014.12.002.

Wang, X., T. Takano, and M. Nedergaard. 2009. "Astrocytic Calcium Signaling: Mechanism and Implications for Functional Brain Imaging." *Methods Mol Biol.* 489 (15): 1–16. https://doi.org/10.1007/978-1-59745-543-5.

Wanner, I. B., M. A. Anderson, B. Song, J. Levine, A. Fernandez, Z. Gray-Thompson, Y. Ao, and M. V. Sofroniew. 2013. "Glial Scar Borders Are Formed by Newly Proliferated, Elongated Astrocytes That Interact to Corral Inflammatory and Fibrotic Cells via STAT3-Dependent Mechanisms after Spinal Cord Injury." *Journal of Neuroscience* 33 (31): 12870–86. https://doi.org/10.1523/JNEUROSCI.2121-13.2013.

Wapinski, O. L., Q. Y. Lee, A. C. Chen, R. Li, M. R. Corces, C. E. Ang, B. Treutlein, et al. 2017. "Rapid Chromatin Switch in the Direct Reprogramming of Fibroblasts to Neurons." *Cell Reports* 20 (13): 3236–47. https://doi.org/10.1016/j.celrep.2017.09.011.

Wapinski, O. L., T. Vierbuchen, K. Qu, Q. Y. Lee, S. Chanda, D. R. Fuentes, P. G. Giresi, et al. 2013. "Hierarchical Mechanisms for Direct Reprogramming of Fibroblasts to Neurons." *Cell* 155 (3): 621–35. https://doi.org/10.1016/j.cell.2013.09.028.

Wei, Y., S. Pattingre, S. Sinha, M. Bassik, and B. Levine. 2008. "JNK1-Mediated Phosphorylation of Bcl-2 Regulates Starvation-Induced Autophagy." *Molecular Cell* 30 (6): 678–88. https://doi.org/10.1016/j.molcel.2008.06.001.

White, R., and E. M. Krämer-Albers. 2014. "Axon-Glia Interaction and Membrane Traffic in Myelin Formation." *Frontiers in Cellular Neuroscience* 7 (January): 1–8. https://doi.org/10.3389/fncel.2013.00284.

Wilczynska, K. M., S. K. Singh, B. Adams, L. Bryan, R. R. Rao, K. Valerie, S. Wright, I. Griswold-Prenner, and T. Kordula. 2009. "Nuclear Factor i Isoforms Regulate Gene Expression during the Differentiation of Human Neural Progenitors to Astrocytes." *Stem Cells* 27 (5): 1173–81. https://doi.org/10.1002/stem.35.

Willis, C. M., A. Ménoret, E. R. Jellison, A. M. Nicaise, A. T. Vella, and S. J. Crocker. 2017. "A Refined Bead-Free Method to Identify Astrocytic Exosomes in Primary Glial Cultures and Blood Plasma." *Frontiers in Neuroscience* 11: 1–12. https://doi.org/10.3389/fnins.2017.00335.

Wilson, C. H., I. Gamper, A. Perfetto, J. Auw, T. D. Littlewood, and G. I. Evan. 2014. "The Kinetics of ER Fusion Protein Activation in Vivo." *Oncogene* 33 (40): 4877–80. https://doi.org/10.1038/onc.2014.78.

Wong, F. K., K. Bercsenyi, V. Sreenivasan, A. Portalés, M. Fernández-Otero, and O. Marín. 2018. "Pyramidal Cell Regulation of Interneuron Survival Sculpts Cortical Networks." *Nature* 557 (7707): 668–73. https://doi.org/10.1038/s41586-018-0139-6.

Wylie, L. A., L. J. A. Hardwick, T. D. Papkovskaia, C. J. Thiele, and A. Philpott. 2015. "Ascl1 Phospho-Status Regulates Neuronal Differentiation in a Xenopus Developmental Model of Neuroblastoma." *Disease Models & Mechanisms* 8 (5): 429–41.

https://doi.org/10.1242/dmm.018630.

Xie, Y., W. Hou, X. Song, Y. Yu, J. Huang, X. Sun, R. Kang, and D. Tang. 2016. "Ferroptosis: Process and Function." *Cell Death and Differentiation* 23 (3): 369–79. https://doi.org/10.1038/cdd.2015.158.

Yang, N., S. Chanda, S. Marro, Y. H. Ng, J. A. Janas, D. Haag, C. E. Ang, et al. 2017. "Generation of Pure GABAergic Neurons by Transcription Factor Programming." *Nature Methods* 14 (6): 621–28. https://doi.org/10.1038/nmeth.4291.

Yang, N., J. B. Zuchero, H. Ahlenius, S. Marro, Y. H. Ng, T. Vierbuchen, J. S. Hawkins, R. Geissler, B. A. Barres, and M. Wernig. 2013. "Generation of Oligodendroglial Cells by Direct Lineage Conversion." *Nature Biotechnology* 31 (5): 434–39. https://doi.org/10.1038/nbt.2564.

Yang, Y. P., F. Thorel, D. F. Boyer, P. L. Herrera, and C. V. E. Wright. 2011. "Context-Specific α -to- β -Cell Reprogramming by Forced Pdx1 Expression Service Re Programming by Forced Pdx1 Expression." *Genes and Development* 25: 1680–85. https://doi.org/10.1101/gad.16875711.

Yokota, Y. 2001. "Id and Development." *Oncogene* 20 (58 REV. ISS. 8): 8290–98. https://doi.org/10.1038/sj/onc/1205090.

Yoo, A. S., A.X. Sun, L. Li, A. Shcheglovitov, T. Portmann, Y. Li, C. Lee-Messer, R. E. Dolmetsch, R.W. Tsien, and G. R. Crabtree. 2011. "MicroRNA-Mediated Conversion of Human Fibroblasts to Neurons." *Nature* 476 (7359): 228–31. https://doi.org/10.1038/nature10323.

Yu, A. C. H., I. J. Drejer, L. Hertz, and A. Schousboe. 1983. "Pyruvate Carboxylase Activity in Primary Cultures of Astrocytes and Neurons." *Journal of Neurochemistry* 41 (5): 1484–87. https://doi.org/10.1111/j.1471-4159.1983.tb00849.x.

Yu, Y., Y. Xie, L. Cao, L. Yang, M. Yang, M.T. Lotze, H. J. Zeh, R. Kang, and D. Tang. 2015. "The Ferroptosis Inducer Erastin Enhances Sensitivity of Acute Myeloid Leukemia Cells to Chemotherapeutic Agents." *Molecular and Cellular Oncology*. https://doi.org/10.1080/23723556.2015.1054549.

Yuan, Y. W., and S. R. Wessler. 2011. "The Catalytic Domain of All Eukaryotic Cut-and-Paste Transposase Superfamilies." *Proceedings of the National Academy of Sciences* 108 (19): 7884–89. https://doi.org/10.1073/pnas.1104208108.

Yusa, K. 2014. "PiggyBac Transposon." *Microbiology Spectrum* 3 (2): 1–26. https://doi.org/10.1128/microbiolspec.MDNA3.

Yusa, K., L. Zhou, M. A. Li, A. Bradley, and N. L. Craig. 2011. "A Hyperactive PiggyBac Transposase for Mammalian Applications." *Proceedings of the National Academy of Sciences* 108 (4): 1531–36. https://doi.org/10.1073/pnas.1008322108.

Zalckvar, E., H. Berissi, M. Eisenstein, and A. Kimchi. 2009. "Phosphorylation of Beclin 1 by DAP-Kinase Promotes Autophagy by Weakening Its Interactions with Bcl-2 and Bcl-X L." *Autophagy* 5 (July): 1–3. https://doi.org/10.1038/embor.2008.246.1.

Zhang, L., J. C. Yin, H. Yeh, N. X. Ma, G. Lee, X. A. Chen, Y. Wang, et al. 2015. "Small Molecules Efficiently Reprogram Human Astroglial Cells into Functional Neurons." *Cell Stem Cell* 17 (6): 735–47. https://doi.org/10.1016/j.stem.2015.09.012.

Zhang, Y., K. Chen, S. A. Sloan, M. L. Bennett, A. R. Scholze, S. O'Keeffe, H. P. Phatnani, et al. 2014. "An RNA-Sequencing Transcriptome and Splicing Database of Glia, Neurons, and Vascular Cells of the Cerebral Cortex." *Journal of Neuroscience* 34 (36): 11929–47. https://doi.org/10.1523/JNEUROSCI.1860-14.2014.

Acknowledgments

"Collaboration operates through a process in which the successful intellectual achievements of one person arouse the intellectual passions and enthusiasms of others." Alexander von Humboldt

My accomplishment would have not been possible without my supervisor and the amazing opportunity he gave me to explore the world of brain repair, a dream for the future. You have been the first one to show me the importance of networking and gave me access to a great deal of extraordinary minds and researchers, thus creating such an inspiring environment.

I would also like to thank my Doktor Mutter for her evaluation on my work, thus allowing me to attain the highest level of education's title I wanted.

An essential presence along the way has been the postdoc supervising my project, who provided me with outstanding support and guidance for my PhD thesis, from projects' execution to technical issues as well as little personal crisis. Thank you for all the patience and for being such an exemplar model for fellow female researchers.

Part of my work has been carried on as a collaboration with the Department of Molecular, Cellular and Developmental Neurobiology at the Instituto Cajal (Madrid, Spain). I am grateful for the helpful discussions and technical advice I received from my collaborators for such a challenging project.

I would like to thank the Microscopy Core Facility at the Institute of Molecular Biology (IMB Mainz) for granting me access to their equipment and for the kind and professional technical support they provide. I have also benefited from the expertise of the TARC personal, who taught me such a delicate procedure as *in utero* electroporation and patiently trained me. Many thanks to the animal caretakers of the Mouse Behavioural Unit, who took good care of our babies and their mothers.

Many friends and colleagues stood by me during my journey. I am grateful for your constant words of encouragement and for your friendship.

The Berninger lab eased my early-stage growth. In particular, I must thank my colleague for taking the time to help me with electrophysiology.

I also want to thank my family, for all the support you always gave or offered me.

Thank you,

Chiara

CHIARA GALANTE

https://www.linkedin.com/in/chiara-galante/
Date of birth: 23.03.1986
Place of birth: Vicenza, Italy
Nationality: Italian

EDUCATION

2015 – 2019	**PhD candidate, Biology Faculty, Johannes Gutenberg University Mainz (Germany)** PhD project: Factors determining competence for *in vivo* glia-to-neuron conversion
2009 – 2011	**Master of Science in Sanitary Biology, Università degli Studi di Padova (Italy)**
Jan – Aug 2010	**Erasmus Lifelong Learning Program, Biology Faculty, Ludwig-Maximilian University Munich (Germany)** Master project: regulated intramembrane proteolysis of Type III Neuregulin 1
2005 – 2009	**Bachelor of Science in Molecular Biology, Università degli Studi di Padova (Italy)** **Bachelor project**: cloning and phenotypical characterization of a mutant *Mycobacterium smegmatis* strain
2000 – 2005	**Diploma di maturità (A-level), Liceo Scientifico Statale "G.B. Quadri" (Vicenza, Italy)**

EMPLOYMENT HISTORY

Feb 2018-today	**Coordinator of the International Summer School and Postdoc Programme, Institute of Molecular Biology gGmbH Mainz (Germany)**
Nov - Dec 2018	**Trainee of the Scientific Management Office, Institute of Molecular Biology gGmbH Mainz (Germany)**
2013 – 2018	**Research Assistant, University Medical Center Mainz (Germany)**
March 2014	**Teaching Assistant, rmn2 workshop "Single Cell Live Imaging", University Medical Center Mainz (Germany)**
2012 – 2013	**Research Assistant, Ludwig-Maximilian University Munich (Germany)** Project: lineage progression of adult neural stem cells

ADDITIONAL NON-ACADEMIC AFFILIATIONS

Sep 2015 – today	**Co-Founder, Manager & Spokesperson, Neuroscience Graduates' Colloquium Mainz** (www.ngcinmainz.com)
2016 – 2019	**Academic Team member/Berlin Verein Board Member, Deutsche Neurowissenschaften-Olympiade e.V.**
2016 – today	**Student member** **Neurowissenschahftliche Gesellschaft e.V.**

ADDITIONAL TRAINING

2016	**Introduction to Project Management, edX online course, Licence of the University of Adelaide (Australia)**

2016	Introduction to People Management, edX online course, Licence of the Indian Institute of Management Bangalore (India)
2014	Course in Laboratory Animal Practice, Johannes Gutenberg University, Mainz (Germany) Valid as FELASA B certificate.
2013	Advances in Stem Cells Biology, Pasteur Institute (Paris, France)

ADDITIONAL COMPETENCES

LANGUAGES	Italian: mother tongue English: full professional proficiency German: B2-Zertifikat (Telc).
COMPUTER SKILLS	Proficient user of Microsoft Office. Expert user of APE (A Plasmid Editor). Competent in Adobe Photoshop, Adobe Illustrator, Mendeley, GraphPad Prism, FIJI, Wordpress. Basic user of SAP (Unimedizin Mainz), and SPSS.
TECHNICAL SKILLS	Molecular cloning; Cell culture; Primary cultures of cortical astrocytes and subependymal zone neural stem cells; Immunocytochemistry; Immunohystochemistry; Microscopy (confocal and epifluorescence); Production of retroviruses in-house; hiPSCs; *in utero* Electroporation; Cryosections and vibrotome sections; Timelapse videomicroscopy; qRT-PCR; Western blot; basic MALDI-TOF mass spectrometry; Co-immunoprecipitation assays.

PROCEEDINGS AT CONFERENCES

Fleck D., Galante C., Hampel H., Kunath S., Tahirovic S., Kremmer E., Haass C. & Willem M.: ADAMs and BACE1 liberate the EGF-like domain of type III Neuregulin-1. Proceedings of the 11th meeting on Cellular Mechanisms of Neurodegeneration, Eibsee, Germany (2011)

Galante C., Ortega F., Masserdotti G., Berninger B.: *Lineage progression of adult neural stem cells – role of Sox2.* Proceedings of the Abcam meeting "Quantitative Single Cell Biology in Stem Cell Research", Munich, Germany (2013).

Galante C., Ortega F., Masserdotti G., Berninger B. *Lineage progression of adult neural stem cells.* Third biennal meeting of the rmn^2 network, Oberwesel, Germany (2014).

Galante C., Ortega F., Masserdotti G., Berninger B.: *Lineage progression of adult neural stem cells – role of Sox2.* Proceedings of the 9th FENS Forum of Neuroscience, Milan, Italy (2014).

Galante C., Ortega F., Berninger B. *Lineage progression of adult neural stem cells* in vitro. Adult Neurogenesis: Evolution, Regulation and Function-Abcam Meeting, Dresden, Germany (2015).

Galante C., Péron S., Bribian A., Figueres-Oñate M., Lopez-Mascaraque L., Berninger B., *Developing a strategy for studying the clonal origin of astrocytes reprogrammed into neurons in vivo*. Fourth biennial meeting of the rmn^2 network, Oberwesel, Germany (2016).

Galante C., Péron S., Bribian A., Figueres-Oñate M., Lopez-Mascaraque L., Berninger B., *Developing a strategy for studying the clonal origin of astrocytes reprogrammed into neurons in vivo*. Programming and reprogramming the brain – Abcam meeting, Munich, Germany (2017).

Galante C., Péron S., Berninger B., *Influence of posttranslational modifications on Ascl1-mediated conversion of glia into neurons in vivo*. Fifth biennial meeting of the rmn^2 network, Oberwesel, Germany (2018).

LIST OF PUBLICATIONS

The work about the role of pASCL1 in direct glia-to-neuron conversion in vivo will be published as:

Galante C., Péron S., Marichal N., Sharif N. Berninger B.: *Influence of post-translational modifications on Ascl1-mediated glia-to-neurons conversion.* (In preparation)

Additional publications:

Fleck D., van Bebber F., Colombo A., Galante C., Schwenk B., Rabe L., Hampel H., Novak B., Kremmer E., Tahirovic S., Edbauer D., Lichtenthaler S., Schmid B., Willem M., Haass C.: *Dual cleavage of Neuregulin 1 type III by BACE1 and ADAM17 liberates its EGF-like domain and allows paracrine signaling*. JNeurosci, 33(18):7856-7869 (2013)

Dumitru I., Galante C., Cesetti T., Kupke J., Nungeß S., Rangaraju V., Watson M., Schwarz F.: *Deutsche Neurowissenschaften-Olympiade – Official Study Guide*. (2017-2018)